INVESTIGATING ENERGY BALANCE AND HORMONAL INFLUENCE IN AN ELASMOBRANCH FISH THE NORTH PACIFIC SPINY DOGFISH, *SQUALUS SUCKLEYI*

By
Alexandra Nicole Schoen

A thesis submitted to the Faculty of Graduate Studies of
The University of Manitoba
in partial fulfillment of the requirements of the degree of

DOCTOR OF PHILOSOPHY

Department of Biological Sciences
University of Manitoba

Copyright © 2023 Alexandra N. Schoen

Abstract

Appropriate energy balance is fundamental for survival, particularly when the demand for energy increases, such as activation of the endocrine stress axis in vertebrates. Hormonal control of energy balance is critical for fueling the stress response and to reestablish internal equilibrium. In most vertebrates, glucose is a predominate fuel source and is primarily mobilized following a stress event. Elasmobranchs are considered relatively glucose intolerant, in comparison to mammals, and also use ketone bodies (e.g. 3-hydroxybutyrate [3-HB]) extrahepatically as a fuel source in both satiated and starved conditions; thus, it is plausible that elasmobranchs use ketones to fuel the stress response. This thesis aims to investigate energy balance (specifically balance of the energy metabolites: glucose and 3-HB) and hormonal regulation during the stress response using a holistic approach in a representative elasmobranch species, the North Pacific spiny dogfish, *Squalus suckleyi*, by 1) examining metabolite and corticosteroid mobilization *in vivo* following a stress event, 2) assessing changes in metabolite balance following hormonal stimulation is a novel *in situ* liver perfusion, and 3) exploring cellular enzymatic and molecular mechanisms involved in metabolite balance. Data presented here show that metabolite mobilization and usage is likely context-dependent and that *S. suckleyi* is slow to mobilize and use the fuel sources investigated. Further, there is evidence presented that demonstrate an increase in measured plasma corticosteroids following a stress event, but that this is not repeatable across different stressors. However, this thesis highlights hormonal candidates that may serve a role in regulating energy balance, such as 11-deoxycortiosterone. Ultimately, this thesis demonstrates that glucose and 3-HB may serve to fuel the stress response in the relative long-term, but the identity of the hormones that regulate balance of these metabolites remains elusive.

Acknowledgements

First and foremost, I want to thank my advisor Dr. Gary Anderson. He was the driving force moving me to Canada, which has subsequently opened innumerable doors both professionally and personally. Gary has been a dream advisor, a valuable mentor, a motivating collaborator, and ultimately an appreciated friend. In addition, I want to thank my committee members, Dr. Jay Treberg and Dr. Rebecca Davis, for their unwavering support of my work. Gary, Jay, and Rebecca, thank you for believing in my abilities as a scientist and cultivating my confidence as a researcher.

Next, I want to thank the past and present members of the Anderson, Treberg, and Davis labs for their assistance with lab and fieldwork, and comradery over the last five years. Particularly, I want to endlessly thank Dr. Alyssa Weinrauch and Dr. Ian Bouyoucos for their dedication to teaching me and moral support, and Dr. Alison Loeppky and Ryan Wahl for emotional guidance. You all have deeply enriched both my academic career and life.

Finally, I want to thank my family for being my first and consistent teachers and cheerleaders. There is no end to the support and advice you have given me in reaching this milestone and continue to offer moving forward. Thank you to my parents and grandparents, who made it financially possible to move to another country to pursue my goals, as well as for answering the phone when I needed you (sometimes 5-6 times a day). Thank you to my sister, Caitlin, who is on her own PhD journey, for your empathy and making me laugh. Thank you to my partner, Eric, for your level-headedness and wholehearted support of anything I want to accomplish.

I also want to dedicate my thesis to my grandmother, Nicole McGuire, a woman ahead of her time. She fought to go to university when the people around her were unsupportive of her decisions and was passionate about furthering my education (sometimes resorting to ice cream as bribery). I can only hope that I have made her proud.

Table of Contents

Abstract 2

Acknowledgements 3

Abbreviations (alphabetical) 7

List of Tables 9

List of Figures 10

Chapter 1. General Introduction 17

1.1. Review of Major Fuel Substrates in Elasmobranchs 17

1.2. Ketone Bodies 19

1.3. The Stress Response 22

1.4. Corticosteroids in Elasmobranchs 24

1.5. Hormonal Control in Metabolite Balance 25

1.6. Objectives and Hypotheses 30

1.7. Works Cited 33

2. Chapter 2: Energy and corticosteroid mobilization following an induced stress response in an elasmobranch fish, the North Pacific spiny dogfish, Squalus suckleyi. 43

2.1. Abstract 44

2.2. Introduction 44

2.3. Methods 46

2.4. Results 50

2.5. Discussion 52

2.6. Conclusion 55

2.7. Acknowledgements 56

2.8. Figures 57

2.9. Supplemental Figure 60

2.10. Works Cited 61

3. Chapter 3: An adapted liver perfusion in a shark species, Squalus suckleyi: investigation of energy mobilization. 67

3.1. Abstract 68

3.2. Introduction 68

3.3. Methods 70

3.4. Results 76

3.5. Discussion 78

3.6. Conclusions 83

3.7. Acknowledgements 83

3.8. Tables 84

3.9. Figures 90

3.10. Works Cited 101

4. Chapter 4: Effects of corticosteroid and a catecholamine in the perfused liver of an elasmobranch, the North Pacific spiny dogfish, Squalus suckleyi. 106

4.1. Abstract 106

4.2. Introduction 106

4.3. Methods 109

4.4. Results 116

4.5. Discussion 117

4.6. Conclusion 121

4.7. Acknowledgements 122

4.8. Tables 123

4.9. Figures 128

4.10. Works Cited 136

5. Chapter 5: Metabolic indicators of glucose and ketone body energy balance following air exposure in an elasmobranch species, the North Pacific spiny dogfish, Squalus suckleyi. 143
5.1. Abstract 143
5.2. Introduction 144
5.3. Methods 146
5.4. Results 150
5.5. Discussion 152
5.6. Conclusions 159
5.7. Acknowledgements 160
5.8. Tables 161
5.9. Figures 165
5.10. Works Cited 174
6. General Discussion 182
6.1. Thesis Summary 182
6.2. What are the dynamics of key metabolites following a stress response? 185
6.3. What are the dynamics of major corticosteroids following a stress response? 186
6.4. What influence do hormones of interest have on metabolite mobilization? 187
6.5. What is fueling the stress response in elasmobranchs? 189
6.6. Caveats and Future Directions 190
6.7. Conclusion 191
6.8. Works Cited 192

Abbreviations (alphabetical)

ACoAT – aceteocetyl-CoA thiolase

ACTH – adrenocorticotropic hormone

Ang II – angiotensin II

AR – adrenergic receptor

A-V – arterial-venous

B – corticosterone

Ca^{2+} – calcium

CR – corticosteroid receptor

DO – dissolved oxygen

DOC – 11-deoxycorticosterone

E – epinephrine

F – cortisol

GC – glucocorticoid

GLUT – glucose transporter

GP – glycogen phosphorylase

GR – glucocorticoid receptor

G1P – glucose-1-phosphate

G6P – glucose-6-phosphate

HEX – hexokinase

HMG-CoA – ß-hydroxy-ß-methylglutaryl-CoA

MC – mineralocorticoid

MCT – monocarboxylate transporter

MR – mineralocorticoid receptor

NE – norepinephrine

O_2 – oxygen

PC – pre-cannulation

PEP – phosphoenolpyruvate

PEPCK – phosphoenolpyruvate carboxykinase

SCOT – succinyl-CoA transferase

1α-OHB – 1α-hydroxycorticosterone

3-HB (or β-HB) – 3-hydroxybutyrate

αMSH – α-melanocyte-stimulating hormone

3-HBDH (or β-HBDH) – 3-hydroxybutyrate dehydrogenase

List of Tables

Table 3.1. Liver perfusion treatments and specifications. 84
Table 3.2. Linear model outputs for metabolite 'removal' and 'recovery'. 85
Table 3.3. Mean values and 95% confidence intervals of oxygen consumption. Bold rows indicate that 2.5-97.5% confidence intervals do not overlap 0. 85
Table 3.4. Mean values and 95% confidence intervals of glucose. Bold rows indicate that 2.5-97.5% confidence intervals do not overlap 0. 86
Table 3.5. Mean values and 95% confidence intervals of 3-HB. Bold rows indicate that 2.5-97.5% confidence intervals do not overlap 0. 88
Table 4.1. qPCR primer sequences, reaction conditions, efficiency, and sources. 123
Table 4.2. Mean values and 95% confidence intervals of oxygen consumption. Bold rows indicate that 2.5-97.5% confidence intervals do not overlap 0. 125
Table 4.3. Mean values and 95% confidence intervals of glucose. Bold rows indicate that 2.5-97.5% confidence intervals do not overlap 0. 125
Table 4.4. Mean values and 95% confidence intervals of 3-HB. Bold rows indicate that 2.5-97.5% confidence intervals do not overlap 0. 127
Table 5.1. qPCR primer sequences, concentrations, cycling conditions, efficiency, and sources. 161

List of Figures

Figure 1.1. Simplified overview of glucose and ketone body metabolism in a hepatocyte and general extrahepatic tissue cell (i.e. brain, heart, skeletal muscle, and rectal gland; tissues examined in this thesis). Metabolic processes are illustrated in white boxes. Enzymes are denoted in green ovals and abbreviations are as follows: GP, glycogen phosphorylase; HEX, hexokinase; PEPCK, phosphoenolpyruvate carboxykinase; 3-HBDH, 3-hydroxybyturate dehydrogenase; SCOT, succinyl-CoA transferase. Blue transporters represent glucose transporters (GLUT), specifically GLUT1 and GLUT4 for the purpose of this thesis. Yellow transporters represent ketone and lactate transporters (MCT), specifically MCT1 and MCT2 for the purpose of this thesis. Additional abbreviations are as follows: G1P, glucose-1-phosphate; G6P, glucose-6-phosphate; PEP, phosphoenolpyruvate; 3-HB, 3-hyroxybyturate. Figure created using BioRender. 21

Figure 1.2. Basic pattern of biochemical synthesis of major mineralocorticoids (MCs) and glucocorticoids (GCs) and supposed corticosteroids in vertebrates. 23

Figure 1.3. Overview of the putative endocrine and metabolic responses following exposure to a stressor in elasmobranchs. Dark blue arrow illustrates innervation of chromaffin tissue by sympathetic ganglia, red arrow illustrates release of hypothalamic hormones that stimulate pituitary hormone release, light blue arrows illustrate release of pituitary hormones that stimulate corticosteroid release from interrenal gland, yellow arrows illustrate release of catecholamines and binding with hepatic and extrahepatic adrenergic receptors, green arrows illustrate release of corticosteroids and binding with hepatic and extrahepatic corticosteroid receptors, and purple arrows hepatic efflux, release, and extrahepatic influx of glucose and ketones. Purple circles denote mechanisms associated with glucose and ketone metabolism. Blue transporters represent GLUT transporters, specifically GLUT1 and GLUT4 for the purpose of this thesis. Yellow transporters represent MCT transporters, specifically MCT1 and MCT2 for the purpose of this thesis. Abbreviations are as followed: CRF, corticosteroid releasing factor; ACTH, adrenocorticotropic hormone; αMSH, α-melanocyte-stimulating hormone; ARs, adrenergic receptors; CRs, corticosteroid receptors. Figure created using BioRender. 30

Figure 2.1. Changes in plasma metabolite and corticosteroid concentrations in *Squalus suckleyi* following control (c, closed circles and solid line), air-exposed (a, open triangles and dashed line), or B-injected (b, open squares and dotted line) treatments. Values are expressed as a mean +/- SEM. Letters indicate means that are significantly different ($p < 0.05$) from respective PC (pre-

cannulation) values within each treatment. An asterisk (*) indicates means that are significantly different ($p < 0.05$) from control values at the same timepoint (n = 6-8). Time-0 min occurred 24 to 48 hours following cannulation. 57
Figure 2.2. Correlations between metabolite and hormone concentrations during control and air-exposed treatments in *Squalus suckleyi*. A) β-HB (mM) and glucose (mM) concentrations (n = 203; $R^2 = -0.296$; $p < 0.001$). B) B ($ng \cdot mL^{-1}$) and 1α-OHB ($ng \cdot mL^{-1}$) concentrations (n = 212; $R^2 = 0.466$; $p < 0.001$). C) Glucose (mM) and 1α-OHB ($ng.mL^{-1}$) concentrations (n= 202; $R^2 = 0.016$; p= 0.818). D) β-HB (mM) and 1α-OHB ($ng \cdot mL^{-1}$) concentrations (n = 203; $R^2 = 0.230$; p = 0.001). E) Glucose (mM) and B ($ng \cdot mL^{-1}$) concentrations (n = 220; $R^2 = 0.349$; $p < 0.001$). F) β-HB (mM) and B ($ng \cdot mL^{-1}$) concentrations (n = 212; $R^2 = 0.180$; p = 0.008)..... 58
Figure 2.3. Changes in plasma lactate, pH, and osmolality in *Squalus suckleyi* at different times following control (c, closed circles and solid line), air-exposed (a, open triangles and dashed line), or B-injected (b, open squares and dotted line) treatments. Values are expressed as a mean +/- SEM. Letters indicate means that are significantly different ($p < 0.05$) from respective PC (pre-cannulation) values within each treatment. An asterisk (*) indicates means that are significantly different ($p < 0.05$) from control values at the same timepoint (n = 6-8). 59
Figure S2.1. Individual serial sampling in control (solid line, open triangle) and air-exposed (dashed line, closed circle) *Squalus suckleyi*, including outliers. Fish were included if they contained all 9 timepoints. A) Glucose (mM) concentration (n = 24). B) β-HB (mM) concentration (n = 24). C) 1α-OHB ($ng \cdot mL^{-1}$) concentration (n = 25). D) Corticosterone ($ng \cdot mL^{-1}$) concentration (n = 25)..... 60
Figure 3.1. Diagram of the major vasculature and cannulations associated with the adapted liver perfusion in *Squalus suckleyi.* Blue vasculature indicates venous systems and red vasculature indicates arterial systems (1: hepatic vein, 2: hepatic sinuses, 3: sinus venosus, 4: atrium, 5: ventricle). Orange indicates cannulation tubing (6: inflowing, 7: outflowing, 8: airtight cryovial for oxygen consumption measurements). 90
Figure 3.2. Oxygen consumption ($ng\ O_2 \cdot min^{-1} \cdot g\ wet\ tissue^{-1}$) of *Squalus suckleyi* liver preparations, as determined by the modified Fick's equation, for 3hr perfusions (n = 11). Boxplots represent the mean (solid black line inside box), interquartile range (box edges), and maximum and minimum (box whiskers) of oxygen consumption data. Dotted line indicates null oxygen

consumption (0) and confidence intervals that do not overlap with 0 are denoted with an asterisk (*). 91
Figure 3.3. A-V difference of metabolites (mM) in *Squalus suckleyi* liver preparations prior to (initial baseline; Ringer with both glucose and 3-HB), during (metabolite removal), and following (baseline; Ringer with both glucose and 3-HB) removal of metabolites from inflow (n=4). A) [A-V glucose] of perfusions with removal of both 2mM glucose and 1mM 3-HB. B) [A-V 3-HB] of perfusions with removal of both 2mM glucose and 1mM 3-HB. C) [A-V glucose] of perfusions with removal of 2mM glucose. D) [A-V 3-HB] of perfusions with removal of 2mM glucose. E) [A-V glucose] of perfusions with removal of 1mM 3-HB. F) [A-V 3-HB] of perfusions with removal of 1mM 3-HB. Dotted lines (0) indicate metabolite balance where outflow metabolite concentration is equal to inflow metabolite concentration. Boxplots represent the mean (solid black line inside box), interquartile range (box edges), and maximum and minimum (box whiskers) of A-V difference of metabolite data. Shaded boxes indicate metabolite removal (10-30min), followed by metabolite recovery (40-60min). Confidence intervals that do not overlap with 0 are denoted with a plus sign (+). Statistical significance ($\alpha = 0.05$) of the mean metabolite balance between subsequent timepoints and the initial baseline is indicated with an asterisk (*). 93
Figure 3.4. Flow rate ($mL \cdot min^{-1}$) during *Squalus suckleyi* liver preparations prior to (initial baseline; Ringer with both glucose and 3-HB), during (metabolite removal), and following (baseline; Ringer with both glucose and 3-HB) removal of metabolites from inflow (n = 4). A) Removal of both 2mM glucose and 1mM 3-HB. B) Removal of 1mM 3-HB. C) Removal of 2mM glucose. Boxplots represent the mean (solid black line inside box), interquartile range (box edges), and maximum and minimum (box whiskers) of flow rate data. Shaded boxes indicate metabolite removal (10-30min), followed by metabolite recovery (40-60min). Inflowing rate (dotted line) and outflowing rate (black circles). Statistical significance ($\alpha = 0.05$) of the mean flow rate between subsequent timepoints and the initial baseline is indicated by an asterisk (*). 94
Figure 3.5. Flow rate ($mL \cdot min^{-1}$) during *Squalus suckleyi* liver preparations prior to (initial baseline), during (hormone treatment), and following (baseline) addition of peptide hormones to inflow (Series B and C; n = 5). B) Perfusions treated with 30μM Ang II. C) Perfusions treated with 10nM insulin. D) Perfusions treated with 10nM glucagon. Boxplots represent the mean (solid black line inside box), interquartile range (box edges), and maximum and minimum (box whiskers) of flow rate data. Shaded boxes indicate metabolite removal (10min), followed by metabolite

recovery (20-30min). Inflowing rate (dotted line) and outflowing rate (black circles). Statistical significance (α = 0.05) of the mean flow rate between subsequent timepoints and the initial baseline is indicated by an asterisk (*). 96
Figure 3.6. A-V difference of metabolites (mM) during *Squalus suckleyi* liver preparations prior to (initial baseline), during (hormone treatment), and following (baseline) addition of hormones to inflow (n = 5). A) [A-V glucose] of perfusions treated with 10nM insulin. B) [A-V 3-HB] of perfusions treated with 10nM insulin. C) [A-V glucose] of perfusions treated with 10nM glucagon. D) [A-V 3-HB] of perfusions treated with 10nM glucagon. Boxplots represent the mean (solid black line inside box), interquartile range (box edges), and maximum and minimum (box whiskers) of A-V difference of metabolite data. Shaded boxes indicate metabolite removal (10min), followed by metabolite recovery (20-30min). Dotted lines (0) indicate metabolite balance where outflow metabolite concentration is equal to inflow metabolite concentration. Confidence intervals that do not overlap with 0 are denoted with a plus sign (+)..... 98
Figure 3.7. Conceptual models of liver preparations under A) initial baseline conditions with no endogenous mechanisms altering outflow metabolite concentration. B) Perfusion conditions where removal and reintroduction of metabolite produces equal, but inverse, slopes of outflow metabolite concentrations over time. C) Perfusion conditions where removal of metabolite produces a steeper slope than the inverse recovery slope, but outflow metabolite concentration does not recover to initial baseline concentrations. D) Perfusion conditions where removal of metabolite produces a steeper slope than the inverse recovery slope due to endogenous production/reduced consumption of metabolite (red bracket), thus increasing outflow metabolite concentration..... 100
Figure 4.1. Effect of corticosteroid perfusion on oxygen consumption (ng $O_2 \cdot min^{-1} \cdot g$ wet tissue^{-1}) of *Squalus suckleyi* livers. A) 1μM B (n = 5-6). B) 10nM DOC (n = 5). C) 0.034% ethanol vehicle control (n = 10-11). Boxplots represent the mean (solid black line inside box), interquartile range (box edges), and maximum and minimum (box whiskers) of oxygen consumption data. Individual oxygen consumption values are represented by open circles. Boxplots represent the mean (solid black line inside box), interquartile range (box edges), and maximum and minimum (box whiskers) of oxygen consumption data. Shaded boxes indicate hormone perfusion (15min), followed by Ringer's solution (30-45min). Statistical significance (α = 0.05) of the mean oxygen consumption from initial baseline is indicated by an asterisk (*). Statistical significance of confidence intervals from 0 (dotted line) is indicated by a plus sign (+). 128

Figure 4.2. Effects of hormone perfusion on inflow (mL·min^{-1}; red circles) and outflow rate (mL·min^{-1}; black circles). A) 1μM B (n = 5-6). B) 10nM DOC (n = 5). C) 0.034% ethanol vehicle control (n = 10-11). D) 50nM E (n = 5). Boxplots represent the mean (solid black line inside box), interquartile range (box edges), and maximum and minimum (box whiskers) of flow rate data. Individual flow rate values are represented by open circles. Boxplots represent the mean (solid black line inside box), interquartile range (box edges), and maximum and minimum (box whiskers) of flow rate data. Shaded boxes indicate hormone perfusion (15min), followed by Ringer's solution (30-45min). Statistical significance (α = 0.05) of the mean flow rate from initial baseline is indicated by a different letter (A or B), which is only compared within inflow or outflow over time. 130

Figure 4.3. Effects of hormones on [A-V glucose] (mM). A) 1μM B (n = 5-6). B) 10nM DOC (n = 5). C) 0.034% ethanol vehicle control (n = 10-11). E) 50nM E (n = 4). Boxplots represent the mean (solid black line inside box), interquartile range (box edges), and maximum and minimum (box whiskers) of [A-V glucose] data. Individual [A-V glucose] values are represented by open circles. Shaded boxes indicate hormone perfusion (15min), followed by Ringer's solution (30-45min). There is no statistical significance of mean [A-V glucose] from initial baseline or 0 (dotted line). 132

Figure 4.4. Effects of hormones on [A-V 3-HB] (mM). A) 1μM B (n = 5-6). B) 10nM DOC (n = 5). C) 0.034% ethanol vehicle control (n = 10-11). E) 50nM E (n = 5). Boxplots represent the mean (solid black line inside box), interquartile range (box edges), and maximum and minimum (box whiskers) of [A-V 3-HB] data. Individual [A-V 3-HB] values are represented by open circles. Shaded boxes indicate hormone perfusion (15min), followed by Ringer's solution (30-45min). There is no statistical significance the mean [A-V 3-HB] from initial baseline. Statistical significance of confidence intervals from 0 (dotted line) is indicated by a plus sign (+)..... 133

Figure 4.5. Effects of hormones on enzyme activity (absolute U·mg protein^{-1}) as compared to controls. A) 3-HBDH. B) SCOT. C) GP. D) PEPCK. Boxplots represent the mean (solid black line inside box), interquartile range (box edges), and maximum and minimum (box whiskers) of enzyme activity data. Individual enzyme activity values are represented by open circles. Statistical significance (α = 0.05) of the mean enzyme activity from control is indicated by an asterisk (*). 134

Figure 4.6. Effects of hormones on relative hepatic mRNA transcript abundance as compared to controls. A) *glut1*. B) *glut4*. C) *mct1*. D) *mct2*. E) *gr*. Boxplots represent the mean (solid black line inside box), interquartile range (box edges), and maximum and minimum (box whiskers) of transcript abundance data. Individual transcript abundance values are represented by open circles. Statistical significance (α = 0.05) of the mean relative transcript abundance from controls is indicated by an asterisk (*). 135
Figure 5.1. Plasma A) glucose concentrations (mM; n = 6-7), B) 3-HB concentrations (mM; n = 6-8), C) lactate concentrations (mM; n = 5-6), D) osmolality (mmol·kg^{-1}; n = 5-6), E) 1α-OHB concentrations (ng·mL^{-1}; n = 6-8), F) B concentrations (ng·mL^{-1}; n = 5-6), and G) F concentrations (ng·mL^{-1}; n = 6) over time in *Squalus suckleyi*. Boxplots represent the mean (solid black line inside box), interquartile range (box edges), and maximum and minimum (box whiskers) of respective data. Statistical significance (α = 0.05) of the mean from 0min is indicated by an asterisk (*). 166
Figure 5.2. Enzyme activity (U·mg protein^{-1}) of A) HEX (n = 3-6), B) GP (n = 3-6), C) 3-HBDH (n = 4-6), D) SCOT (n = 4-6), and E) PEPCK (n = 6) in various tissues over time in *Squalus suckleyi*. Boxplots (0min = black circles, 30min = red squares, and 1hr = blue diamonds) represent the mean (solid black line inside box), interquartile range (box edges), and maximum and minimum (box whiskers) of enzyme activity data. Statistical significance (α = 0.05) of the mean over time within tissue is indicated by different letters (A or B)..... 167
Figure 5.3. Transcript abundance of A) *glut1* (n = 5-7), B) *glut4* (n = 5-7), C) *mct1* (n = 5-7), D) *mct2* (n = 5-7), and E) *gr* (n = 5-7) in various tissues over time (relative to 0min within tissue) in *Squalus suckleyi*. Boxplots (0min = black circles, 30min = red squares, and 1hr = blue diamonds) represent the mean (solid black line inside box), interquartile range (box edges), and maximum and minimum (box whiskers) of transcript abundance data. Statistical significance (α = 0.05) of the mean over time within tissue is indicated by different letters (A or B). 168
Figure 5.4. Plasma A) glucose concentrations (mM; n = 6), B) 3-HB concentrations (mM; n = 6), C) lactate concentrations (mM; n = 6), D) osmolality (mmol·kg^{-1}; n = 6), E) 1α-OHB concentrations (ng·mL^{-1}; n = 6), F) B concentrations (ng·mL^{-1}; n = 4-5), and G) F concentrations (ng·mL^{-1}; n = 4-5) over time in *Squalus suckleyi*. Boxplots represent the mean (solid black line inside box), interquartile range (box edges), and maximum and minimum (box whiskers) of respective data. Statistical significance (α = 0.05) of the mean from 0min is indicated by an asterisk (*)..... 169

Figure 5.5. Enzyme activity (U·mg protein^{-1}) of A) HEX (n = 5-6), B) GP (n = 4-6), C) 3-HBDH (n = 5-6), D) SCOT (n = 4-6), and E) PEPCK (n = 6) in various tissues over time in *Squalus suckleyi*. Boxplots (controls = black circles, air exposure treatment = red squares) represent the mean (solid black line inside box), interquartile range (box edges), and maximum and minimum (box whiskers) of enzyme activity data. Statistical significance ($\alpha = 0.05$) of the mean over time within tissue is indicated by an asterisk (*). 172
Figure 5.6. Transcript abundance of A) *glut1* (n = 4-6), B) *glut4* (n = 4-6), C) *mct1* (n = 5-6), D) *mct2* (n = 4-6), and E) *gr* (n = 5-6) in various tissues over time (relative to 0min within tissue) in *Squalus suckleyi*. Boxplots (controls = black circles, air exposure treatment = red squares) represent the mean (solid black line inside box), interquartile range (box edges), and maximum and minimum (box whiskers) of transcript abundance data. Statistical significance ($\alpha = 0.05$) of the mean over time within tissue is indicated by an asterisk (*). 173

Chapter 1. General Introduction

Organisms must acquire and store energy to fuel physiological and behavioral processes. The vertebrate endocrine system plays a critical regulatory role in controlling energy balance, particularly during periods of increased energy demand. Examples of hormones involved in energy balance that have been relatively well-conserved on an evolutionary timescale include growth hormone (Kawauchi et al., 2002) and somatostatin (Conlon et al., 1985), which act to regulate insulin-like growth factors primarily in the liver; thyroid hormones (T_3 and T_4) (Leary et al., 1999; Taylor and Heyland, 2017), which are known to influence early development and regulate basal metabolic rate (Little and Seebacher, 2014); and insulin and glucagon (Van de Pol et al., 2017), which are classically thought to antagonistically control plasma glucose levels (Leibson and Plisetskaya, 1968; Patent, 1970), as well as regulate glycogen stores in the liver, heart, and skeletal muscle (Leibson and Plisetskaya, 1968; Navarro et al., 1999). Beyond daily energy costs, organisms must allocate energy to maintain internal homeostasis during situations that require an increase of fuel. Costly physiological or behavioral activities include but are not limited to reproduction, hunting or foraging, and the stress response. The endocrine stress axis in vertebrates is a mechanism that reestablishes internal homeostasis in response to external change. Activation of the stress axis by definition demands mobilization and use macromolecules (metabolites) to fuel the stress response.

1.1. Review of Major Fuel Substrates in Elasmobranchs

Plasma glucose is a predominate fuel source for oxidative metabolism in most tetrapods (Krebs et al., 1963; Newsholme and Start, 1973; Pardridge, 1983). When the demand for energy increases, as is the case during the stress response, glucose is produced through glycogenolysis and gluconeogenesis. These processes synthesize glucose from stored glycogen and other macromolecules, respectively. Glycogen is stored in a variety of tissues, but predominately in the liver, which is also the major site of gluconeogenesis in vertebrates (Newsholme and Start, 1973); although, these mechanisms occur in extrahepatic tissues as well, such as glycogenolysis in exercised muscle fibers (Richter et al., 1982) or gluconeogenesis in the mammalian kidney (Krebs et al., 1963).

Teleosts and elasmobranchs differ from mammals in that these taxa are relatively glucose intolerant, meaning an increased bolus of glucose takes significantly longer to metabolize or clear

from circulation (Deck et al., 2017b; Patent, 1970; Polakof et al., 2012). Thus, there may be a comparatively lower reliance on glucose as a fuel source. For example, hepatic phosphoenolpyruvate carboxykinase (PEPCK) – the rate limiting step for gluconeogenesis – activity in the lesser-spotted dogfish, *Scyliorhinus canicula*, did not increase during starvation, inferring that liver gluconeogenesis may not be the primary method of fuel production under these conditions (Zammit and Newsholme, 1979). Furthermore, 60% of exogenous lactate and alanine was directed towards oxidation rather than serving as gluconeogenetic precursors in isolated hepatocytes of the little skate, *Leucoraja erinacea* (Mommsen and Moon, 1987). On the contrary, a maintenance of plasma glucose over prolonged fasting might infer that gluconeogenesis may be more important during starvation (Wood et al., 2010). Yet, there is also a deficiency of PEPCK extrahepatically, which limits gluconeogenesis as compared to more derived vertebrates (Ballantyne, 1997). Further, endogenous glycogen may serve as a sustainable fuel source in tissues such as the heart of *L. erinacea* (Driedzic and Hart, 1984) and brain of the North Pacific spiny dogfish, *Squalus suckleyi* (deRoos, 1994), supporting the limited use of exogenous glucose; although, the change in glycogen content of tissues was not directly measured in these studies. However, metabolite preference may be tissue-specific, in that some tissues are glucose dependent such as the rectal gland of *S. suckleyi* (Deck et al., 2017a; Walsh et al., 2006).

An additional fuel source in many fishes are fatty acids (Speers-Roesch and Treberg, 2010; Zammit and Newsholme, 1979); however, this appears to be limited to specific tissues in elasmobranchs (Driedzec and Hart, 1984; Speers-Roesch and Treberg, 2010; Zammit and Newsholme, 1979). Fatty acids are thought to be primarily stored in adipose and liver tissue in tetrapods and teleosts and the liver of elasmobranchs thus far investigated. There are several lines of evidence to support that elasmobranchs have a limited, tissue-specific ability to use fatty acids as a fuel source, specifically long-chain fatty acids. In those elasmobranchs examined to date there is a lack of plasma albumin, an essential fatty acid transport molecule (Metcalf and Gemmell, 2005), and therefore concentrations of plasma non-esterified fatty acids, a key indication of lipid metabolism, are low compared to other vertebrate taxa (Ballantyne, 1997; Speers-Roesch and Treberg, 2010; Zammit and Newsholme, 1979). Additionally, several elasmobranch species are deficient in carnitine palmitoyltransferase (CPT), an enzyme necessary for mitochondrial long-chain fatty acid oxidation in teleosts and tetrapods (Kerner and Hoppel, 2000), in skeletal and cardiac muscle (Speers-Roesch et al., 2006; Speers-Roesch and Treberg, 2010; Zammit and

Newsholme, 1979). Previous studies have also demonstrated an inability to metabolize long-chain fatty acids in red muscle of the spiny dogfish, *Squalus acanthias* (Moyes et al., 1990), heart of *L. erinacea* (Driedzic and Hart, 1984), and white muscle of *S. suckleyi* (Richards et al., 2003).

1.2. Ketone Bodies

Given the proposed reduced reliance on glucose and inability to oxidize long-chain fatty acids extrahepatically, it has been suggested that elasmobranchs may use another class of metabolites as a fuel source: ketone bodies. Ketone bodies represent three molecules: acetone, acetoacetate, and 3-ß-hydroxybutyrate (ß-HB or 3-HB; to date, these metabolites have the same physiological role but the use of either the ß- or 3- nomenclature is specified in each chapter of this thesis). Ketone production increases in the liver during periods of starvation in mammals (Newsholme and Start, 1973) when glucose reserves are low (Newsholme and Start, 1973; Pardridge, 1983), and notably causes ketoacidosis in poorly controlled diabetic humans (Laffel, 1999). If there is not enough glucose production or a lack of cellular glucose uptake to support the citric acid cycle, ketogenesis is upregulated due to the abundance of acetyl-CoA – essential to the citric acid cycle. Two acetyl-CoAs combine via aceteocetyl-CoA thiolase (ACoAT) to form acetoactyl-CoA, which is then converted to ß-hydroxy-ß-methylglutaryl-CoA (HMG-CoA) by HMG-CoA synthase. HMG-CoA is lysed to produce, acetoacetate, which is then converted to acetone spontaneously and to 3-HB by 3-hydroxybutyrate dehydrogenase (3-HBDH) (Laffel, 1999; Newsholme and Start, 1973).

While some studies deduce that several teleost species contain 3-HBDH, there is general consensus that ketones do not play a major role as an energy source in teleosts (Ballantyne, 1997). Contrary to teleosts and mammals, elasmobranchs produce ketones in both satiated and starved conditions (Wood et al., 2010; Zammit and Newsholme, 1979). Zammit and Newsholme (1979) were the first to comprehensively illustrate that elasmobranchs rely heavily on ketone bodies as an extrahepatic fuel source rather than fatty acids, showing that hepatic 3-HBDH and plasma 3-HB increase in *S. canicula* during starvation. Certain amino acids also seem to be important metabolic fuels (Chamberlin and Ballantyne, 1992; Newsholme and Start, 1973), but as nitrogen donors, these metabolites may be conserved for the purpose of urea production (Ballantyne, 1997; Kajimura et al., 2006) since elasmobranchs are ureotelic and ureosmotic (Smith, 1935). It has also been suggested that amino acids may be substrates in hepatic ketogenesis, particularly leucine

(Mommsen and Moon, 1987) and alanine (Anderson, 1990). Elevated activity of enzymes related to ketone oxidation have been found in the skeletal muscle, heart, and rectal gland of several elasmobranch species (Driedzec and de Almeida-Val, 1996; Speers-Roesch et al., 2006; Walsh et al., 2006; Zammit and Newsholme, 1979). In ketotic *S. acanthias,* hepatic mitochondrial ACoAT activity was elevated, although this was not reflected in a change in HMG-CoA synthase or 3-HBDH activity (Treberg et al., 2006). Treberg et al. (2006) also showed that hepatic CPT was less sensitive to inhibition under fed conditions, as compared to mammals, and demonstrated similar regulation to increase activity (thus increasing beta-oxidation) during fasting. Further, acetoacetate was preferred over fatty acids in the perfused heart of *L. erinacea* (Driedzec and Hart, 1984) and there were high rates of acetoacetate and 3-HB catabolism in red muscles and the heart of *S. suckleyi* (Moyes et al., 1990). Interestingly, acetoacetate was not oxidized by liver mitochondria of *L. erinacea,* suggesting negligible hepatic ketone usage (Moyes et al. 1986). Together these data indicate that ketones are predominately synthesized in the liver and consumed in tissues with high oxidative rates.

Given the important role ketones appear to play as a metabolic fuel in elasmobranchs, it is conceivable that release of these molecules may play a significant function in fueling extrahepatic metabolic processes when the demand for energy increases. Previous work had measured plasma 3-HB in the Atlantic stingray, *Dasyatis sabina*, during 30 minutes of air exposure, but the results were inconclusive (Lambert et al., 2018). In angled shortfin mako sharks, *Isurus oxyrinchus*, plasma 3-HB was negatively correlated with increasing sea surface temperature, suggesting a decrease in 3-HB production or an increase in 3-HB consumption with thermal stress (French et al., 2015). Beyond plasma analysis, low pyruvate dehydrogenase activity and a significant influx of 3-HB in perfused white muscle of *S. suckleyi* post-exhaustive exercise indicated that 3-HB may be the recovery fuel of choice over glucose (Richards et al., 2003). In hypoxia exposed smooth dogfish, *Mustelus canis*, glycogen did not significantly decrease in the heart and lactate depressed contractile function, suggesting that glycogen is not a major metabolite in this tissue during hypoxia stress (Driedzec, 1978). Moreover, there was very little change in flux of glucose in the perfused brain of fasted *S. suckleyi,* while 3-HB significantly increased the rate of influx (deRoos, 1994).

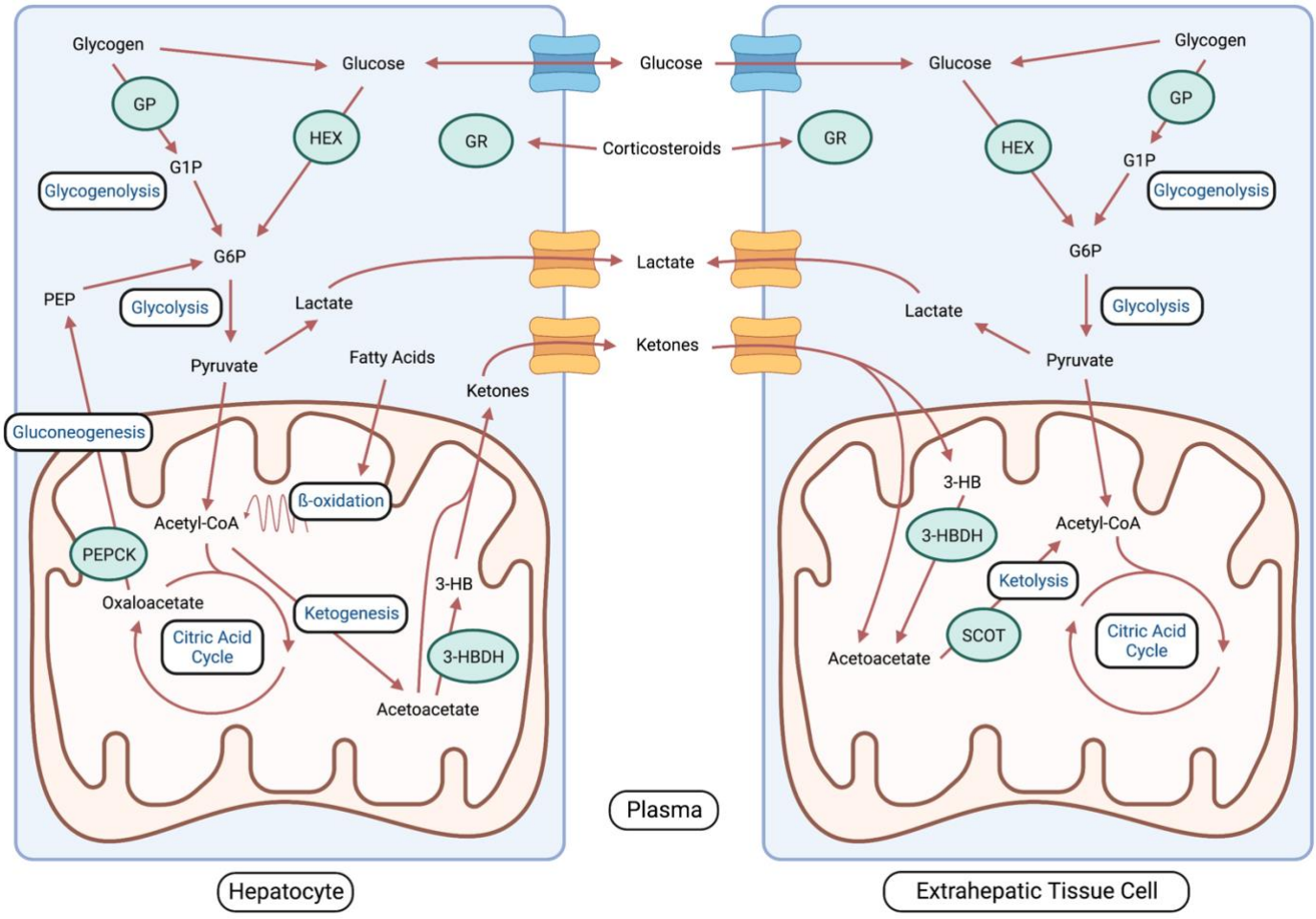


Figure 1.1. Simplified overview of glucose and ketone body metabolism in a hepatocyte and general extrahepatic tissue cell (i.e. brain, heart, skeletal muscle, and rectal gland; tissues examined in this thesis). Metabolic processes are illustrated in white boxes. Enzymes are denoted in green ovals and abbreviations are as follows: GP, glycogen phosphorylase; HEX, hexokinase; PEPCK, phosphoenolpyruvate carboxykinase; 3-HBDH, 3-hydroxybyturate dehydrogenase; SCOT, succinyl-CoA transferase. Blue transporters represent glucose transporters (GLUT), specifically GLUT1 and GLUT4 for the purpose of this thesis. Yellow transporters represent ketone and lactate transporters (MCT), specifically MCT1 and MCT2 for the purpose of this thesis. Additional abbreviations are as follows: G1P, glucose-1-phosphate; G6P, glucose-6-phosphate; PEP, phosphoenolpyruvate; 3-HB, 3-hyroxybyturate. Figure created using BioRender.

1.3. The Stress Response

The typical vertebrate endocrine response first requires perception of the stressor by the brain. Ganglionic neurons in the vertebral column innervate chromaffin tissue and initially stimulate the release of catecholamines (epinephrine [E] and norepinephrine [NE]) through release of the neurotransmitter acetylcholine that binds to cholinergic receptors in chromaffin tissue (Reid et al., 1998). Catecholamines then bind to adrenergic receptors, thus resulting in the short-term "fight-or-flight" response (Cannon, 1915). This response increases ventilation, oxygen uptake, plasma glucose, and regulates mineral balance (depending on the tissue) allowing the organism to quickly respond to the stressor (Chrousos and Gold, 1992; Romero and Butler, 2007; Wendelaar Bonga, 1997).

A persistent stressor will continue to activate a long-term stress response, which acts along the hypothalamic-pituitary-adrenal axis in tetrapods (Wright and Jones, 1955; Wurtman and Axelrod, 1966; Hess 2002). This causes the release of corticotropin releasing hormone (CRH) from the hypothalamus that stimulates the release of adrenocorticotropin hormone (ACTH) from the pituitary gland. ACTH targets adrenocortical cells to increase synthesis and release of corticosteroids that regulate metabolite and mineral balance (Chrousos and Gold, 1992). Corticosteroids are the product of a biosynthetic pathway that begins with the modification of cholesterol and ultimately influence the genomic response of target tissues by binding to an intracellular receptor. There is also evidence of non-genomic effects of corticosteroids that requires a plasma membrane-bound receptor and has the capacity to elicit cellular changes within minutes (Faught and Vijayan, 2016; Das and Vijayan, 2023), although this is not discussed in this thesis. Similar to tetrapods, teleosts utilize a "fight-or-flight" reaction for an immediate stress response and a chronic stress scheme that acts along the hypothalamic-pituitary-interrenal axis (Wendelaar Bonga, 1997). It is presumed that elasmobranchs use the catecholamine and corticosteroid endocrine responses, although the stress response is not as well defined in this taxon. In elasmobranchs, chromaffin tissue, distributed in bundles along the kidney (Gelsleichter and Evans, 2012) excretes both E and NE (Reid et al., 1998). The interrenal gland (analogous to the adrenal gland in tetrapods) is the primary source of corticosteroids in elasmobranchs and is composed of compact adrenal tissue that is separate from, although closely associated with, the kidneys (Butler, 1973).

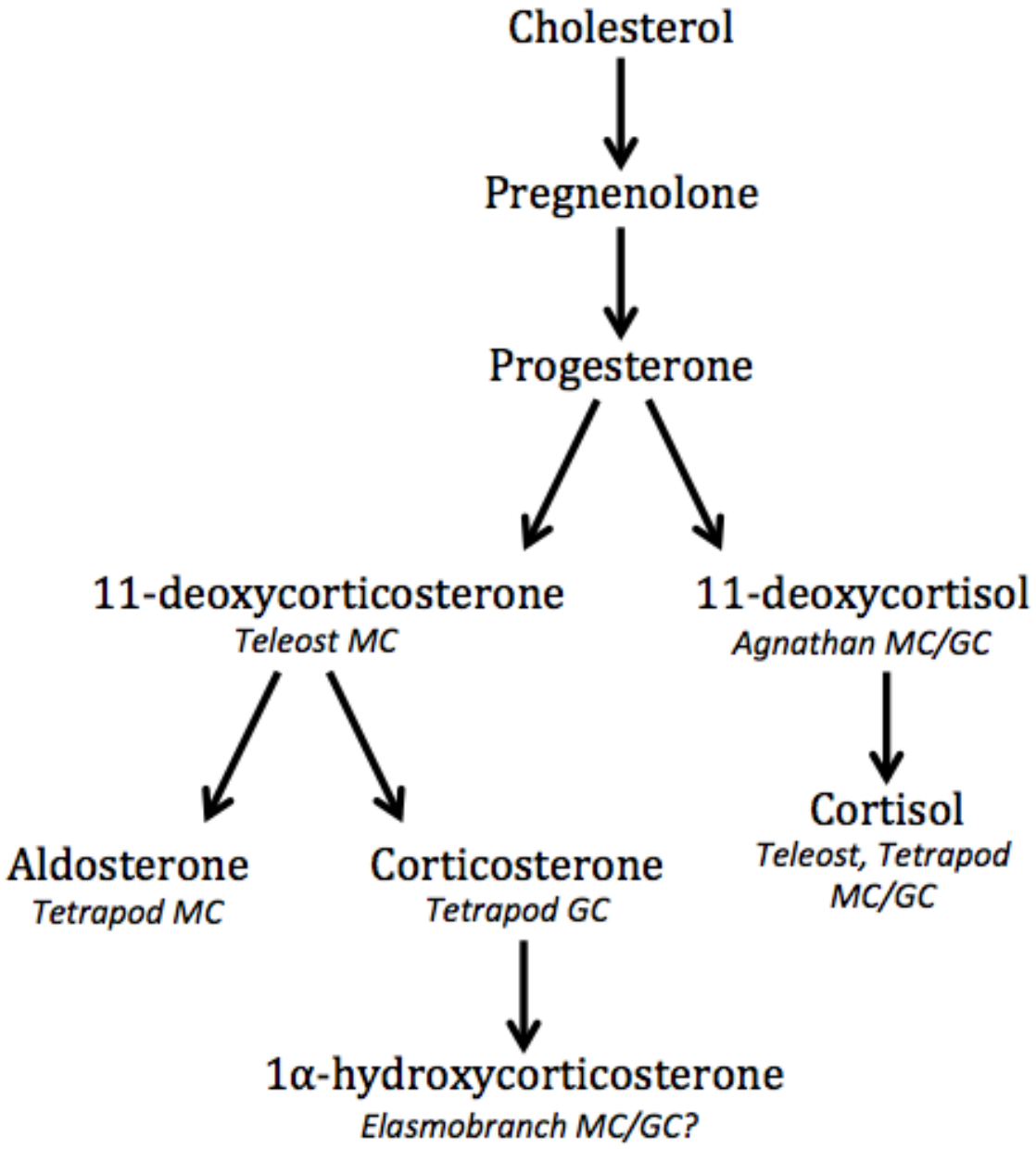


Figure 1.2. Basic pattern of biochemical synthesis of major mineralocorticoids (MCs) and glucocorticoids (GCs) and supposed corticosteroids in vertebrates.

1.4. Corticosteroids in Elasmobranchs

There are two types of responses to corticosteroids in vertebrates: mineralocorticoids (MCs), which act through mineralocorticoid receptors (MRs) to regulate mineral balance, and glucocorticoids (GCs), which act through glucocorticoid receptors (GRs) to regulate metabolite balance, primarily glucose. Cortisol (F) and corticosterone (B) are the major GCs in tetrapods (Bury and Sturm, 2007; Romero and Butler, 2007) and are derivatives of 11-deoxycortisol and 11-deoxycorticosterone (DOC), respectively. Early studies predicted that aldosterone and B were the major elasmobranch corticosteroids because treatment with mammalian ACTH increased the plasma concentrations of these steroids (Bern et al., 1962). However, subsequent research demonstrated that elasmobranchs have a distinct corticosteroid, 1α-hydroxycorticosterone (1α-OHB) (Idler and Truscott, 1966), which is hypothesized to dually act as a MC and GC (Evans et al., 2010). Following its initial discovery, administration of 1α-OHB in mice resulted in an increase in plasma sodium in adrenalectomized mice (Idler et al., 1967) and an increase in sodium movement across the toad bladder (Grimm et al., 1969), indicating a potential MC role. When placed in a hyposaline environment, *S. canicula* experienced an increase in circulating levels of 1α-OHB, which was thought to cause an increase in plasma osmolyte retention (Hazon and Henderson, 1984). Armour, et al. (1993) further elucidated the effect of 1α-OHB on osmoregulation by feeding *S. canicula* a low protein diet, thus reducing the dogfishes' capacity to produce urea through a reduction in dietary nitrogen. Subsequently, circulating levels of 1α-OHB increased and corresponded with an increase in plasma sodium compared to controls that were fed a normal protein diet (Armour et al., 1993). Thus, evidence to date suggests an MC role for 1α-OHB in elasmobranchs.

Conversely, the role of 1α-OHB in the GC response of elasmobranchs has not been thoroughly described and is largely based on indirect evidence. Early studies suggest that mammalian ACTH increases plasma glucose concentrations in *S. suckleyi*, possibly through the action of 1α-OHB (deRoos and deRoos, 1973). Although, four species of interenalectomized skates did not show a change in plasma glucose following the procedure, but did exhibit a 65% decrease in hepatic glycogen compared to controls, indicating an effect on glycogenolysis (Hartman et al., 1944). However, attempts to replicate this procedure did not yield similar results (Idler et al., 1969). Using a sensitive reporter assay, 1α-OHB was found to activate the GR in *L. erinacea* at concentrations 200-fold greater than the MR; it was hypothesized that the increased

requirement of 1α-OHB for GR activation would be indicative of an increase in circulating levels of the steroid following exposure to a stressful event, yet this has not been empirically tested (Carroll et al., 2008). Most recently, plasma 1α-OHB was found to increase following surgical cannulation, handling, air exposure, and fasting in the Japanese banded houndshark, *Triakis scyllium* (Iki et al., 2020); as well as positively correlate with plasma glucose following air exposure in *S. canicula* (Ruiz-Jarabo et al., 2019).

The presumptive precursor to 1α-OHB, B (Anderson, 2012), has also been investigated for GC activity. Patent (1970) showed that an intramuscular injection of B over 10 days caused hyperglycemia in *S. acanthias* and increased hepatic lipolysis, potentially for ß-oxidation of lipids or ketones. Circulating levels of B have also been shown to increase in response to gillnet capture in the bonnethead shark, *Sphyrna tiburo* (Manire et al., 2007); transport stress in the Cururu stingray, *Potamotrygon histrix* (Brinn et al., 2012); and following surgery, handling, air exposure, and fasting in *T. scyllium* (Iki et al., 2020). Interestingly, both B, and the presumed biosynthetic precursor of B, DOC, activate the GR with about 3- and 16-fold greater sensitivity than 1α-OHB, respectively (Carroll et al., 2008); thus, these corticosteroids merit examination into their roles as GC's in elasmobranchs.

1.5. Hormonal Control in Metabolite Balance

Catecholamines first stimulate glycogenolysis in vertebrates by activating glycogen phosphorylase (GP), predominately in the liver (Fischer et al., 1978). Glucose is rapidly liberated from hepatic glycogen into circulation to support extrahepatic function, but glycogenolysis also occurs within tissues that have endogenous glycogen stores. To date, it is unclear if elasmobranch GP is similarly activated by catecholamines (Fischer et al., 1978) or another mechanism of activation (Nathanson and Mariwalla, 1996). Intramuscular administration of E in *S. acanthias* (Patent, 1970) and intravascularly in *S. suckleyi* (deRoos and deRoos, 1978) caused hyperglycemia. Interestingly, both intravascular and intramuscular NE injections caused greater hyperglycemia in the *L. erinacea* that lasted longer than the same concentration of E (Grant et al., 1969); in contrast, hyperglycemia in *S. suckeyi* in response to NE was significantly blunted as compared to E (deRoos and deRoos, 1978). Despite the mechanism, these results suggest that catecholamines exert an effect on glucose mobilization. Additionally, catecholamines stimulate lipolysis from lipid stores (Guzmán and Geelen, 1993) in mammals, which can serve to supplement

oxidative metabolism or provide glycerol as a de novo gluconeogenic substrate. E and NE decreased hepatic fatty acid stores in the nurse shark, *Ginglymostoma cirratum* (Lipshaw et al., 1972), potentially for ketogenesis.

GCs effect glucose balance primarily through stimulation of gluconeogenesis to replenish catabolized glycogen lost following the catecholamine response (Romero and Beattie, 2022). Further, GCs in part increase plasma glucose by directing the internalization of insulin-sensitive GLUT transporters in extrahepatic tissues, which is a well-described response in mammals (Dimitriadis et al., 1997) and some teleosts (Capilla et al, 2002; Díaz et al., 2007), primarily GLUT4 in skeletal muscle and adipose tissue. GLUT4 internalization in skeletal muscle is part of a process that cycles GLUT4 protein between intracellular vesicles and the plasma membrane depending on factors such as cellular conditions or hormonal stimulation (Gould and Holman, 1993; Widnell, 1995). GLUT1, in a mammalian BHK cell line, also follows a similar cycling process under stress conditions such as heat shock (Widnell, 1995). However, there is conflicting evidence if GLUT1 is insulin-sensitive, which has been shown in mammals, although less efficiently as compared to GLUT4, (Gould and Holman, 1993). Indeed, *glut1* transcript abundance was effected by insulin in rainbow trout, *Oncorhynchus mykiss*, to a lesser extent than *glut4* transcript abundance; transcript abundance of both GLUTs also demonstrated changes in response to insulin growth factor-1, showing hormonal regulation of GLUTs in this species (Díaz et al. 2009). In *S. suckleyi*, transcript abundance of *glut4* in white muscle was shown to be insulin-sensitive (Deck et al., 2017b), and both *glut1* and *4* transcript abundance increased in white muscle following a glucose bolus, suggesting some stimulatory effect; still, it remains to be determined if corticosteroids effect this or other GLUT transporters in elasmobranchs.

Beyond corticosteroids, additional regulatory hormones play major roles in energy regulation. For example, insulin and glucagon antagonistically regulate plasma glucose and hepatic glycogen stores. Treatment with heterologous insulin caused a hypoglycemic effect in *S. suckleyi* (Deck et al., 2017b; deRoos and deRoos, 1979; deRoos et al., 1985), as well as homologous insulin in *S. canicula* (Anderson et al., 2002). In *S. suckleyi*, an intravascular glucose injection caused an increase in hepatic and white muscle glycogen, potentially due to insulin acting to increase transcript abundance of glucose transporters (Deck et al., 2017b). In contrast to insulin, glucagon is largely responsible for catabolizing hepatic and muscle glycogen for glycolysis in the absence of free plasma glucose. However, studies argue that intravascular glucagon injections in several

elasmobranch species caused a trivial hyperglycemic effect (Grant, 1964; Patent, 1970), and little change in glycogen stores (Patent, 1970). Furthermore, homologous glucagon did not change glucose uptake rates in perfused rectal glands of *S. suckleyi* in either fed or fasted treatments (Deck et al., 2017a), indicating that glucagon may serve a minor role in energy regulation.

In mammals, ketogenesis is largely regulated by insulin and glucagon ratios, and as previously mentioned, E. Insulin reduces lipolysis and increases malonyl-CoA production that allosterically inhibits mitochondrial fatty acid transport; glucagon promotes the opposite physiological effect (Laffel, 1999). Insulin does not appear to have the same effect on ketogenesis in elasmobranchs as an intravascular injection of homologous insulin in *S. canicula* (Anderson et al., 2002) and heterologous insulin in *S. suckleyi* (deRoos et al., 1985) did not significantly change plasma 3-HB. There are no studies that explore the effects of glucagon on ketones in elasmobranchs, although the IC_{50} of malonyl-CoA increases with prolonged fasting (more malonyl-CoA needed to inhibit mitochondria transport of fatty acids) as is found in mammals (Treberg et al., 2006), potentially as a hormonal signal to increase ketogenesis. It also remains unclear if corticosteroids serve a role in ketone balance. Patent (1970) showed a decrease in hepatic lipid content following 10 days of sequential intramuscular B injections, although the fate of these fatty acids is unknown. Further, stimulation with heterologous ACTH did not change plasma 3-HB concentrations in *S. suckleyi* (deRoos and deRoos, 1992), suggesting that ketone balance may not be controlled by the release of corticosteroids.

Little is known about ketone transport in elasmobranchs and mostly is inferred from mammalian physiology where ketones are transported by the MCT (monocarboxylate) transporter family, which also transports lactate (Halestrap, 2013; Halestrap and Price, 1999; Jackson and Halestrap, 1996). MCT1 and 2 have been located in the brain of the redspotted catshark, *Schroedericthys chilensis* (Balmaceda-Aguilera et al., 2012), and the rectal gland of *S. suckleyi* (Deck et al., 2016), and MCT4 has also been found in the brain of *S. chilensis* (Balmaceda-Aguilera et al., 2012). To date, there is no evidence of corticosteroid regulation of MCTs, although an increase in B in response to high frequency stimulation of the sciatic nerve is rats, *Rattus norvegicus*, was correlated with an increase in MCT1 and 2 neural expression (Huang et al., 2022). In teleosts, changes in *mct* transcript abundance was associated with changes in lactate transport following post-exhaustive exercise in *O. mykiss* (Omlin and Weber, 2013); and hypoxia in zebrafish, *Danio rerio* (Ngan and Wang, 2009); lactate uptake of MCT2 and 4 expressed in

Xenopus oocytes also decreased with cold-shock in *D. rerio* (Tseng et al., 2014). Finally, there was an increase in *mct1* and *2* transcript abundance in the rectal gland of *S. suckleyi* during an environmental hyposaline stress (Deck et al., 2016) and a decrease in MCT1 and 4 protein expression in the brain of *S. chilensis* during hypoxia (Balmaceda-Aguilera et al., 2012), showing a potential relationship between MCT expression and stress events, although again it remains unclear if this is an effect of ketone or lactate transport.

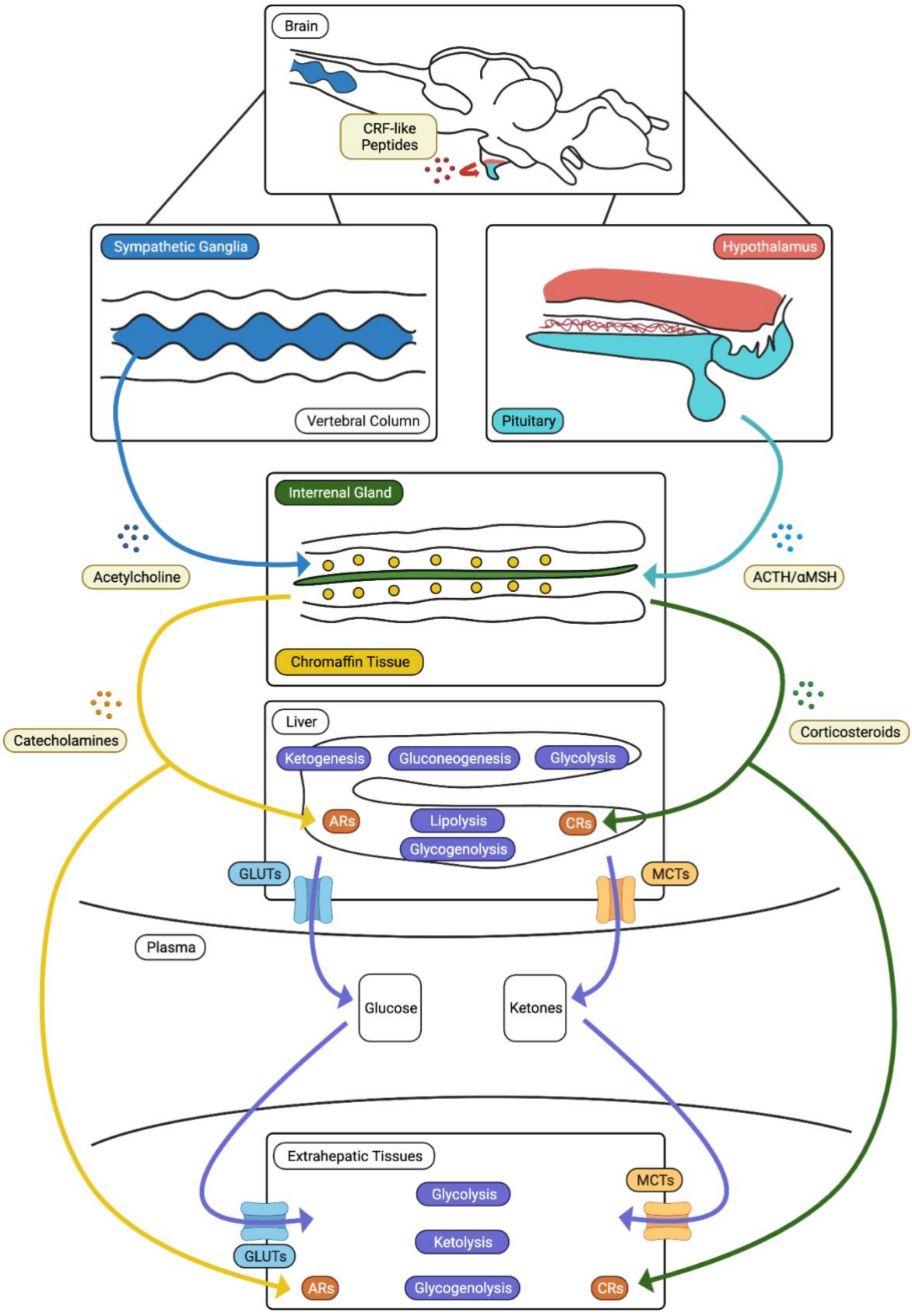

Brain
CRF-like Peptides
Sympathetic Ganglia
Vertebral Column
Hypothalamus
Pituitary
Interrenal Gland
Chromaffin Tissue
Acetylcholine
ACTH/αMSH
Catecholamines
Corticosteroids
Liver
Ketogenesis
Gluconeogenesis
Glycolysis
ARs
Lipolysis
CRs
Glycogenolysis
GLUTs
MCTs
Plasma
Glucose
Ketones
Extrahepatic Tissues
Glycolysis
Ketolysis
Glycogenolysis
MCTs
GLUTs
ARs
CRs

Figure 1.3. Overview of the putative endocrine and metabolic responses following exposure to a stressor in elasmobranchs. Dark blue arrow illustrates innervation of chromaffin tissue by sympathetic ganglia, red arrow illustrates release of hypothalamic hormones that stimulate pituitary hormone release, light blue arrows illustrate release of pituitary hormones that stimulate corticosteroid release from interrenal gland, yellow arrows illustrate release of catecholamines and binding with hepatic and extrahepatic adrenergic receptors, green arrows illustrate release of corticosteroids and binding with hepatic and extrahepatic corticosteroid receptors, and purple arrows hepatic efflux, release, and extrahepatic influx of glucose and ketones. Purple circles denote mechanisms associated with glucose and ketone metabolism. Blue transporters represent GLUT transporters, specifically GLUT1 and GLUT4 for the purpose of this thesis. Yellow transporters represent MCT transporters, specifically MCT1 and MCT2 for the purpose of this thesis. Abbreviations are as followed: CRF, corticosteroid releasing factor; ACTH, adrenocorticotropic hormone; αMSH, α-melanocyte-stimulating hormone; ARs, adrenergic receptors; CRs, corticosteroid receptors. Figure created using BioRender.

1.6. Objectives and Hypotheses

The objective of my thesis is to evaluate glucose and 3-HB production and consumption following stress in a representative elasmobranch species, *S. suckleyi*, as well as investigate hormonal control of these metabolites.

In Chapter 2 I take an *in vivo* approach and concurrently measure plasma metabolites (glucose and 3-HB) and corticosteroids (1α-OHB and B) following a series of stress events: surgical cannulation, handling, and air exposure. I test the hypotheses that 1) plasma metabolites and corticosteroids will change following stress and 2) plasma metabolites will correlate with corticosteroids. I predicted that circulating levels of metabolite and corticosteroids would increase following stress events, and that 1α-OHB would positively correlate with both glucose and 3-HB, thus supporting a GC role for 1α-OHB in this species.

In Chapter 3 I describe a liver perfusion for the first time in a shark species that was designed to measure changes in hepatic flux of metabolites (glucose and 3-HB) with and without hormonal stimulation. I test the hypotheses that 1) the perfusion will be viable as determined by hormones with known physiological effects (angiotensin II, insulin, and glucagon) and oxygen consumption and 2) I will be able to measure changes between inflowing and outflowing

metabolites in the isolated perfused preparation which may indicate changes in metabolite use by the liver. I predicted that this preparation would demonstrate oxygen consumption, vasoconstriction following angiotensin II stimulation, a decrease in outflowing glucose following glucagon stimulation, and an increase in outflowing glucose following insulin stimulation. Further, I predicted that the preparation would show hepatic production of both glucose and 3-HB.

In Chapter 4 I used the liver perfusion described in Chapter 3, as well as incorporating enzymatic and molecular techniques, to determine the effects of catecholamine (E) and corticosteroid (B and DOC) stimulation on hepatic metabolite balance (glucose and 3-HB). I test the hypotheses that 1) hormonal stimulation will change outflowing metabolite balance as compared to inflowing metabolite balance and 2) these changes will be reflected in appropriate enzyme activity (HEX, GP, 3-HBDH, SCOT, and PEPCK) and molecular transcript abundance (*glut1*, *glut4*, *mct1*, *mct2*, and *gr*). I predicted that B would decrease hepatic 3-HB production (negative correlation in Chapter 2) and E would increase hepatic glucose production and vasodilation. Further, these changes following B stimulation would reflect as a decrease in hepatic 3-HBDH activity and *mct* transcript abundance, and following E stimulation would reflect as an increase in GP activity and *glut* transcript abundance.

In Chapter 5 I employ a similar handling and air exposure stress to concurrently measure plasma metabolites (glucose and 3-HB) and corticosteroids (1α-OHB, B, and F), as well as enzyme activity (HEX, GP, 3-HBDH, SCOT, and PEPCK) and molecular transcript abundance (*glut1*, *glut4*, *mct1*, *mct2*, and *gr*) from the liver and four extrahepatic tissues (heart, white muscle, rectal gland, and brain). I test the hypotheses that 1) plasma metabolites and corticosteroids will change following stress and 2) these changes will be reflected in appropriate enzyme activity (HEX, GP, 3-HBDH, SCOT, and PEPCK) and molecular transcript abundance (*glut1*, *glut4*, *mct1*, *mct2*, and *gr*). I predicted that circulating levels of metabolites and corticosteroids will reflect the results of Chapter 2 (increase in all parameters following stress), which will be represented in an increase in hepatic GP and 3-HBDH activity and *glut* and *mct* transcript abundance. Further, I predict that extrahepatically that there will be an increase in endpoints associated with 3-HB catabolism but a decrease in endpoints associated with glucose catabolism in white muscle.

Finally, in Chapter 6 I synthesize the findings in this thesis, which demonstrates balance of the major metabolites (glucose and 3-HB) in elasmobranchs following stress from a whole organism to molecular level. This work is critical in understanding glucose and 3-HB utilization

in a more phylogenetically ancient vertebrate taxa, which seems to greatly differ to that of more derived vertebrates.

1.7. Works Cited

Anderson, P. M. (1990). Ketone Body and Phosphoenolpyruvate Formation by Isolated Hepatic Mitochondria From *Squalus acanthias* (Spiny Dogfish). *Journal of Experimental Biology* **254**.

Anderson, W. G. (2012). The endocrinology of 1α-hydroxycorticosterone in elasmobranch fish: A review. *Comparative Biochemistry and Physiology Part A: Molecular & Integrative Physiology* **162**, 73-80.

Anderson, W. G., Ali, M. F., Einarsdóttir, I. E., Schäffer, L., Hazon, N. and Conlon, J. M. (2002). Purification, Characterization, and Biological Activity of Insulins from the Spotted Dogfish, *Scyliorhinus canicula*, and the Hammerhead Shark, *Sphyrna lewini*. *General and Comparative Endocrinology* **126**, 113-122.

Armour, K. J., O'Toole, L. B. and Hazon, N. (1993). The effect of dietary protein restriction on the secretory dynamics of 1α-hydroxycorticosterone and urea in the dogfish, *Scyliorhinus canicula*: a possible role for 1α-hydroxycorticosterone in sodium retention. *Journal of Endocrinology* **138**, 275-282.

Ballantyne, J. S. (1997). Jaws: The Inside Story. The Metabolism of Elasmobranch Fishes. *Comparative Biochemistry and Physiology Part B: Biochemistry and Molecular Biology* **118B**, 703-742.

Balmaceda-Aguilera, C., Cortés-Campos, C., Cifuentes, M., Peruzzo, B., Mack, L., Tapia, J. C., Oyarce, K., García, M. A. and Nualart, F. (2012). Glucose Transporter 1 and Monocarboxylate Transporters 1, 2, and 4 Localization within the Glial Cells of Shark Blood-Brain-Barriers. *PloS One* **7**, e32409.

Bern, H. A., deRoos, C. C. and Biglieri, E. G. (1962). Aldosterone and Other Corticosteroids from Chondrichthyean Interrenal Glands. *Gen Comp Endocrinol* **2**, 490-494.

Brinn, R. P., Marcon, J. L., McComb, D. M., Gomes, L. C., Abreu, J. S. and Baldisseroto, B. (2012). Stress responses of the endemic freshwater cururu stingray (*Potamotrygon* cf. *histrix*) during transportation in the Amazon region of the Rio Negro. *Comparative Biochemistry and Physiology Part A: Molecular & Integrative Physiology* **162A**, 139-145.

Bury, N. and Sturm, A. (2007). Evolution of the corticosteroid receptor signalling pathway in fish. *General and Comparative Endocrinology* **153**, 47-56.

Butler, D. G. (1973). Structure and Function of the Adrenal Gland of Fishes. *American Zoologist* **13**, 839-879.

Cannon, W. B. (1915). Bodily changes in pain, hunger, fear, and rage, an account of recent researches into the function of emotional excitement. London and New York: D. Appleton and Co.

Capilla, E., Díaz, M., Gutiérrez, J. and Planas, J. V. (2002). Physiological regulation of the expression of a GLUT4 homolog in fish skeletal muscle. *American Journal of Physiology Endocrinology and Metabolism* **283**, E44-E49.

Carroll, S. M., Bridgham, J. T. and Thornton, J. W. (2008). Evolution of Hormone Signaling in Elasmobranchs by Exploitation of Promiscuous Receptors. *Molecular Biology and Evolution* **25**, 2643-2652.

Chamberlin, M. E. and Ballantyne, J. S. (1992). Glutamine Metabolism in Elasmobranch and Agnatahn Muscle. *Journal of Experimental Zoology* **264**, 267-272.

Chrousos, G. P. and Gold, P. W. (1992). The Concepts of Stress and Stress System Disorders: Overview of Physical and Behavioral Homeostasis. *The Journal of the American Medical Association* **267**, 1244-1252.

Conlon, J. M., Agoston, D. V. and Thim, L. (1985). An Elasmobranch Somatostatin: Primary Structure and Tissue Distribution in *Torpedo marmorata*. *General and Comparative Endocrinology* **60**.

Das, C. and Vijayan, M. M. (2023). Cortisol Rapidly Facilitates Glucocorticoid Receptor Translocation to the Plasma Membrane in Primary Trout Hepatocytes. *Biology* **12**, 311.

Deck, C. A., Anderson, W. G., Conlon, J. M. and Walsh, P. J. (2017a). The activity of the rectal gland of the North pacific spiny dogfish *Squalus suckleyi* is glucose dependent and stimulated by glucagon-like peptide-1. *Journal of Comparative Physiology B: Biochemical, Systematic, and Environmental Physiology* **187**, 1155-1161.

Deck, C. A., Anderson, W. G. and Walsh, P. J. (2017b). Effects of glucose and insulin administration on glucose transporter expression in the North Pacific spiny dogfish (*Squalus suckleyi*). *Gen Comp Endocrinol* **247**, 46-52.

Deck, C. A., Bockus, A. B., Seibel, B. A. and Walsh, P. J. (2016). Effects of short-term hyper- and hypo-osmotic exposure on the osmoregulatory strategy of unfed North Pacific spiny dogfish (*Squalus suckleyi*). *Comparative Biochemistry and Physiology Part A* **193**, 29-35.

deRoos, R. (1994). Plasma ketone, glucose, lactate, and alanine levels in the vascular supply to and from the brain of the spiny dogfish shark (Squalus acanthias). *Journal of Experimental Zoology* **268**, 354-363.

deRoos, R. and deRoos, C. C. (1973). Elevation of Plasma Glucose Levels by Mammalian ACTH in the Spiny Dogfish Shark (*Squalus acanthias*). *General and Comparative Endocrinology* **21**, 403-409.

deRoos, R. and deRoos, C. C. (1978). Elevation of Plasma Glucose Levels by catecholamines in Elasmobranch Fish. *General and Comparative Endocrinology* **34**, 447-452.

deRoos, R. and deRoos, C. C. (1979). Sever Insulin-Induced Hypoglycemia in the Spiny Dogfish Shark (*Squalus acanthias*). *General and Comparative Endocrinology* **37**, 186-191.

deRoos, R. and deRoos, C. C. (1992). Effects of Mammalian ACTH on Potential Fuels and Gluconeogenic Substrates in the Plasma of the Spiny Dogfish Shark (*Squalus acanthias*). *General and Comparative Endocrinology* **87**, 149-158.

deRoos, R., deRoos, C. C., Werner, C. S. and Werner, H. (1985). Plasma Levels of Glucose, Alanine, Lactate, and ß-Hydroxybutyrate in the Unfed Spiny Dogfish Shark (*Squalus acanthias*) after Surgery and following Mammalian Insulin Infusion. *General and Comparative Endocrinology* **58**, 28-43.

Dimitriadis, G., Leighton, B., Parry-Billings, M., Sasson, S., Young, M., Krause, U., Bevan, S., Piva, T., Wegener, G. and Newsholme, E. A. (1997). Effects of glucocorticoid excess on the sensitivity of glucose transport and metabolism to insulin in rat skeletal muscle. *Biochemical Journal* **321**.

Driedzec, W. R. (1978). Carbohydrate Metabolism in the Perfused Dogfish Heart. *Physiological Zoology* **51**, 42-50.

Driedzec, W. R. and de Almeida-Val, V. M. F. (1996). Enzymes of Cardiac Energy Metabolism in Amazonian Teleosts and the Fresh-Water Stingray (*Potomotrygon hystrix*). *Journal of Experimental Zoology* **274**, 327-333.

Driedzec, W. R. and Hart, T. (1984). Relationship bewteen exogenous fuel avaiability and performance by teleost and elasmobranch hearts. *Journal of Comparative Physiology B: Biochemical, Systematic, and Environmental Physiology* **154**, 593-599.

Driedzic, W. R. and Hart, T. (1984). Relationship bewteen exogenous fuel avaiability and performance by teleost and elasmobranch hearts. *Journal of Comparative Physiology B: Biochemical, Systematic, and Environmental Physiology* **154**, 593-599.

Díaz, M., Antonescu, C., Capilla, E., Klip, A. and Planas, J. (2007). Fish Glucose Transporter (GLUT)-4 Differs from Rat GLUT4 in Its Traffic Characteristics but Can Translocate to the Cell Surface in Response to Insulin in Skeletal Muscle Cells. *Endocrinology* **148**, 5248-5257.

Evans, A. N., Rimoldi, J. M., Gadepalli, R. S. V. S. and Nunez, S. (2010). Adaptation of a corticosterone ELISA to demonstrate sequence-specific effects of angiotensin II peptides and C-type natriuretic peptide on 1α-hydroxycorticosterone synthesis and steroidogenic mRNAs in the elasmobranch interrenal gland. *Journal of Steroid Biochemistry and Molecular Biology* **120**, 149-154.

Fischer, E. H., Alaba, J. O., Brautigan, D. L., Kerrick, W. G. L., Malencik, D. A., Moeschler, H. J., Picton, C. and Pocinwong, S. (1978). Evolutionary aspects of the structure and regulation of phosphorylase kinase. In *Versatility of Proteins*, (ed. C. H. Li), pp. 133-149. New York, New York: Academic Press.

French, R. P., Lyle, J., Tracey, S., Currie, S. and Semmens, J. M. (2015). High survivorship after catch-and-release fishing suggests physioloical resilience in the endothermic shortfun mako shark (*Isurus oxyrinchus*). *Conservation Physiology* **3**, cov044.

Gould, G. W. and Holman, G. D. (1993). The glucose transporter family: structure, function and tissue-specific expression. *Biochemical Journal* **295**, 329-341.

Grant, W. C. (1964). Effect of insulin and glucagon on blood glucose levels in the skate, *R. erinacea. American Zoologist* **4**, 325-326.

Grant, W. C., Hendler, F. J. and Banks, P. M. (1969). Studies on Blood-Sugar Regulation in the Little Skate *Raja erinacea*. *Physiological Zoology* **42**, 231-247.

Grimm, A. S., O'Halloran, M. J. and Idler, D. R. (1969). Stimulation of Sodium Transport Across the Isolated Toad Bladder by 1α-Hydroxycorticosterone from an Elasmbranch. *Journal of the Fisheries Research Board of Canada* **26**, 1823-1835.

Guzmán, M. and Geelen, M. J. H. (1993). Regulation of fatty acid oxidation in mammalian liver. *Biochimica et Biophysica Acta* **1167**, 227-241.

Halestrap, A. P. (2013). Monocarboxylic Acid Transport. *Comprehensive Physiology* **3**, 1611-1643.

Halestrap, A. P. and Price, N. T. (1999). The proton-linked monocarboxylate transporter (MCT) family: structure, fuction and regulation. *Biochemical Journal* **343**, 281-299.

Hartman, F. A., Lewis, L. A., Brownell, K. A., Angerer, C. A. and Shelden, F. F. (1944). Effect of Interrenalectomy on Some Blood Constituents in the Skate. *Physiological Zoology* **17**, 228-238.

Hazon, N. and Henderson, I. W. (1984). Secretory dynamics of 1a-hydroxycorticosterone in the elasmobranch fish, *Scyliorhimus canicula*. *Journal of Endocrinology* **103**, 205-211.

Hess, L. (2002). Corticosteroid synthesis and metabolism in birds. *Seminars in Avian and Exotic Pet Medicine* **11**, 65-70.

Huang, R., Han, S., Qiu, Y., Zhou, T., Wu, Y., Du, H., Xu, J. and Wei, X. (2022). Glucocorticoid regulation of lactate release from spinal astrocytes contributes to the induction of spinal LTP of C-fiber-evoked field potentials and the development of mechanical allodynia. *Neuropharmacology* **219**, 109253.

Idler, D. R., Freeman, H. C. and Truscott, B. (1967). Biological Activity and Protein-Binding of 1a-Hydroxycorticosterone: An Interrenal Steroid in Elasmbranch Fish. *General and Comparative Endocrinology* **9**, 207-213.

Idler, D. R., O'Halloran, M. J. and Horne, D. A. (1969). Interrenalectomy and hypophysectomy in relation to liver glycogen levels in the skate (Raja erinacea). *General and Comparative Endocrinology* **13**, 303-306.

Idler, D. R. and Truscott, B. (1966). 1a-hydroxycorticosterone from cartilagenous fish: a new adrenal steroid in blood. *Journal of the Fisheries Research Board of Canada* **23**, 615–619.

Iki, A., Anderson, G., Deck, C. A., Ogihara, M. H., Ikeba, K., Kataoka, H. and Hyodo, S. (2020). Measurement of 1a-hydroxycorticosterone in the Japanese banded houndshark, *Triakis scyllium*, following expsure to a series of stressors. *General and Comparative Endocrinology* **292**, 113440.

Jackson, V. N. and Halestrap, A. P. (1996). The Kinetics, Substrate, and Inhibitor Specificity of the Monocarboxylate (Lactate) Transporter of Rat Liver Cells Determined Using the Fluorescent Intracellular pH Indicator, 2',7'-Bis(carboxyethyl)-5(6)-carboxyfluorescein*. *The Journal of Biological Chemistry* **271**, 861-868.

Kajimura, M., Walsh, P. J., Mommsen, T. P. and Wood, C. M. (2006). The Dogfish Shark (*Squalus acanthias*) Increases both Hepatic and Extrahepatic Ornithine Urea Cycle Enzyme Activities for Nitrogen Conservation after Feeding. *Physiology and Biochemical Zoology* **79**, 602-613.

Kawauchi, H., Suzuki, K., Yamazaki, T., Moriyama, S., Nozaki, M., Yamaguchi, K., Takahashi, A., Youson, J. and Sower, S. (2002). Identification of Growth Hormone in the Sea Lamprey, an Extant Representative of a Group of the Most Ancient Vertebrates. *Endocrinology* **143**, 4916-4921.

Kerner, J. and Hoppel, C. (2000). Fatty acid import into mitochondria. *Biochimica et Biophysica Acta* **1486**, 1-17.

Krebs, H. A., Bennett, A. H., de Gasquet, P., Gascoyne, T. and Yoshida, T. (1963). Renal Gluconeogenesis: The Effect of Diet on the Gluconeogenic Capacity of Rat-Kidney-Cortex Slices. *Biochemical Journal* **86**, 22-27.

Laffel, L. (1999). Ketone Bodies: a Review of Physiology, Pathophysiology and Application of Monitoring to Diabetes. *Diabetes/Metabolism Research and Review* **15**, 412-426.

Lambert, F. N., Treberg, J. R., Anderson, W. G., Brandt, C. and Evans, A. N. (2018). The physiological stress response of the Atlantic stingray (*Hypanus sabinus*) to aerial exposure. *Comparative Biochemistry and Phsiology, Part A* **219-220**, 38-43.

Leary, S. C., Ballantyne, J. S. and Leatherland, J. F. (1999). Evaluation of Thyroid Hormone Economy in Elasmobranch Fishes, With Measurements of Hepatic 5'-Monodeiodinase Activity in Wild Dogfish. *Journal of Experimental Biology* **284**, 492-499.

Leibson, L. and Plisetskaya, E. (1968). Effect of Insulin on Blood Sugar Level and Glycogen Content in Organs of Some Cyclostomes and Fish. *General and Comparative Endocrinology* **11**, 381-392.

Little, A. G., and Seebacher, F. (2014). The evolution of endothermy is explained by thyroid hormone-mediated responses to cold in early vertebrates. *Journal of Experimental Biology* **217**, 1642-1648.

Lipshaw, L. A., Patent, G. J. and P, F. P. (1972). Effects of Epinephrine and Norepinephrine on the Hepatic Lipids of the Nurse Shark, *Ginglymostoma cirratum*. *Hormone and Metabolic Research* **4**, 34-38.

Long, C. N. H. (1938). The Adrenal Cortex and Carbohydrate Metabolism. *Sigma Xi, The Scientific Research Society* **26**, 175-186.

Manire, C. A., Rasmussen, L. E. L., Maruska, K. P. and Tricas, T. C. (2007). Sex, seasonal, and stress-related variations in elasmobranch corticosterone concentrations. *Comparative Biochemistry and Physiology, Part A* **148**, 926-935.

Metcalf, V. J. and Gemmell, N. J. (2005). Fatty acid transport in cartilaginous fish: absence of albumin and possible utilization of lipoproteins. *Fish Physiology and Biochemistry* **31**, 55-64.

Mommsen, T. P. and Moon, T. W. (1987). The Metabolic Potential of Hepatocytes and Kidney Tissue in the Little Skate, *Raja erinacea*. *Journal of Experimental Zoology* **244**, 1-8.

Moyes, C. D., Buck, L. T. and Hochachka, P. W. (1990). Mitochondrial and peroxisomal fatty acid oxidation in elasmobranchs. *American Physiological Society* **258**, 756-762.

Moyes, C. D., Moon, T. W., and Ballantyne, J.S. (1986). Oxidation of Amino Acids, Krebs Cycle Intermediates, Fatty Acids and Ketone Bodies by *Raja erinacea* Liver Mitochondria. *Journal of Experimental Zoology* **237**, 119-128.

Nathanson, M. H. and Mariwalla, K. (1996). Characterization and function of ATP receptors on hepatocytes from the little skate *Raja erinacea*. *American Physiological Society* **270**, R561-R570.

Navarro, I., Leibush, B., Moon, T. W., Plisetskaya, E., Baños, N., Méndez, E., Planas, J. and Gutiérrez, J. (1999). Insulin, insulin-like grwoth factor-I (IGF0I) and glucagon: the evolution of their receptors. *Comparative Biochemistry and Physiology, Part B* **122**, 137-153.

Newsholme, E. A. and Start, C. (1973). Regulation in metabolism. London and New York: Wiley Interscience.

Ngan, A. K. and Wang, Y. S. (2009). Tissue-specific transcriptional regulation of monocarboxylate transporters (MCTs) during short-term hypoxia in zebrafish (*Danio rerio*). *Comparative Biochemistry and Physiology, Part B* **154**, 396-405.

Omlin, T. and Weber, J.-M. (2013). Exhausting exercise and tissue-specific expression of monocarboxylate transporters in rainbow trout. *American Journal of Physiology Regulatory, Integrative, and Comparative Physiology* **304**, R1036-R1043.

Pardridge, W. M. (1983). Brain Metabolism: A Perspective From the Blood-Brain Barrier. *American Physiological Society* **63**, 1481-1535.

Patent, G. J. (1970). Comparision of Some Hormonal Effects on Carbohydrate Metabolism in an Elasmobranch (*Squalus acanthias*) and a Holocephalan (*Hydrolagus colliei*). *General and Comparative Endocrinology* **14**, 215-242.

Polakof, S., Panserat, S., Soengas, J. L. and Moon, T. W. (2012). Glucose metabolism in fish: a review. *Journal of Comparative Physiology B* **182**, 1015-1045.

Reid, S. G., Bernier, N. J. and Perry, S. F. (1998). The adrenergic stress response in fish: control of catecholamine storage and release. *Comparative Biochemistry and Physiology, Part C* **120**, 1-27.

Richards, J. G., Heigenhauster, J. F. and Wood, C. M. (2003). Exercise and recovery metabolism in the pacific spiny dogfish (*Squalus acanthias*). *Journal of Comparative Physiology, Part B* **173**, 463-474.

Richter, E. A., Ruderman, N. B., Gavras, H., Belur, E. R. and Galbo, H. (1982). Muscle glycogenolysis during exercise: dual control by epinephrine and contractions. *American Journal of Physiology- Endocrinology and Metabolism* **242**, E25-E32.

Romero, L. M. and Beattie, U. K. (2022). Common myths of glucocorticoid function in ecology and conservation. *Journal of Experimental Zoology, Part A* **337**, 7-14.

Romero, M. L. and Butler, L. K. (2007). Endocrinology of Stress. *International Journal of Comparative Psychology* **20**, 89-95.

Ruiz-Jarabo, I., Berragán-Méndez, C., Jerez-Cepa, I., Fernández-Castro, M., Sobrino, I., Mancera, J. M. and Aerts, J. (2019). Plasma 1α-Hydroxycorticosterone as Biomarker for Acute Stress in Catsharks (*Scyliorhinus canucula*). *Frontiers in Physiology* **10**.

Smith, H. W. (1935). The Rentention and Physiological Role of Urea in the Elasmobranchii. *BIological Reviews* **11**, 49-82.

Speers-Roesch, B., Ip, Y. K. and Ballantyne, J. S. (2006). Metabolic organization of freswater, euryhaline, and marine elasmobranchs: implications for the evolution of energy metabolism in sharks and rays. *Journal of Experimental Biology* **209**, 2495-2508.

Speers-Roesch, B. and Treberg, J. R. (2010). The unusual energy metabolism of elasmobranch fishes. *Comparative Biochemistry and Physiology, Part A* **155**, 417-434.

Taylor, E. and Heyland, A. (2017). Evolution of thyroid hormone signaling in animals: Non-genomic and genomic modes of action. *Molecular and Cellular Endocrinology* **459**, 14-20.

Treberg, J. R., Crockett, E. L. and Driedzec, W. R. (2006). Activation of Liver Carnitine Palmitoyltransferase-1 and Mitchondrial Acetoacetyl-CoA Thiolase Is Associated with Elevated Ketone Body Levels in the Elasmobranch *Squalus acanthias*. *Physiological and Biochemical Zoology* **79**, 899-908.

Tseng, Y.-C., Liu, S.-T., Hu, M. Y., Chen, R.-D., Lee, J.-R. and Hwang, P.-P. (2014). Brain functioning under acute hypothermic stress supported by dynamic monocarboxylate utilization and transport in ectothermic fish. *Frontiers in Zoology* **11**, 53.

Van de Pol, I., Flik, G. and Gorissen, M. (2017). Comparative Physiology of Energy Metabolism: Fishing for Endocrine Signals in the Early Vertebrate Pool. *Frontiers in Endocrinology* **8**, 1-18.

Vijayan, M. M. and Moon, T. W. (1992). Acute Handling Stress Alters Hepatic Glycogen Metabolism in Food-Deprived Rainbow Trout (*Oncorhynchus mykiss*). *Canadian Journal of Fisheries and Aquatic Sciences* **49**, 2260-2266.

Vijayan, M. M. and Moon, T. W. (1994). The stress response and the plasma disappearance of corticosteroid and glucose in a marine teleost, the sea raven. *Canadian Journal of Zoology* **72**, 379-386.

Walsh, P. J., Kajimura, M., Mommsen, T. P. and Wood, C. M. (2006). Metabolic organization and effects of feeding on ezyme activities of the dogifsh shark (*Squalus acanthias*) rectal gland. *Journal of Experimental Biology* **209**, 2929-2938.

Wendelaar Bonga, S. E. (1997). The Stress Response in Fish. *Physiological Reviews* **77**, 591-625.

Widnell, C. C. (1995). Control of Glucose Transport by GLUT1: Regulated Secretion in an Unexpected Environment. *Bioscience Reports* **15**, 427-443.

Wood, C. M., Walsh, P. J., Kajimura, M., McClelland, G. B. and Chew, S. F. (2010). The influence of feeding and fasting on plasma metabolites in the dogfish shark (*Squalus acanthias*). *Comparative Biochemistry and Physiology, Part A* **155**, 435-444.

Wright, A. and Jones, I. C. (1955). Chromaffin Tissue in the Lizard Adrenal Gland. *Nature* **175**, 1001-1002.

Wurtman, R. J. and Axelrod, J. (1966). Control of Enzymatic Synthesis of Adrenaline in the Adrenal Medulla by Adrenal Cortical Steroids. *The Journal of Biological Chemistry* **241**, 2301-2305.

Zammit, V. A. and Newsholme, E. A. (1979). Activities of Enzymes of Fat and Ketone-Body Metabolism and Effects of Starvation on Blood Concentrations of Glucose and Fat Fuels in Teleost and Elasmobranch Fish. *Biochemical Journal* **184**, 313-322.

2. Chapter 2: Energy and corticosteroid mobilization following an induced stress response in an elasmobranch fish, the North Pacific spiny dogfish, *Squalus suckleyi*.

This manuscript has been published in the journal General and Comparative Endocrinology. As the lead author on the manuscript, I was responsible for the experimental design, data collection, analysis, writing of the initial manuscript, and synthesis of revisions. J.R. Treberg assisted with metabolite assays and revision of manuscript. C.J. Wheaton assisted with hormone assays and revision of manuscript. N.D. Mylniczenko assisted with revision of manuscript. W.G. Anderson assisted with experimental design, metabolite and hormones assays, and revision of manuscript.

Schoen, A.N., J.R. Treberg, C.J. Wheaton, N.D. Mylniczenko, W.G. Anderson. 2021. Energy and corticosteroid mobilization following an induced stress response in an elasmobranch fish, the North Pacific spiny dogfish (*Squalus acanthias suckleyi*). 310: 113799.

2.1. Abstract

The dominant corticosteroid in elasmobranchs, 1α-hydroxycorticosterone (1α-OHB), has a described role in mineral regulation but a presumptive role in energy balance. Energy demand in vertebrates following exposure to a stressor typically involves an immediate but transient release of glucocorticoids as a means of mobilizing available energy stores, usually in the form of glucose. Although a glucocorticoid role for 1α-OHB would be expected, direct glucocorticoid function of this steroid has yet to be reported in any elasmobranch. In addition, elasmobranchs also utilize the metabolite β-hydroxybutyrate (β-HB), which is thought to replace the role fatty acids play in most vertebrates as a predominant fuel source in extrahepatic tissues. To determine the mobilization of metabolites and corticosteroids during a stress event, North Pacific spiny dogfish, *Squalus suckleyi*, were cannulated and held in a darkened isolation box to recover (24-48hr) before being subjected to an acute air exposure or corticosterone (B) injection. Dogfish were then serially blood sampled at nine timepoints over 48h. Glucose, β-HB, 1α-OHB, B, as well as lactate, pH, and osmolality were quantified in plasma samples. All measured variables increased in control and treatment groups within 48 hours from the start of experimentation, and β-HB and 1α-OHB remained elevated for the duration of the experiment. There was no linear correlation between glucose and 1α-OHB, but there was a weak ($R^2 = 0.230$) although significant ($p = 0.001$), positive correlation between β-HB and 1α-OHB. Interestingly, there were also significant correlations between increasing circulating glucose and B ($R^2 = 0.349$; $p < 0.001$), and decreasing β-HB and B concentrations ($R^2 = 0.180$; $p = 0.008$). Our data suggest that following successive stressors of capture, surgery, and confinement, 1α-OHB was not correlated with circulating glucose, only weakly correlated with circulating β-HB concentrations ($R^2 = 0.230$; $p = 0.001$), and that B may also serve a role in energy mobilization in this species.

2.2. Introduction

The endocrine stress response is a well-established, and in most cases, accepted phenomenon across vertebrates. Corticosteroids in vertebrates are defined by the action elicited following release, typically in regulating energy and mineral balance. The primary glucocorticoid in vertebrates is lineage specific, with cortisol (F) and corticosterone (B) being the major glucocorticoids in tetrapods (Cockrem, 2013) and F being the dominant glucocorticoid in ray-finned fishes (Wendelaar Bonga, 1997; Barton, 2002; Gorissen and Flik 2016). The primary

circulating corticosteroid in chondrichthyans, 1α-hydroxycorticosterone (1α-OHB) (Idler and Truscott, 1966; Idler et al., 1967; Grimm et al., 1969; Hazon and Henderson, 1984, Armour et al., 1993), is thus far unique to this taxa and is the only vertebrate corticosteroid where a complete steroidogenic pathway has yet to be determined (Wiens et al., 2018). Further, while a role for 1α-OHB in mineral balance has been described (Armour et al., 1993) a direct role in regulating energy balance has yet to be demonstrated (Anderson, 2012).

Glucocorticoids are so named for their role in mobilization of metabolic fuels, typically in the form of glucose, which is a universal response in vertebrates following exposure to a stressful event (Krebs et al., 1963; Patent, 1970; Newsholme and Start, 1973; Pardridg,e 1983;Wendelaar Bonga, 1997). In elasmobranchs, circulating glucose concentrations have been shown to increase following exposure to a variety of stressors, (Hoffmayer and Parsons, 2001; Mandelman and Farrington, 2007; Cicia et al., 2012; Skomal and Mandelman, 2012; Guida et al., 2016; Bouyoucos et al., 2018; Lambert et al., 2018). However, much of the evidence supporting a direct glucocorticoid function for 1α-OHB is correlative and equivocal (for review see: Anderson, 2012). Recently, a positive correlation between circulating levels of 1α-OHB and glucose was suggested in the air-exposed European catshark, *Scyliorhinus canicula* (Ruiz-Jarabo et al., 2019), providing potential evidence of a glucocorticoid role for 1α-OHB in elasmobranchs.

Assigning the classic vertebrate glucocorticoid definition to 1α-OHB in elasmobranchs may be complicated by the unusual metabolic strategy adopted by these fishes. In mammals, glucose and fatty acids are mobilized to fuel extrahepatic tissues, followed by ketone bodies (primarily β-hydroxybutyrate [β-HB]) to fuel brain function (Pardridge, 1983) during periods of starvation (Newsholme and Start, 1973; Rauch and Behrisch, 1980; Laffel, 1999). Similarly, teleosts catabolize fatty acids (Vijayan and Moon, 1992), but have low activities of the enzymes necessary for β-HB production and catabolism, as well as low circulating levels of ketone bodies, which are consistent with little reliance on these as oxidative fuels (Zammit and Newsholme, 1979). It is currently understood that elasmobranchs are likely deficient in extrahepatic long-chain fatty acid oxidation (Crabtree and Newsholme, 1972; Newsholme and Start, 1973; Zammit and Newsholme, 1979; Moyes et al., 1990; Ballantyne, 1997; Speers-Roesch et al., 2006; Ballantyne, 2016) and lack fatty acid transport proteins such as albumin (Metcalf and Gemmell, 2005; Ballantyne, 2016), and thus may instead rely heavily on ketone bodies as an extrahepatic fuel source in both satiated and starved conditions (Zammit and Newsholme, 1979; Ballantyne, 1997).

High activities of β-HBDH (Zammit and Newsholme, 1979; Speers-Roesch et al., 2006; Walsh et al., 2006), as well as high rates of ketone body catabolism have been found in oxidative tissues of several elasmobranch species (Driedzic, 1978; Moyes et al., 1990; Chamberlin and Ballantyne, 1992). Therefore, given the important role ketone bodies play as a metabolic fuel in elasmobranchs, it is reasonable to assume that the release of these molecules may play a significant function in fueling recovery from a stressor.

To our knowledge, a single study has examined circulating levels of β-HB and glucose following exposure to an acute stressor in the Atlantic stingray, *Hypanus sabinus* (Lambert et al., 2018). Stingrays air-exposed for 30 minutes showed a predictable and transient increase in circulating levels of glucose following exposure. However, plasma β-HB was highly variable before, during, and after air exposure and thus no definitive conclusion could be made in relation to the role β-HB may have played in fueling recovery from the stress event (Lambert et al., 2018). Additionally, under a chronic stress of starvation, plasma concentrations of β-HB in the North Pacific spiny dogfish, *Squalus suckleyi*, increased following 15 days of food deprivation, while plasma glucose remained constant (Wood et al., 2010), further suggesting that β-HB may be an important fuel source under at least some stressful conditions in this species.

In the present study we tested the hypothesis that 1α-OHB would act as a primary regulator of energy mobilization. We report, for the first-time, changing circulating levels of glucose, β-HB, 1α-OHB, and B under simulated stressors in a representative elasmobranch, the North Pacific spiny dogfish, *S. suckleyi*. We predicted that circulating levels of 1α-OHB would be positively correlated to circulating levels of both glucose and β-HB, thus supporting a glucocorticoid role for 1α-OHB in this species.

2.3. Methods

Animal Care

Male North Pacific spiny dogfish (1.50-2.64kg) were caught by rod and line in Barkley Sound, Vancouver Island, British Columbia, during July of 2018 and 2019. Fish were transferred to and housed in the Bamfield Marine Science Centre holding tank (155,000L) with flow-through seawater (12°C) and aeration, where they were fed North Pacific hake, *Merluccius productus, ad libitum* every other day. Fish were held for at least five days and fed two days prior to experimentation. Experiments were completed in accordance with the Canadian Council of

Animal Care standards, and with the approval of the Bamfield Marine Science Centre and University of Manitoba animal care committees.

Surgical Cannulations and Recovery

Fish were hand caught from the holding tank and placed in an immersion anesthetic ($0.2g \cdot L^{-1}$ tricaine methanesulfonate (MS-222), Syndel Labs, Vancouver, British Columbia, Canada). Body mass to the nearest gram was taken and fish were then placed ventral side up on a surgical V-board. A maintenance dose of anesthetic ($0.06g \cdot L^{-1}$ MS222) was then pumped across the gills through the oral cavity from a chilled recirculating anesthetic bath positioned below the fish. A 2mL pre-cannulation (PC) blood sample was taken from the caudal vessel with a heparinized 3mL ($100IU \cdot mL^{-1}$ ammonia heparin) syringe and 25-gauge needle. The PC timepoint was chosen based on previous work using the same cannulation methodology in this species (deRoos and deRoos, 1992). The caudal vessel was then cannulated using an 18-gauge Touhy needle and PE-50 cannula (Intramedic, Fisher Scientific). The cannula was fed into the dorsal aorta to approximately just anterior of the first dorsal fin (~15cm) (Deck et al., 2017). The cannula was flushed with heparinized elasmobranch Ringer's solution (257mM NaCl, 7mM Na_2SO_4, 3mM $MgSO_4$, 4mM KCl, 2mM $CaCl_2$ dihydrate, 0.1mM Na_2HPO_4 dibasic, 6mM $NaHCO_3$, 400mM urea, 80mM TMAO, 5mM glucose), secured to the caudal peduncle with three sterile sutures (KRUUSE, Silk Suture, 25mm), and sealed by melting the exposed end of the cannula. The fish was then placed in an individual blacked-out isolation box (33L) supplied with aerated flow-through seawater at ~12°C. The cannulation and isolation box paradigm has been established previously in teleosts to investigate hormone mobilization following a stress event (for review see: Gamperl et al., 1994). The entire procedure took less than 15 minutes to complete. A minimum of 24hr and maximum of 48hr recovery was provided prior to any further manipulation of the experimental animal. The duration of post-operative recovery was previously shown to not have a significant effect on plasma glucose concentrations between 24hr and 120hr in the spiny dogfish (deRoos and deRoos, 1973), and thus 24hr to 48hr was expected to be an acceptable recovery range.

Air Exposure and Corticosterone Loading

After 24hr or 48hr recovery, a 2mL time-0 blood sample was taken via the indwelling cannula following the blood sampling procedure outlined in deRoos and deRoos (1973). Fish then received one of three treatments (n = 6-8 per treatment): an injection of saline (control, 1mL saline.kg.fish^{-1}), 10min intermittent air exposure, or an intra-arterial administration of B (0.04μg·mL^{-1}·kg fish^{-1}) dissolved in dichloromethane (DCM)/saline (final concentration of DCM was 0.0017%). A B injection was chosen as an upstream biosynthetic proxy for 1α-OHB (Nunez and Trant, 1999), as to date, there is no reliable source of synthetic 1α-OHB. Air exposure was achieved by draining the blacked-out isolation box and starting a timer for 5min when the water level in the box was below the fish's gills. After 5min, water was reintroduced into the box and a timer was started for a 3min recovery when the water level in the box was above the fish's gills. The process was immediately repeated a second time for a total of 10min air exposure. The injected B concentration was determined as double the circulating levels of B in this species (Truscott and Idler, 1972). Two mL serial blood samples were taken at 30min, 1, 3, 6, 12, 24, and 48hr following treatment. Blood samples were immediately centrifuged for 3min at 13,000g at room temperature to separate plasma from cellular constituents. Plasma samples were decanted into a clean tube, pH was measured immediately, and the remainder of plasma was frozen and stored at -80°C for later analysis.

pH and Osmolality

Following centrifugation, pH was measured in 20μL of plasma (Fisher Scientific Accumet ® model AE 150) and osmolality (via vapor pressure) of each sample was measured using 10μL of plasma (Wescor Inc Vapro ®, model no. 5520).

Glucose, β-HB, and Lactate Assays

Plasma glucose concentrations were determined using an enzymatic hexokinase assay outlined in Treberg et al. (2007) and adapted for a 96-well plate. Plasma lactate concentrations were measured using an enzymatic lactate dehydrogenase assay outlined in Morrison et al. (2020). Plasma β-HB concentrations were measured using an enzymatic ß-HBDH assay. Briefly, reaction buffer was made with 0.1M glycine and 15mM NAD^+ (pH 9.5, room temperature). Samples were appropriately diluted and plated onto a 96-well plate in duplicate, and compared to a serial dilution of standards (β-HB). β-HBDH (0.43IU·mL^{-1}) was added to each well, except the control wells,

which had an equal volume of DI water. 200µL of reaction buffer was added to each well and the assay was immediately read spectrophotometrically at 340nm for 50min by measuring the conversion of NAD^+ to NADH. For all assays, an initial validation was conducted using a pool of 4-6 haphazardly chosen samples. A standard dilution, determined by the validation, was used to dilute all samples. However, if a sample fell below (negative control) or above (top standard) detection range of an assay, samples were appropriately rediluted and rerun. All metabolite concentrations were determined by subtracting the first recorded value (immediately following addition of respective enzymes) from the final recorded value (when the enzyme reaction was complete) and interpolating values from the assay specific standard curve. The time variation in adding enzyme to an assay across the 96-well plate was less than 30sec. All assays were run at room temperature and conducted using a plate reader (Power wave XS2, Biotek) with Gen5 software (Biotek, Winooski, VT, USA).

1α-OHB and B Assays

Samples were extracted using one part plasma and 1.5 parts 100% ice-cold acetonitrile, vortexed gently for 30sec to thoroughly mix the precipitate, and centrifuged at 5°C, 8000 RPM, for 20min (Eppendorf 5804 R centrifuge with 30x2mL conical centrifuge tube rotor, model #FA-45-30-11 with aerosol-tight lid). The supernatants were decanted and evaporated at 35°C and 200mBar for one hour to remove the acetonitrile, and then reduced to 50mBar for two hours to remove the water phase. All samples were reconstituted in 200µL Enzyme Linked Immunosorbent assay (ELISA) buffer. Plasma 1α-OHB concentrations were determined using the methods outlined in Wheaton et al. (2018) with 1α-OHB standards provided by CJW. Ten µL of the remaining sample was diluted for B analysis by an in-house B ELISA (Wheaton et al. 2018). The cross-reactivity of B standards on the 1α-OHB assay was 16.1% (Wheaton et al. 2018), and the 1α-OHB standards on the B assay was 15.1%. Other important cross-reactants in the assay which may be intermediates in the stress-axis pathway include 11-dehydrocorticosterone (166%) and cortisone (25%) (Wheaton et al. 2018). Absorbance was measured with an Emax Plus plate reader (test wavelength of 450nm and reference wavelength of 650nm) with SoftMax Pro software (version 6.4.2, Molecular Devices LLC). Extraction efficiencies, determined by comparing a set of corticosteroid-spiked acetonitrile blanks (spiked with respective standard, 1α-OHB = ~33.8ng·mL^{-1}, B = ~5.9ng·mL^{-1}) that underwent the extraction process with neat standard (same

concentrations), of 1α-OHB and B were 60.9% and 54.6%, respectively. 1α-OHB intra- and inter-assay variations were 8.3% and 8.0% (n = 15 assays), respectively, and B intra- and inter-assay variations were 8.6% and 6.4% (n= 14 assays), respectively. All chemicals were purchased from Sigma Aldrich unless otherwise noted.

Statistical Analysis

All data sets (glucose, β-HB, lactate, pH, osmolality, 1α-OHB, and B) were subject to Grubb's outlier tests (α = 0.05). All data points from an individual fish were removed from a treatment if there were four or more outliers (out of nine timepoints sampled) for that fish. No more than two fish were removed from any data set. Shapiro-Wilks and Levine's tests were used to assess normality and equal variance, respectively, of data sets. If these assumptions were not met, data sets were transformed using a rank transformation.

One-way ANOVAs with Tukey's HSD post-hoc tests ('glht' function in 'multcomp' package) (Hothorn et al. 2008) were used to determine the significance of treatments within individual time points. Linear mixed effects models ('lmer' function in 'lme4' package) (Bates et al. 2015) with Tukey's HSD post-hoc tests were used to determine the significance of each treatment over time, as compared to PC values. Fish identification was added to the model as a random effect, thus accounting for repeat sampling of each fish and non-independence (Zeger and Karim 1991).

Correlation plots were analyzed using Pearson Product-Moment Correlations. Data sets consisted of control and air exposure treatments combined, and were again subject to Grubb's outlier tests (α = 0.05). Two fish were considered outliers in the glucose, β-HB, and 1α-OHB parameters and were removed from respective correlation analyses (plots with outliers provided in Supplementary Material). All statistical analyses were performed in R (v3.5.2) and statistical significance was accepted at α = 0.05.

2.4. Results

Plasma glucose and β-HB were elevated at time-0, when compared to respective PC values, in all treatments. However, the increase in plasma glucose at time-0 in the air-exposed treatment, as well as plasma β-HB at time-0 in the control treatment, was not significantly different from respective PC values. Plasma glucose returned to levels similar to PC within 24hr in the B

treatment and 48hr in all other treatments (Figure 2.1A). Plasma β-HB returned to levels similar to PC within 48hr in the control treatment only (Figure 2.1B).

Plasma 1α-OHB was significantly elevated at all timepoints in respect to PC values ($p < 0.05$), and did not return to values similar to PC throughout the experiment (Figure 2.1C). Plasma B similarly was significantly elevated at time-0 ($p < 0.05$), and remained elevated in all treatments until 12h. As expected, plasma B was significantly elevated 30min following the B injection ($p < 0.05$), with respect to the control group at this timepoint (Figure 2.1D). There was a considerable amount of individual variation in metabolite and hormone concentrations, most notably at the PC compared to 0min timepoints indicating that many fish did not return to their PC values by the end of the surgical recovery period, or following continued confinement only (Figure S2.1).

There was a significant negative correlation between circulating plasma glucose and β-HB (Figure 2.2A; $p < 0.001$), as well as a significant positive correlation between circulating 1α-OHB and B (Figure 2.2B; $p < 0.001$). Additionally, there was no correlation between circulating plasma glucose and 1α-OHB (Figure 2.2C). There was a significant positive correlation between circulating plasma β-HB and 1α-OHB (Figure 2.2D; $p = 0.001$). Furthermore, there was a significant positive correlation between circulating plasma glucose and B (Figure 2.2E; $p < 0.001$), in addition to a significant negative correlation between circulating plasma β-HB and B (Figure 2.2F; $p = 0.008$).

Plasma lactate did not significantly differ from PC values at time-0 in air-exposed and control treatments, but was elevated at time-0 in the B treatment. There was a significant increase in plasma lactate in the air-exposed treatment at 30min ($p < 0.05$), respective to PC values. There was a significant difference from PC values in all treatments at 1hr ($p < 0.05$), although plasma lactate was significantly greater than PC values in the air exposed treatment and significantly less than PC values in the B and control treatments. Plasma lactate values were not significantly different from PC values within 3h in the air-exposed treatment, and all treatments demonstrated significantly less plasma lactate than PC values within 24hr ($p < 0.05$). Plasma lactate in the air-exposed treatment was significantly greater than control values at 30min and 1hr (Figure 2.3A; $p < 0.05$).

Plasma pH decreased at 30min in the air-exposed treatment. However, only the B treatment was significantly different from the respective PC values at 30min ($p < 0.05$). The air-exposed treatment was significantly less than control values at 30min ($p < 0.05$). The air-exposed and

control treatments remain consistent for the duration of the experiment, except for a significant increase in plasma pH in the control treatment at 24hr ($p < 0.05$), compared to PC values. Plasma pH also increased in the air-exposed treatment at 24hr, but this change was not significant. Plasma pH in the B treatment remained significantly elevated for the duration of the experiment ($p < 0.05$), except at 24hr, compared to PC values (Figure 2.3B).

Plasma osmolality was relatively stable over the duration of experimentation, and was only significantly less than the respective PC value in the air-exposed treatment at 12hr (Figure 2.3C; $p < 0.05$).

2.5. Discussion

The goal of this study was to determine if circulating concentrations of the primary corticosteroid, 1α-OHB, in an elasmobranch fish, *S. suckleyi*, were correlated to circulating levels of the primary energy metabolites, glucose and β-HB, following exposure to a stress event. To our knowledge, this is the first study to simultaneously measure changes in circulating levels of glucose, β-HB, and the presumptive glucocorticoid 1α-OHB in any elasmobranch species. Our data did not fully support our hypothesis that 1α-OHB is a primary regulator of energy mobilization following a series of repeated stressors in this species. Both plasma 1α-OHB and B significantly increased following the recovery period in air-exposed fish and were significantly correlated with one another. However, 1α-OHB exhibited a stronger response overall with plasma concentrations of 1α-OHB five to seven-fold greater than B. A similar result was recently reported in the air-exposed Japanese houndshark, *Triakis scyllia*, (Iki et al., 2020) where concomitant measurement of B confirmed that 1α-OHB was the major circulating corticosteroid following exposure to a stressful event in the houndshark (Iki et al., 2020). However, unlike dogfish in the present study, circulating levels of both steroids returned to baseline within 6hr post-air exposure in the houndshark. The differences in duration of response between species are unknown but it is important to note that the study conducted in the houndshark did not use isolation boxes but rather larger aquarium tanks post-stressor (Iki et al., 2020), thus the impact of confinement was likely much reduced in comparison to the present study.

Consideration of multiple stressors within our study design may help explain why circulating concentrations of both metabolites and steroids increased in all treatments following the recovery period in the isolation box. It is possible that the fish used in this study experienced

acute stressors during capture and surgical implantation of the cannula followed by the chronic stressor of confinement in the isolation box, as seen in numerous teleosts under the same experimental paradigm (Gamperl et al., 1994). Previous work has established that confinement stimulates the secondary stress response in spiny dogfish (Mandelman and Farrington, 2007) and *S. canicula*, (Torres et al., 1986), supporting the concept that confinement in the darkened box may have acted as a stressor prior to or concurrently with air exposure or B injection in the present study. Importantly, plasma glucose did not recover to PC values until 48hr in all treatments. This delay in recovery of glucose has been shown previously in this species (Patent, 1970) and the return of circulating glucose to PC values shows an ultimate recovery from the successive stress events, as expected during the vertebrate stress response.

The significant increase in plasma lactate alongside transient acidosis post-air exposure supports the presence of an anaerobic stress and is similar to previous studies utilizing such a stressor in elasmobranchs (Hoffmayer and Parsons, 2001; Cicia et al., 2012; Lambert et al., 2018). However, this stressor was not reflected by an increase in glucose and β-HB concentrations between time-0 and 30min, as might be expected in a classic acute vertebrate stress response involving glucocorticoids. Furthermore, changes in osmolality following a stress event in fish is often suggestive of a compromise in gill function between respiration and osmoregulation (Wood and Randall, 1973; Wendelaar Bonga, 1997). A significant reduction in plasma osmolality was only observed 12h post-treatment in the air-exposed fish relative to controls, indicating that treatments had a transient effect on solute and water balance.

Although not significant, plasma β-HB concentrations increased across all treatments following the initial recovery and remained elevated thereafter. There was considerable variation in plasma β-HB levels among fish (Zammit and Newsholme, 1979; Lambert et al., 2018), a characteristic in elasmobranchs that may be related to the fed or fasted status of the individual (Speers-Roesch and Treberg, 2010; Wood et al., 2010). While all fish used in this study were fasted for a minimum of two days prior to experimentation, we have no knowledge of their fed state prior to capture, which would likely lead to some variation in circulating levels of β-HB. A similar result was observed in the Atlantic stingray, where there was a highly variable but insignificant increase in plasma levels of β-HB following 30min of air exposure (Lambert et al., 2018). In contrast, the net flux of β-HB increased across electrically stimulated white muscle of spiny dogfish (Richards et al., 2003), suggesting that it may be used as a recovery fuel in this tissue during periods of

increased energy demand. Unlike plasma glucose levels, the increase in circulating β-HB was maintained throughout the course of the experiment, which may be a result of fasting, leading to preferential mobilization of β-HB over glucose in these fish as previously theorized (Zammit and Newsholme, 1979; Wood et al., 2010). This notion is further supported by the negative correlation between glucose and β-HB in this study and the European catshark (Gutiérrez et al., 1987).

While understanding that the interaction between cannulation, confinement, and treatment effects complicate interpretation of the results of mobilization of energy stores and steroids in the spiny dogfish, we were, for the first time, able to examine the relationship between 1α-OHB and both primary energy metabolites. Contrary to previous work (Ruiz-Jarabo et al., 2019) in the European catshark, we found no correlation between circulating plasma glucose and 1α-OHB over the time course of our experiment. Although plasma glucose predictably increased following the stress event, values remained within the normal range for this species (deRoos et al., 1985; Wood et al., 2010) and were not associated with increases in circulating 1α-OHB. However, there was a weak positive linear correlation between plasma β-HB and 1α-OHB suggesting that 1α-OHB may preferentially mobilize β-HB from hepatic stores during periods of energy demand.

Previous studies have demonstrated that glucose may not be sufficient in maintaining energy requirements of cardiac tissues during periods of increased energy demand, such as in hypoxia-exposed smooth dogfish, *Mustelus canis* (Driedzic, 1978) and glycolysis inhibited little skates, *Leucoraja erinacea* (Driedzic and Hart, 1984). Additionally, both plasma β-HB (Zammit and Newsholme, 1979; Walsh et al., 2006) and 1α-OHB (Iki et al., 2020) increase during fasting, suggesting that both may be more involved energetically during long-term stress. However, these measurements were determined along much different timelines than the current study (i.e., Zammit and Newsholme, 1979, 40-150 days fasted; Walsh et al., 2006, one week fasted; Iki et al., 2020, three weeks fasted), which likely serves a role in the magnitude of metabolite and corticosteroid mobilization (see Wood et al., 2010). Previously, it has been shown that plasma F increased during fasting in several teleost species (Pottinger and Brierley, 1997; Peterson and Small, 2004; Barcellos et al., 2010), although this has been linked to both hyper and hypoglycemic effects (Mommsen et al., 1999). Classically, teleosts and tetrapods will utilize fatty acids during long-term starvation (Newsholme and Start, 1973; Zammit and Newsholme, 1979; Speers-Roesch and Treberg, 2010), which is also in part corticosteroid-mediated (Jeanrenaud, 1967; Vijayan et al.,

1996; Laffel, 1999). Therefore, it can be postulated that 1α-OHB may have the same effect on plasma β-HB under similar conditions.

Unsurprisingly, there was a further, transient increase in plasma B following *in vivo* B administration. However, this was not reflected in a subsequent increase in 1α-OHB in this treatment. In previous studies B has been shown to increase during capture stress in bonnethead sharks, *Sphyrna tiburo* (Manire et al., 2007), as well as transport stress in Cururu stingrays, *Potamotrygon wallacei* (Brinn et al., 2012). It is unclear from these studies how much interference with 1α-OHB may have occurred in the assays, which has been consistently higher in elasmobranchs where both corticosteroids were measured (Anderson, 2012). Furthermore, a sensitive reporter assay showed that glucocorticoid receptors isolated from the little skate were activated by B at concentrations that were orders of magnitude lower than 1α-OHB (Carroll et al., 2008), and injections of B in spiny dogfish were previously shown to produce a hyperglycemic effect (Patent, 1970). Thus, B cannot be ruled out as having a potential role in energy balance, in addition to its assumed function as a biosynthetic precursor to 1α-OHB. Indeed, the positive correlation between plasma B and glucose in the present study may support this concept.

While we have observed positive correlations between 1α-OHB and B to β-HB and glucose, respectively, they are relatively weak, implying that additional hormonal factors may be involved in regulating circulating levels of these key metabolites in *S. suckleyi* and likely other elasmobranch fishes during repeated or chronic stress. Candidate hormones could include glucagon and insulin, which are important hormones in hepatic ketogenesis in mammals (Laffel, 1999) but have been minimally investigated in elasmobranchs (Anderson et al., 2002); and thyroid hormone, which has been shown to produce hyperglycemia in some teleosts but not others (Plisetskaya et al., 1983). It is likely that combinations of these hormones are important in regulating the unusual metabolic strategy in elasmobranch fishes.

2.6. Conclusion

In all vertebrates, the activation of the stress axis stimulates an almost immediate, but often transient release of glucocorticoids, which in turn are responsible for initial increases in energy mobilization. This study confirms an increase in key metabolites (glucose and β-HB) and corticosteroids (1α-OHB and B) following an acute (cannulation) and potentially chronic stressor (confinement) but it remains unclear which, if either, corticosteroid acts as a primary

glucocorticoid during the stress response in *S. suckleyi*. The arguably weak correlations between the metabolites and corticosteroids in this study suggest that other hormonal factors may be at play in regulating energy metabolism following exposure to repeated or chronic stressors in this species.

2.7. Acknowledgements

The authors would like to acknowledge the staff at Bamfield Marine Science Centre and Dr. Eric Clelland for their support of experiments, access to facilities, and care of fish; Dr. Shāna Lavin and Dr. Mandi Schook for support and use of the hormone lab at Disney's Animal Kingdom®; Emily Bach for assistance with hormone assays; and Dr. Jennifer Jeffrey for assistance with statistical analysis. We would also like the thank four anonymous reviewers and Dr. Andrea Morash for their constructive feedback, which significantly improved the quality of this manuscript. Funding for this work was provided by the University of Manitoba Faculty of Science Fieldwork support program, Natural Science and Engineering Research Council of Canada Discovery grant (05348-15) awarded to WGA, and Bamfield Marine Science Centre's Dick and Leona Peter Student Bursary awarded to ANS.

2.8. Figures

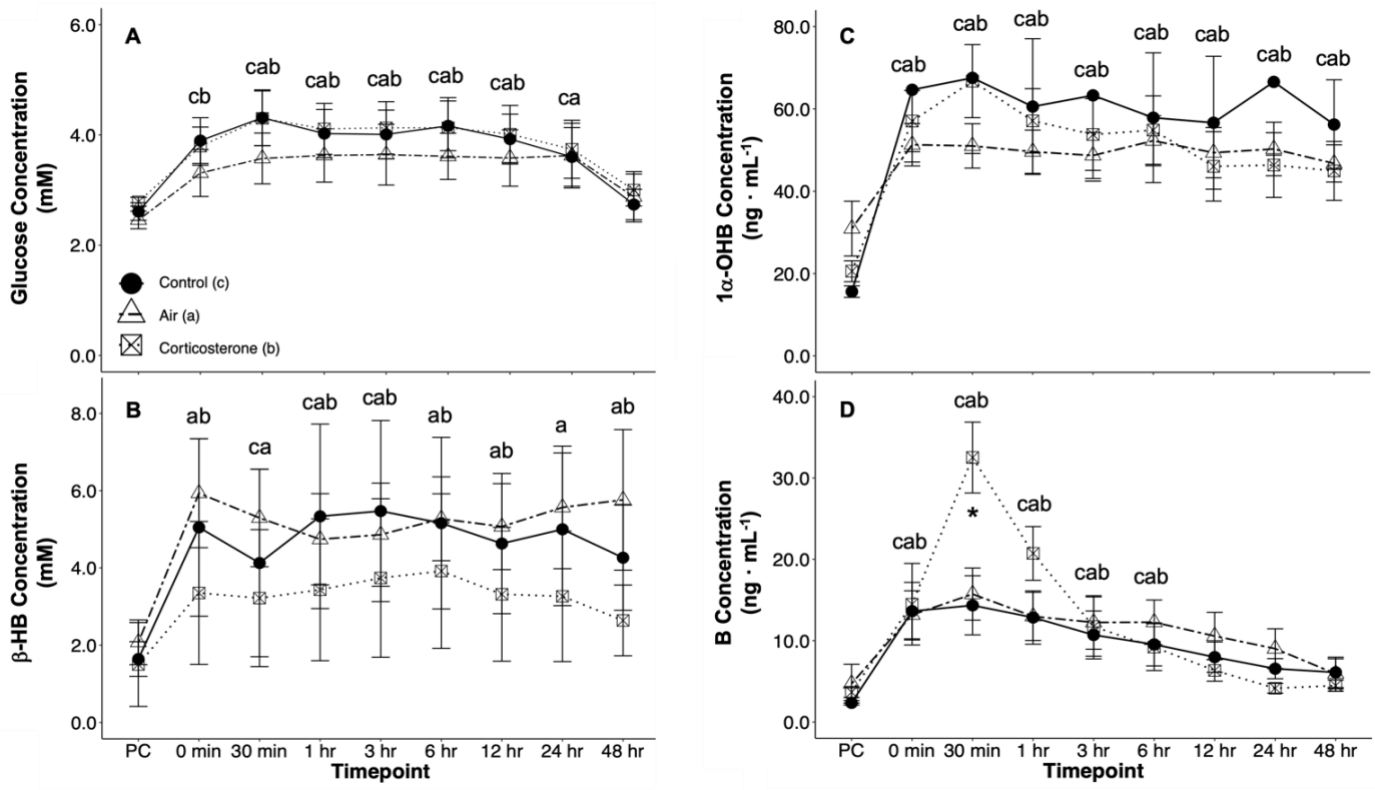


Figure 2.1. Changes in plasma metabolite and corticosteroid concentrations in *Squalus suckleyi* following control (c, closed circles and solid line), air-exposed (a, open triangles and dashed line), or B-injected (b, open squares and dotted line) treatments. Values are expressed as a mean +/- SEM. Letters indicate means that are significantly different ($p < 0.05$) from respective PC (pre-cannulation) values within each treatment. An asterisk (*) indicates means that are significantly different ($p < 0.05$) from control values at the same timepoint ($n = 6$-8). Time-0 min occurred 24 to 48 hours following cannulation.

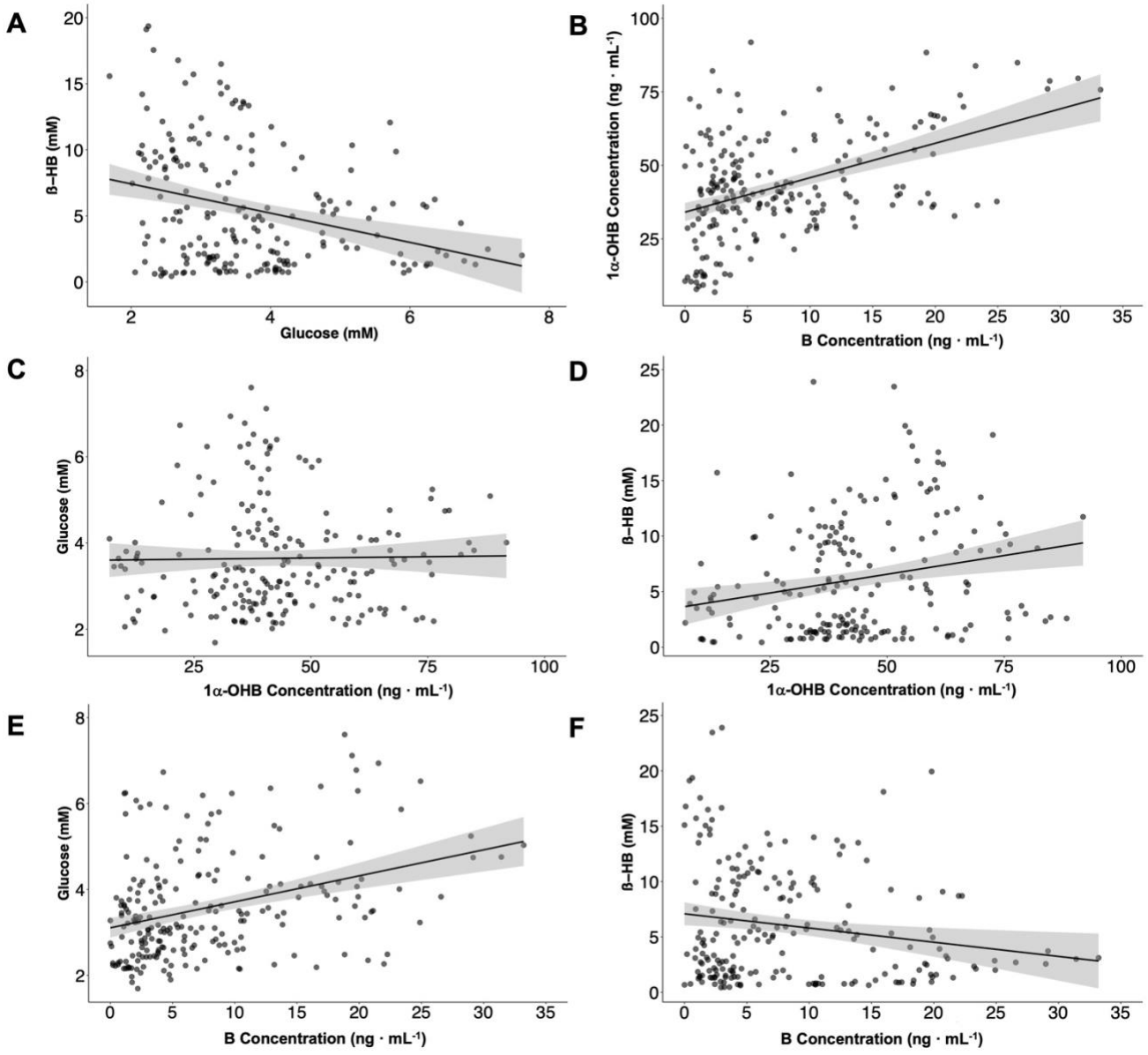


Figure 2.2. Correlations between metabolite and hormone concentrations during control and air-exposed treatments in *Squalus suckleyi*. A) β-HB (mM) and glucose (mM) concentrations (n = 203; R^2 = -0.296; p < 0.001). B) B (ng·mL^{-1}) and 1α-OHB (ng·mL^{-1}) concentrations (n = 212; R^2 = 0.466; p < 0.001). C) Glucose (mM) and 1α-OHB (ng.mL^{-1}) concentrations (n= 202; R^2 = 0.016; p= 0.818). D) β-HB (mM) and 1α-OHB (ng·mL^{-1}) concentrations (n = 203; R^2 = 0.230; p = 0.001). E) Glucose (mM) and B (ng·mL^{-1}) concentrations (n = 220; R^2 = 0.349; p < 0.001). F) β-HB (mM) and B (ng·mL^{-1}) concentrations (n = 212; R^2 = 0.180; p = 0.008).

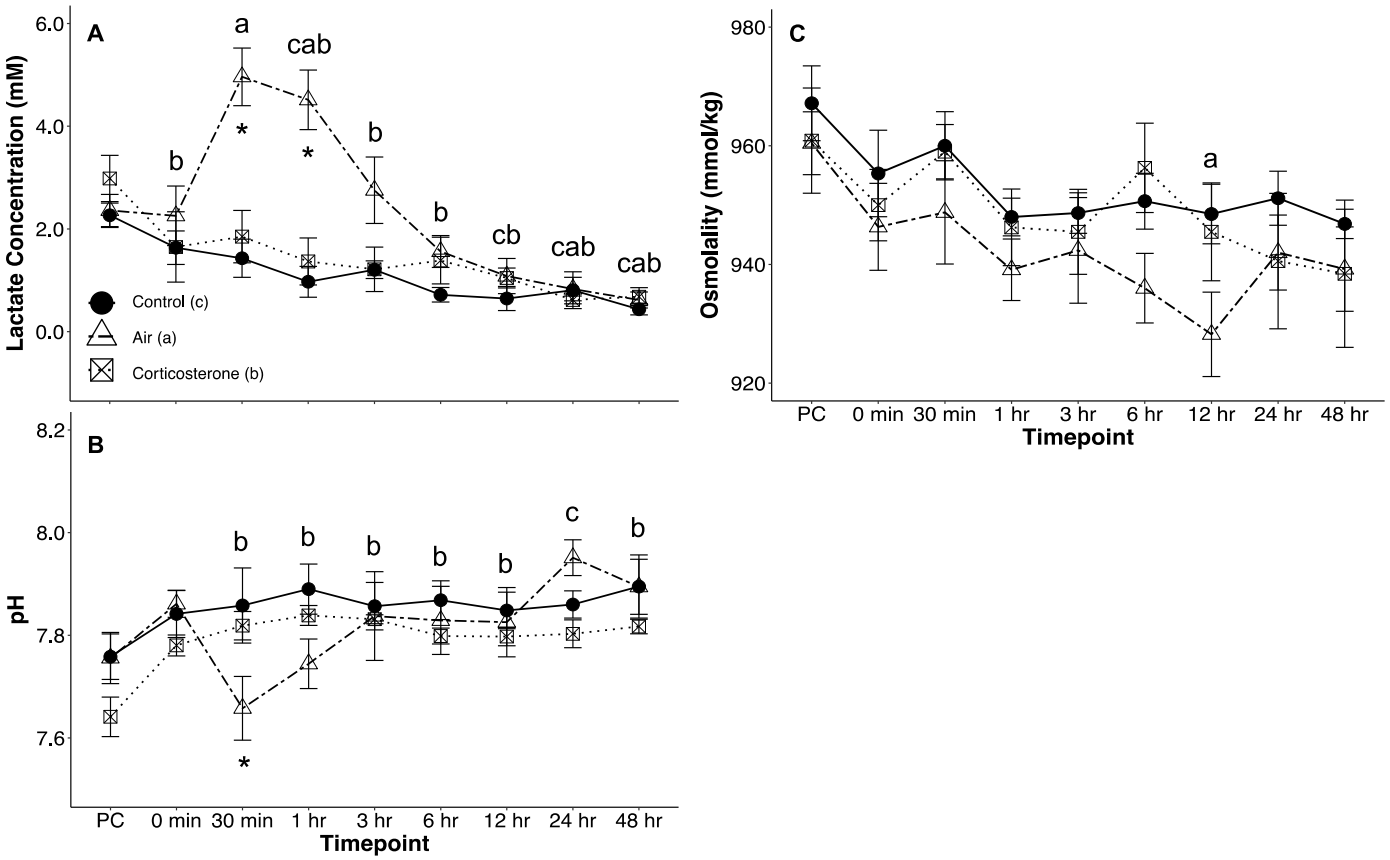


Figure 2.3. Changes in plasma lactate, pH, and osmolality in *Squalus suckleyi* at different times following control (c, closed circles and solid line), air-exposed (a, open triangles and dashed line), or B-injected (b, open squares and dotted line) treatments. Values are expressed as a mean +/- SEM. Letters indicate means that are significantly different ($p < 0.05$) from respective PC (pre-cannulation) values within each treatment. An asterisk (*) indicates means that are significantly different ($p < 0.05$) from control values at the same timepoint ($n = 6$-8).

2.9. Supplemental Figure

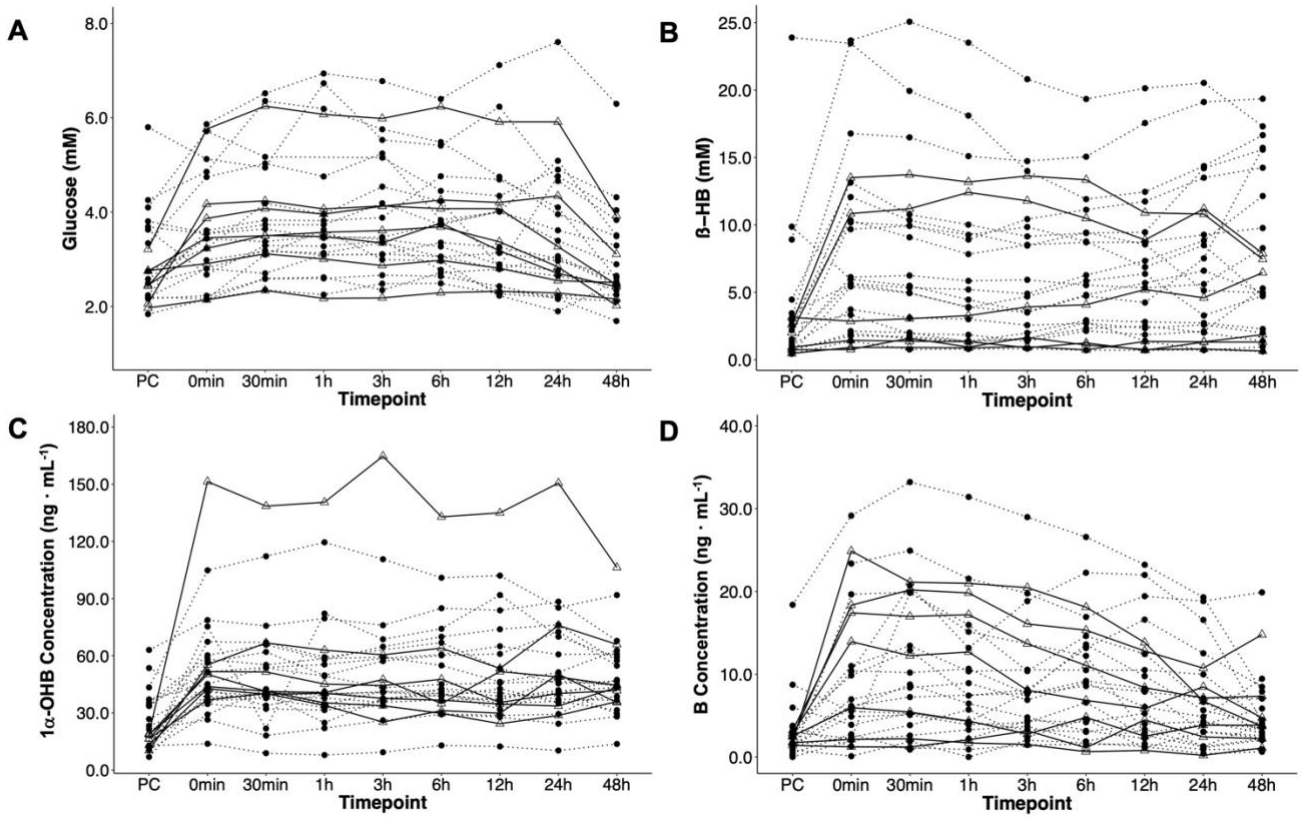


Figure S2.1. Individual serial sampling in control (solid line, open triangle) and air-exposed (dashed line, closed circle) *Squalus suckleyi*, including outliers. Fish were included if they contained all 9 timepoints. A) Glucose (mM) concentration (n = 24). B) β-HB (mM) concentration (n = 24). C) 1α-OHB ($ng \cdot mL^{-1}$) concentration (n = 25). D) Corticosterone ($ng \cdot mL^{-1}$) concentration (n = 25).

2.10. Works Cited

Anderson, W. G. (2012). The endocrinology of 1[alpha]-hydroxycorticosterone in elasmobranch fish: A review. *Comparative Biochemistry and Physiology Part A: Molecular & Integrative Physiology* **162**, 73-80.

Anderson, W. G., Ali, M. F., Einarsdóttir, I. E., Schäffer, L., Hazon, N. and Conlon, J. M. (2002). Purification, Characterization, and Biological Activity of Insulins from the Spotted Dogfish, *Scyliorhinus canicula*, and the Hammerhead Shark, *Sphyrna lewini*. *Gen Comp Endocrinol* **126**, 113-122.

Armour, K. J., O'Toole, L. B. and Hazon, N. (1993). The effect of dietary protein restriction on the secretory dynamics of 1a-hydroxycorticosterone and urea in the dogfish, *Scyliorhinus canicula*: a possible role for 1a-hydroxycorticosterone in sodium retention. *Journal of Endocrinology* **138**, 275-282.

Ballantyne, J. S. (1997). Jaws: The Inside Story. The Metabolism of Elasmobranch Fishes. *Comparative Biochemistry and Physiology Part B: Biochemistry and Molecular Biology* **118B**, 703-742.

Ballantyne, J. S. (2016). Metabolism of Elasmobrachs (Jaws II). London, San Diego, Waltham and Oxford: Academic Press.

Barcellos, L. J. G., Marqueze, A., Trapp, M., Quevedo, R. M. and Ferreira, D. (2010). The effects of fasting on cortisol, blood glucose and liver and muscle glycogen in adult jundiá *Rhamdia quelen*. *Aqauculture* **300**, 231-236.

Barton, B. A. (2002). Stress in Fishes: A Diversity of Responses with Particular Reference to Changes in Circulating Corticosteroids. *Integrative and Comparative Biology* **42**, 517-525.

Bates, D., Mächler, M., Bolker, B. M. and Walker, S. C. (2015). Fitting Linear Mixed-Effects Models Using lme4. *Journal of Statistical Software* **67**.

Bouyoucos, I. A., Weideli, O. C., Planes, S., Simpfendorfer, C. A. and Rummer, J. L. (2018). Dead tired: evaluating the physiological status and survival of neonatal reef sharks under stress. *Conservation Physiology* **6**.

Brinn, R. P., Marcon, J. L., McComb, D. M., Gomes, L. C., Abreu, J. S. and Baldisseroto, B. (2012). Stress responses of the endemic freshwater cururu stingray (*Potamotrygon* cf. *histrix*) during transportation in the Amazon region of the Rio Negro.

Comparative Biochemistry and Physiology Part A: Molecular & Integrative Physiology **162A**, 139-145.

Carroll, S. M., Bridgham, J. T. and Thornton, J. W. (2008). Evolution of Hormone Signaling in Elasmobranchs by Exploitation of Promiscuous Receptors. *Molecular Biology and Evolution* **25**, 2643-2652.

Chamberlin, M. E. and Ballantyne, J. S. (1992). Glutamine Metabolism in Elasmobranch and Agnathan Muscle. *Journal of Experimental Zoology* **264**, 267-272.

Cicia, A. M., Schlenker, L. S., Sulikowski, J. A. and Mandelman, J. (2012). Seasonal variations in the physiological stress response to discrete bouts of aerial exposure in the little skate, *Leucoraja erinacea*. *Comparative Biochemistry and Physiology Part A: Molecular & Integrative Physiology* **162**, 130-138.

Cockrem, J. F. (2013). Individual variation in glucocorticoid stress responses in animals. *Gen Comp Endocrinol* **181**, 45-58.

Crabtree, B. and Newsholme, E. A. (1972). The Activities of Lipases and Carnitine Palmitoyltransferase in Muscles from Vertebrates and Invertebrates. *Biochemical Journal* **130**, 697-705.

Deck, C. A., Anderson, W. G. and Walsh, P. J. (2017). Effects of glucose and insulin administration on glucose transporter expression in the North Pacific spiny dogfish (*Squalus suckleyi*). *Gen Comp Endocrinol* **247**, 46-52.

deRoos, R. and deRoos, C. C. (1973). Elevation of Plasma Glucose Levels by Mammalian ACTH in the Spiny Dogfish Shark (*Squalus acanthias*). *Gen Comp Endocrinol* **21**, 403-409.

deRoos, R., deRoos, C. C., Werner, C. S. and Werner, H. (1985). Plasma Levels of Glucose, Alanine, Lactate, and ß-Hydroxybutyrate in the Unfed Spiny Dogfish Shark (*Squalus acanthias*) after Surgery and following Mammalian Insulin Infusion. *Gen Comp Endocrinol* **58**, 28-43.

Driedzic, W. R. (1978). Carbohydrate Metabolism in the Perfused Dogfish Heart. *Physiological Zoology* **51**, 42-50.

Driedzic, W. R. and Hart, T. (1984). Relationship bewteen exogenous fuel avaiability and performance by teleost and elasmobranch hearts. *Journal of Comparative Physiology B: Biochemical, Systematic, and Environmental Physiology* **154**, 593-599.

Gamperl, A. K., Vijayan, M. M. and Boutilier, R. G. (1994). Epinephrine, norepinephrine, and cortisol concentrations in cannulated seawater-acclimated rainbow trout (*Oncorhynchus mykiss*) following black-box confinement and epinephrine injection. *Journal of Fish Biology* **45**, 313-324.

Gorissen, M. and Flik, G. (2016). The Endocrinology of the Stress Response in Fish: An Adaptation-Physiological View. In *Fish Physiology*, vol. 35 eds. C. B. Schreck L. Tort A. P. Farrell and C. J. Brauner), pp. 75-111.

Grimm, A. S., O'Halloran, M. J. and Idler, D. R. (1969). Stimulation of Sodium Transport Across the Isolated Toad Bladder by 1α-Hydroxycorticosterone from an Elasmbranch. *Journal of the Fisheries Research Board of Canada* **26**, 1823-1835.

Guida, L., Walker, T. I. and Reina, R. D. (2016). Temperature Insensitivity and Behavioural Reduction of the Physiological Stress Response to Longline Capture by the Gummy Shark, *Mustelus antarcticus*. *PloS One* **11**, e0148829.

Gutiérrez, J., Fernández, J. and Planas, J. (1987). Seasonal Variations of Insulin and Some Metabolites in Dogfish Plasma, *Scyliorhinus canicula*, L. *Gen Comp Endocrinol* **70**, 1-8.

Hazon, N. and Henderson, I. W. (1984). Secretory dynamics of 1a-hydroxycorticosterone in the elasmobranch fish, *Scyliorhimus canicula*. *Journal of Endocrinology* **103**, 205-211.

Hoffmayer, E. R. and Parsons, G. R. (2001). The physiological response to capture and handling stress in the Atlantic sharpnose shark, *Rhizoprionodon terraenovae*. *Fish Physiology and Biochemistry* **25**, 277-285.

Hothorn, T., Bretz, F. and Westfall, P. (2008). Simultaneous Inference in General Parametric Models. *Biometrical Journal* **50**, 346-363.

Idler, D. R., Freeman, H. C. and Truscott, B. (1967). Biological Activity and Protein-Binding of 1a-Hydroxycorticosterone: An Interrenal Steroid in Elasmbranch Fish. *Gen Comp Endocrinol* **9**, 207-213.

Idler, D. R. and Truscott, B. (1966). 1a-hydroxycorticosterone from cartilagenous fish: a new adrenal steroid in blood. *Journal of the Fisheries Research Board of Canada* **23**, 615–619.

Iki, A., Anderson, G., Deck, C. A., Ogihara, M. H., Ikeba, K., Kataoka, H. and Hyodo, S. (2020). Measurement of 1a-hydroxycorticosterone in the Japanese banded houndshark, *Triakis scyllium*, following expsure to a series of stressors. *Gen Comp Endocrinol* **In Review**.

Jeanrenaud, B. (1967). Effect of Glucocorticoid Hormones on Fatty Acid Mobilization and Re-esterification in Rat Adipose Tissue. *Biochemical Journal* **103**, 627-633.

Krebs, H. A., Bennett, A. H., de Gasquet, P., Gascoyne, T. and Yoshida, T. (1963). Renal Gluconeogenesis: The Effect of Diet on the Gluconeogenic Capacity of Rat-Kidney-Cortex Slices. *Biochemical Journal* **86**, 22-27.

Laffel, L. (1999). Ketone Bodies: a Review of Physiology, Pathophysiology and Application of Monitoring to Diabetes. *Diabetes/Metabolism Research and Review* **15**, 412-426.

Lambert, F. N., Treberg, J. R., Anderson, W. G., Brandt, C. and Evans, A. N. (2018). The physiological stress response of the Atlantic stingray (*Hypanus sabinus*) to aerial exposure. *In Review*.

Mandelman, J. and Farrington, M. A. (2007). The physiological status and mortality associated with otter-trawl capture, transport, and captivity of an exploited elasmobranch, *Squalus acanthias*. *ICES Journal of Marine Science* **64**, 122-130.

Manire, C. A., Rasmussen, L. E. L., Maruska, K. P. and Tricas, T. C. (2007). Sex, seasonal, and stress-related variations in elasmobranch corticosterone concentrations. *Comparative Biochemistry and Physiology Part A: Molecular & Integrative Physiology* **148**, 926-935.

Mommsen, T. P., Vijayan, M. M. and Moon, T. W. (1999). Cortisol in teleosts: dynamics, mechanisms of action, and metabolic regulation. *Reviews in Fish Biology and Fisheries* **9**, 211-268.

Moyes, C. D., Buck, L. T. and Hochachka, P. W. (1990). Mitochondrial and peroxisomal fatty acid oxidation in elasmobranchs. *American Physiological Society* **258**, 756-762.

Newsholme, E. A. and Start, C. (1973). Regulation in metabolism. London and New York: Wiley Interscience.

Pardridge, W. M. (1983). Brain Metabolism: A Perspective From the Blood-Brain Barrier. *American Physiological Society* **63**, 1481-1535.

Patent, G. J. (1970). Comparision of Some Hormonal Effects on Carbohydrate Metabolism in an Elasmobranch (*Squalus acanthias*) and a Holocephalan (*Hydrolagus colliei*). *Gen Comp Endocrinol* **14**, 215-242.

Peterson, B. C. and Small, B. C. (2004). Effects of fasting on circulating IGF-binding proteins, glucose, and cortisol in channel catfish (*Ictalurus punctatus*). *Domestic Animal Endocrinology* **26**, 231-240.

Plisetskaya, E., Woo, N. Y. S. and Murat, J.-C. (1983). Thyroid hormones in cyclostomes and fish and their role in regulation of intermediary metabolism. *Comparative Biochemistry and Physiology Part A: Molecular & Integrative Physiology* **74**, 179-187.

Pottinger, T. G. and Brierley, I. (1997). A putative cortisol receptor in the rainbow trout erythrocyte: stress prevents starvation-induced increased in specific binding of cortisol. *Journal of Experimental Biology* **200**, 2035-2043.

Rauch, J. C. and Behrisch, H. W. (1980). Ketone bodies: a source of energy during hibernation. *Canadian Journal of Zoology* **59**, 754-760.

Richards, J. G., Heigenhauster, J. F. and Wood, C. M. (2003). Exercise and recovery metabolism in the pacific spiny dogfish (*Squalus acanthias*). *Journal of Comparative Physiology B: Biochemical, Systematic, and Environmental Physiology* **173**, 463-474.

Ruiz-Jarabo, I., Berragán-Méndez, C., Jerez-Cepa, I., Fernández-Castro, M., Sobrino, I., Mancera, J. M. and Aerts, J. (2019). Plasma 1a-Hydroxycorticosterone as Biomarker for Acute Stress in Catsharks (*Scyliorhinus canucula*). *Frontiers in Physiology* **10**.

Skomal, G. and Mandelman, J. (2012). The physiological response to anthropogenic stressors in marine elasmbranch fishes: A review with a focus on the secondary response. *Comparative Biochemistry and Physiology Part A: Molecular & Integrative Physiology* **162**, 146-155.

Speers-Roesch, B., Ip, Y. K. and Ballantyne, J. S. (2006). Metabolic organization of freswater, euryhaline, and marine elasmobranchs: implications for the evolution of energy metabolism in sharks and rays. *Journal of Experimental Biology* **209**, 2495-2508.

Speers-Roesch, B. and Treberg, J. R. (2010). The unusual energy metabolism of elasmobranch fishes. *Comparative Biochemistry and Physiology Part A: Molecular & Integrative Physiology* **155**.

Torres, P., Tort, L., Planas, J. and Flos, R. (1986). Effects of confinement stress and additional zinc treatment on some blood parameters in the dogfish *Scyliorhinus canicula*. *Comparative Biochemistry and Physiology Part C: Pharmacology, Toxicology and Endocrinology* **83C**, 89-92.

Truscott, B. and Idler, D. R. (1972). Corticosteroids in Plasma of Elasmobranchs. *Comparative Biochemistry and Physiology Part A: Molecular & Integrative Physiology* **41**, 41-50.

Vijayan, M. M., Mommsen, T. P., Glémet, H. C. and Moon, T. W. (1996). Metabolic Effects of Cortisol Treatment in a Marine Teleost, the Sea Raven. *Journal of Experimental Biology* **199**, 1509-1514.

Vijayan, M. M. and Moon, T. W. (1992). Acute Handling Stress Alters Hepatic Glycogen Metabolism in Food-Deprived Rainbow Trout (*Oncorhynchus mykiss*). *Canadian Journal of Fisheries and Aquatic Sciences* **49**, 2260-2266.

Walsh, P. J., Kajimura, M., Mommsen, T. P. and Wood, C. M. (2006). Metabolic organization and effects of feeding on ezyme activities of the dogifsh shark (*Squalus acanthias*) rectal gland. *Journal of Experimental Biology* **209**, 2929-2938.

Wendelaar Bonga, S. E. (1997). The Stress Response in Fish. *Physiological Reviews* **77**, 591-625.

Wheaton, C. J., Mylniczenko, N. D., Rimoldi, J. M., Gadepalli, R. S. V. S., Hart, R., O'Hara, B. R. and Evans, A. N. (2018). Challenges, pitfalls and surprises: development and validation of a monoclonal antibody for enzyme immunoassay of the steroid 1a-hydroxycorticosterone in elasmobranch species. *Gen Comp Endocrinol* **265**, 83-89.

Wood, C. M. and Randall, D. J. (1973). The Influence of Swimming Activity on Sodium Balance in the Rainbow Trout (*Salmo gairdneri*). *Journal of Comparative Physiology* **82**, 207-233.

Wood, C. M., Walsh, P. J., Kajimura, M., McClelland, G. B. and Chew, S. F. (2010). The influence of feeding and fasting on plasma metabolites in the dogfish shark (*Squalus acanthias*). *Comparative Biochemistry and Physiology Part A: Molecular & Integrative Physiology* **155**, 435-444.

Zammit, V. A. and Newsholme, E. A. (1979). Activities of Enzymes of Fat and Ketone-Body Metabolism and Effects of Starvation on Blood Concentrations of Glucose and Fat Fuels in Teleost and Elasmobranch Fish. *Biochemical Journal* **184**, 313-322.

Zeger, S. L. and Karim, M. R. (1991). Generalized Linear Models With Random Effects; A Gibbs Sampling Approach. *Journal of American Statistical Association* **86**, 79-86.

3. Chapter 3: An adapted liver perfusion in a shark species, *Squalus suckleyi*: investigation of energy mobilization.

This manuscript has been published in the journal American Journal of Physiology: Regulatory, Integrative and Comparative Physiology. As the lead author on the manuscript, I was responsible for the experimental design, data collection, analysis, writing of the initial manuscript, and synthesis of revisions. J.R. Treberg assisted with metabolite assays and revision of manuscript. C.J. Wheaton assisted with hormone assays and revision of manuscript. N.D. Mylniczenko assisted with revision of manuscript. W.G. Anderson assisted with experimental design, metabolite and hormones assays, and revision of manuscript.

Schoen, A.N., A.N. Weinrauch, I.A. Bouyoucos, W.G. Anderson. 2023. An adapted liver perfusion in a shark species, *Squalus suckleyi*: investigation of energy mobilization. (Accepted, published online).

3.1. Abstract

The liver is an essential energy storage organ in all vertebrates thus far examined. In teleosts and elasmobranchs, previous studies examining hepatic energetics have used isolated hepatocytes. While these studies have been informative the high fat content in the elasmobranch liver limits isolation of hepatocytes and therefore the utility of this method to understand hepatic metabolic processes. In the present study we developed an *in situ* liver perfusion in the North Pacific spiny dogfish, *Squalus suckleyi*. Perfusions were conducted by cannulating the hepatic portal vein (inflowing cannulation) and the sinus venosus through the heart (outflowing cannulation). Changes in major elasmobranch metabolites (glucose and 3-hydroxybutarate [3-HB]) were determined by the arterial (inflow)-venous (outflow) difference in glucose and 3-HB concentrations. Liver preparations were considered viable due to consistent oxygen consumption over 3hrs and the maintenance of predictable vasoconstriction following administration of homologous 10^{-7}M angiotensin II. Removal and reintroduction of glucose and 3-HB from the perfusate showed endogenous 3-HB production in the isolated perfused livers but unaffected glucose balance. However, the arterial-venous difference of both glucose and 3-HB did not change following perfusion with insulin and glucagon, which may be due to the glucose intolerant nature of elasmobranchs. Ultimately, we show the viability of this perfusion for the investigation of hepatic metabolite mobilization in sharks.

3.2. Introduction

Metabolic processes in the liver are fundamental to whole-body energy balance in all vertebrates. Notably, the liver serves a role in carbohydrate and lipid metabolism, primarily as an energy reserve to fuel extrahepatic tissues (reviewed in Rui, 2014). In most vertebrates, glycogen is mobilized from the liver following hormonal stimulation, which can be dependent on the physiological condition of the organism (i.e., seasonality, feeding status, stress status, etc.). A classic method to understand hormonal control of hepatic energy balance is *in vivo* administration of stimulatory or inhibitory agents. For example, in rats, *Rattus sp.*, *in vivo* administration of the glucocorticoid, cortisol, led to an increase in hepatic glycogen deposition (Bellamy and Leonard, 1964; Bellamy et al., 1968), as well as protein catabolism (Bellamy and Leonard, 1964), inferring a correlation between glucocorticoids and gluconeogenesis to replenish depleted glycogen stores. Direct insight into hormonal control of metabolite balance in the liver has been made possible by

the isolation of hepatocytes (i.e., (Berry and Friend, 1969; Birnbaum et al., 1976; Danulat and Mommsen, 1990; Mommsen et al., 1987; Mommsen and Moon, 1987; Mommsen et al., 2001; Vijayan et al., 1993). The significant benefit of isolated hepatocytes is the direct contact of cells with incubation media containing nutrients, oxygen, and hormones. In elasmobranchs, several studies have used isolated hepatocytes from the little skate, *Leucoraja erinacea*, to assess metabolite uptake and oxidation (Ballatori and Boyer, 1988; Mommsen and Moon, 1987; Shuttleworth and Goldstein, 1984; Smith et al., 1987) and a single study has used isolated hepatocytes to investigate hormonal influence on urea production in *L. erinacea* (Mommsen and Moon, 1987).

Mommsen and Moon (1987) outlined CO_2 (oxidation), glucose (gluconeogenesis), and 3-hydroxybutyrate (3-HB) production (ketogenesis) with select oxidative substrates. Hepatocytes were concluded to be a major site of 3-HB synthesis to fuel extrahepatic tissues, which is thought to be a preferential energy metabolite over long-chain fatty acids extrahepatically in elasmobranchs (Speers-Roesch and Treberg, 2010; Zammit and Newsholme, 1979). Additionally, the authors demonstrated that teleost insulin and porcine glucagon significantly increased urea formation, possibly linked to an increase in amino acid metabolism. Of note in Mommsen and Moon (1987) is the suggestion that isolated hepatocytes from *L. erinacea* are only seasonally successful, with collections of hepatocytes from late summer being ineffective due to the high hepatic lipid content. This presents a problem in isolating hepatocytes from other elasmobranchs, as hepatic lipids can often vary in profile and concentration across species (Bakes and Nichols, 1995). For example, the elasmobranch Family *Squalidae* contains species that have liver oil contents ranging between 52-83% of total liver mass (Wetherbee and Nichols, 2000). Indeed, prior to the present study, we had many failed attempts of isolating hepatocytes from the North Pacific spiny dogfish, *Squalus suckleyi*, because of the high lipid content. A further problem with isolated hepatocytes in fish is a high rate of endogenous glucose production following isolation due to elevated glycogen levels as compared to mammals (Mommsen, 1986). Therefore, gluconeogenic rates may be overestimated in teleost, and presumably elasmobranch, hepatocytes (Deck et al., 2017b; Patent, 1970). Given these challenges, other methods of studying hormonal effects on hepatic tissue in elasmobranchs should be explored, such as whole-tissue perfusions, which may be more stable in terms of endogenous glycogenolysis (Mommsen, 1986).

Whole-tissue liver perfusions have been performed previously in *L. erinacea* to examine properties of bile secretion and composition (Ballatori et al., 1999; Reed et al., 1982; Simmons et al., 1991; Weisiger et al., 1984) and in the blue-spotted stingray, *Neotrygon kuhlii*, to compare liver morphology and function to that of teleosts and mammals (Arab et al., 1998), as well as exogenous albumin transport (Roberts et al., 1998). Perfusions in *L. erinacea* were all conducted *in vitro*, while *N. kuhlii* perfusions were conducted *in situ*, both of which were successful in smaller species with relatively smaller livers. To our knowledge, there are no published whole liver perfusion studies in any squaliform species. Thus, here we describe and validate an *in situ* liver perfusion for the first time in a shark species, *S. suckleyi*. We first demonstrate the viability of the preparation through oxygen consumption and flow measurements, then demonstrate changes in glucose and 3-HB concentrations exiting the liver following administration of hormones with known roles in regulation of hepatic metabolism in vertebrates. We propose that the isolated perfused liver preparation is a viable alternative to isolated hepatocytes in understanding the metabolic role of this important organ in elasmobranch fishes.

3.3. Methods

Fish Collection

Twenty-four male (1.76-2.85kg) and one female (0.86kg) *S. suckleyi* were caught by rod and line in Barkley Sound, Vancouver Island, British Columbia, during July of 2019 (n = 9), 2021 (n = 11), and 2022 (n = 5) using approved Department of Fisheries and Oceans Canada collection permits (XR-99-2019; XR-139-2021 and XR199-2022). Fish were transferred to and housed in a holding tank (155,000L) with flow-through seawater (12°C) and aeration at Bamfield Marine Science Centre. Fish were fed North Pacific hake, *Merluccius productus*, *ad libitum* every other day and food was withheld for at least two days prior to experimentation. Experiments were completed in accordance with the Canadian Council of Animal Care standards, and with the approval of the Bamfield Marine Science Centre (RS-2019-03; RS-2021-06; RS-22-01) and University of Manitoba (F19-006) animal care committees.

Liver Preparation Set-Up

On the day of experimentation, fish were hand caught from the holding tank and immersed in anesthetic ($0.2 g \cdot L^{-1}$ tricaine methanesulfonate [MS-222], Syndel Labs, Vancouver, British

Columbia, Canada) until sedated, which was determined by the loss of an escape reflex via a pinch on the caudal peduncle. Then, body mass to the nearest gram was taken, the cervical column was severed just posterior to the brain, and the brain was destroyed. Fish were then placed ventral side up on a surgical V-board. Liver perfusions were conducted in a similar manner to previous perfusions in *N. kuhlii* (Arab et al., 1998; Roberts et al., 1998), as an *in situ* approach was adopted. Fish were dissected along the midline of the ventral surface to expose the abdominal and pericardial cavities. The gonads were tied off with bailer twine at the intersecting junctions with the liver to prevent perfusion of these organs. The cardiac stomach was also tied off as close to the esophagus as possible to restrict flow into the gastrointestinal tract. Next, the hepatic portal vein was cannulated in the direction of the liver with PE160 tubing (Figure 3.1). Heparinized elasmobranch Ringer's solution (257mM NaCl, 7mM Na_2SO_4, 3mM $MgSO_4$, 4mM KCl, 2mM $CaCl_2$ dihydrate, 0.1mM Na_2HPO_4 dibasic, 6mM $NaHCO_3$, 400mM urea, 80mM TMAO, 0.2mM alanine, 0.03mM glutamine, 50IU·mL^{-1} sodium heparin, pH 7.8) was perfused via a pressure head placed 28cm above the liver preparation to reflect resting mean arterial pressure in this species (Swenson et al., 2005). The perfusion rate from the pressure head equated to approximately 1.8ml·min^{-1}. In subsequent preparations this perfusion rate was used to perfuse the livers directly via a peristaltic pump (Table 3.1). The conus arteriosus of the heart was then tied-off and the ventricle was cut open. A PE240 cannula was fed through the ventricle and atrium into one side of the sinus venosus (Figure 3.1) and tied off at the ventricular-atrial node. The V-board and fish were positioned at a ~30° angle on the vertical plane such that all hepatic perfusate drained into the cannulated sinus. Perfusate from the sinus venosus was collected via the outflowing cannula and were denoted 'outflow'. All inflowing Ringer and treatment solutions from the inflowing cannula were supersaturated with oxygen (specialty gas mix of 99.7% O_2 and 0.3% CO_2) and were denoted 'inflow'.

Three types of experiments were used to validate this preparation: tissue oxygen consumption (Series A), glucose and 3-HB removal (Series B) or hormone addition (Series C and D). A summary of perfusion Series and sampling specifications are provided in Table 3.1. A higher concentration of glucose and 3-HB was used in Series B to allow increased resolution of small changes in metabolite concentration when these metabolites were removed. To begin, livers were perfused for a minimum of 50min with heparinized Ringer's solution until outflow was visually clear of blood in all experiments. Once the outflow was clear, the experiment commenced with a

period of inflow using non-heparinized Ringer. This period was termed baseline as it did not involve any manipulation of the preparation but varied in duration depending on the experimental aim. A period of baseline perfusion occurred before and after each experimental manipulation. For oxygen consumption experiments, baseline was perfused for 3hrs to understand the viability of an unmanipulated perfused liver preparation over this period. In Series B, baseline was perfused for 30min to determine production/consumption dynamics of glucose and 3-HB in the unmanipulated preparation prior to hormone addition. In Series C and D, baseline was perfused for 50min because some hormones were added to the same preparation and separated temporally, so the baseline perfusions were lengthened to allow the first perfused hormone to clear the liver before adding the second.

Series A: Oxygen Consumption

Oxygen consumption was measured over a 3hr period to determine if liver tissue was metabolically active for the duration of the perfusion. Oxygen probes (430μm Bare fiber oxygen microsensor, FireStingO2, PyroScience, Graz, Austria) were used to measure the percent oxygen saturation (Pyro Workbench software, V1.2.3.1406, PyroScience, Graz, Austria) in inflow and outflow at 15min intervals. To account for oxygen equilibrium with air, a chamber was created with a 1.7mL cryovial, which was situated at the collection end of the outflowing cannula (Figure 1). Perfusate from the liver entered the chamber and flowed through a secondary cannula, which was used to collect outflow and insert the oxygen probe. Thus, percent oxygen saturation in outflow fluid was measured without any exposure to air.

Percent oxygen saturation of both inflow and outflow was converted to dissolved oxygen concentrations (DO; mg $O_2 \cdot mL^{-1}$) using the equations in Mortimer (1956), assuming 1atm at sea-level and 12°C of Ringer, which was temperature controlled using a constant flow-through seawater bath. Oxygen consumption of liver tissue (ng $O_2 \cdot min^{-1} \cdot g$ wet $weight^{-1}$) during perfusion was modified from Fick's principle (Equation 1) and determined as the difference between oxygen concentration (ng $O_2 \cdot mL^{-1}$) between the inflow and outflow from the whole liver perfusion and accounting for total liver mass (g).

Equation 1. Modified Fick's equation for oxygen consumption of liver perfusion.

$$Oxygen\ Consumption\left(\frac{ng\ O_2}{min}/g\right) = \left(Outflow\ \left(\frac{mL}{min}\right) * \left(DO\ Inflow\ \left(\frac{ng\ O_2}{mL}\right) - DO\ Outflow\left(\frac{ng\ O_2}{mL}\right)\right)\right)/Wet\ Mass\ (g)$$

Series B: Glucose and 3-HB Removal

This series of experiments was used to evaluate 1) if reductions in glucose and 3-HB concentrations of the inflowing perfusate would be detectable in the outflowing perfusate and 2) if there was a change in glucose and 3-HB balance (inflow vs outflow concentration), which might infer consumption or production of these metabolites. There were three treatments in this Series: 1) removal of only 5mM glucose, 2) removal of only 2mM 3-HB, 3) removal of both 5mM glucose and 2mM 3-HB. Glucose and 3-HB were removed from inflow for a total of 30min. All three treatments were conducted in the same preparation, although the order of removal was haphazard in each fish to account for order effect. Between removal treatments within the same preparation, baseline was introduced for 30min with both glucose and 3-HB present.

Outflow was collected in 50mL Falcon tubes, and outflow rate of perfusion ($mL \cdot min^{-1}$) was determined by weighing the amount of outflow collected at each interval and correcting this value for seawater (density = $1.03 g \cdot mL^{-1}$). One mL of outflow was then immediately centrifuged (1min, 13,000g) and the supernatant was removed and frozen at -20°C for later glucose and 3-HB analysis. Inflow rate of perfusion ($mL \cdot min^{-1}$) for preparations using a 28cm H_2O pressure head was determined by the speed of the peristaltic pump maintaining the pressure head at a constant height. Inflow rate was constant ($1.8 mL \cdot min^{-1}$) for preparations where the liver was perfused directly by the peristaltic pump (Series B and D).

Series C: Angiotensin II

This series of experiments was used to assess the hemodynamic function of liver preparations following perfusion of a known vasopressive hormone, angiotensin II (Ang II). Thirty μM homologous Ang II was perfused for 15min, followed by 15min of baseline. Outflow was collected and treated as previously described.

Series D: Insulin and Glucagon

This series of experiments was used to evaluate the metabolic function of liver preparations following exposure to known metabolically active hormones, insulin and glucagon. Ten nM heterologous bovine insulin and 10nM homologous glucagon were perfused for 10min each in the

same preparation and separated temporally by 50min of baseline to ensure that the first hormone perfused was cleared from the liver. The order that insulin and glucagon were added was switched in half the perfusions to account for order of hormone perfusion. Outflow was collected and treated as previously described.

Glucose and 3-HB Assays

Perfusate was assayed in Series B and D for glucose and 3-HB as previously conducted in Schoen et al., (2021). In brief, glucose concentrations were determined using an enzymatic hexokinase assay and 3-HB concentration with an enzymatic 3-hydroxybutyrate dehydrogenase assay (β-hydroxybutyrate dehydrogenase assay was conducted in Chapter 2; a minor change was the addition of $0.5 IU \cdot mL^{-1}$ enzyme in the present chapter after revalidation of the assay with a different source of enzyme [Sigma-Aldrich, Missouri, USA versus Roche, Basel, Switzrland). Samples were assayed in duplicate and read spectrophotometrically (Powerwave XS2, Biotek) at 340nm for 50min (glucose) or 120min (3-HB) with Gen5 software (Biotek, Winooski, VT, USA). All samples were compared to a serially diluted standard curve. The absolute change in glucose and 3-HB was calculated as the difference in inflow metabolite concentration (mM) and outflow metabolite concentration (mM), which was denoted the A-V difference (arterial-venous difference; Equation 2). Importantly, inflow glucose and 3-HB concentrations were 0 when respective metabolites were removed in Series B.

Equation 2. Glucose and 3-HB consumption or production equation.

$$A - V\ Difference\ (mM) = (Inflow\ (mM) - Outflow\ (mM)) * -1$$

In the absence of radiolabeled metabolites, we were unable to assess if endogenous production or consumption for each liver perfusion was sourced from exogenous metabolites. Therefore, net production and consumption was inferred from equation 2, which produced a positive value if outflow glucose and 3-HB concentration was greater than inflow glucose and 3-HB concentration, thus indicating a net production (or decreased consumption) of the given metabolite. Conversely, a negative value would indicate a net consumption (or decreased production) of the given metabolite. A value of 0 indicated neither a net increase or decrease in consumption or production from the inflow metabolite concentration, so 0 was used as a statistical

reference point to determine if glucose and 3-HB concentration at any given timepoint was significantly greater or less than inflow glucose and 3-HB concentration.

Statistical Analysis

Oxygen consumption, flow rate, and A-V difference were first analyzed within treatments over time and compared to values obtained during the initial baseline Ringer perfusion. Linear mixed effect models ('lmer' function in 'lmer4' package) (Bates et al., 2015) were used with individual liver preparation identification added to each model as a random effect to account for repeated sampling (Zeger and Karim, 1991). Model residuals were visually assessed for normality and equal variance ('check_model' function in 'performance' package) (Lüdecke et al., 2021). If model assumptions were not met, datasets were transformed using a rank transformation. For all models, Tukey's post-hoc tests ('glht' function in 'multcomp' package) (Hothorn et al., 2008) were used to determine significance of treatments across time relative to initial baseline Ringer perfusion, and were accepted as statistically significant at $\alpha = 0.05$.

In Series B, timepoints were also divided into respective 'metabolite removal' (time 10min, 20min, and 30min) and 'metabolite recovery' (time 40min, 50min, and 60min) for each treatment, and analyzed using linear mixed effect models. Fick's second law of diffusion dictates that exponential models may be the most accurate to use under metabolite manipulation, but given that only 2-3 timepoints were used in these models, we did not deem this amount of data valid to inform an exponential model; thus, linear mixed effects models were used as a conservative metric of metabolite change over time. The slopes of linear models were assessed for significance ($\alpha = 0.05$) and confidence intervals of slopes were also compared between respective treatment 'removal' and 'recovery' models. The '3-HB removal' model did not include the 10min timepoint, as one datapoint was missing from this timepoint that caused the slope to be insufficiently described by a linear model. Finally, models were extrapolated from 10min or 40min, using slopes, to determine experimental intercepts at time 0min and time 30min, respectively.

Next, oxygen consumption at every timepoint was compared to the statistical reference point 0 to determine if oxygen consumption was statistically greater than 0 (no oxygen consumption). A-V difference at every timepoint was compared to the statistical reference point 1 to deduce if metabolite concentration in the outflow was statistically greater or less than metabolite concentration in the inflow. Confidence intervals of mean estimates of fixed effects terms (95%

confidence intervals) were produced from 1000 posterior simulations ('arm' package) (Gelman and Su, 2022; Hasler et al., 2016) to determine significance of timepoints from 0. All statistical analysis was conducted in R v.1.3.1093 (R Core Team 2020).

3.4. Results

Series A

Oxygen consumption was constant and significantly greater than 0 throughout the entire 3-hour perfusion period, indicative of a metabolically active tissue. (Figure 3.2; Table 3.3). It is important to note that given the size of the liver, the tissue was likely not equally oxygenated, which may alter the final value of oxygen consumption; nevertheless, the liver preparations consistently consumed oxygen.

Series B

In treatments where both glucose and 3-HB were removed and in the treatment that only removed glucose, A-V difference in glucose concentration ([A-V glucose]) significantly increased from the initial baseline for at least 30min (Linear Mixed Effects Model and Tukey post-hoc; $p < 0.001$; Figure 3E) and 20 min (Linear Mixed Effects Model and Tukey post-hoc; $p = 0.001$; Figure 3A), respectively. Additionally, [A-V glucose] was significantly less than the initial baseline at 40min, after reintroduction of baseline Ringers (Figure 3.3A, 3.3E) in both treatments (Linear Mixed Effects Model and Tukey post-hoc; $p < 0.045$). There was no change in [A-V glucose] from the initial baseline in the treatment that only removed 3-HB (Figure 3.3C). Furthermore, confidence intervals in the treatments that removed glucose demonstrated that [A-V glucose] significantly increased from 0 for at least 30min following glucose removal (Figure 3.3A, 3.3E; Table 3.4); thus, outflow in these preparations during metabolite removal had a greater glucose concentration than inflow. Conversely, [A-V glucose] significantly decreased from 0 at 40min in the treatment that removed both metabolites, and at 40 and 50min in the treatment that only removed glucose (Figure 3.3A, 3.3E; Table 3.4), following reintroduction of glucose. This denotes that after reintroduction of baseline Ringer, outflow glucose concentration in these preparations was lower that inflow glucose concentration.

In treatments that removed 3-HB, A-V difference in 3-HB concentration ([A-V 3-HB]) significantly increased from initial baseline for the duration of metabolite removal (Linear Mixed

Effects Model and Tukey post-hoc; both treatments $p < 0.050$); moreover, [A-V 3-HB] was significantly less than initial baseline at 40min, after reintroduction of baseline (Linear Mixed Effects Model and Tukey post-hoc; both treatments $p < 0.020$; Figures 3.3D, 3.3F). There was no change in [A-V 3-HB] from initial baseline in the treatment that only removed glucose (Figure 3.3B). Confidence intervals in the treatments that only removed 3-HB or only removed glucose were significantly elevated above 0 at the initial baseline and for the duration of experimentation (Figures 3.3B, 3.3D; Table 3.5), indicating that outflow concentration of 3-HB in these preparations was greater than inflow. In the treatment that only removed 3-HB, confidence intervals were significantly raised above 0 at the initial baseline, for the duration of metabolite removal, and at 60min (after reintroduction of metabolites) (Figure 3.3F; Table 3.5).

All slopes of linear mixed effects models of metabolite removal and recovery were significant (Linear Mixed Effects Model; all $p < 0.031$; Table 3.2), showing that these models effectively fit each dataset. In treatments that removed glucose, the negative slopes of the linear models after glucose removal (no glucose only = -0.87, no glucose and 3-HB = -0.77) closely matched the slope after glucose recovery (no glucose only = 0.87, no glucose and 3-HB = 0.83). Absolute confidence intervals between removal of glucose and recovery of glucose overlapped along the entire interval in these treatments. Intercepts of the glucose removal slopes in these treatments were close to or below the 5mM glucose added to the initial baseline Ringer (no glucose only = 5.04, no glucose and 3-HB = 4.52) (Table 3.2). In treatments that removed 3-HB, the negative slopes of the linear models after 3-HB removal (no 3-HB only = -0.58, no glucose and 3-HB = -0.56) were greater than the slope after 3-HB recovery (no 3-HB only = 0.20, no glucose and 3-HB = 0.32). Absolute confidence intervals slightly overlapped in these treatments, but not along the entire interval. Intercepts of the 3-HB removal slopes in these treatments were above the 2mM 3-HB added to the initial baseline Ringer (no 3-HB only = 4.06, no glucose and 3-HB = 3.34) (Table 3.2).

The outflow rate was consistent in all the metabolite treatments (Figure 3.4) except for a significant decrease in outflow at 40min, after reintroduction of baseline in the treatment that removed only 3-HB from inflow (Linear Mixed Effects Model and Tukey post-hoc; $p = 0.047$; Figure 4B). Inflow rate was set to $1.8 mL \cdot min^{-1}$ in these perfusions and was consistently greater than outflow rate (Figure 3.4).

Series C

The outflow rate in the Ang II treatment significantly decreased following exposure to Ang II and at 30min, post-treatment (Linear Mixed Effects Model and Tukey post-hoc; both timepoints $p < 0.003$; Figure 3.5A).

Series D

There was a significant decrease in outflow rate from the initial baseline following perfusion of the liver with both insulin (Figure 3.5B) and glucagon (Figure 3.5C). This decrease in flow persisted at 20min post-insulin administration (Linear Mixed Effects Model and Tukey post-hoc; $p < 0.001$; Figure 3.5B) and at 30min post-glucagon administration (Linear Mixed Effects Model and Tukey post-hoc; $p < 0.004$; Figure 3.5C).

[A-V glucose] and [A-V 3-HB] did not significantly deviate from the respective initial baselines following either insulin or glucagon treatments (Figure 3.6). Confidence intervals for [A-V glucose] were significantly greater than 0 for all timepoints in both insulin and glucagon treatments (Figures 3.6A, 3.6C; Table 3.4). Similarly, confidence intervals for [A-V 3-HB] were significantly greater than 0 for all timepoints in the glucagon treatment (Figure 3.6D; Table 3.5), but only at 20min in the insulin treatment (Figure 3.6B; Table 3.5). These data indicate that outflow metabolite concentration was consistently greater than inflow metabolite concentration in all treatments except [A-V 3-HB] in the insulin treatment.

3.5. Discussion

In the present study, we describe a liver perfusion preparation in a shark species, *S. suckleyi*. Foremost, the preparations were deemed viable for at least three hours as oxygen consumption remained stable and elevated for this period, indicating aerobic metabolic activity (Series A). Furthermore, hemodynamic function of the preparation was confirmed following a predictable decrease in outflow rate in response to Ang II exposure (Series C), a known vasoconstrictor in elasmobranchs (Hamano et al., 1998; Hazon et al., 1995). Together, consistent oxygen consumption above 0 alongside predicted changes in hemodynamics indicate a functional *in situ* perfusion.

In Series B, glucose and 3-HB were removed from inflow to investigate if changes were detectable in the collected outflow, as well as to determine endogenous glucose and 3-HB release

or uptake, prior to the addition of hormones that were predicted to be involved in regulation of hepatic metabolic function. In all treatments, [A-V glucose] of initial baselines did not deviate from 0, which is conceptualized in Figure 3.7A and suggests no net glucose production or consumption in initial baselines. In the treatments that removed glucose, there was a rapid increase in [A-V glucose], followed by a consistent decrease in [A-V glucose] over 30min. This decrease was mirrored by a parallel increase in [A-V glucose] when glucose was reintroduced to the preparations. The inverse relationship between these slopes and overlapping confidence intervals suggests that the changes in [A-V glucose] are most likely reflective of inflow glucose concentrations; in other words, tissue-derived glucose balance mechanisms did not account for the changes in [A-V glucose], which is illustrated in Figure 3.7B. This was not unexpected as elasmobranchs are relatively glucose intolerant as compared to mammals, taking up to 48hrs to fully process a bolus glucose injection (Deck et al., 2017b; Patent, 1970). Given the low carbohydrate diet of elasmobranchs, a slow rate of glucose utilization would be beneficial to reserve energy for processing other macromolecules; thus, 30min of glucose removal followed by the subsequent 30min of reintroduction may have been too short of a time to initiate hepatic mechanisms involved with glucose release or uptake. Indeed, liver glycogen content increased 6hrs after a bolus glucose injection in *S. suckleyi* (Deck et al., 2017b), although there were no timepoints taken between 0 and 6hrs in this study so it is unclear at what time liver glycogen started significantly accumulating in the previous study.

In contrast to [A-V glucose], the [A-V 3-HB] of initial baselines in all treatments were significantly greater than 0, thus inferring an endogenous release of 3-HB under initial baseline conditions. Endogenous 3-HB production is further confirmed in the treatment that only removed glucose, as all timepoints are significantly elevated above 0. It is largely assumed that elasmobranch livers are the site of 3-HB synthesis for extrahepatic use (Moon and Mommsen, 1987; Zammit and Newsholme, 1979). Considering 3-HB appears to be preferential to other measured metabolites in tissues such as the heart (Driedzic and Hart, 1984) and of importance for recovery of white muscle post-exercise (Richards et al., 2003), it would stand to reason that there would be a net release of hepatic 3-HB.

In treatments that removed 3-HB, [A-V 3-HB] significantly increased from initial baseline 10min after removal, followed by a steady decline in [A-V 3-HB] (similar to the pattern observed for [A-V glucose]). In contrast to glucose concentrations following reintroduction of glucose, [A-

V 3-HB] demonstrated a shallower positive slope after reintroduction of 3-HB. Confidence intervals between the removal and recovery 3-HB slopes overlapped in both treatments that removed 3-HB, although to a lesser degree than the glucose slopes. Therefore, given the variable slopes and elevated outflow of 3-HB in initial baselines, it can be inferred that endogenous hepatic mechanisms altered [A-V 3-HB] when 3-HB was removed or reintroduced. As illustrated by Figure 3.7C, the differences between the slopes when 3-HB is removed and reintroduced could be described by hepatic mechanisms that slow the rate of 3-HB recovery following 3-HB reintroduction, causing a dampened recovery slope compared to the removal slope. However, this would result in an overall reduced concentration of 3-HB in the outflow (as compared to initial baseline) after 30min, which is not what occurred in the present study. More likely, the scenario depicted in Figure 3.7D represents what is occurring in the preparations. A rapid increase in [A-V 3-HB] (endogenous 3-HB production or reduced consumption) within the first 10min of 3-HB removal caused a steeper removal slope and shallower recovery slope that returns [A-V 3-HB] to initial baseline levels. In fact, this can be shown using the intercepts of the linear models outlined in Table 2, which represent the concentrations within the liver preparations when glucose and 3-HB were removed. When glucose was removed the [A-V glucose] intercepts were close to 5, indicative of the 5mM of glucose that was added to the initial baseline. In contrast, when 3-HB was removed the [A-V 3-HB] intercepts were well above the 2mM 3-HB added to the initial baseline, suggestive of endogenous ketogenesis that is consistent with previous studies (Moon and Mommsen, 1987; Zammit and Newsholme, 1979).

Outflow rate of Series B preparations did not deviate from the initial baselines for the duration of experimentation in either the treatment that removed both glucose and 3-HB and the treatment that only removed glucose. There was a slight significant decrease in outflow rate at 40min, post-reintroduction of 3-HB, in the treatment that only removed 3-HB. While not considered a typical effector of hemodynamic change, there is some evidence of changes in glucose causing vasodilation in perfused rat kidneys (Kasiske et al., 1985) and vasoconstriction in suspended aortic rings of New Zealand white rabbits, *Orctolagus cuniculus* (Tesfamariam and Cohen, 1992). Although, in both cases glucose is the first step in a cascade of signaling mechanisms involved in hemodynamic change and likely does not act directly. Research is lacking in terms of metabolite control of hemodynamics in other vertebrates, and it remains unclear if 3-HB plays any role in this function, though our results indicate it might under certain conditions.

Notably, the inflow rate is greater than the outflow rate in all preparations in all Series, indicative of leakage in the preparation. Importantly, the outflow rate of unmanipulated preparations remained relatively stable and consistent across perfusions.

In Series D, hormones with known metabolic actions in other vertebrates were administered to determine if they influenced glucose and 3-HB concentrations. In the vertebrate liver, insulin typically promotes glycogen synthesis and inhibits glycogenolysis, thereby reducing hepatic glucose release (Cherrington et al., 1998). In the present study, insulin did not influence [A-V glucose], although this may be a result of the perfusion time (15min). Injections of bovine insulin *in vivo* in *S. suckleyi* have demonstrated a decrease in plasma glucose concentrations, usually followed by extended hypoglycemia (Deck et al., 2017b; deRoos and deRoos, 1979; deRoos et al., 1985; Patent, 1970), although these observations were only initially significant between 6-12hrs after insulin injection. Additionally, these studies measured glucose in the plasma and therefore were whole-body and likely involved insulin-mediated glucose influx into extrahepatic tissues in addition to any hepatic effect. Furthermore, there is indication that bovine insulin and elasmobranch insulin may have varying degrees of efficacy, as shown in *Scyliorhinus canicula* exhibiting delayed hypoglycemia (between 12 and 48hrs) after injection with homologous dogfish insulin (Anderson et al., 2002). Thus, the use of homologous hormone at equivalent concentrations may elicit significant changes in glucose and 3-HB handling in the timeframe of our experiment.

Contrary to our expectations, the classical antagonist to insulin, glucagon, did not alter glucose balance in the perfused liver. In vertebrates, including numerous teleost species, glucagon causes inhibition of insulin pathways and an increase in glycogenolysis, thus resulting in hepatic glucose efflux (Plisetskaya and Mommsen, 1996). Previous work in elasmobranchs has suggested hyperglycemia in response to heterologous bovine glucagon, although this increase was much slower than that of other vertebrates and a relatively large dose of glucagon was needed to elicit a response (Grant, 1964; Patent, 1970). For example, in Patent (1970), $2 mg \cdot kg^{-1}$ of bovine glucagon was injected into *S. suckleyi*, while the concentration of circulating plasma glucagon in a number of teleost species and *S. canicula* was measured in $ng \cdot mL^{-1}$ (Gutiérrez et al., 1986), which could indicate that a glucagon concentration several fold higher than circulating was injected into *S. suckleyi*. In the liver perfusions for the present study, a 10nM concentration of *S. suckleyi* glucagon was used, which is equivalent to approximately 7.12µg of glucagon flowing into a 200g liver

(35.6μg·kg^{-1}) over 10min at a flow rate of 1.8ml·min^{-1} and a molecular weight of 3954.9 Da (Deck et al., 2017a). Therefore, although *S. suckleyi* glucagon was utilized in this study, it may have not been at a sufficient dose to generate a hyperglycemic response.

In contrast to glucose, the effects of insulin and glucagon on 3-HB concentrations are largely unknown in elasmobranchs. The consensus in the literature is that insulin does not impact plasma 3-HB concentrations, which is consistent with both bovine insulin (deRoos et al., 1985) and dogfish insulin (Anderson et al., 2002). To date, there are no studies that explore the impact of glucagon on 3-HB levels in any elasmobranch and our data suggest a negligible effect. Interestingly, [A-V glucose] and [A-V 3-HB] for almost all timepoints in insulin and glucagon treatments were significantly elevated above 0, suggesting an increase in release of the metabolites from the perfused liver. This is consistent with Series B [A-V 3-HB] and further supports the notion of consistent hepatic ketogenesis; however, [A-V glucose] in Series B is only elevated above 0 when glucose was removed and not under baseline conditions. Discrepancies between Series B and D might be explained by fasting status. Additional experiments manipulating the perfusate concentration of glucose and 3-HB for longer periods may aid in understanding the balance between production and consumption of these key metabolites.

In mammals, both insulin and glucagon have demonstrated vasodilatory effects (Manrique et al., 2014; Muniyappa and Yavuz, 2013; Sélley et al., 2016); however, in our data the decrease in outflow rate following hormone administration is indicative of vasoconstrictive actions. In diabetic humans insulin has been shown to have vasoconstrictive properties, and the persistent state of ketosis in elasmobranchs is comparable to ketonemia or ketoacidosis in untreated diabetics (De Roos, 1994; Speers-Roesch and Treberg, 2010). Under normal non-ketotic circumstances in mammals, there is a balance between insulin mediated vasodilation and vasoconstriction, tending towards vasodilation through activation of nitric oxide pathways. In the case of metabolic disorders characterized by insulin resistance, such as type II diabetes, this balance is shifted towards vasoconstriction via endothelin-1 pathways (Manrique et al., 2014; Muniyappa and Yavuz, 2013). Therefore, vasoconstriction in response to insulin may be an indication of a degree of insulin-resistance in *S. suckleyi*, which is conceivable given elasmobranchs relative glucose intolerance, as compared to mammals, and their reliance on ketone bodies (Patent, 1970; Polakof et al., 2012). In the case of glucagon, the mechanism of vasodilation in mammals is also thought to involve nitric oxide, amongst other messengers such as carbon monoxide (Sélley et al., 2016). There is

very little evidence of direct vasoconstriction in response to glucagon in vertebrates, although this study shows the possibility of glucagon's constricting effects and must be further studied to confirm this action in elasmobranchs.

3.6. Conclusions

Data presented show that the adapted liver perfusion is viable in a larger elasmobranch species. Oxygen consumption, changes in hemodynamics, and measurable changes in outflow glucose and 3-HB concentrations all serve to validate the perfusion for future use. However, this preparation did not detect changes in glucose and 3-HB concentrations following insulin and glucagon exposure. Further research is recommended to determine if this preparation is useful in determining deviations in metabolite balance in response to other agonists such as catecholamines and corticosteroids.

3.7. Acknowledgements

The authors thank Bamfield Marine Science Centre for the use of facilities and financial assistance to A.N.S. through the Dick and Leona Peter Student Bursary, Ryan Wahl and Dr. Tamzin Blewett for assistance with sample collection, and Dr. Jason Treberg for assistance with data analysis. Further, we thank the additional funding sources of the Natural Science and Engineering Research Council of Canada (NSERC) Discovery grant awarded to W.G.A. the University of Manitoba Graduate Fellowship awarded to A.N.S., a NSERC PDF awarded to A.R.W., and the University of Manitoba Faculty of Science Field work support program. We also acknowledge that the Bamfield Marine Sciences Centre sits within the traditional territory of the Huu-ay-aht First Nations and the University of Manitoba campuses are located on the original lands of the Anishinaabeg, Cree, Oji-Cree, Dakota, and Dene peoples, and on the homeland of the Métis Nation.

3.8. Tables

Table 3.1. Liver perfusion treatments and specifications.

Series	Treatment	Measurement	Fish Number (n)	Year	Peristaltic Pump or Pressure Head	Time Between Sampling (minutes)	Glucose Concentration in Ringer	3-HB Concentration in Ringer
A	None	Percent Oxygen Saturation	11	2021	Pressure Head	15	2mM	1mM
B	Metabolite Removal - no glucose and 3-HB, no glucose, and no 3-HB	Flow, Metabolites	4	2019	Pump	10	5mM	2mM
C	Angiotensin	Flow	5	2022	Pressure Head	15	2mM	1mM
D	Insulin and Glucagon	Flow, Metabolites	5	2019	Pump	10	2mM	1mM

Table 3.2. Linear model outputs for metabolite 'removal' and 'recovery'.

Treatment		Slope	2.5%	97.5%	p-value	Intercept
No Glucose Only	Glucose Removal	-0.87	-1.19	-0.56	<0.01	5.04
	Glucose Recovery	0.87	0.45	1.29	<0.01	-3.26
No 3-HB Only	3-HB Removal	-0.58	-0.93	-0.23	0.01	4.06
	3-HB Recovery	0.20	0.11	0.30	<0.01	0.32
No Glucose and 3-HB	Glucose Removal	-0.77	-0.96	-0.58	<0.01	4.52
	Glucose Recovery	0.83	0.46	1.19	<0.01	-3.25
	3-HB Removal	-0.56	-0.89	-0.24	0.03	3.34
	3-HB Recovery	0.32	0.23	0.42	<0.01	-0.25

Table 3.3. Mean values and 95% confidence intervals of oxygen consumption. Bold rows indicate that 2.5-97.5% confidence intervals do not overlap 0.

Oxygen Consumption		(Relative to 0)	
	Mean	2.5%	97.5%
Intercept	**161.78**	**126.82**	**198.97**
Timepoint 1	**147.82**	**114.05**	**183.18**
Timepoint 2	**154.94**	**119.40**	**191.51**
Timepoint 3	**165.83**	**134.01**	**200.57**
Timepoint 4	**140.86**	**106.05**	**176.91**
Timepoint 5	**150.25**	**116.00**	**186.19**
Timepoint 6	**150.47**	**116.89**	**187.68**
Timepoint 7	**154.28**	**120.01**	**188.78**
Timepoint 8	**140.44**	**104.56**	**175.94**
Timepoint 9	**138.17**	**102.89**	**171.98**
Timepoint 10	**127.98**	**94.63**	**162.75**
Timepoint 11	**152.20**	**116.25**	**188.78**

Table 3.4. Mean values and 95% confidence intervals of glucose. Bold rows indicate that 2.5-97.5% confidence intervals do not overlap 0.

Glucose Balance		(Relative to 0)		
Hormone		Mean	2.5%	97.5%
Insulin	**Intercept**	**2.07**	**1.07**	**3.12**
	Timepoint 2	**2.03**	**1.07**	**2.99**
	Timepoint 3	**1.39**	**0.38**	**2.39**
	Timepoint 4	**1.40**	**0.32**	**2.41**
Glucagon	**Intercept**	**1.23**	**0.31**	**2.18**
	Timepoint 2	**1.37**	**0.53**	**2.27**
	Timepoint 3	**1.47**	**0.63**	**2.34**
	Timepoint 4	**1.44**	**0.55**	**1.30**
Remove Glucose Only	Intercept	-0.25	-1.05	0.57
	Timepoint 2	**4.17**	**3.11**	**5.23**
	Timepoint 3	**3.29**	**2.20**	**4.36**
	Timepoint 4	**2.43**	**1.37**	**3.50**
	Timepoint 5	**-2.44**	**-3.56**	**-1.29**
	Timepoint 6	**-1.43**	**-2.54**	**-0.41**
	Timepoint 7	-0.71	-1.80	0.37
Remove 3-HB Only	Intercept	-0.16	-0.74	0.42
	Timepoint 2	-0.40	-1.03	0.29
	Timepoint 3	-0.26	-0.84	0.32
	Timepoint 4	-0.31	-0.84	0.29
	Timepoint 5	-0.39	-0.98	0.20
	Timepoint 6	0.03	-0.56	0.65
	Timepoint 7	0.18	-0.41	0.73
Remove Glucose and 3-HB	Intercept	-0.49	-1.17	0.21
	Timepoint 2	**3.83**	**3.08**	**4.51**
	Timepoint 3	**2.80**	**2.12**	**3.53**
	Timepoint 4	**2.28**	**1.60**	**2.95**

	Timepoint 5	**-2.56**	**-3.30**	**-1.83**
	Timepoint 6	**-1.07**	**-1.77**	**-0.41**
	Timepoint 7	**-0.78**	**-0.11**	**-1.52**

Table 3.5. Mean values and 95% confidence intervals of 3-HB. Bold rows indicate that 2.5-97.5% confidence intervals do not overlap 0.

3-HB Balance		(Relative to 0)		
Hormone		Mean	2.5%	97.5%
Insulin	Intercept	0.45	-0.08	0.94
	Timepoint 2	0.46	-0.12	1.02
	Timepoint 3	**0.55**	**0.03**	**1.06**
	Timepoint 4	0.27	-0.22	0.76
Glucagon	**Intercept**	**0.50**	**0.20**	**0.75**
	Timepoint 2	**0.66**	**0.39**	**0.96**
	Timepoint 3	**0.36**	**0.03**	**0.66**
	Timepoint 4	**0.43**	**0.13**	**0.72**
Remove Glucose Only	**Intercept**	**0.86**	**0.24**	**1.53**
	Timepoint 2	**1.12**	**0.42**	**1.85**
	Timepoint 3	**1.28**	**0.60**	**1.94**
	Timepoint 4	**0.93**	**0.26**	**1.63**
	Timepoint 5	**1.06**	**0.39**	**1.73**
	Timepoint 6	**1.03**	**0.37**	**1.72**
	Timepoint 7	**1.00**	**0.34**	**1.71**
Remove 3-HB Only	**Intercept**	**1.46**	**1.03**	**1.90**
	Timepoint 2	**3.62**	**3.23**	**4.07**
	Timepoint 3	**2.61**	**2.16**	**3.07**
	Timepoint 4	**2.45**	**2.05**	**2.88**
	Timepoint 5	**0.49**	**0.09**	**0.91**
	Timepoint 6	**0.77**	**0.35**	**1.16**
	Timepoint 7	**0.89**	**0.49**	**1.31**
Remove Glucose and 3-HB	**Intercept**	**1.21**	**0.55**	**1.81**
	Timepoint 2	**2.67**	**2.01**	**3.31**
	Timepoint 3	**2.77**	**2.07**	**3.41**
	Timepoint 4	**2.20**	**1.55**	**2.80**

	Timepoint 5	0.08	-0.64	0.71
	Timepoint 6	0.60	-0.08	1.22
	Timepoint 7	**0.84**	**1.43**	**0.19**

3.9. Figures

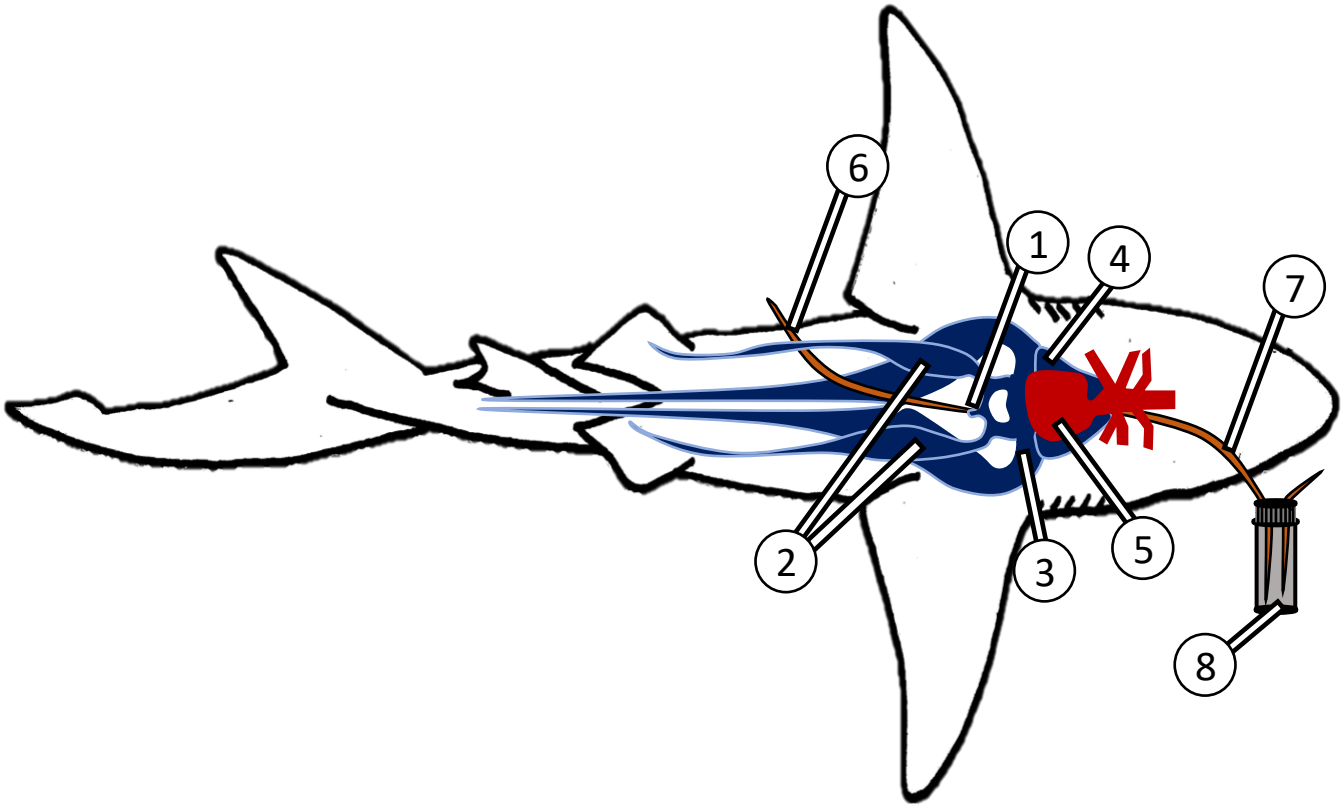


Figure 3.1. Diagram of the major vasculature and cannulations associated with the adapted liver perfusion in *Squalus suckleyi.* Blue vasculature indicates venous systems and red vasculature indicates arterial systems (1: hepatic vein, 2: hepatic sinuses, 3: sinus venosus, 4: atrium, 5: ventricle). Orange indicates cannulation tubing (6: inflowing, 7: outflowing, 8: airtight cryovial for oxygen consumption measurements).

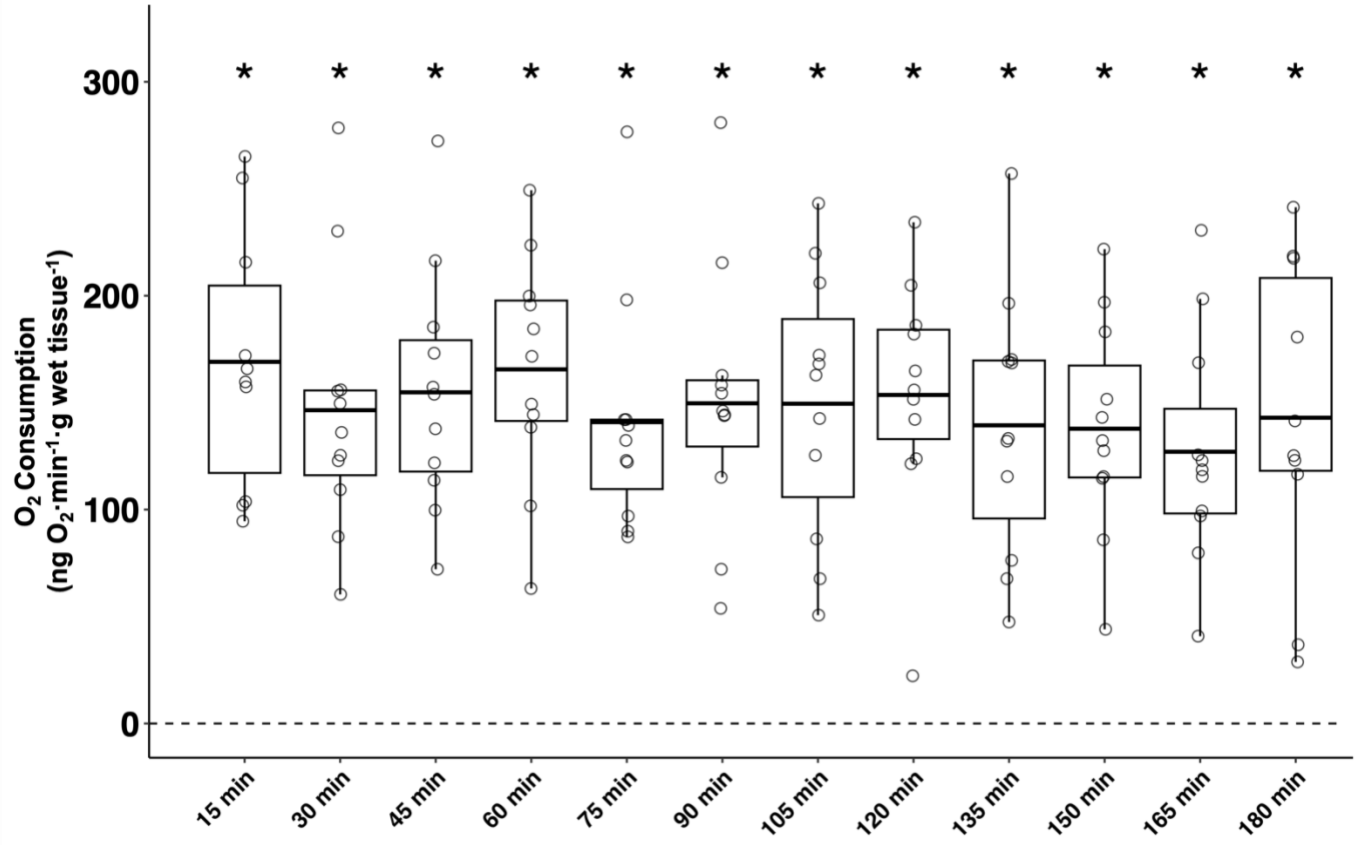


Figure 3.2. Oxygen consumption (ng $O_2 \cdot min^{-1} \cdot g$ wet $tissue^{-1}$) of *Squalus suckleyi* liver preparations, as determined by the modified Fick's equation, for 3hr perfusions (n = 11). Boxplots represent the mean (solid black line inside box), interquartile range (box edges), and maximum and minimum (box whiskers) of oxygen consumption data. Dotted line indicates null oxygen consumption (0) and confidence intervals that do not overlap with 0 are denoted with an asterisk (*).

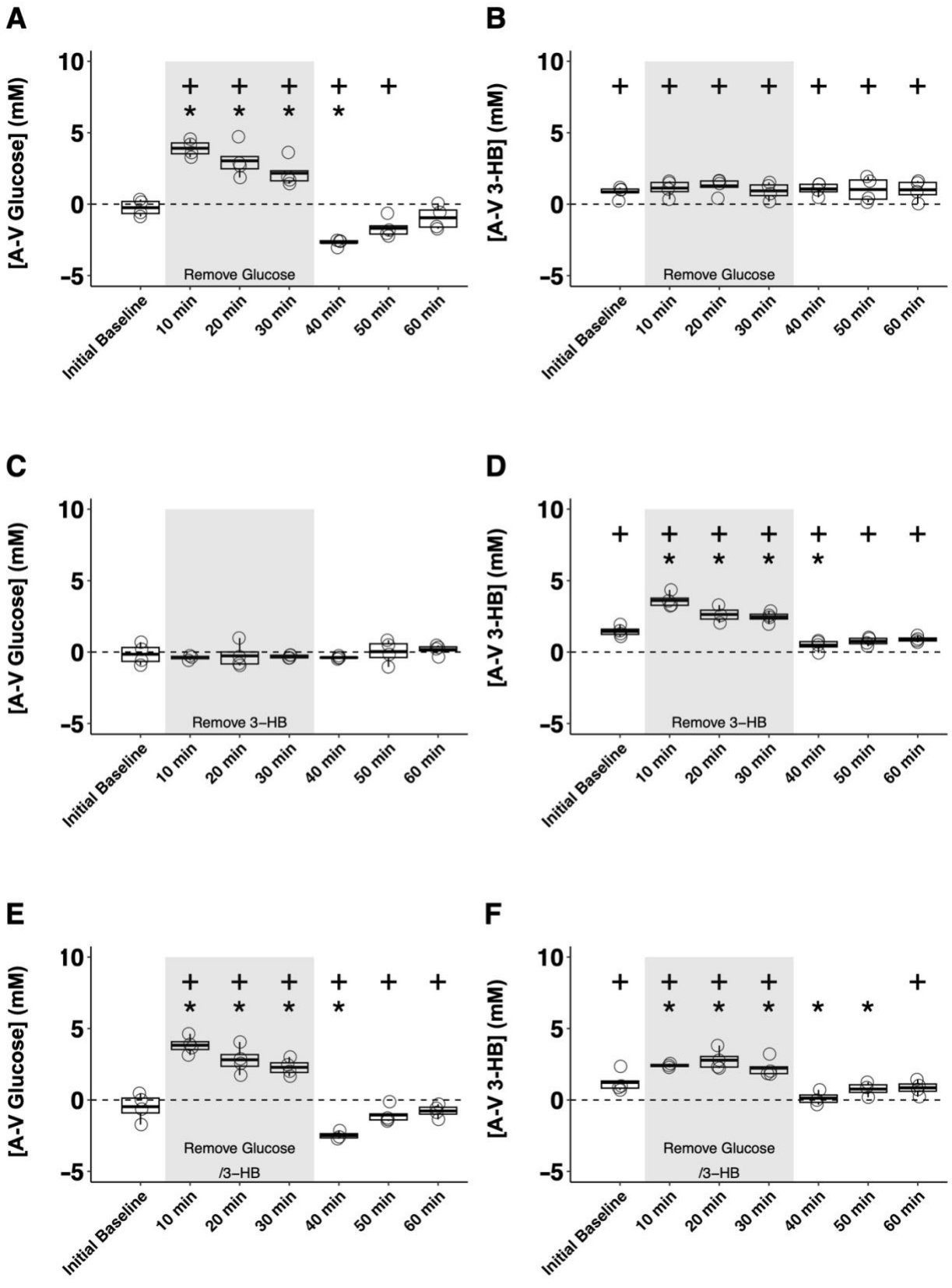

A
B
C
D
E
F
[A-V Glucose] (mM)
[A-V 3-HB] (mM)
10
5
0
−5
Remove Glucose
Remove 3−HB
Remove Glucose
/3−HB
Initial Baseline
10 min
20 min
30 min
40 min
50 min
60 min

Figure 3.3. A-V difference of metabolites (mM) in *Squalus suckleyi* liver preparations prior to (initial baseline; Ringer with both glucose and 3-HB), during (metabolite removal), and following (baseline; Ringer with both glucose and 3-HB) removal of metabolites from inflow (n=4). A) [A-V glucose] of perfusions with removal of both 2mM glucose and 1mM 3-HB. B) [A-V 3-HB] of perfusions with removal of both 2mM glucose and 1mM 3-HB. C) [A-V glucose] of perfusions with removal of 2mM glucose. D) [A-V 3-HB] of perfusions with removal of 2mM glucose. E) [A-V glucose] of perfusions with removal of 1mM 3-HB. F) [A-V 3-HB] of perfusions with removal of 1mM 3-HB. Dotted lines (0) indicate metabolite balance where outflow metabolite concentration is equal to inflow metabolite concentration. Boxplots represent the mean (solid black line inside box), interquartile range (box edges), and maximum and minimum (box whiskers) of A-V difference of metabolite data. Shaded boxes indicate metabolite removal (10-30min), followed by metabolite recovery (40-60min). Confidence intervals that do not overlap with 0 are denoted with a plus sign (+). Statistical significance ($\alpha = 0.05$) of the mean metabolite balance between subsequent timepoints and the initial baseline is indicated with an asterisk (*).

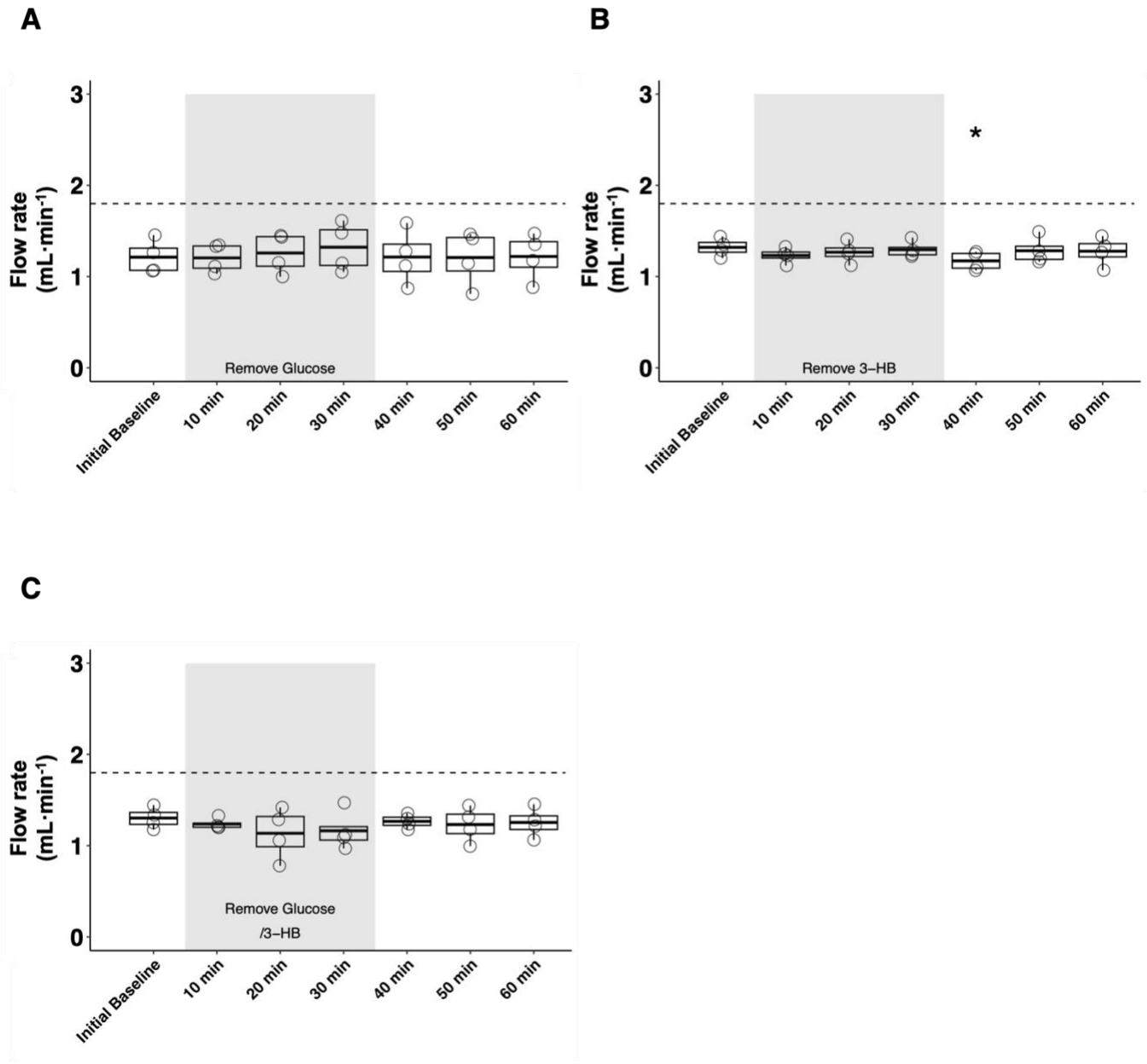


Figure 3.4. Flow rate (mL·min^{-1}) during *Squalus suckleyi* liver preparations prior to (initial baseline; Ringer with both glucose and 3-HB), during (metabolite removal), and following (baseline; Ringer with both glucose and 3-HB) removal of metabolites from inflow (n = 4). A) Removal of both 2mM glucose and 1mM 3-HB. B) Removal of 1mM 3-HB. C) Removal of 2mM glucose. Boxplots represent the mean (solid black line inside box), interquartile range (box edges), and maximum and minimum (box whiskers) of flow rate data. Shaded boxes indicate metabolite removal (10-30min), followed by metabolite recovery (40-60min). Inflowing rate (dotted line) and

outflowing rate (black circles). Statistical significance ($\alpha = 0.05$) of the mean flow rate between subsequent timepoints and the initial baseline is indicated by an asterisk (*).

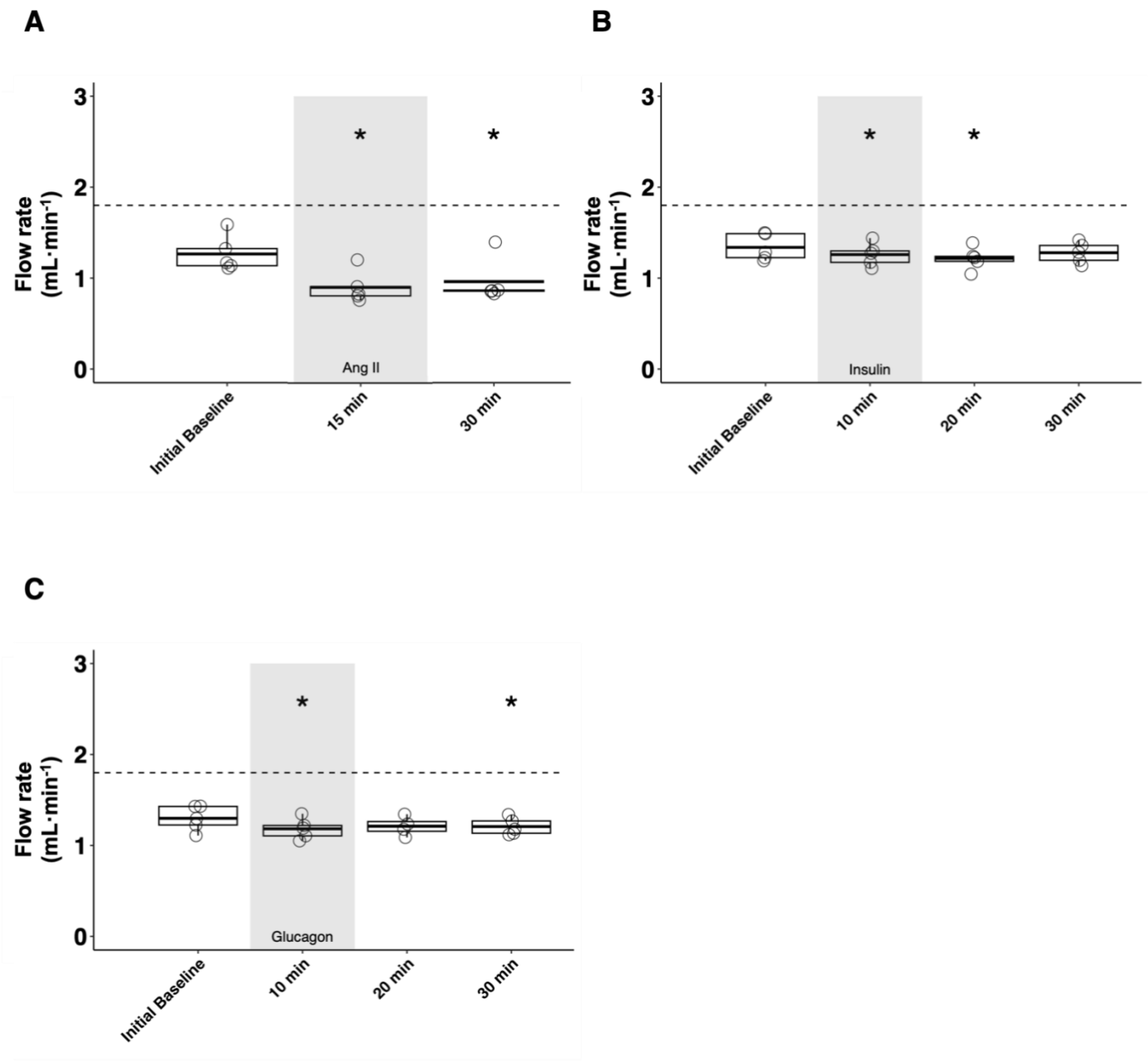


Figure 3.5. Flow rate (mL·min^{-1}) during *Squalus suckleyi* liver preparations prior to (initial baseline), during (hormone treatment), and following (baseline) addition of peptide hormones to inflow (Series B and C; n = 5). B) Perfusions treated with 30μM Ang II. C) Perfusions treated with 10nM insulin. D) Perfusions treated with 10nM glucagon. Boxplots represent the mean (solid black line inside box), interquartile range (box edges), and maximum and minimum (box whiskers) of flow rate data. Shaded boxes indicate metabolite removal (10min), followed by metabolite recovery (20-30min). Inflowing rate (dotted line) and outflowing rate (black circles). Statistical

significance (α = 0.05) of the mean flow rate between subsequent timepoints and the initial baseline is indicated by an asterisk (*).

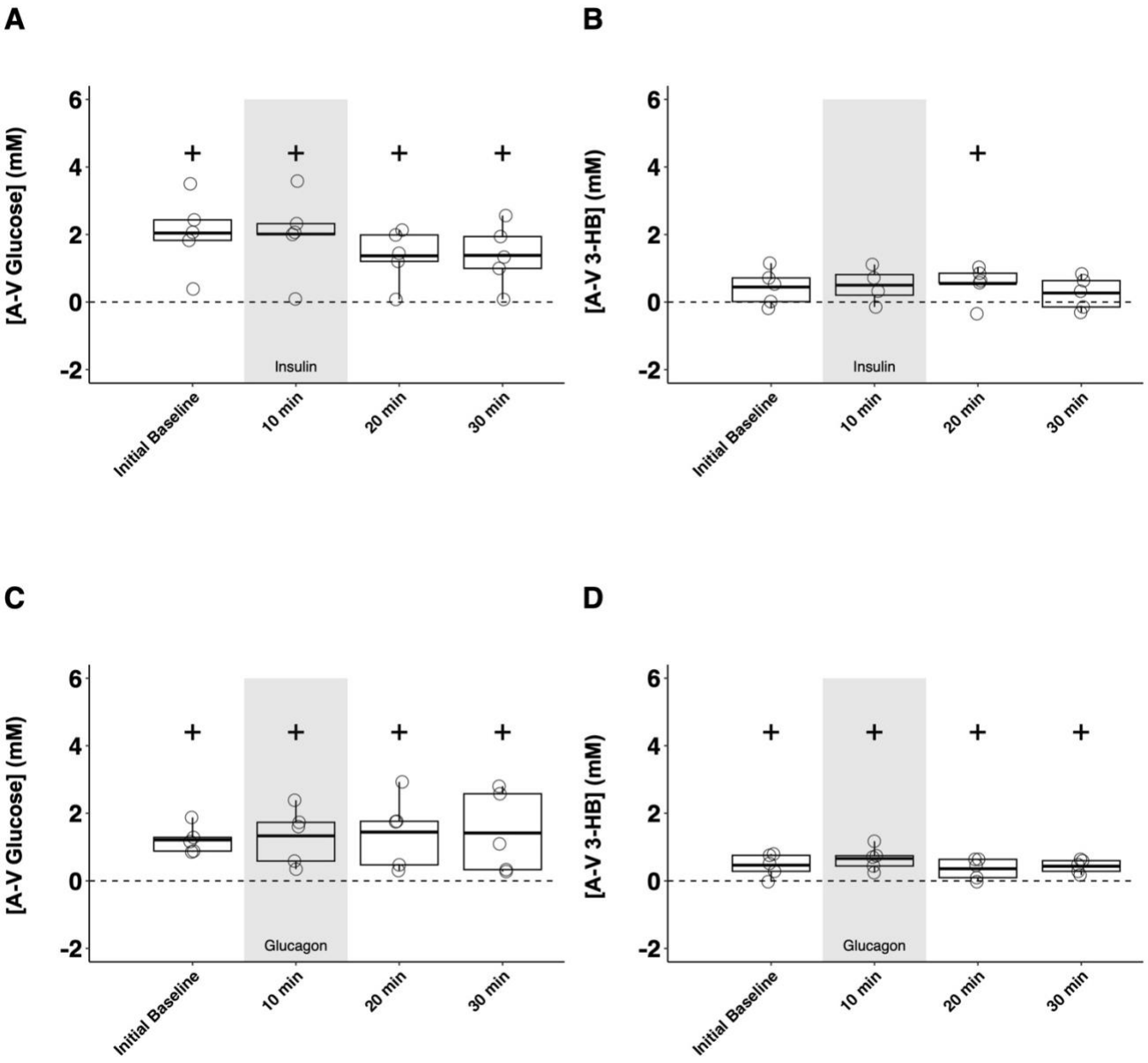


Figure 3.6. A-V difference of metabolites (mM) during *Squalus suckleyi* liver preparations prior to (initial baseline), during (hormone treatment), and following (baseline) addition of hormones to inflow (n = 5). A) [A-V glucose] of perfusions treated with 10nM insulin. B) [A-V 3-HB] of perfusions treated with 10nM insulin. C) [A-V glucose] of perfusions treated with 10nM glucagon. D) [A-V 3-HB] of perfusions treated with 10nM glucagon. Boxplots represent the mean (solid black line inside box), interquartile range (box edges), and maximum and minimum (box whiskers) of A-V difference of metabolite data. Shaded boxes indicate metabolite removal (10min), followed by metabolite recovery (20-30min). Dotted lines (0) indicate metabolite balance where outflow

metabolite concentration is equal to inflow metabolite concentration. Confidence intervals that do not overlap with 0 are denoted with a plus sign (+).

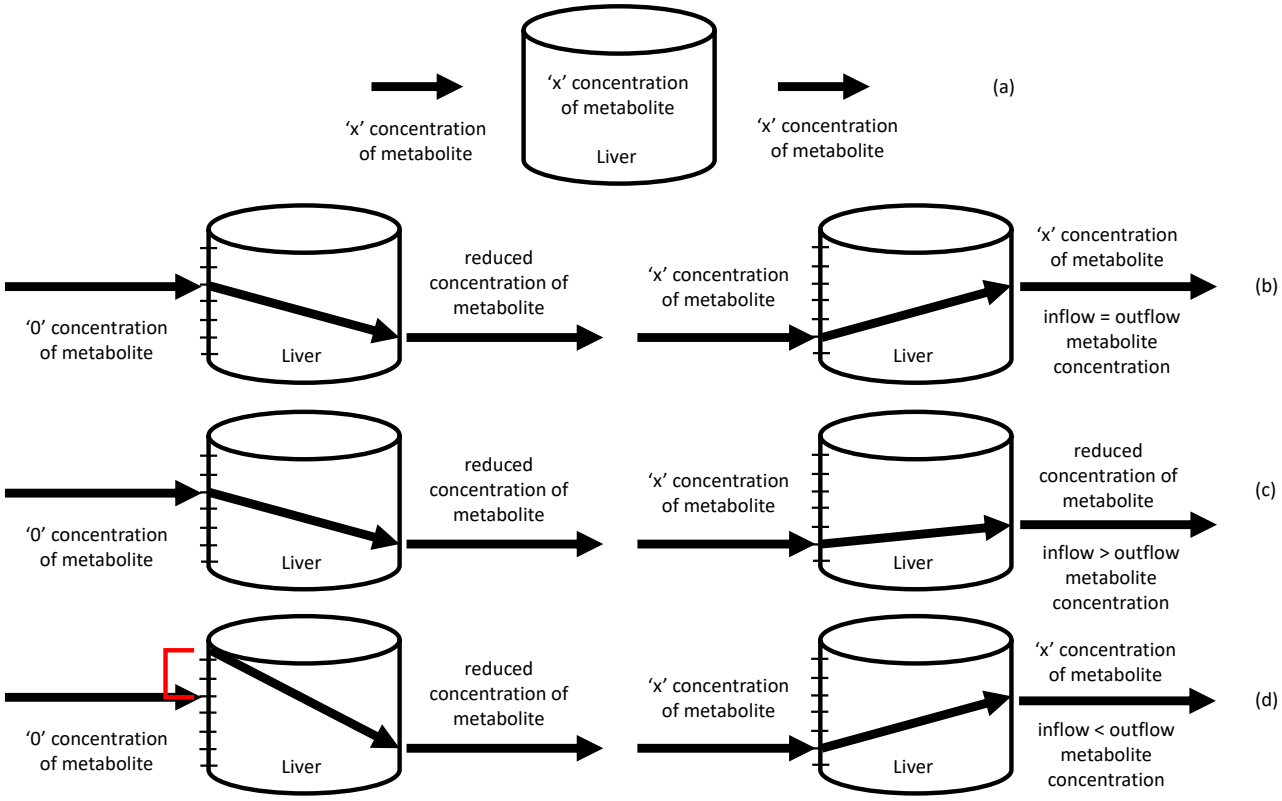


Figure 3.7. Conceptual models of liver preparations under A) initial baseline conditions with no endogenous mechanisms altering outflow metabolite concentration. B) Perfusion conditions where removal and reintroduction of metabolite produces equal, but inverse, slopes of outflow metabolite concentrations over time. C) Perfusion conditions where removal of metabolite produces a steeper slope than the inverse recovery slope, but outflow metabolite concentration does not recover to initial baseline concentrations. D) Perfusion conditions where removal of metabolite produces a steeper slope than the inverse recovery slope due to endogenous production/reduced consumption of metabolite (red bracket), thus increasing outflow metabolite concentration.

3.10. Works Cited

Anderson, W. G., Ali, M. F., Einarsdóttir, I. E., Schäffer, L., Hazon, N. and Conlon, J. M. (2002). Purification, Characterization, and Biological Activity of Insulins from the Spotted Dogfish, Scyliorhinus canicula, and the Hammerhead Shark, Sphyrna lewini. *General and Comparative Endocrinology* **126**, 113-122.

Arab, H., Walker, N. I., Cheung, K., Winterford, C., Hickman, P. E., Potter, J. M. and Roberts, M. S. (1998). Functional and Structural Characterization of Isolated Perfused Stingray Liver Including Effects of Ischaemia/Reperfusion. *Journal of Comparative Pathology* **118**, 221-230.

Bakes, M. J. and Nichols, P. D. (1995). Lipid, fatty acid and squalene composition of liver oil from six species of deep-sea sharks collected in sourthern Australian waters. *Comparative Biochemistry and Physiology, Part B* **110**, 267-275.

Ballatori, N. and Boyer, J. L. (1988). Characteristics of L-alanine uptake and freshly isolated hepatocytes of elasmobranch *Raja erinacea*. *The American Physiological Society* **254**, R801-R808.

Ballatori, N., Hager, D. N., Nundy, S., Miller, D. S. and Boyer, J. L. (1999). Carrier-mediated uptake of lucifer yellow in skate and rate hepatocytes: A fluid-phase marker revisited. *The American Journal of Physiology* **277**, G896-G904.

Bates, D., Mächler, M., Bolker, B. M. and Walker, S. C. (2015). Fitting Linear Mixed-Effects Models Using lme4. *Journal of Statistical Software* **67**.

Bellamy, D. and Leonard, R. A. (1964). The Effect of Cortisol on the Activity of Glutamate-Pyruvate Transaminase and the Formation of Glycogen and Urea in Starved Rats. *Biochemical Journal* **93**, 331-336.

Bellamy, D., Leonard, R. A. and Dulieu, K. (1968). Hepatic Gluconeogenesis in Rats Treated with Cortisol. *General and Comparative Endocrinology* **10**, 434-437.

Berry, M. N. and Friend, D. S. (1969). HIGH-YIELD PREPARATION OF ISOLATED RAT LIVER PARENCHYMAL CELLS. *Journal of Cell Biology* **43**, 506-520.

Birnbaum, M. J., Schultz, J. and Fain, J. N. (1976). Hormone-stimulated glycogenolysis in isolated goldfish hepatocytes. *American Journal of Physiology* **231**, 191-197.

Cherrington, A. D., Edgerton, D. and Sindelar, D. K. (1998). The direct and indirect effects of insulin on hepatic glucose production in vivo. *Diabetologia* **41**, 987-996.

Danulat, E. and Mommsen, T. P. (1990). Norepinephrine: A Potent Activator of Glycogenolysis and Gluconeogenesis in Rockfish Hepatocytes. *Gen Comp Endocrinol* **78**, 12-22.

De Roos, R. (1994). Plasma ketone, glucose, lactate, and alanine levels in the vascular supply to and from the brain of the spiny dogfish shark (Squalus acanthias). *Journal of Experimental Zoology* **268**, 354-363.

Deck, C. A., Anderson, W. G., Conlon, J. M. and Walsh, P. J. (2017a). The activity of the rectal gland of the North pacific spiny dogfish *Squalus suckleyi* is glucose dependent and stimulated by glucagon-like peptide-1. *Journal of Comparative Physiology, Part B* **187**, 1155-1161.

Deck, C. A., Anderson, W. G. and Walsh, P. J. (2017b). Effects of glucose and insulin administration on glucose transporter expression in the North Pacific spiny dogfish (*Squalus suckleyi*). *General and Comparative Endocrinology* **247**, 46-52.

deRoos, R. and deRoos, C. C. (1979). Sever Insulin-Induced Hypoglycemia in the Spiny Dogfish Shark (*Squalus acanthias*). *General and Comparative Endocrinology* **37**, 186-191.

deRoos, R., deRoos, C. C., Werner, C. S. and Werner, H. (1985). Plasma Levels of Glucose, Alanine, Lactate, and ß-Hydroxybutyrate in the Unfed Spiny Dogfish Shark (*Squalus acanthias*) after Surgery and following Mammalian Insulin Infusion. *General and Comparative Endocrinology* **58**, 28-43.

Driedzic, W. R. and Hart, T. (1984). Relationship bewteen exogenous fuel avaiability and performance by teleost and elasmobranch hearts. *Journal of Comparative Physiology, Part B* **154**, 593-599.

Gelman, A. and Su, Y.-S. (2022). arm: Data Analysis Using Regression and Multilevel/Hierarchical Models. https://CRAN.R-project.org/package=arm

Grant, W. C. (1964). Effect of insulin and glucagon on blood glucose levels in the skate, R. erinacea. *American Zoologist* **4**, 325-326.

Gutiérrez, J., Fernandez, J., Blasco, J., Gesse, J. M. and Planas, J. (1986). Plasma Glucagon Levels in Different Species of Fish. *General and Comparative Endocrinology* **63**, 328-333.

Hamano, K., Tierney, M. L., Ashida, K., Takei, Y. and Hazon, N. (1998). Direct vasoconstrictor action of homologous angiotensin II on isolated arterial ring preparations in an elasmobranch fish. *Journal of Endocrinology* **158**, 419-423.

Hasler, C. T., Midway, S. R., Jeffrey, J. D., Tix, J. A., Sullivan, C. and Suski, C. D. (2016). Exposure to elevated *p*CO2 alters post-treatment diel movement patterns of largemouth bass over short time scales. *Freshwater Biology* **61**, 1590-1600.

Hazon, N., Tierney, M. L., Hamano, K., Ashida, K. and Takei, Y. (1995). Endogenous angiotensins, angiotesin II-competitive binding inhibitors and converting enzyme inhibitor in elasmobranch fish. *Netherlands Journal of Zoology* **45**, 117-120.

Hothorn, T., Bretz, F. and Westfall, P. (2008). Simultaneous Inference in General Parametric Models. *Biometrical Journal* **50**, 346-363.

Kasiske, B. L., O'Donnell, M. P. and Keane, W. F. (1985). Glucose-induced Increases in Renal Hemodynamic Function. *Diabetes* **34**, 360-364.

Lüdecke, D., Ben-Shachar, M. S., Patil, I., Waggoner, P. and Makowski, D. (2021). performance: An R Package for Assessment, Comparison and Testing of Statistical Models. *The Journal of Open Source Software* **6**, 3139.

Manrique, C., Lastra, G. and Sowers, J. R. (2014). New insights into insulin action and resistance in the vasculature. *Annals of the New York Academy of Sciences* **1311**, 138-150.

Mommsen, T. P. (1986). Comparative gluconeogenesis in hepatocytes from salmonid fishes. *Canadian Journal of Zoology* **64**, 1110-1117.

Mommsen, T. P., Andrews, P. C. and Plisetskaya, E. (1987). Glucagon-like peptides activate hepatic gluconeogenesis. *FEBS Letters* **219**, 227-232.

Mommsen, T. P. and Moon, T. W. (1987). The Metabolic Potential of Hepatocytes and Kidney Tissue in the Little Skate, Raja erinacea. *Journal of Experimental Zoology* **244**, 1-8.

Mommsen, T. P., Moon, T. W. and Plisetskaya, E. (2001). Effects of Arginine on Pancreatic Hormones and Hepatic Metabolism in Rainbow Trout. *Physiological and Biochemical Zoology* **74**, 668-678.

Moon, T. W. and Mommsen, T. P. (1987). Enzymes of Intermediary Metabolism in Tissues of the Little Skate, *Raja erinacea*. *Journal of Experimental Zoology* **244**, 9-15.

Muniyappa, R. and Yavuz, S. (2013). Metabolic actions of angiotensin II and insulin: A microvascular endothelial balancing act. *Molecular and Cellular Endocrinology* **378**, 59-69.

Patent, G. J. (1970). Comparision of Some Hormonal Effects on Carbohydrate Metabolism in an Elasmobranch (*Squalus acanthias*) and a Holocephalan (*Hydrolagus colliei*). *General and Comparative Endocrinology* **14**, 215-242.

Plisetskaya, E. and Mommsen, T. P. (1996). Glucagon and Glucagon-like Peptides in Fishes. *International Review of Cytology* **168**, 187-257.

Polakof, S., Panserat, S., Soengas, J. L. and Moon, T. W. (2012). Glucose metabolism in fish: a review. *Journal of Comparative Physiology, Part B* **182**, 1015-1045.

Reed, J. S., Smith, N. D. and Boyer, J. L. (1982). Hemodynamic effects on oxygen consumption and bile flow in isolated skate liver. *American Journal of Physiology* **242**.

Richards, J. G., Heigenhauster, J. F. and Wood, C. M. (2003). Exercise and recovery metabolism in the pacific spiny dogfish (Squalus acanthias). *Journal of Comparative Physiology, Part B* **173**, 463-474.

Roberts, M. S., Ballinger, L. N. and Weiss, M. (1998). Relative Dispersions of Intra-albumin Transit Times across Rat and Elasmobranch Perfused Livers, and Implications for Intra- and Inter-species Scaling of Hepatic Clearance using Microsomal Data. *Journal of Pharmacy and Pharmacology* **50**, 865-870.

Shuttleworth, T. J. and Goldstein, L. (1984). β-Alanine transport in the isolated hepatocytes of the elasmobranchRaja erinacea. *Journal of Experimental Zoology* **231**, 39-44.

Simmons, T. W., Hinchman, C. A. and Ballatori, N. (1991). Polarity of Hepatic Glutathione and Glutathione *S*-Conjugate Efflux, and Intraorgan Mercapturic Acid Formation in the Skate. *Biochemical Pharmacology* **42**, 2221-2228.

Smith, D. J., Grossbard, M., Gordon, E. R. and Boyer, J. L. (1987). Taurocholate uptake by isolated skate hepatocytes: effect of albumin. *The American Journal of Physiology* **252**, G479-G484.

Speers-Roesch, B. and Treberg, J. R. (2010). The unusual energy metabolism of elasmobranch fishes. *Comparative Biochemistry and Physiology, Part A* **155**, 417-434.

Sélley, E., Kun, S., Szijártó, I., Kertész, M., Wittmann, I. and Molnár, G. (2016). Vasodilator Effect of Glucagon: Receptorial Crosstalk Among Glucagon, GLP-1, and Receptor for Glucagon and GLP-1. *Hormone and Metabolic Research* **48**, 476-483.

Tesfamariam, B. and Cohen, R. A. (1992). Free radicals mediate endothelial cell dysfunction caused by elevated glucose. *Heart and Circulatory Physiology* **263**, H321-H326.

Vijayan, M. M., Foster, G. D. and Moon, T. W. (1993). Effects of cortisol on hepatic carbohydrate metabolism and responsiveness to hormones in the sea raven, *Hemitripterus americanus*. *Fish Physiology and Biochemistry* **12**, 327-335.

Weisiger, R. A., Zacks, C. M., Smith, N. D. and Boyer, J. L. (1984). Effect of Albumin Binding on Extraction of Sulfobromophthalein by Perfused Elasmobranch Liver: Evidence for Dissociation-Limited Uptake. *Hepatology* **4**, 492-501.

Wetherbee, B. M. and Nichols, P. D. (2000). Lipid composition of the liver oil of deep-sea sharks from the Chatham Rise, New Zealand. *Comparative Biochemistry and Physiolog*, *Part B* **125**, 511-521.

Wood, C. M., Walsh, P. J., Kajimura, M., McClelland, G. B. and Chew, S. F. (2010). The influence of feeding and fasting on plasma metabolites in the dogfish shark (*Squalus acanthias*). *Comparative Biochemistry and Physiology*, *Part A* **155**, 435-444.

Zammit, V. A. and Newsholme, E. A. (1979). Activities of Enzymes of Fat and Ketone-Body Metabolism and Effects of Starvation on Blood Concentrations of Glucose and Fat Fuels in Teleost and Elasmobranch Fish. *Biochemical Journal* **184**, 313-322.

Zeger, S. L. and Karim, M. R. (1991). Generalized Linear Models With Random Effects; A Gibbs Sampling Approach. *Journal of American Statistical Association* **86**, 79-86.

4. Chapter 4: Effects of corticosteroid and a catecholamine in the perfused liver of an elasmobranch, the North Pacific spiny dogfish, *Squalus suckleyi.*

4.1. Abstract

Hormonal influence on hepatic function is a critical aspect of whole-body energy balance in vertebrates. Catecholamines and corticosteroids both influence hepatic energy mobilization through glycogenolysis and gluconeogenesis. In elasmobranchs, determining hepatic energy balance may be complicated by this taxon's unique metabolic strategy of mobilizing and using ketone bodies and demonstrating relative glucose intolerance. Therefore, a liver perfusion for a shark species was used to investigate the effects of catecholamine (epinephrine [E]) and corticosteroid (corticosterone [B] and 11-deoxycorticosterone [DOC]) stimulation on hepatic glucose and ketone (3-hydroxybutyrate [3-HB]) balance in the North Pacific Spiny dogfish, *Squalus suckleyi*. Further, a second set of hormone perfusions were conducted to collect tissue samples for enzyme activity (3-hydroxybutyrate dehydrogenase, 3-HBDH [ketogenesis/ketolysis]; succinyl-CoA transferase, SCOT [ketolysis]; glycogen phosphorylase, GP [glycogenolysis]; and phosphoenolpyruvate carboxykinase, PEPCK [gluconeogenesis]) and mRNA transcript abundance (*glut1* and *glut4* [glucose transport], *mct1* and *mct2* [3-HB transport], and *gr* [glucocorticoid receptor]). There were no changes in the arterial-venous difference of either metabolite in all hormone perfusions. However, DOC increased *gr* transcript abundance and decreased flow rate of perfusions, suggesting a regulatory role for this corticosteroid. PEPCK activity increased following all hormone treatments, which may suggest gluconeogenic function; E also increased 3-HBDH activity and did not change SCOT activity, suggesting a function in ketogenesis. Interestingly, E did not cause any changes in flow rate or the arterial-venous difference of glucose, contrary to the known function of E in vertebrates. This may indicate an alternative mechanism of hepatic E function.

4.2. Introduction

In vertebrates the liver serves a fundamental role in macromolecule storage and catabolism. This is particularly important during the highly conserved role of hepatic metabolite mobilization following exposure to a stressor (Romero and Gormally, 2019; Romero and Butler, 2007). Immediate metabolite liberation from the liver occurs following catecholamine stimulation by

activating glycogenolysis and subsequent release of glucose (Kuo et al., 2015; Romero and Butler, 2007). In the medium to long term, increased circulating levels of corticosteroids target hepatic nuclear receptors to upregulate gluconeogenic pathways (Kuo et al., 2015; Romero and Butler, 2007), which enhances glucose mobilization, further fueling the animals response to a stressor; a response that is consistent across all vertebrate taxa thus far examined (Bouyoucos et al., 2021).

In mammals (Fischer et al., 1978) and to some degree in teleosts (Fabbri et al., 1998), catecholamines (epinephrine [E] and norepinephrine) primarily act through adrenergic receptors to regulate glycogenolysis by activating glycogen phosphorylase (GP) via cAMP and intracellular calcium (Ca^{2+}) pathways. Similar to more derived vertebrates, increased circulating levels of catecholamines induce hyperglycemia in elasmobranchs (deRoos and deRoos, 1978; Patent, 1970). However, previous work in skeletal muscle of the spiny dogfish, *Squalus acanthias*, suggests that elasmobranchs may demonstrate a more primitive mechanism of GP activation that only relies on Ca^{2+} and less on catecholamine stimulation (Fischer et al., 1978). To a lesser extent, catecholamines also increase gluconeogenesis in teleosts by inhibiting pyruvate kinase, thus increasing gluconeogenic precursors (Mommsen et al., 1988; Wright et al., 1989). However, very little is known if these pathways are similar in elasmobranchs.

Corticosteroids affecting glucose metabolism are broadly called glucocorticoids. In mammals and teleosts, glucocorticoids bind to nuclear glucocorticoid receptors (GR) to activate gluconeogenesis (Long, 1938; Newsholme and Start, 1973; Wendelaar Bonga, 1997). Elasmobranchs (e.g., sharks and rays) may operate in a similar manner; for example, four species of interenalectomized skates exhibited a decrease in hepatic glycogen as compared to controls, indicating an effect on glycogenesis (Hartman et al., 1944), possibly as a result of reduced glucocorticoid-mediated gluconeogenesis. However, glucocorticoids have not yet been identified in elasmobranchs and corticosteroids may serve a nonclassical role in this group and act to mobilize alternative fuel sources. For example, elasmobranchs have an increased reliance on ketone bodies, primarily 3-hydroxybutyrate (3-HB) and acetoacetate, as preferential extrahepatic fuels over fatty acids (Ballantyne, 1997; Speers-Roesch and Treberg, 2010; Zammit and Newsholme, 1979). Indeed, high activity of 3-hydroxybutyrate dehydrogenase (3-HBDH), an enzyme essential for ketogenesis and ketolysis, has been found in the hepatic tissue of several elasmobranch species (Speers-Roesch et al., 2006), as well as relatively low activity of phosphoenolpyruvate carboxykinase (PEPCK), a rate limiting enzymatic step for gluconeogenesis

(Ballantyne, 1997; Zammit and Newsholme, 1979) via the conversion of oxaloacetate in the citric acid cycle to phosphoenolpyruvate. However, hepatic PEPCK may also be involved in triglyceride derived ketogenesis, because of the rapid formation of phosphoenolpyruvate, which is hypothesized to be used for lipid synthesis (Anderson, 1990); although, this would require the reversal of PEPCK (Carlsen et al., 1988). Regardless, to date there is no direct evidence of corticosteroids acting on hepatic metabolite mobilization in elasmobranchs, which is a significant knowledge gap in our understanding of energy balance in this taxon.

Classical methods of determining hormonal action on metabolite mobilization include whole-organism hormonal injections and tissue-specific cell incubations. Intramuscular corticosterone (B) injections in *S. acanthias* (Patent, 1970) demonstrated a hyperglycemic effect. However, this was not the case following intravascular B injections in the North Pacific spiny dogfish, *Squalus suckleyi* (Chapter 2), although circulating plasma B correlated positively with glucose using the data across several treatment groups in this study (B also negatively correlated with 3-HB). These results suggest that B may mobilize hepatic glucose under certain conditions, although the mechanisms of action remain unclear. To gain further insight into hepatic function under hormonal stimulation, isolated hepatocytes have been used in multiple studies on teleosts (i.e. (Birnbaum et al., 1976; Danulat and Mommsen, 1990; Mommsen et al., 1987; Mommsen et al., 2001; Vijayan et al., 1993; Wright et al., 1989) and a single elasmobranch species (Mommsen and Moon, 1987); however, this has not been performed using corticosteroids or catecholamines in elasmobranchs and may in fact overestimate glucose production given the high rate of endogenous glycogen catabolism following hepatocyte isolation seen in teleosts (Mommsen, 1986). Additionally, isolating hepatocytes in elasmobranchs with a greater liver lipid content has proven difficult (Mommsen and Moon, 1987).

In the present study, we investigated the effect of corticosteroids, B and 11-deoxycorticosterone (DOC) and the catecholamine (E), on hepatic metabolite balance of key energy metabolites (glucose and 3-HB) using an *in situ* whole-liver perfusion (Chapter 3), in *S. suckleyi*. The advantages of liver perfusions over previously described techniques include direct administration of hormones to the living tissue, sampling of liver tissue immediately following hormonal administration, and avoiding the need to separate hepatocytes from the lipid dense tissue. E was chosen as a candidate catecholamine because of known hyperglycemic actions in elasmobranchs *in vivo* (deRoos and deRoos, 1978; Patent, 1970). The dominant corticosteroid, 1α-

hydroxycorticosterone (1α-OHB), is not currently available for experimental use, and thus B and DOC were chosen as candidate corticosteroids since both are presumed biosynthetic precursors of 1α-OHB (Anderson, 2012; Truscott and Idler, 1972). Ligand exploitation theory postulates that B and/or DOC, as precursors to 1α-OHB, may serve as alternative ligands that can activate the GR; indeed, previous work in *L. erinacea* shows that 1α-OHB activates the GR with the least sensitivity amongst circulating corticosteroids (Carroll et al., 2008), although this is coupled with 1α-OHB concentrations being consistently higher in circulation than other corticosteroids in a number of elasmobranch species (Anderson, 2012; Schoen et al., 2021; Truscott and Idler, 1972; Chapter 2). Both DOC and B activate the GR with about 3- and 16-fold greater sensitivity than 1α-OHB, respectively (Carroll et al., 2008); however, there is no direct evidence of these corticosteroids acting as glucocorticoids during the stress response.

Beyond hepatic metabolite handling, liver tissue was sampled post-hormonal perfusion to assess changes in enzyme activity associated with metabolite production and consumption. These included: GP as an indication of glycogenolysis; 3-HBDH as an indication of ketogenesis/ketolysis; succinyl CoA transferase [SCOT] as an indication of ketolysis; and PEPCK, as an indication of gluconeogenesis. Furthermore, mRNA transcript abundance of transporters involved in metabolite influx and efflux were examined with a focus on *glut1* and *glut4* as an indication of hepatic glucose transport (Deck et al., 2017); and *mct1* and *mct2* as an indication of hepatic 3-HB transport (Balmaceda-Aguilera et al., 2012). Finally, we examined mRNA transcript abundance for the glucocorticoid receptor (*gr*) as an indication of activation or suppression of glucocorticoid mediated pathways. We hypothesized that hormones would cause changes in hepatic metabolite balance; specifically, that B would cause an increase in hepatic glucose and a decrease in 3-HB mobilization, and that E would cause an increase in hepatic glucose mobilization. Furthermore, we hypothesized that these changes in metabolites would be reflected in appropriate enzyme activity and transcript abundance; specifically, that B would increase PEPCK activity and *glut* and *gr* transcript abundance, and decrease 3-HBDH activity and *mct* transcript abundance, and that E would increase GP activity and *glut* transcript abundance.

4.3. Methods

Fish Collection

Sixteen adult male (1.81-2.85kg) *S. suckleyi* were caught by rod and line in Barkley Sound, Vancouver Island, British Columbia, during July 2021 (n = 11) and 2022 (n = 5). Fish were housed in the Bamfield Marine Sciences Centre holding tank (155,000L) with flow-through seawater (12°C) and aeration, and fed North Pacific hake, *Merluccius productus*, *ad libitum* every other day. Fish were held in the holding tank and not fed for at least two days prior to experimentation. Experiments were completed in accordance with the Canadian Council of Animal Care standards, and with the approval of the Bamfield Marine Sciences Centre (RS-2019-03; RS-2021-06) and University of Manitoba (F19-006) animal care committees.

Liver Perfusions

Fish were immersed in an overdose of anesthetic ($0.2 g \cdot L^{-1}$ tricaine methanesulfonate (MS-222), Syndel Labs, Vancouver, British Columbia, Canada) until respiration and escape reflex ceased. Body mass to the nearest gram was recorded, and the cervical column was severed just posterior to the brain. *In situ* liver perfusions were conducted according to the protocol outlined in Chapter 3 with minor changes. Inflowing elasmobranch Ringer's solution (257mM NaCl, 7mM Na_2SO_4, 3mM $MgSO_4$, 4mM KCl, 2mM $CaCl_2$ dihydrate, 0.1mM Na_2HPO_4, 6mM $NaHCO_3$, 400mM urea, 80mM TMAO, 2mM glucose, 1mM 3-HB, 0.2mM alanine, 0.03mM glutamine, pH 7.8) was perfused into the liver via a PE160 cannula placed in the hepatic vein from a constant pressure head placed 28cm above the liver preparations, which was maintained by a peristaltic pump. The pressure head was equivalent to the reported resting mean arterial pressure in this species (Swenson et al., 2005). As the height of the pressure head changed, the speed of the pump was altered to sustain the 28cm pressure head; thus, the speed of the pump was used to calculate the changes in inflow rate. Additionally, inflow Ringer's solution was supersaturated with a specialty gas mix of 99.7% O_2 and 0.3% CO_2. Outflowing perfusate was collected from the sinus venosus via a PE240 cannula threaded through the atrium and conus arteriosus of the heart and placed in the sinus venosus. Prior to experimentation, livers were perfused for 50min with heparinized Ringer's solution (50 $IU \cdot mL^{-1}$ sodium heparin) until outflow was visually clear of blood. Following heparization, non-heparinized Ringer's solution was perfused into preparations for 50min to determine baseline responses of the preparation. In total, each liver preparation was perfused for no more than 160min as the previous study in Chapter 3 demonstrated viability of the preparation for at least 180min.

Series A: Effect of Corticosteroid and E Perfusion on Metabolites

Series A was conducted using the methods outlined in Chapter 3, where preparations were perfused with known concentrations of hormone, and outflow rate and concentrations of key metabolites (glucose and 3-HB) were determined and compared to values with Ringer only (initial baseline). One μM B (n = 5-6), 10nM DOC (n = 5), or 50nM E (n = 5) were perfused into liver preparations for 15min. These hormone concentrations were determined as approximately double the measured circulating concentrations of B (Chapter 2) in *S. suckleyi* and E in (Opdyke et al., 1982) *S. acanthias* following respective stress events, and DOC in several elasmobranch species (Truscott and Idler, 1972). Since corticosteroids were dissolved in ethanol, a vehicle control of 0.034% ethanol in Ringer's solution was tested in the same preparations as corticosteroids. Delivery of corticosteroids and vehicle control was randomized to avoid order effects on the measured variables. Following treatment, Ringer's solution only was perfused for another 30min in corticosteroid and vehicle control treatments and 15min in the E treatment. Outflow was collected every 15min in 50mL Falcon tubes. Outflow flow rate was determined gravimetrically, assuming a specific gravity of Ringers as $1.03 g \cdot mL^{-1}$. One mL of outflow was centrifuged (1min, 13,000g) and the supernatant was frozen at -20°C for metabolite analysis.

Finally, in corticosteroid treatments, oxygen consumption of liver tissue was recorded and calculated in the same manner as Chapter 3 using oxygen probes (430μm Bare fiber oxygen microsensor, FireStingO2, PyroScience, Graz, Austria) to measure percent oxygen saturation with Pyro Workbench software (V1.2.3.1406, PyroScience, Graz, Austria). Probes were situated in the inflow reservoir and an airtight 1.7mL cryovial at the outflow cannula. Using the equations in Mortimer (1956), percent oxygen saturation was converted to dissolved oxygen concentrations (DO; mg $O_2 \cdot mL^{-1}$), assuming 1atm at sea-level and 12°C of Ringer (temperature controlled using a constant flow-through seawater bath). Oxygen consumption (ng $O_2 \cdot min^{-1} \cdot$g wet mass of $liver^{-1}$) was modified from Fick's principle (Equation 1).

Equation 1. Modified Fick's equation for oxygen consumption of liver perfusion.

$$Oxygen\ Consumption = \left(Outflow\ \left(\frac{mL}{min}\right) * \left(DO\ Inflow\ \left(\frac{ng\ O_2}{mL}\right) - DO\ Outflow \left(\frac{ng\ O_2}{mL}\right)\right)\right) / \ Liver\ Wet\ Mass\ (g)$$

Series B: *Effect of Corticosteroid and E Perfusion on Enzyme Activity and mRNA Transcript Abundance*

This set of experiments was performed to investigate hormonal influence on hepatic enzyme activity and mRNA transcript abundance of candidate proteins and genes, respectively, likely involved in regulating hepatic glucose and 3-HB balance. Liver perfusions were conducted as described above, then perfused with corticosteroids or E for 15min, followed by a 15min perfusion of Ringer only. Perfusions were then terminated and a sample of liver tissue was removed from the directly cannulated lobe, approximately halfway between the bifurcation of the lobes and the terminal end of the lobe. Tissue was immediately frozen in liquid nitrogen for enzyme activity or stored in RNALater per the manufacturer's instructions (ThermoFisher Scientific, Waltham, MA, USA) for subsequent molecular analysis. Samples were also collected from a control treatment (n = 6) where fish were immediately sampled following sacrifice in anesthetic (livers were not perfused).

Glucose and 3-HB Assays

Outflow and inflow samples were assayed for metabolites (glucose and 3-HB) as previously described in Schoen et al. (2021). In brief, an enzymatic hexokinase assay was used to determine glucose concentrations and an enzymatic 3-HBDH assay was used to determine 3-HB concentrations from inflow and outflow samples of the perfused livers. All samples were run in duplicate and measured at 340nm for 50min (glucose assays) or 120min (3-HB assays) using a Powerwave spectrophotometer and Gen5 software (Powerwave XS2, Biotek, Winooski, VT, USA). The difference between inflow and outflow metabolite concentration was denoted the A-V difference (arterial-venous difference; Equation 2).

Equation 2. Metabolite consumption or production equation.

$$A - V\ Difference\ (mM) = (Inflow\ (mM) - Outflow\ (mM)) * -1$$

Enzyme Activity

Liver samples were assayed for maximal enzyme activity (Absolute U [nmol·min] ·mg protein) of GP, 3-HBDH, SCOT, and PEPCK. First, samples were homogenized in liquid nitrogen using mortar and pestle, and a subsample was homogenized with assay-specific ice-cold

homogenization buffer in a ceramic bead homogenizer for 30sec at speed 5 (Mini Bead Mill 4; VWR). The volume of homogenization buffer used was determined by a previously conducted serial dilution of a haphazardly chosen subset of samples within each tissue. All samples were centrifuged for 20min at 4°C (9,500 g), and then supernatants were centrifuged again at the same parameters to remove lipid constituents. Supernatants were flash frozen in liquid nitrogen for subsequent analysis. Immediately prior to assays, samples were thawed on ice and assay buffers were warmed to room temperature. Assays were conducted on 96-well plates, with each well containing 10μL sample and 200μL assay-specific buffer. Samples were assayed in duplicate, along with duplicate controls, and read kinetically (Powerwave XS2, Biotek) with Gen5 software (Biotek, Winooski, VT, USA) at room temperature. Assays were validated by assessing kinetic curves for linearity following addition of sample. The slope of the linear portion of the curve was used to determine maximum enzyme activity. Enzyme activity was standardized to protein concentration using a Bradford's protein assay as per the manufacturer's instructions (ThermoFisher Scientific, Waltham, MA, USA).

3-HBDH

3-HBDH activity was determined using the protocols in LeBlanc and Ballantyne (2000) and Speers-Roesch et al. (2006). Homogenization buffer: 50mM imidazole, 1mM EDTA, pH 7.4 at 20°C. Assay buffer: 50mM imidazole, 50mM nicotinamide, 2mM dithiothreitol, 11.25mM NAD^+, 0.03μg·mL^{-1} rotenone, 25mM 3-HB (omitted in control wells), pH 8 at 20°C. Assays were read at 340nm ($\in_{340}$, 6.22).

SCOT

SCOT activity was determined using the protocol in Moon and Mommsen (1987). Homogenization buffer: 50mM imidazole, pH 7.4 at 20°C. Assay buffer: 50mM imidazole, 5mM $MgCl_2$, 0.1mM acetoacetyl CoA, 1mM succinate (omitted in control wells), pH 8 at 20°C. Assays were read at 310nm ($\in_{310}$, 11.9).

GP

GP activity was determined using the protocols in Moon et al. (1999), Foster and Moon (1990), and Milligan (2003). Homogenization buffer: 50mM imidazole, 30mM ß-

mercaptoethanol, 5mM EDTA, 5mM EGTA, 100mM KF, 20ug·mL^{-1} aprotinin, pH 7.4 at 20°C. Assay buffer: 50mM phosphate buffer, 0.4mM NAD^+, 10uM glucose 1,6-biphosphate, 15mM $MgCl_2$, 0.25mM EDTA, 2mM AMP, 1.4IU·mL^{-1} phosphoglucomutase, 0.5IU·mL^{-1} G6PDH, 2mg·mL^{-1} dialyzed oyster glycogen (omitted in control wells), pH 7 at 20°C. Assays were read at 340nm ($\in_{340}$, 6.22).

PEPCK

PEPCK activity was determined using the protocol in Mommsen et al. (1980). Homogenization buffer: 50mM imidazole, 50mM KCl, 150mM sucrose, 1mM EDTA, pH 6.8 at 20°C. Assay buffer: 50mM imidazole, 20mM $NaHCO_3$, 0.5mM phosphoenolpyruvic acid, 1mM $MnCl_2$, 0.1mM NADH, 10IU malate dehydrogenase, 0.2mM dGDP (omitted in control wells). Assays were read at 340nm ($\in_{340}$, 6.22).

mRNA Transcript Abundance

mRNA transcript abundance for five genes of interest were investigated in liver samples: *glut1*, *glut4*, *mct1*, *mct2*, and *gr* RNA (1µg) was extracted from samples stored in RNALater with a PureLink RNA mini kit (Invitrogen, CA, USA) as specified by the manufacturer's instructions. Integrity of RNA was determined by gel electrophoresis and quantity by NanoDrop One (Thermofisher Scientific, MS, USA). RNA was treated with DNase I (Invitrogen, CA, USA) and cDNA was generated using Superscript III kits (Invitrogen, CA, USA) as specified by the manufacturer's instructions.

To identify the Pacific spiny dogfish glucocorticoid receptor sequence, glucocorticoid receptors in six chondrichthyan species were obtained from NBCI GenBank (https://www.ncbi.nlm.nih.gov/nuccore) or SkateBase (http://skatebase.org [Wyffels et al., 2014]): elephant shark, *Callorhinchus milii*, (AEF12274); Atlantic stingray, *Hypanus sabinus*, (AEF12278); little skate, *L. erinacea*, (ABD46744.1); Atlantic sharpnose shark, *Rhizoprionodon terraenovae*, (AEF12275); brownbanded bamboo shark, *Chiloscyllium punctatum*, (AEF12276); and small-spotted catshark, *Scyliorhinus canicula*, (AEF12277) (Carroll et al., 2011). Curated sequences were uploaded to MUSCLE (Edgar, 2004) for multiple sequence alignment and the ligand binding domain (LBD) was identified to be highly conserved across these species (Carroll et al., 2011). Thus, *gr* primers (Forward: TCCCATGATTTCGATCCTTGAG; Reverse:

GGTGAAACCGGAGCTGTT**)** were designed from the *S. canicula* LBD sequence only. Reverse transcriptase PCR was performed on *S. suckleyi* liver cDNA using the Phusion High-Fidelity PCR Kit (New England BioLabs, Ipswich, MA, USA) per the manufacturer's instructions with the following cycling conditions: 98°C for 30sec; 35 cycles of 98°C for 10sec, 58°C for 30sec, and 72°C for 30sec; and 72°C for 10min. The PCR product was then run on a 1X TAE gel and the ~750 base pair band was extracted and purified with a E.Z.N.A Gel Extraction kit (Omega Bio-Tek, GA, USA) per the manufacturer's instructions. The product was then shipped to The Centre for Applied Genomics, The Hospital for Sick Children (Toronto, Canada) for sequencing. The returned *S. suckleyi* glucocorticoid receptor sequence was then utilized to design quantitative real-time PCR (qPCR) primers (Table 1). qPCR primers for other genes of interest in *S. suckleyi* were obtained from Deck et al. (2016a,b). qPCR was performed in 96-well qPCR plates with a Bio-Rad CFXConnect qPCR machine (Bio-Rad Laboratories, CA, USA).

Gene specific primer efficiency was determined using a serial dilution slope equation. Genes of interest, primer sequences and concentrations, cycling conditions, and primer efficiencies are reported in Table 4.1. qPCR reactions contained 5μL SYBR Green master mix (Bio-Rad Laboratories, CA, USA), variable gene specific primer sets, 2.5μL cDNA (diluted 1:4 in nuclease-free water) and nuclease-free water to a total of 10 μL. Melt curves were added following the end of the cycling phase. Gene transcript abundance was normalized to the control treatment using NORMA-gene (Heckmann et al., 2011) and analyzed using the comparative C_t method (Schmittgen and Livak, 2008).

Statistical Analysis

Analysis within each hormone treatment and over time was conducted for each measured variable (oxygen consumption, flow rate, and respective A-V metabolite concentration) using linear mixed effects models ('lmer' function in 'lmer4' package) (Bates et al., 2015). Individual liver perfusion identification was added as a random effect to account for repeated sampling (Zeger and Karim, 1991). Shapiro-Wilks and Levine's tests were used to assess normality and equal variance respectively in all models. Datasets were transformed using rank (DOC outflow rate, DOC inflow rate) or square-root (vehicle control inflow rate) transformations if assumptions were not met. For A-V glucose concentration in the E treatment, Grubbs outlier tests were conducted

on each timepoint, and it was determined that one fish was a statistical outlier; this fish was removed from this dataset.

Tukey's post-hoc tests ($\alpha = 0.05$; 'glht' function in 'multcomp' package) (Hothorn et al., 2008) were used on normally distributed data to determine significance of treatments across time. For oxygen consumption and metabolite balance, confidence intervals of mean estimates of fixed effects terms (95% confidence intervals) were produced from 1000 posterior simulations ('arm' package) (Gelman and Su, 2022; Hasler et al., 2016) to determine significance of timepoints from 0. Enzyme activity and gene transcript abundance were analyzed within the same treatment and against the control treatment using one-way ANOVA models with Tukey's post-hoc tests ($\alpha = 0.05$) (Hothorn et al., 2008). All models were subject to Shapiro-Wilks and Levine's tests to assess normality and equal variance, respectively. If these assumptions were not met, datasets were transformed using a rank (PEPCK activity, *glut1* transcript abundance, *glut4* transcript abundance, and *mct2* transcript abundance) or double square root (SCOT activity) transformation. All statistical analysis was conducted in R v.1.3.1093.

4.4. Results

Oxygen consumption of liver preparations perfused with corticosteroids in Series A was significantly elevated above 0 for the duration of experimentation, in both hormone exposure and vehicle control treatments (Figure 4.1; Table 4.2). There was a significant decrease in oxygen consumption at 30 and 45min following DOC perfusion, as compared to initial baseline (Figure 4.1B). Outflow rate significantly decreased from initial baseline immediately following DOC perfusion and recovered at 30min, after DOC perfusion (Figure 4.2B). Inflow rate also decreased significantly at 45min, as compared to 15min during DOC perfusion (Figure 4.2B). There were no changes in inflow or outflow rate in the B (Figure 4.2A), vehicle control (Figure 4.2C), or E treatments (Figure 4.2D).

There were no significant changes in either A-V glucose concentration ([A-V glucose]) or A-V 3-HB concentration ([A-V 3-HB]), with respect to initial baseline, in any corticosteroid, vehicle control, or E treatments (Figure 4.3 and 4.4). Furthermore, [A-V glucose] was not different from 0 in any treatment (Figure 4.3; Table 4.3). [A-V 3-HB] in all timepoints in DOC and vehicle control treatments were significantly less than 0 (Figure 4.4B, 4.4C; Table 4.4), showing that outflow 3-HB concentrations were less than inflow 3-HB concentrations. Similarly, [A-V 3-HB]

in the B treatment were significantly less than 0 in the initial baseline and at 30min (Figure 4.4A). However, [A-V 3-HB] was significantly elevated above 0 in all timepoints in the E treatment (Figure 4.4D; Table 4.4), indicating that outflow 3-HB concentrations were greater than inflow concentrations.

In Series B, 3-HBDH and PEPCK activity were significantly elevated in the E treatment, as compared to the control treatment (Figure 4.5A, 4.5D). PEPCK activity was also greater than the time 0 treatment in both B and DOC treatments (Figure 4.5D). SCOT and GP activity did not deviate from the time 0 treatment following any hormone exposure (Figure 4.5B, 4.5C). Finally, relative *glut1*, *glut4*, *mct1*, and *mct2* transcript abundance did not change in any treatment, with respect to the time 0 treatment (Figure 4.6A-4.6D). However, relative *gr* transcript abundance significantly increased after DOC perfusion, as compared to time 0 (Figure 4.6E).

4.5. Discussion

In the present study, we investigated catecholamine and corticosteroid-mediated hepatic metabolite balance in a shark species, *S. suckleyi*. Interestingly, there were no changes in [A-V glucose] or [A-V 3-HB] relative to initial baselines in either corticosteroid, vehicle control, or E treatments. These results are mirrored in the negligible changes in *glut* and *mct* transcript abundance, as compared to controls across all hormone treatments, suggesting limited change in influx or efflux of metabolites. However, there was an increase in *gr* transcript abundance following DOC perfusion, implying that DOC may serve a role in altering hepatic GR activity. DOC addition also decreased hepatic oxygen consumption and perfusion flow rate, further suggesting a regulatory role of this hormone.

Effects of B on Glucose and 3-HB

There was no effect of B on oxygen consumption, flow rate, or [A-V glucose] in liver preparations. Further, enzyme activities and molecule endpoints associated with glucose balance or glucocorticoid activity (*gr* transcript abundance) did not change. Previously, B increased after gillnet capture in bonnethead sharks, *Sphyrna tiburo* (Manire et al., 2007); in air-exposed and confined neonate blacktip reef sharks, *Carcharhinus melanopterus* (Schoen et al., 2021); in surgically-manipulated, air-exposed, and fasting Japanese banded houndsharks, *Triakis scyllium* (Iki et al., 2020); and in surgically-manipulated, anesthetized, and confined *S. suckleyi* (Chapter

2). Additionally, B injections resulted in hyperglycemia in *S. suckleyi* (Patent, 1970) and there was a significant, albeit weak, positive correlation between B and glucose in Chapter 2. However, in the aforementioned study, the authors were not able to directly replicate a hyperglycemic effect immediately following a B injection in *S. suckleyi*, which is consistent with the negligible change in outflow glucose concentrations following B perfusion in the present study.

There was no change in [A-V 3-HB], as well as enzyme and molecular endpoints associated with 3-HB balance, during B perfusion. This is contradicting to the results of Chapter 2, which demonstrated a significant negative correlation between plasma 3-HB and B concentrations in *S. suckleyi*. Although, an *in vivo* approach was taken in Chapter 2, thus B could have a negligible effect on 3-HB at the hepatic level, but a negative effect at the whole-animal level. The liver of elasmobranchs is the primary site of 3-HB production for extrahepatic use (Mommsen and Moon, 1987; Zammit and Newsholme, 1979), which has been shown to increase in *S. suckleyi* white muscle perfusions following exhaustive exercise (Richards et al., 2003) and brain perfusions during fasting (deRoos, 1994). Potentially the negative relationship between B and 3-HB is a result of uptake by these tissue types.

Feeding status also plays a significant role in plasma 3-HB balance in elasmobranchs (deRoos, 1994; Wood et al., 2010; Zammit and Newsholme, 1979) and may influence the results of the present study. Given fish were offered food *ad libitum* and feeding was not monitored, fish could have very recently fed. As such one would predict hepatic 3-HB release and associated enzymatic and molecular markers to be lower than in starved individuals. Under starved conditions, we would predict that confidence intervals for [A-V 3-HB] would be elevated above 0, suggesting a significant release of 3-HB (Chapter 3), which was consistent with [A-V 3-HB] in the E treatment; however, this was not the case for either corticosteroid or vehicle control treatment. In fact, these treatments were either not significantly different or significantly less than 0, indicating hepatic consumption or reduced production. While the elasmobranch liver is not considered a ketone body consuming tissue, there is still evidence of consumption via SCOT activity (Moon and Mommsen, 1987; Zammit and Newsholme, 1979); although, this enzyme has not yet been shown to change in the liver with feeding status nor is it significantly elevated compared to controls in any hormone treatments in this study and liver mitochondria in *L. erinacea* did not oxidize acetoacetate (Moyes et al. 1986).

Finally, there was an increase in PEPCK activity following perfusion with B, compared to controls, which is an expected indicator of gluconeogenic function of glucocorticoids (Mommsen et al., 1999; Romero and Butler, 2007). However, *gr* transcript abundance did not change after B exposure, suggesting that an alternate mechanism may be employed to increase PEPCK activity rather than the classic glucocorticoid activation via the GR. Further, given the lack of an increase in [A-V glucose] following B perfusion, gluconeogenic substrates may be to preferentially used to increase glycogen reserves rather than directly mobilize glucose (Romero and Beattie, 2022).

Effects of DOC on Glucose and 3-HB

The function of DOC is unknown in elasmobranchs, as no studies have performed DOC injections *in vivo* nor are there any reports of circulating levels of DOC in elasmobranchs. There was a significant decrease in oxygen consumption within 15min following DOC perfusion. In contrast, the dominant circulating corticosteroid in teleosts, cortisol, has been shown to increase whole-body oxygen consumption in the Japanese eel, *Anguilla japonica* (Chan and Woo, 1978) and coastal cutthroat trout, *Oncorhynchus clarkii clarkii* (Morgan and Iwama, 1996), as well as transiently *in vivo* (De Boeck et al., 2001) and in homogenized liver tissue (Pfalzgraff et al., 2022) in rainbow trout, *Oncorhynchus mykiss*. However, whole-body oxygen consumption was unchanged 24hrs after cortisol implantation in coho salmon, *Oncorhynchus kisutch*, inferring that cortisol may act synergistically with other mechanisms to alter metabolic rate (Davis and Schreck, 1997). Here, it is curious that DOC decreases hepatic oxygen consumption, which would infer inhibition of metabolic processes by the corticosteroid. As a proposed biosynthetic precursor of 1α-OHB, it may be that there are opportunistic functional roles for DOC, although further research is needed to confirm if this is the case.

Additionally, there was a significant decrease in outflow rate, relative to initial baseline, during DOC perfusion and in inflow rate 30min following DOC perfusion. A change in flow rate may indicate that DOC exerts a hemodynamic effect, although it is not known if this is a result of a direct interaction of this hormone with a corticosteroid receptor or an indirect mechanism of regulation. DOC did not alter [A-V glucose] in the present study; however, similar to B, an increase in PEPCK activity was noted. Further, there was a significant increase in *gr* transcript abundance following DOC perfusion, as compared to controls. As previously stated, the classic vertebrate stress response results in the release of glucocorticoids to augment glucose mobilization, primarily

by activating nuclear glucocorticoid receptors (Bouyoucos et al., 2021). However, glucocorticoids are also primarily responsible for restoring glycogen stores depleted by catecholamine stimulation rather than increasing plasma glucose concentrations (Romero and Beattie, 2022). This is not to say that under longer-term stress situations that glucocorticoids do not serve a critical role in metabolite balance, but in the present study, a 15min perfusion of DOC may have signaled to upregulate *gr* to restore hepatic glycogen stores through gluconeogenesis prior to mobilization of metabolites extrahepatically. Alternatively, there may be a corticosteroid threshold to activate the GR, as suggested in some teleosts (Vijayan et al., 1991). DOC may have initiated the transcription of *gr* but there may not have been a high enough DOC concentration or long enough perfusion to fully activate the glucocorticoid response and release glucose extrahepatically.

Effects of E on Glucose and 3-HB

Curiously, E, which is a potent vasoconstrictor in elasmobranchs (Opdyke and Holcombe, 1978; Wyman and Lutz, 1932) did not alter inflow or outflow rate. Further, E did not cause a change in [A-V glucose], which is supported by the lack of a change in enzymatic GP activity following E perfusion (Fabbri et al., 1998; Mommsen et al., 1988). In mammals, GP activation requires both activation by intracellular Ca^{2+} and cAMP phosphorylation (Exton, 1987; Fischer et al., 1978), which is stimulated by catecholamines binding to hepatic adrenergic receptor subtypes (α and β) (Fischer et al., 1978). While both α- (Fabbri et al., 1994; Zhang et al., 1992) and β-adrenergic (reviewed in Fabbri et al. 1998) pathways have been detected in teleost species and catecholamines stimulate hepatic glucose production, it is unclear as to what degree a hepatic adrenergic system may serve in glycogenolysis given inconsistencies across species (Fabbri et al., 1998). In elasmobranchs, the connection between catecholamines and hepatic glycogenolysis remains undescribed and is hypothesized to only involve Ca^{2+} pathways (Fischer et al., 1978), which would potentially represent a more ancient method of GP activation. However, an α-adrenergic agonist, phenylephrine, did not increase intracellular Ca^{2+} in isolated little skate, *L. erinacea*, hepatocytes, inferring the absence of α-adrenergic receptors in hepatocytes (Nathanson and Mariwalla, 1996). However, it was determined that both α- and β-adrenergic receptor mRNA transcripts were present in liver tissue used in this study (data not shown; rtPCR using primers designed from a *S. acanthias* α-adrenergic receptor sequence [NCBI GenBank, ES606805.1] and β-adrenergic receptor sequence [NCBI Genbank, EE721839.1]. Since liver tissue in the present

study is not isolated to a specific cell type, such as the hepatocyte in Nathanson and Mariwalla (1996), it might be possible the absence of a change in [A-V glucose] following E perfusion suggests that this hormone might act on other cell types present within the liver tissue (e.g. neural tissue innervating the liver) that may be inactivated as a result of the *in situ* methodology.

E stimulation also induced an increase in PEPCK activity. Catecholamine-mediated gluconeogenesis has been observed in teleosts (Janssens and Waterman, 1988; Mommsen et al., 1988; Wright et al., 1989) , although likely to a lesser degree than glycogenolysis. However, in the present study, no change in GP activity suggests that E may have induced gluconeogenic pathways preferentially. Interestingly, there was no change in [A-V 3-HB], but there was an increase in 3-HBDH activity following E exposure. While little is known about the direct effect of catecholamines on ketone body mobilization in elasmobranchs, E did cause an increase in hepatic lipolysis in the nurse shark, *Ginglymostoma cirratum* (Lipshaw et al., 1972), which is a preliminary step in ketogenesis. Thus, an increase in 3-HBDH activity would be consistent with an increase in ketogenesis. Indeed, all confidence intervals for [A-V 3-HB] in the E treatment were significantly elevated above 0, inferring that there was a net release of 3-HB, which would explain the elevated 3-HBDH activity.

4.6. Conclusion

Here, we used a liver perfusion in a shark species to investigate the effects of corticosteroids and catecholamines on hepatic metabolite balance. Hormonal stimulation provides equivocal results as to the function of corticosteroids in metabolite balance; although DOC does increase *gr* transcript abundance, which might indicate an effect on metabolite balance that may be elucidated over a longer perfusion time. DOC may also serve to regulate flow rate and oxygen consumption. In addition, the lack of a glucose or flow rate response to E perfusion may indicate an alternative method of catecholamine-mediated glycogenolysis, as compared to more derived vertebrates; E may also play a role in hepatic lipolysis and ketogenesis. It is important to note that the liver in all vertebrates is a significant source of energy, and thus the A-V metabolite differences may have been complicated by the self-contained production and consumption of these metabolites, of which additional enzyme and molecular endpoints may elucidate. Finally, it may be critical to determine appropriate feeding status of fish prior to establishing this preparation in

order to provide clear insight into the efficacy and physiological relevance of these hormones in regulating hepatic metabolic processes.

4.7. Acknowledgements

The authors thank Bamfield Marine Science Centre for the use of facilities and financial assistance to A.N.S. through the Dick and Leona Peter Student Bursary, and to Ryan Wahl and for assistance with sample collection. Further, we thank the additional funding sources of the Natural Science and Engineering Research Council of Canada (NSERC) Discovery grant awarded to W.G.A. the University of Manitoba Graduate Fellowship awarded to A.N.S., a NSERC PDF awarded to A.R.W., and the University of Manitoba Faculty of Science Field work support program. We also would like to acknowledge that the Bamfield Marine Sciences Centre sits within the traditional territory of the Huu-ay-aht First Nations and the University of Manitoba campuses are located on the original lands of the Anishinaabeg, Cree, Oji-Cree, Dakota, and Dene peoples, and on the homeland of the Métis Nation.

4.8. Tables

Table 4.1. qPCR primer sequences, reaction conditions, efficiency, and sources.

Target Gene	Forward Primer	Reverse Primer	Primer Concentration	Cycling Conditions	Primer Efficiency	Source
glut1	AGTCGGATTGTT CGTCAACC	GCCGGAGTAGAT GCCAATAA	400nM	95°C for 10min, and 40 cycles of 95°C for 10sec and 60°C for 15sec	96.20%	(Deck et al., 2016b)
glut4	GTGGATGTGCGA TTCTGATG	GATGAAATTTGC GGTCCAGT	200nM	95°C for 3min, and 40 cycles of 95°C for 15sec, 58.5°C for 30sec, and 72°C for 30sec	107.91%	(Deck et al., 2016b)
mct1	CAGCAGTCTCCT GGTGAACA	AGTTGAAGGCGA GTCCAAGA	400nM	95°C for 10min, and 40 cycles of 95°C for 10sec and 60°C for 15sec	108.59%	(Deck et al., 2016a)
mct2	GTGAGGCCAAG GATCCAGTA	TCCCAGAAGTAC AGGGCAAC	200nM	95°C for 3min, and 40 cycles of 95°C for 15sec, 61.5°C for 30sec, and 72°C for 30sec	97.28%	(Deck et al., 2016a)

gr	CGGTCTTGGCTG GAGATCTTA	TGCATCCGTTCC TCATTGAG	400nM	95°C for 10min, and 40 cycles of 95°C for 10sec and 60°C for 15sec	104.56%	This paper

Table 4.2. Mean values and 95% confidence intervals of oxygen consumption. Bold rows indicate that 2.5-97.5% confidence intervals do not overlap 0.

Glucose Balance		(Relative to 0)		
Hormone		Mean	2.5%	97.5%
DOC	**Intercept**	**180.45**	**123.96**	**243.24**
	Timepoint 2	**161.15**	**99.85**	**220.95**
	Timepoint 3	**138.74**	**75.73**	**201.21**
	Timepoint 4	**137.13**	**77.60**	**200.14**
B	**Intercept**	**145.74**	**101.09**	**195.95**
	Timepoint 2	**184.19**	**137.63**	**232.28**
	Timepoint 3	**148.11**	**98.33**	**194.96**
	Timepoint 4	**143.95**	**91.69**	**193.66**
Ethanol Vehicle Control	**Intercept**	**154.54**	**114.83**	**194.92**
	Timepoint 2	**146.11**	**104.90**	**184.57**
	Timepoint 3	**140.86**	**100.54**	**179.82**
	Timepoint 4	**151.83**	**111.91**	**193.64**

Table 4.3. Mean values and 95% confidence intervals of glucose. Bold rows indicate that 2.5-97.5% confidence intervals do not overlap 0.

Glucose Balance		(Relative to 0)		
Hormone		Mean	2.5%	97.5%
DOC	Intercept	0.27	-0.21	0.76
	Timepoint 2	0.33	-0.13	0.82
	Timepoint 3	0.30	-0.18	0.78
	Timepoint 4	0.21	-0.27	0.71
B	Intercept	0.20	-0.51	0.86
	Timepoint 2	0.37	-0.36	1.08
	Timepoint 3	0.35	-0.38	0.98
	Timepoint 4	0.49	-0.28	1.16

Ethanol Vehicle Control	Intercept	0.27	-0.03	0.54
	Timepoint 2	0.21	-0.08	0.49
	Timepoint 3	0.17	-0.12	0.43
	Timepoint 4	0.25	-0.02	0.53
E	Intercept	0.24	-0.05	0.50
	Timepoint 2	0.24	-0.02	0.50
	Timepoint 3	0.20	-0.07	0.46

Table 4.4. Mean values and 95% confidence intervals of 3-HB. Bold rows indicate that 2.5-97.5% confidence intervals do not overlap 0.

3-HB Balance		(Relative to 0)		
Hormone		Mean	2.5%	97.5%
DOC	**Intercept**	**-0.43**	**-0.72**	**-0.14**
	Timepoint 2	**-0.49**	**-0.79**	**-0.20**
	Timepoint 3	**-0.41**	**-0.69**	**-0.11**
	Timepoint 4	**-0.44**	**-0.72**	**-0.14**
B	**Intercept**	**-0.36**	**-0.56**	**-0.15**
	Timepoint 2	-0.08	-0.28	0.15
	Timepoint 3	**-0.26**	**-0.47**	**-0.04**
	Timepoint 4	-0.15	-0.40	0.09
Ethanol Vehicle Control	**Intercept**	**-0.26**	**-0.44**	**-0.07**
	Timepoint 2	**-0.35**	**-0.53**	**-0.15**
	Timepoint 3	**-0.38**	**-0.55**	**-0.20**
	Timepoint 4	**-0.30**	**-0.48**	**-0.12**
E	**Intercept**	**1.43**	**0.87**	**2.00**
	Timepoint 2	**1.43**	**0.85**	**1.97**
	Timepoint 3	**1.46**	**0.94**	**2.01**

4.9. Figures

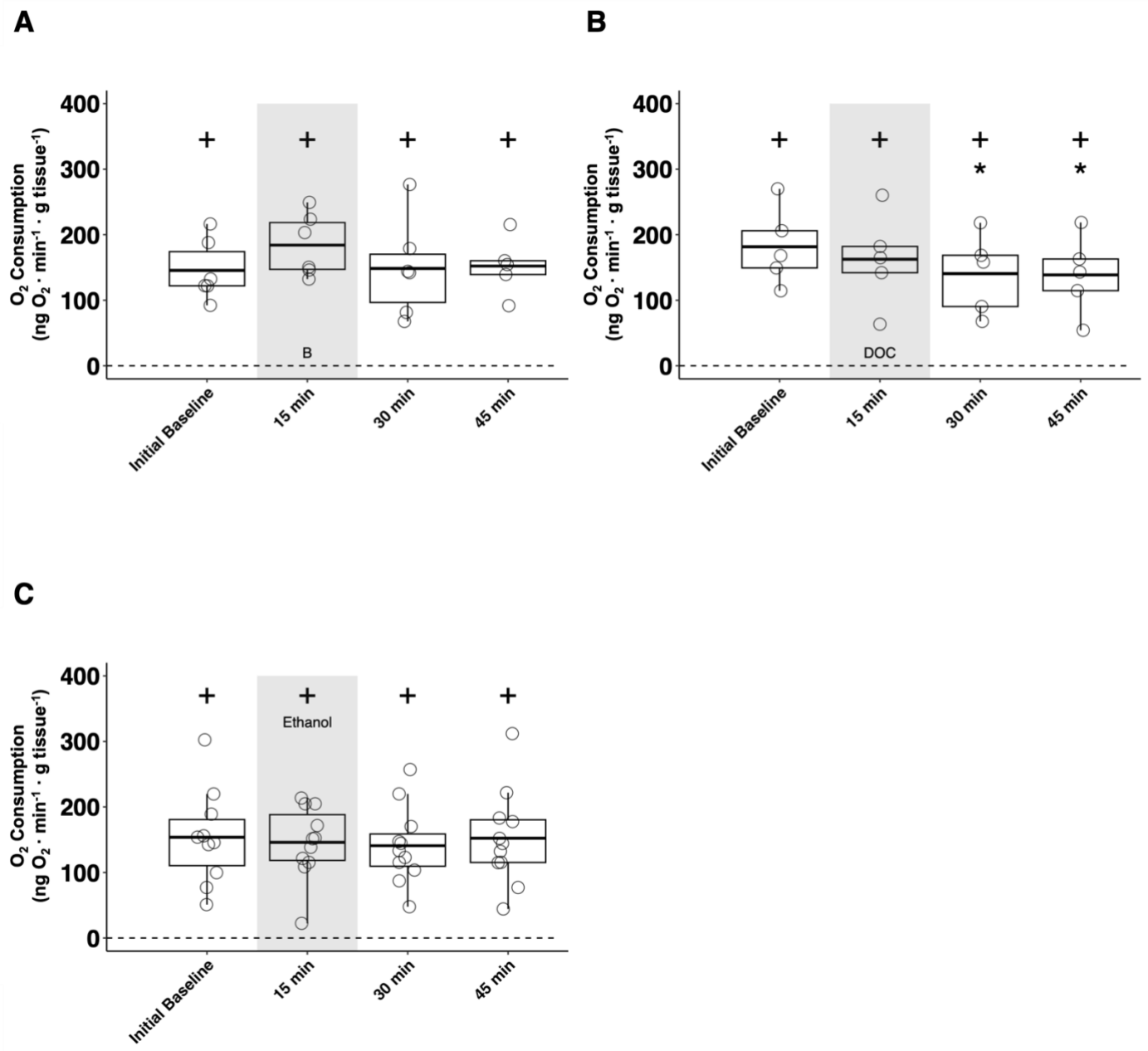


Figure 4.1. Effect of corticosteroid perfusion on oxygen consumption (ng $O_2 \cdot min^{-1} \cdot g$ wet $tissue^{-1}$) of *Squalus suckleyi* livers. A) 1μM B (n = 5-6). B) 10nM DOC (n = 5). C) 0.034% ethanol vehicle control (n = 10-11). Boxplots represent the mean (solid black line inside box), interquartile range (box edges), and maximum and minimum (box whiskers) of oxygen consumption data. Individual oxygen consumption values are represented by open circles. Boxplots represent the mean (solid black line inside box), interquartile range (box edges), and maximum and minimum (box whiskers)

of oxygen consumption data. Shaded boxes indicate hormone perfusion (15min), followed by Ringer's solution (30-45min). Statistical significance ($\alpha = 0.05$) of the mean oxygen consumption from initial baseline is indicated by an asterisk (*). Statistical significance of confidence intervals from 0 (dotted line) is indicated by a plus sign (+).

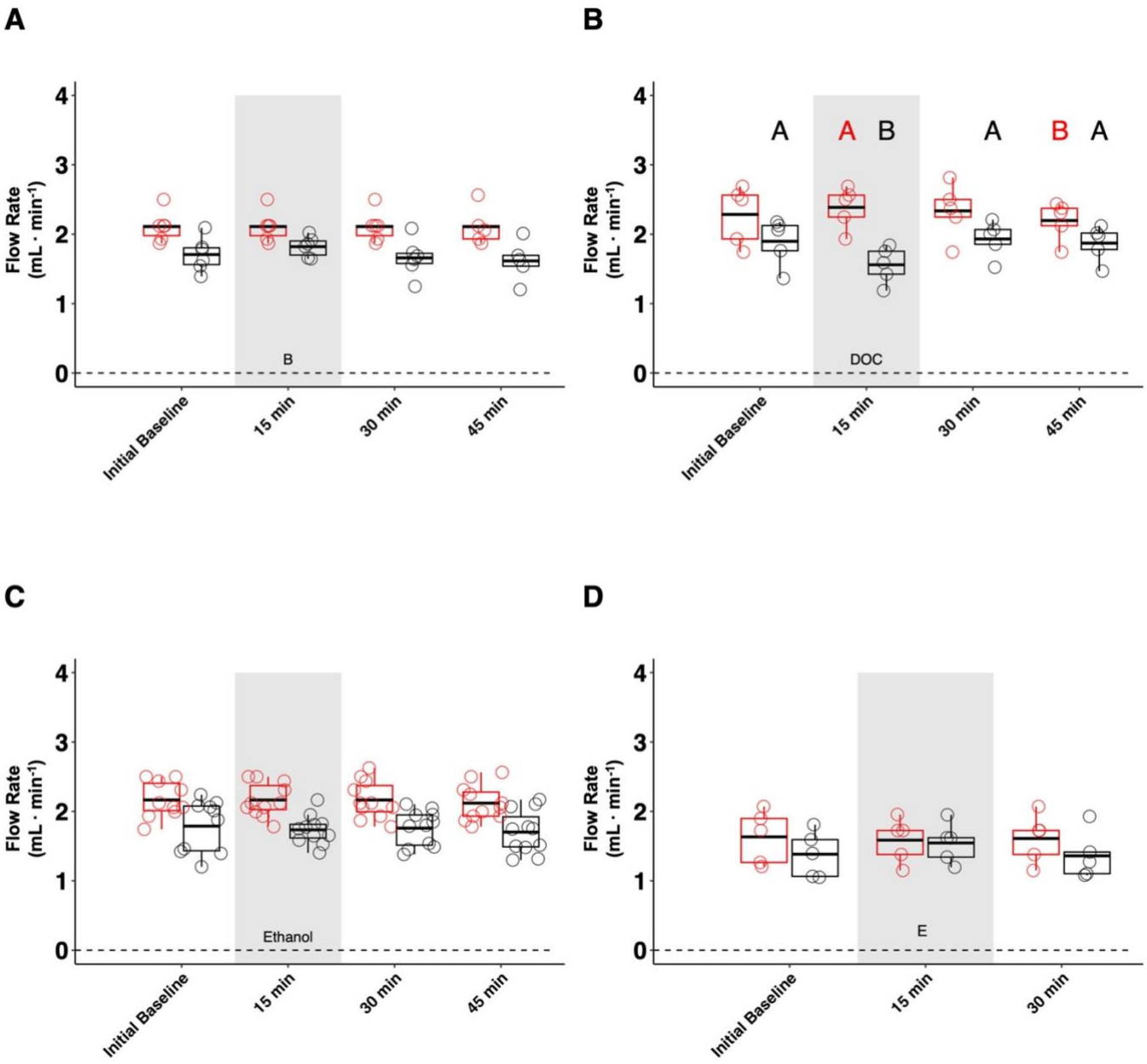


Figure 4.2. Effects of hormone perfusion on inflow ($mL \cdot min^{-1}$; red circles) and outflow rate ($mL \cdot min^{-1}$; black circles). A) 1μM B (n = 5-6). B) 10nM DOC (n = 5). C) 0.034% ethanol vehicle control (n = 10-11). D) 50nM E (n = 5). Boxplots represent the mean (solid black line inside box), interquartile range (box edges), and maximum and minimum (box whiskers) of flow rate data. Individual flow rate values are represented by open circles. Boxplots represent the mean (solid black line inside box), interquartile range (box edges), and maximum and minimum (box whiskers) of flow rate data. Shaded boxes indicate hormone perfusion (15min), followed by Ringer's solution

(30-45min). Statistical significance (α = 0.05) of the mean flow rate from initial baseline is indicated by a different letter (A or B), which is only compared within inflow or outflow over time.

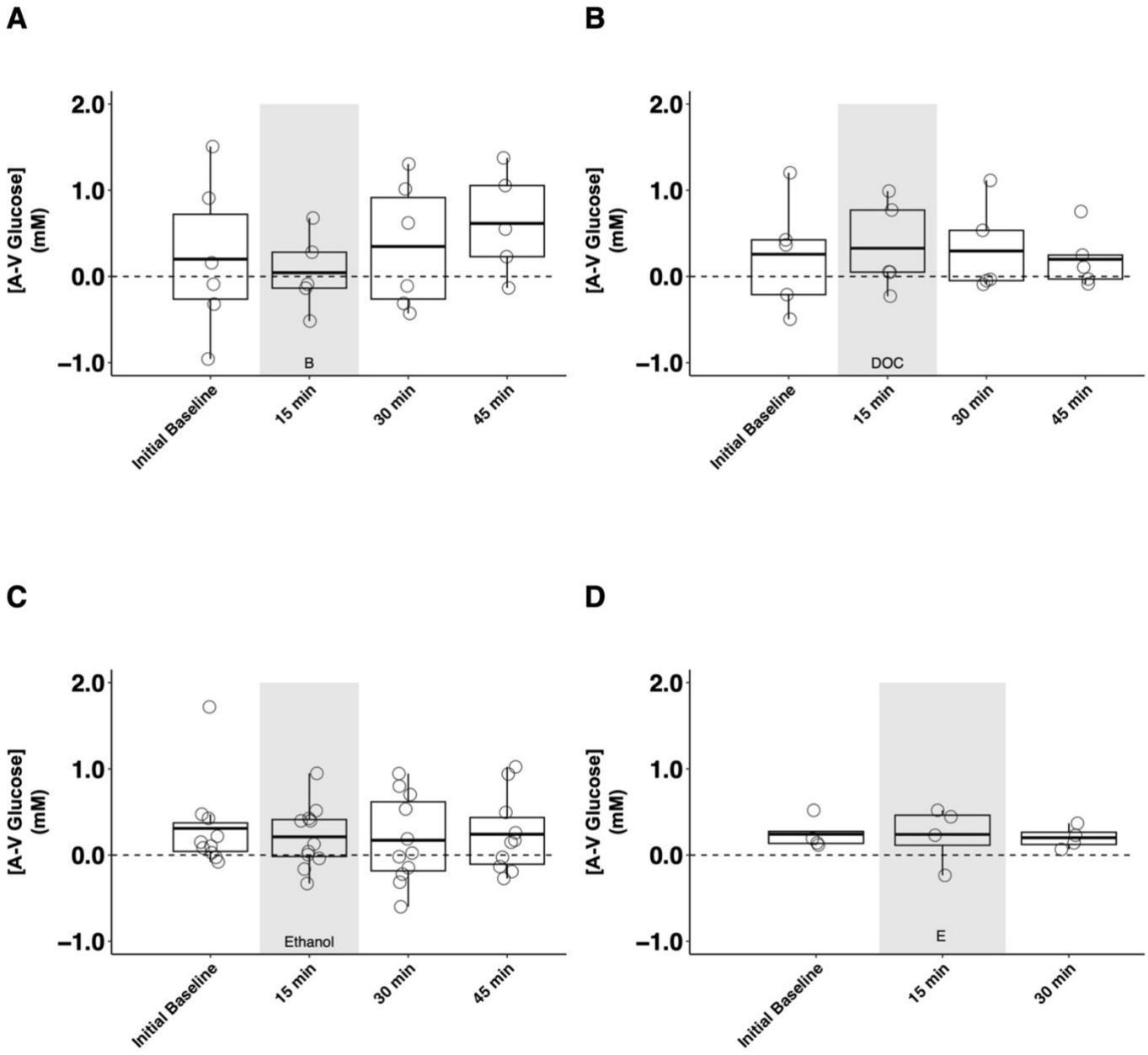


Figure 4.3. Effects of hormones on [A-V glucose] (mM). A) 1μM B (n = 5-6). B) 10nM DOC (n = 5). C) 0.034% ethanol vehicle control (n = 10-11). E) 50nM E (n = 4). Boxplots represent the mean (solid black line inside box), interquartile range (box edges), and maximum and minimum (box whiskers) of [A-V glucose] data. Individual [A-V glucose] values are represented by open circles. Shaded boxes indicate hormone perfusion (15min), followed by Ringer's solution (30-45min). There is no statistical significance of mean [A-V glucose] from initial baseline or 0 (dotted line).

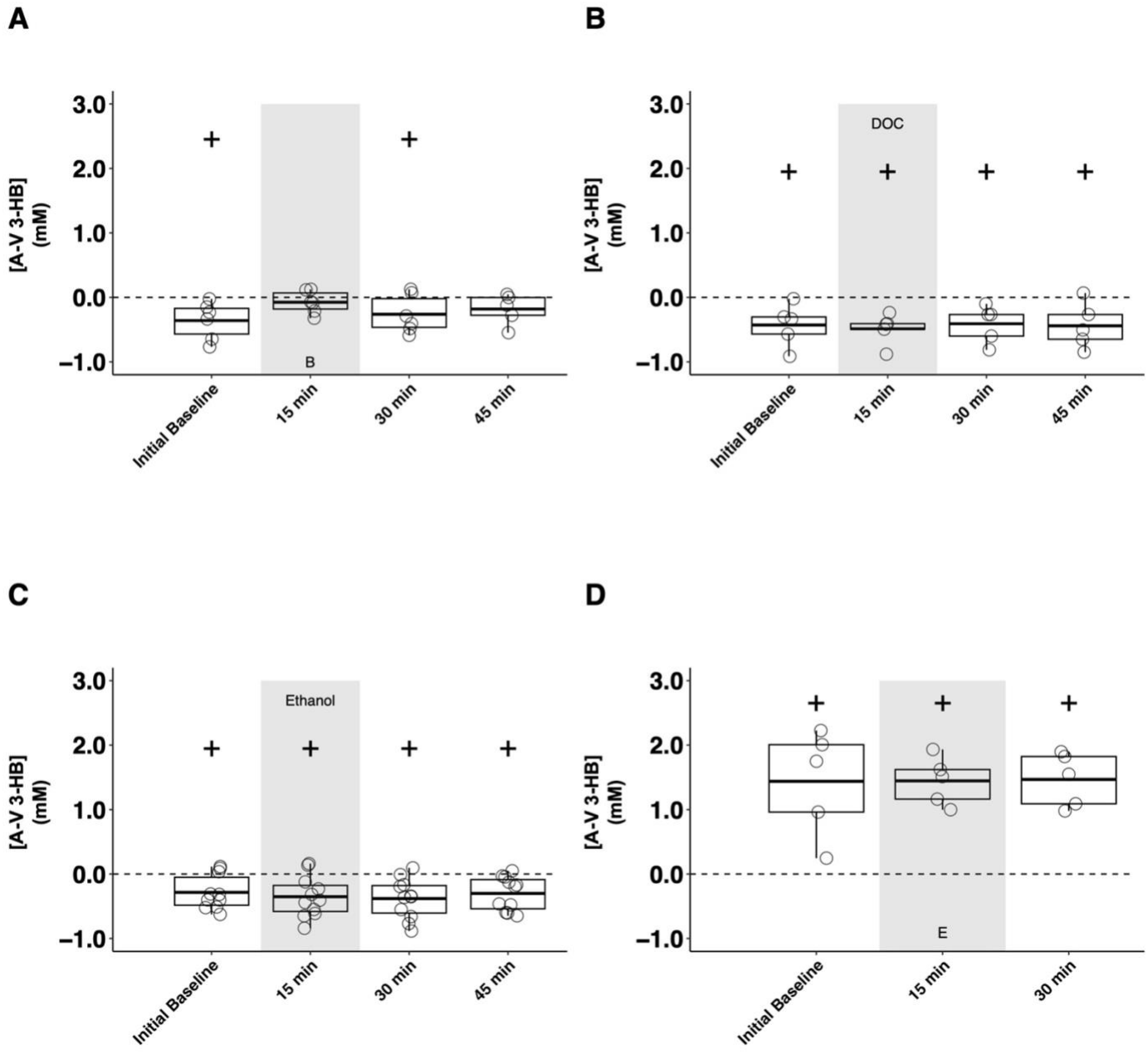


Figure 4.4. Effects of hormones on [A-V 3-HB] (mM). A) 1μM B (n = 5-6). B) 10nM DOC (n = 5). C) 0.034% ethanol vehicle control (n = 10-11). E) 50nM E (n = 5). Boxplots represent the mean (solid black line inside box), interquartile range (box edges), and maximum and minimum (box whiskers) of [A-V 3-HB] data. Individual [A-V 3-HB] values are represented by open circles. Shaded boxes indicate hormone perfusion (15min), followed by Ringer's solution (30-45min). There is no statistical significance the mean [A-V 3-HB] from initial baseline. Statistical significance of confidence intervals from 0 (dotted line) is indicated by a plus sign (+).

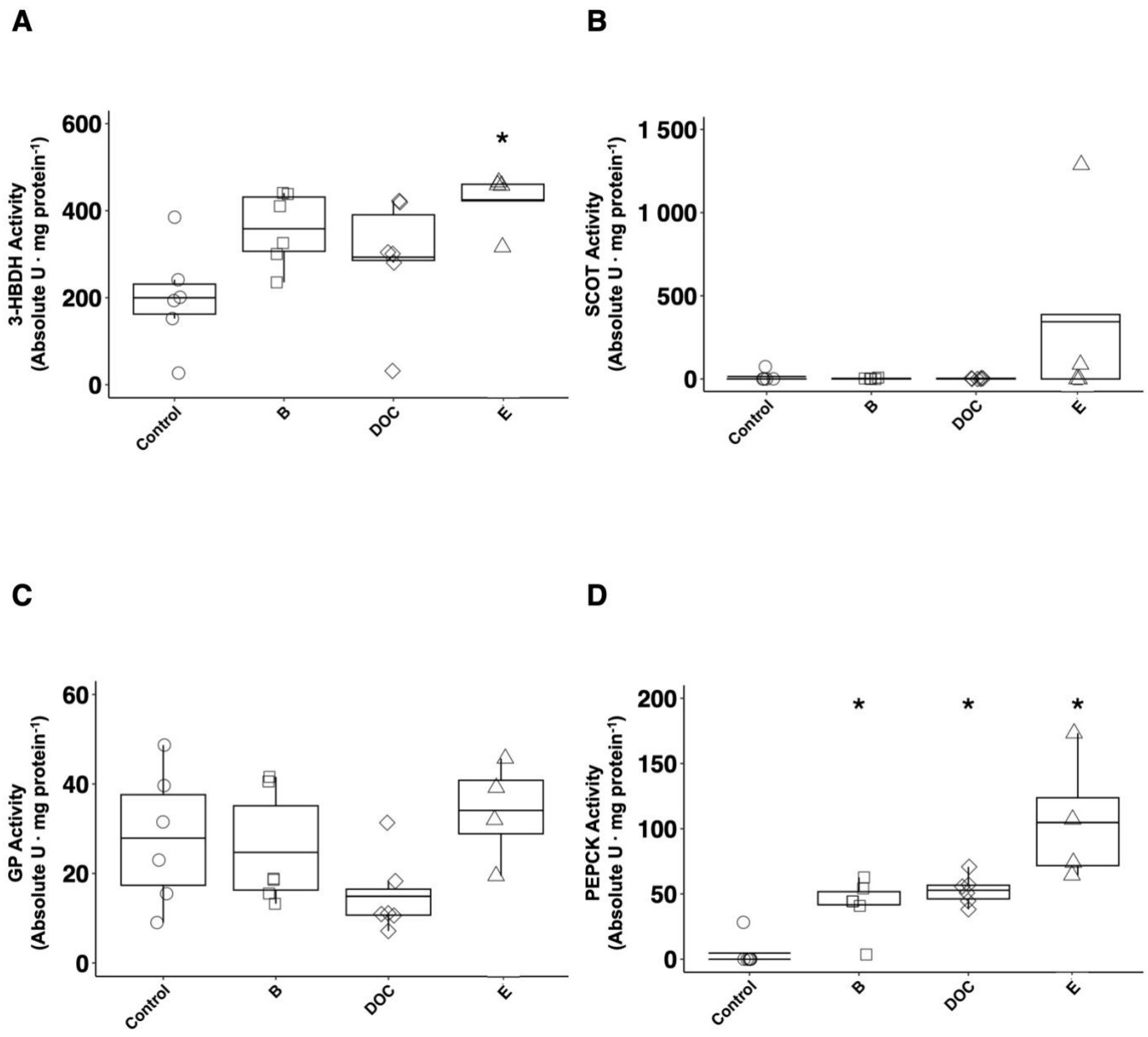


Figure 4.5. Effects of hormones on enzyme activity (absolute U·mg protein^{-1}) as compared to controls. A) 3-HBDH. B) SCOT. C) GP. D) PEPCK. Boxplots represent the mean (solid black line inside box), interquartile range (box edges), and maximum and minimum (box whiskers) of enzyme activity data. Individual enzyme activity values are represented by open circles. Statistical significance ($\alpha = 0.05$) of the mean enzyme activity from control is indicated by an asterisk (*).

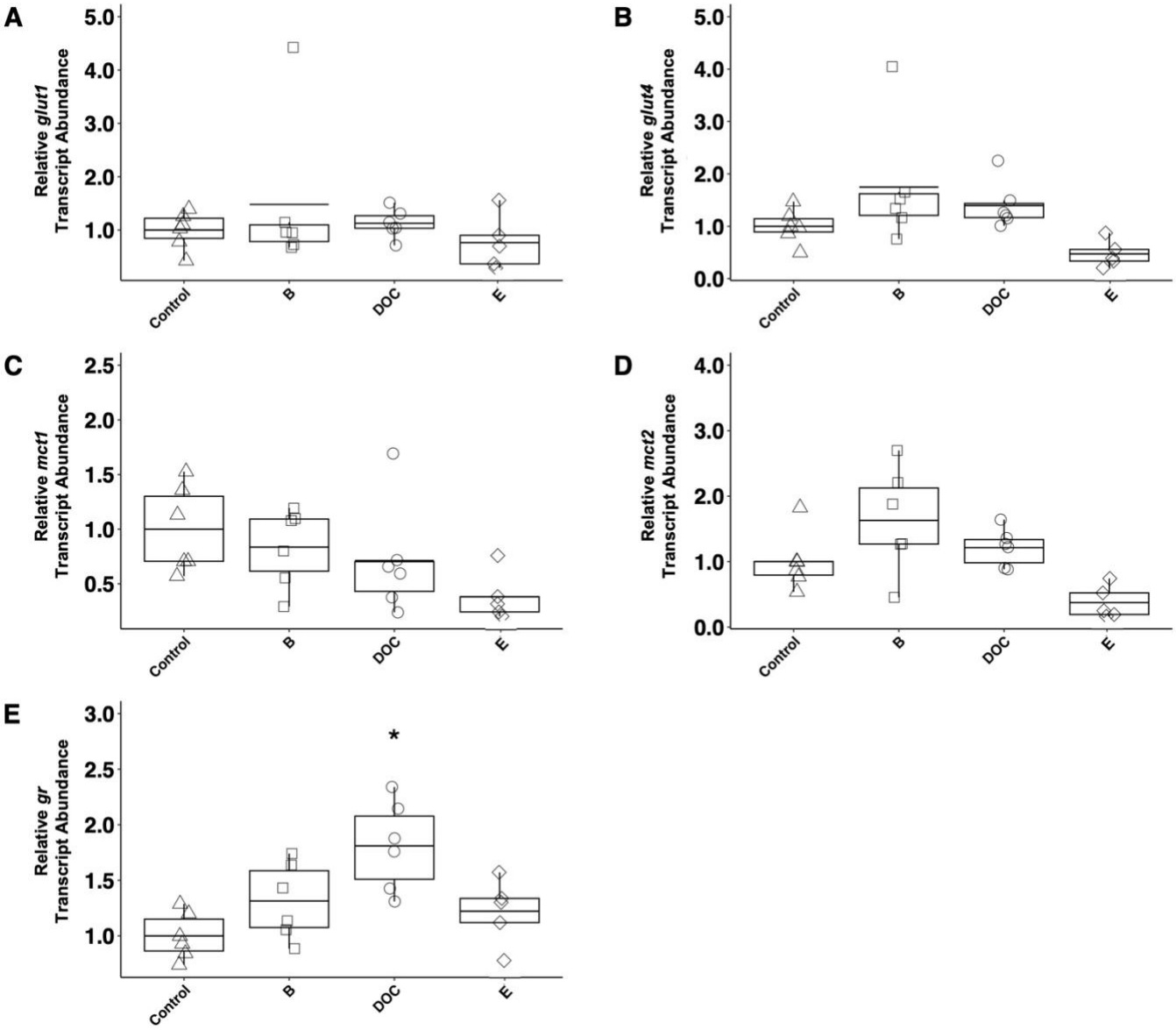


Figure 4.6. Effects of hormones on relative hepatic mRNA transcript abundance as compared to controls. A) *glut1*. B) *glut4*. C) *mct1*. D) *mct2*. E) *gr*. Boxplots represent the mean (solid black line inside box), interquartile range (box edges), and maximum and minimum (box whiskers) of transcript abundance data. Individual transcript abundance values are represented by open circles. Statistical significance (α = 0.05) of the mean relative transcript abundance from controls is indicated by an asterisk (*).

4.10. Works Cited

Anderson, P. M. (1990). Ketone Body and Phosphoenolpyruvate Formation by Isolated Hepatic Mitochondria From *Squalus acanthias* (Spiny Dogfish). *Journal of Experimental Biology* **254**.

Anderson, W. G. (2012). The endocrinology of 1α-hydroxycorticosterone in elasmobranch fish: A review. *Comparative Biochemistry and Physiology Part A: Molecular & Integrative Physiology* **162**, 73-80.

Armour, K. J., O'Toole, L. B. and Hazon, N. (1993). The effect of dietary protein restriction on the secretory dynamics of 1α-hydroxycorticosterone and urea in the dogfish, *Scyliorhinus canicula*: a possible role for 1α-hydroxycorticosterone in sodium retention. *Journal of Endocrinology* **138**, 275-282.

Ballantyne, J. S. (1997). Jaws: The Inside Story. The Metabolism of Elasmobranch Fishes. *Comparative Biochemistry and Physiology*, **118B**, 703-742.

Balmaceda-Aguilera, C., Cortés-Campos, C., Cifuentes, M., Peruzzo, B., Mack, L., Tapia, J. C., Oyarce, K., García, M. A. and Nualart, F. (2012). Glucose Transporter 1 and Monocarboxylate Transporters 1, 2, and 4 Localization within the Glial Cells of Shark Blood-Brain-Barriers. *PloS One* **7**, e32409.

Bates, D., Mächler, M., Bolker, B. M. and Walker, S. C. (2015). Fitting Linear Mixed-Effects Models Using lme4. *Journal of Statistical Software* **67**.

Birnbaum, M. J., Schultz, J. and Fain, J. N. (1976). Hormone-stimulated glycogenolysis in isolated goldfish hepatocytes. *American Journal of Physiology* **231**, 191-197.

Bouyoucos, I. A., Schoen, A. N., Wahl, R. C. and Anderson, W. G. (2021). Ancient fishes and the functional evolution of the corticosteroid stress response in vertebrates. *Comparative Biochemistry and Physiology, Part A* **260**, 111024.

Carroll, S. M., Bridgham, J. T. and Thornton, J. W. (2008). Evolution of Hormone Signaling in Elasmobranchs by Exploitation of Promiscuous Receptors. *Molecular Biology and Evolution* **25**, 2643-2652.

Carroll, S. M., Ortlund, E. A. and Thornton, J. W. (2011). Mechanisms for the Evolution of a Derived Function in the Ancestral Glucocorticoid Receptor. *PLoS Genetics* **7**, e1002117 (1-7).

Carlsen, B. D., Lambeth, D. O., Ray, P. D. (1988). Synthesis of malate from phosphoenolpyruvate by rabbit liver mitochondria: implications for lipogenesis. *Biochimica et Biophysica Acta* **965**, 1-8.

Chan, D. K. O. and Woo, N. Y. S. (1978). Effect of Cortisol on the Metabolism of the Eel, *Anguilla japanica*. *General and Comparative Endocrinology* **35**, 205-2015.

Danulat, E. and Mommsen, T. P. (1990). Norepinephrine: A Potent Activator of Glycogenolysis and Gluconeogenesis in Rockfish Hepatocytes. *General and Comparative Endocrinology* **78**, 12-22.

Davis, L. E. and Schreck, C. B. (1997). The Energetic Response to Handling Stress in Juvenile Coho Salmon. *Transactions of the American Fisheries Society* **126**, 248-258.

De Boeck, G., Alsop, D. and Wood, C. (2001). Cortisol Effects on Aerobic and Anaerobic Metabolism, Nitrogen Excretion, and Whole-Body Composition in Juvenile Rainbow Trout. *Physiological and Biochemical Zoology* **74**, 858-868.

Deck, C. A., Anderson, W. G. and Walsh, P. J. (2017). Effects of glucose and insulin administration on glucose transporter expression in the North Pacific spiny dogfish (*Squalus suckleyi*). *General and Comparative Endocrinology* **247**, 46-52.

Deck, C. A., Bockus, A. B., Seibel, B. A. and Walsh, P. J. (2016a). Effects of short-term hyper- and hypo-osmotic exposure on the osmoregulatory strategy of unfed North Pacific spiny dogfish (*Squalus suckleyi*). *Comparative Biochemistry and Physiology, Part A* **193**, 29-35.

Deck, C. A., Lemoine, C. M. R. and Walsh, P. J. (2016b). Phylogenetic analysis and tissue distribution of elasmobranch glucose transporters and their response to feeding. *Biology Open* **5**, 256-261.

deRoos, R. (1994). Plasma ketone, glucose, lactate, and alanine levels in the vascular supply to and from the brain of the spiny dogfish shark (Squalus acanthias). *Journal of Experimental Zoology* **268**, 354-363.

deRoos, R. and deRoos, C. C. (1978). Elevation of Plasma Glucose Levels by catecholamines in Elasmobranch Fish. *General and Comparative Endocrinology* **34**, 447-452.

Edgar, R. C. (2004). MUSCLE: multiple sequence alignment with high accuracy and high throughput. *Nucleic Acids Research* **32**, 1792-1797.

Exton, J. H. (1987). Mechanisms of Hormonal Regulation of Hepatic Glucose Metabolism. *Diabetes/Metabolism Reviews* **3**, 163-183.

Fabbri, E., Capuzzo, A. and Moon, T. W. (1998). The role of circulating catecholamines in the regulation of fish metabolism: An overview. *Comparative Biochemistry and Physiology, Part C* **120**, 177-192.

Fabbri, E., Cristina Puviani, A., Ottolenghi, C. and Capuzzo, A. (1994). Identification of alpha-Adrenergic Receptors in Catfish Liver and Their Involement in Glucose Release. *General and Comparative Endocrinology* **95**, 457-463.

Fischer, E. H., Alaba, J. O., Brautigan, D. L., Kerrick, W. G. L., Malencik, D. A., Moeschler, H. J., Picton, C. and Pocinwong, S. (1978). Evolutionary aspects of the structure and regulation of phosphorylase kinase. In *Versatility of Proteins*, (ed. C. H. Li), pp. 133-149. New York, New York: Academic Press.

Gelman, A. and Su, Y.-S. (2022). arm: Data Analysis Using Regression and Multilevel/Hierarchical Models. https://cran.r-project.org/web/packages/arm/index.html

Hartman, F. A., Lewis, L. A., Brownell, K. A., Angerer, C. A. and Shelden, F. F. (1944). Effect of Interrenalectomy on Some Blood Constituents in the Skate. *Physiological Zoology* **17**, 228-238.

Hasler, C. T., Midway, S. R., Jeffrey, J. D., Tix, J. A., Sullivan, C. and Suski, C. D. (2016). Exposure to elevated *p*CO2 alters post-treatment diel movement patterns of largemouth bass over short time scales. *Freshwater Biology* **61**, 1590-1600.

Hazon, N. and Henderson, I. W. (1984). Secretory dynamics of 1a-hydroxycorticosterone in the elasmobranch fish, *Scyliorhimus canicula*. *Journal of Endocrinology* **103**, 205-211.

Heckmann, L.-H., Sørensen, P. B., Krogh, P. H. and Sørensen, J. G. (2011). NORMA-Gene: A simple and robust method for qPCR normalization based on target gene data. *BMC Bioinformatics* **12**, 250.

Hothorn, T., Bretz, F. and Westfall, P. (2008). Simultaneous Inference in General Parametric Models. *Biometrical Journal* **50**, 346-363.

Iki, A., Anderson, G., Deck, C. A., Ogihara, M. H., Ikeba, K., Kataoka, H. and Hyodo, S. (2020). Measurement of 1a-hydroxycorticosterone in the Japanese banded houndshark, *Triakis scyllium*, following expsure to a series of stressors. *Gen Comp Endocrinol* **292**, 113440.

Janssens, P. A. and Waterman, J. (1988). Hormonal Regulation of Gluconeogenesis and Glycogenolysis in carp (*Cyprinus carpio*) liver pieces cultured *in vitro*. *Comparative Biochemistry and Physiology, Part A* **91A**, 451-455.

Kuo, T., McQueen, A., Chen, T.-C. and Wang, J.-C. (2015). Regulation of Glucose Homeostasis by Glucocorticoids. *Advances in Experimental Medicine and Biology* **872**, 99-126.

Lipshaw, L. A., Patent, G. J. and P, F. P. (1972). Effects of Epinephrine and Norepinephrine on the Hepatic Lipids of the Nurse Shark, *Ginglymostoma cirratum*. *Hormone and Metabolic Research* **4**, 34-38.

Long, C. N. H. (1938). The Adrenal Cortex and Carbohydrate Metabolism. *Sigma Xi, The Scientific Research Society* **26**, 175-186.

Manire, C. A., Rasmussen, L. E. L., Maruska, K. P. and Tricas, T. C. (2007). Sex, seasonal, and stress-related variations in elasmobranch corticosterone concentrations. *Comparative Biochemistry and Physiology, Part A* **148**, 926-935.

Mommsen, T. P. (1986). Comparative gluconeogenesis in hepatocytes from salmonid fishes. *Canadian Journal of Zoology* **64**, 1110-1117.

Mommsen, T. P., Andrews, P. C. and Plisetskaya, E. (1987). Glucagon-like peptides activate hepatic gluconeogenesis. *FEBS Letters* **219**, 227-232.

Mommsen, T. P. and Moon, T. W. (1987). The Metabolic Potential of Hepatocytes and Kidney Tissue in the Little Skate, *Raja erinacea*. *Journal of Experimental Zoology* **244**, 1-8.

Mommsen, T. P., Moon, T. W. and Plisetskaya, E. (2001). Effects of Arginine on Pancreatic Hormones and Hepatic Metabolism in Rainbow Trout. *Physiological and Biochemical Zoology* **74**, 668-678.

Mommsen, T. P., Vijayan, M. M. and Moon, T. W. (1999). Cortisol in teleosts: dynamics, mechanisms of action, and metabolic regulation. *Reviews in Fish Biology and Fisheries* **9**, 211-268.

Mommsen, T. P., Walsh, P. J., Perry, S. F. and Moon, T. W. (1988). Interactive Effects of Catecholamines and Hypercapnia on Glucose Production in Isolated Trout Hepatocytes. *General and Comparative Endocrinology* **70**, 63-73.

Moon, T. W. and Mommsen, T. P. (1987). Enzymes of Intermediary Metabolism in Tissues of the Little Skate, *Raja erinacea*. *Journal of Experimental Zoology* **244**, 9-15.

Morgan, J. D. and Iwama, G. K. (1996). Cortisol-induced changes in oxygen consumption and ionic regulation in coastal cutthroat throut (*Oncorhynchus clarki clarki*) parr. *Fish Physiology and Biochemistry* **15**, 385-394.

Moyes, C. D., Moon, T. W., and Ballantyne, J.S. (1986). Oxidation of Amino Acids, Krebs Cycle Intermediates, Fatty Acids and Ketone Bodies by *Raja erinacea* Liver Mitochondria. *Journal of Experimental Zoology* **237**, 119-128.

Nathanson, M. H. and Mariwalla, K. (1996). Characterization and function of ATP receptors on hepatocytes from the little skate *Raja erinacea*. *American Physiological Society* **270**, R561-R570.

Newsholme, E. A. and Start, C. (1973). Regulation in metabolism. London and New York: Wiley Interscience.

Opdyke, D. F., Carroll, R. G. and Keller, N. E. (1982). Catecholamine release and blood pressure changes induced by exercise in dogfish. *American Journal of Physiology- Regulatory, Integrative and Comparative Physiology* **242**, R163-R408.

Opdyke, D. F. and Holcombe, R. F. (1978). Effect of angiotensins and epinephrine on vascular resistance of isolated dogfish gut. *American Journal of Physiology* **234**, R196-R200.

Patent, G. J. (1970). Comparision of Some Hormonal Effects on Carbohydrate Metabolism in an Elasmobranch (*Squalus acanthias*) and a Holocephalan (*Hydrolagus colliei*). *General and Comparative Endocrinology* **14**, 215-242.

Pfalzgraff, T., Lund, I. and Skov, P. V. (2022). Prolonged cortisol elevation alters whole body and tissue metabolism in rainbow trout (*Oncorhynchus mykiss*). *Comparative Biochemistry and Phsiology, Part A* **263**, 111098.

Richards, J. G., Heigenhauster, J. F. and Wood, C. M. (2003). Exercise and recovery metabolism in the pacific spiny dogfish (*Squalus acanthias*). *Journal of Comparative Physiology, Part B* **173**, 463-474.

Romero, L. M. and Beattie, U. K. (2022). Common myths of glucocorticoid function in ecology and conservation. *Journal of Experimental Zoolog,y Part A* **337**, 7-14.

Romero, L. M. and Gormally, B. M. G. (2019). How Truly Conserved Is the "Well-Conserved" Vertebrate Stress Response? *Integrative and Comparative Biology* **59**, 273-281.

Romero, M. L. and Butler, L. K. (2007). Endocrinology of Stress. *International Journal of Comparative Psychology* **20**, 89-95.

Schmittgen, T. D. and Livak, K. J. (2008). Analyzing real-time PCR data by the comparative CT method. *Nature Protocols* **3**, 1101-1108.

Schoen, A. N., Bouyoucos, I. A., Anderson, W. G., Wheaton, C. J., Planes, S., Mylniczenko, N. D. and Rummer, J. L. (2021). Simulated heatwave and fishing stressors alter corticosteroid and energy balance in neonate blacktip reef sharks, *Carcharhinus melanopterus*. . *Conservation Physiology* **9**, coab067.

Speers-Roesch, B., Ip, Y. K. and Ballantyne, J. S. (2006). Metabolic organization of freswater, euryhaline, and marine elasmobranchs: implications for the evolution of energy metabolism in sharks and rays. *Journal of Experimental Biology* **209**, 2495-2508.

Speers-Roesch, B. and Treberg, J. R. (2010). The unusual energy metabolism of elasmobranch fishes. *Comparative Biochemistry and Physiology, Part A* **155**, 417-434.

Sturm, A., Bury, N. R., Dengreville, L., Fagart, J., Flouriot, G., Rafestin-Oblin, M. E. and Prunet, P. (2005). 11-Deoxycorticosterone Is a Potent Agonist of the Rainbow Trout (*Oncorhynchus mykiss*) Mineralcorticoid Receptor. *Endocrinology* **146**, 47-55.

Swenson, K. E., Eveland, R. L., Gladwin, M. T. and Swenson, E. R. (2005). Nitric Oxide (NO) in Normal and Hypoxic Vascular Regulation of the Spiny Dogfish, *Squalus acanthias*. *Journal of Experimental Zoology* **303A**, 154-160.

Truscott, B. and Idler, D. R. (1972). Corticosteroids in Plasma of Elasmobranchs. *Comparative Biochemistry and Physiology, Part A* **41**, 41-50.

Vijayan, M. M., Ballantyne, J. S. and Leatherland, J. F. (1991). Cortisol-Induced Changes in Some Aspects of the Intermediary Metabolism of *Salvenlinus fontinalis*. *General and Comparative Endocrinology* **82**, 476-486.

Vijayan, M. M., Foster, G. D. and Moon, T. W. (1993). Effects of cortisol on hepatic carbohydrate metabolism and responsiveness to hormones in the sea raven, *Hemitripterus americanus*. *Fish Physiology and Biochemistry* **12**, 327-335.

Wendelaar Bonga, S. E. (1997). The Stress Response in Fish. *Physiological Reviews* **77**, 591-625.

Wood, C. M., Walsh, P. J., Kajimura, M., McClelland, G. B. and Chew, S. F. (2010). The influence of feeding and fasting on plasma metabolites in the dogfish shark (*Squalus acanthias*). *Comparative Biochemistry and Physiology, Part A* **155**, 435-444.

Wright, P. A., Perry, S. F. and Moon, T. W. (1989). Regulation of hepatic gluconeogenesis and glycogenolysis by catecholamines in rainbow trout during exvironmental hypoxia. *Journal of Experimental Biology* **147**, 169-188.

Wyffels, J., King, B. L., Vincent, J., Chen, C., Wu, C. H. and Polson, S. W. (2014). SkateBase, an elasmobranch genome project and collection of molecular resources for chondrickthyan fishes. *F1000 Research* **3**, 191.

Wyman, L. C. and Lutz, B. R. (1932). The Effect of Adrenalin on the Blood Pressure of the Elasmobranch, *Squalus acanthias*. *Biological Bulletin* **62**, 17-22.

Zammit, V. A. and Newsholme, E. A. (1979). Activities of Enzymes of Fat and Ketone-Body Metabolism and Effects of Starvation on Blood Concentrations of Glucose and Fat Fuels in Teleost and Elasmobranch Fish. *Biochemical Journal* **184**, 313-322.

Zeger, S. L. and Karim, M. R. (1991). Generalized Linear Models With Random Effects; A Gibbs Sampling Approach. *Journal of American Statistical Association* **86**, 79-86.

Zhang, J., Désilets, M. and Moon, T. W. (1992). Evidence for the modulation of cell calcium by epinephrine in fish hepatocytes. *American Phsiological Society* **263**, 512-519.

5. Chapter 5: Metabolic indicators of glucose and ketone body energy balance following air exposure in an elasmobranch species, the North Pacific spiny dogfish, *Squalus suckleyi*.

5.1. Abstract

Plasma glucose is an important energy source in most vertebrates when the demand for energy increases, such as the endocrine stress response. Hormones stimulate metabolic processes to initially liberate glucose through glycogenolysis and gluconeogenesis. However, it is unclear what metabolites are preferentially mobilized in elasmobranchs, which have an unusual energy metabolism of using of ketone bodies (3-hydroxybutyrate [3-HB] and acetoacetate) in both satiated and starved states, suggesting an increased reliance on these metabolites during periods of increased energy demand. To investigate the patterns of metabolite (glucose and 3-HB) use in elasmobranchs, we induced two stress events using the north Pacific spiny dogfish, *Squalus suckleyi*: 1) short-term handling and air exposure (10min) and 2) air exposure (10min) and long-term holding (7 days). Fish were sampled for plasma, glucose, 3-HB, lactate, pH, osmolality, and corticosteroid concentrations. Furthermore, tissue samples of liver, heart, white muscle, rectal gland, and brain were assessed for activity of the following key metabolic enzymes hexokinase (HEX), glycogen phosphorylase (GP), 3-hydroxybutyrate dehydrogenase (3-HBDH), succinyl-CoA transferase (SCOT), and phosphoenolpyruvate carboxykinase (PEPCK); and mRNA transcript abundance of glucose transporters, *glut1* and *glut4*; putative ketone transporters, *mct1* and *mct2*; and the glucocorticoid receptor (*gr*). In the short-term experiment there were no changes in plasma glucose, corticosteroids, or tissue enzyme activity; however, there were predictable changes in *glut* transcript abundance that suggests internalization of glucose transporters in white muscle. There was also a decrease in SCOT activity in the heart, inferring a reduced capacity for flux through the pathways associated with ketolysis under these conditions in this tissue. In the long-term experiment, there was a greater capacity for flux through pathways associated with the catabolism of glucose, as demonstrated by an increase in HEX and GP activity in the heart and rectal gland. Additionally, there was an increase in 3-HBDH and SCOT activity in the heart and rectal gland, as well as an increase in 3-HBDH activity in the liver, indicating an increase in the capacity for flux through pathways associated with hepatic ketogenesis and extrahepatic ketolysis. Ultimately, it remains unclear what the predominate fuel source is in the short-term following a

short-term air exposure stress event, but it is evident that both glucose and 3-HB serve a role in fueling the long-term stress event.

5.2. Introduction

Plasma glucose is an important fuel source for oxidative metabolism in most vertebrates (Bouyoucos et al., 2021; Krebs et al., 1963; Newsholme and Start, 1973; Pardridge, 1983). When the need for energy increases, such as periods of stress, glucose is produced through glycogenolysis and gluconeogenesis. These processes synthesize glucose from the storage molecule glycogen and other energy molecules (i.e. glycerol, amino acids, etc.) a process that predominately occurs in the liver (Krebs et al., 1963; Newsholme and Start, 1973), but can also occur extrahepatically (Krebs et al., 1963). Tetrapods and teleosts also have the capacity to directly oxidize fatty and amino acids following glycogen depletion and will often employ this strategy during periods of starvation (Newsholme and Start, 1973; Zammit and Newsholme, 1979).

Elasmobranchs are unusual in that they seem to employ an metabolic strategy of using liver-derived ketone bodies (3-hydroxybutyrate [3-HB] and acetoacetate) rather than long-chain fatty acids extrahepatically (reviewed in (Speers-Roesch and Treberg, 2010)). While other taxa use ketones, particularly in the brains of fasted mammals (Laffel, 1999), elasmobranchs use ketones in both satiated and starved states (Ballantyne, 1997; Zammit and Newsholme, 1979). In some cases, ketones are a more efficient or preferential fuel type over carbohydrates in perfused tissues such as the heart of the little skate, *Leucoraja erinacea*, (Driedzic and Hart, 1984) or the white muscle of North Pacific spiny dogfish, *Squalus suckleyi*, post-exercise (Richards et al., 2003). Given the important role ketones appear to play as a metabolic fuel in elasmobranchs it is conceivable that release of these molecules may play a significant function in fueling extrahepatic metabolic processes following exposure to a stressor.

Broadly, energy balance in vertebrates following stress events is regulated by the endocrine stress system, which releases a variety of hormones that act to reestablish homeostasis. Catecholamines are released rapidly (second to minutes) to fuel the initial 'fight-or-flight' response and corticosteroids are secondarily released (minutes to hours) to further modulate metabolite mobilization and use. Catecholamines (epinephrine [E] and norepinephrine) rapidly liberate hepatic glucose from glycogen stores by activating glycogen phosphorylase (GP) (Fischer et al., 1978). While catecholamine injections do increase plasma glucose concentrations in

elasmobranchs (deRoos and deRoos, 1978; Patent, 1970), the hormonal control of GP activation in this taxa is still unclear (Fischer et al., 1978; Nathanson and Mariwalla, 1996). Further, catecholamines may also act to mobilize hepatic lipids for ketogenesis, as demonstrated by an increase in hepatic lipolysis following catecholamine stimulation in the nurse shark, *Ginglymostoma cirratum* (Lipshaw et al., 1972). Less is known about the catecholamine influence on metabolite catabolism in extrahepatic tissues of teleosts and elasmobranchs, although a species and stress-event specific increase in white and cardiac muscle glycogenolysis may be reasonably anticipated (Fabbri et al., 1998).

Corticosteroids, more specifically glucocorticoids, are responsible for the long-term re-establishment of energy balance in vertebrates, which is accomplished first through upregulation of hepatic gluconeogenesis to replenish depleted glycogen stores (Romero and Butler, 2007). In elasmobranchs, low activity of phosphoenolpyruvate carboxykinase (PEPCK) – a rate-limiting enzyme in gluconeogenesis – has been detected in the liver of fasted lesser-spotted dogfish, *Scyliorhinus canicula*, concurrently with elevated levels of 3-hydroxybutyrate dehydrogenase (3-HBDH) – an enzyme essential for the reversible conversion of 3-HB to acetoacetate (Zammit and Newsholme, 1979), suggesting a reliance on ketone mobilization over gluconeogenesis. Therefore, it is unclear if gluconeogenic or ketogenic pathways would be preferential following a stress event in elasmobranchs; although, the target response is likely similar to more derived vertebrates: mobilize macromolecules to fuel extrahepatic tissues.

In mammalian muscle glucocorticoids have been shown to effect circulating plasma glucose by stimulating the internalization of insulin sensitive glucose transporters (primary GLUT4) (Dimitriadis et al., 1997). GLUT1 may also be insulin sensitive, although the evidence is conflicting as this transporter is more ubiquitously expressed under basal conditions (Gould and Holman, 1993; Widnell, 1995) Insulin sensitivity of GLUT4 has been demonstrated in some teleosts (Díaz et al., 2007; Díaz et al., 2009) and there is evidence that GLUT1 in rainbow trout, *Oncorhynchus mykiss*, is insulin growth factor-1 sensitive (Capilla et al., 2002; Díaz et al., 2009), suggesting that these transporters may still be under some hormonal regulation. Ultimately, the internalization of glucose transporters elevates plasma glucose by limiting the influx of this metabolite into peripheral tissues to presumably allow selective uptake of glucose in tissues that are critical for responding to a stress event (e.g. the brain). Deck et al. (2017b) showed that GLUT4 in elasmobranch white muscle is insulin sensitive (Deck et al., 2017b) and that both *glut1* and *glut4*

transcript abundance increased after a glucose bolus; however, it is unclear if transcript abundance of these transporters are inversely effected by corticosteroids.

In regards to ketone transport, most studies are mammalian focused and conclude that the MCT family of transporters are responsible for the transport of monocarboxylates such as lactate, pyruvate, and ketone bodies (Halestrap, 2013; Halestrap and Price, 1999). Hepatic export of ketones has been shown to use MCTs in rats, *Rattus norvegicus*, (Jackson and Halestrap, 1996), and MCT1 is ubiquitously expressed in mammalian extrahepatic tissues (Halestrap, 2013). In elasmobranchs, MCT 1, 2, and 4 has been found in the brain of the redspotted catshark, *Schroedericthys chilensis* (Balmaceda-Aguilera et al., 2012), and MCT 1 and 2 in the rectal gland of *S. suckleyi* (Deck et al., 2016a), and are assumed to be involved in similar transport processes as mammals. While there is no direct evidence of glucocorticoid regulation of MCTs, high frequency stimulation of the sciatic nerve in *R. norvegicus* increased neural expression of MCT1 and 2, which was associated with an increase in plasma corticosterone (B) (Huang et al., 2022). In teleosts, induced stress events such as post-exhaustive exercise (Omlin and Weber, 2013), hypoxia (Ngan and Wang, 2009), and cold-shock (Tseng et al., 2014) stimulated changes in MCT transcript abundance and protein kinetics, although these variations were only investigated in association with lactate metabolism. Finally, environmental hyposaline stress increased *mct1* and *2* transcript abundance in the rectal gland of *S. suckleyi* (Deck et al., 2016a) and hypoxia decreased MCT1 and 4 protein expression in the brain of *S. chilensis* (Balmaceda-Aguilera et al., 2012), suggesting a relationship between MCT expression and some stress conditions.

In the present study, we aimed to investigate enzymatic and molecular mechanisms involved in glucose and ketone (3-HB) metabolism by evoking an endocrine stress response in a representative elasmobranch species, *S. suckleyi.* Two stress protocols were used: 1) air exposure (10min total) to examine endpoints in the relative short-term following a stress event, and 2) air exposure (10min total) to examine endpoints in the relative long-term (7 days) following a stress event. We hypothesize that endpoints associated with hepatic mobilization and extrahepatic oxidation of glucose and 3-HB will change following a stress event; further, these endpoints will be correlated with dominant circulating plasma corticosteroids.

5.3. Methods

Fish Collection and Care

Thirty male (1.45-2.47kg) *S. suckleyi* were caught by rod and line in Barkley Sound, Vancouver Island, British Columbia, during July 2021. Fish were housed in the Bamfield Marine Science Centre holding tank (155,000L) with flow-through seawater (12°C) and aeration, and fed North Pacific hake, *Merluccius productus*, *ad libitum* every other day. Fish were held in the holding tank for at least four days prior to experimentation. Experiments were completed in accordance with the Canadian Council of Animal Care standards, and with the approval of the Bamfield Marine Science Centre (RS-2021-06; RS-22-01) and University of Manitoba (F19-006) animal care committees.

Short-term Stress Protocol (Short-term)

This protocol was conducted to determine enzyme activity, mRNA transcript abundance, and circulating corticosteroids and metabolites in the relative short-term following a stress event. Fish were transferred to holding tanks (5,000L), with flow-through seawater (12°C) and aeration, in pairs two days prior to experimentation and fed immediately *ad libitum*. Air exposure protocols were adapted from Iki et al. (2020) and Chapter 2. On the day of experimentation, fish were hand caught from holding tanks and individually placed in a 190L plastic tub without water for 5min of air exposure. Then, fish were released back into holding tanks for 3min to briefly recover, hand-caught again, and placed back into the plastic tub without water for another 5min of air exposure. Fish were then reintroduced to the holding tank and held for 30min (n = 6) or 1hr (n = 6). A control treatment (0min) was taken from holding tanks and immediately placed in a terminal bath of anesthetic (n = 6).

Long-term Stress Protocol (Long-term)

This protocol was conducted to assess enzyme activity, mRNA transcript abundance, and circulating corticosteroids and metabolites in the relative long-term following a stress event. Six fish were transferred to a holding tank (5,000L), with flow-through seawater (12°C) and aeration. Fish were immediately fed *ad libitum*, held for two days, and air exposed using the same protocol as the short-term stress. Fish were then held in the holding tank for 7 days. A control treatment (n = 6) was not air-exposed and held in holding tanks in pairs for 7 days. Both treatment and control groups were not fed for the 7 days of holding.

Blood and Tissue Sampling

After respective holding time, fish were immersed in an anesthetic bath ($0.2 g \cdot L^{-1}$ tricaine methanesulfonate (MS-222), Syndel Labs, Vancouver, British Columbia, Canada) until loss of operculum movement. Body mass to the nearest gram was recorded, and the cervical column was severed just posterior to the brain. Two mLs of blood was immediately collected via the caudal vessel with a 3mL syringe and 18-gauge needle. Blood was centrifuged (2min, 13,000g) and plasma was frozen at -20°C for metabolite analysis. Fish were then dissected along the ventral surface to expose the abdominal and pericardial cavities. Tissues samples were collected from the liver (halfway between the bifurcation of the liver lobes and the terminal end of the liver lobe closest to the hepatic vein), ventricle of the heart, rectal gland, and white muscle (white muscle; laterally to the caudal peduncle). Fish were then dissected along the dorsal surface to expose the braincase and brain, which was also sampled (whole brain). Tissue samples were divided and either flash-frozen in liquid nitrogen for enzyme analysis, or stored in RNALater for molecular analysis.

Plasma Analysis

Plasma samples were analyzed for circulating levels of glucose, 3-HB (described in Chapters 2 and 3) 1α-hydroxycorticosterone (1α-OHB), and B (described in Chapter 2). Circulating levels of cortisol (F) were also measured using an in-house Enzyme Linked Immunosorbent assay provided by collaborators at Disney's Animal Kingdom and conducted using the same method for corticosteroid assays outlined in Chapter 2. Lactate was measured using a Lactate Scout® Unit (EKF Diagnostics, Boerne, TX, USA) and osmolality was measured using a Osmette III® osmometer (Precision Systems, Natick, MA, USA), respectively using 5μL of plasma and per the manufacturer's instructions.

Enzyme Activity

All tissue samples were assayed for maximal enzyme activity of 3-HBDH (ketogenesis and catabolism), succinyl-CoA transferase (SCOT; ketone catabolism), and glycogen phosphorylase (GP; glycogenolysis). Additionally, heart, rectal gland, and brain samples were assayed for hexokinase activity (HEX; glycolysis), which was not successfully conducted in liver or white

muscle samples because of unidentified assay interference in these tissues. Liver samples were also assayed for phosphoenolpyruvate carboxykinase (PEPCK; gluconeogenesis). Enzyme assays were conducted using the same protocols as outlined in Chapter 4. Liver and white muscle samples were processed in the same manner as Chapter 4, in that homogenates were appropriately diluted in homogenization buffer (determined by a previously conducted serial dilution of a haphazardly chosen subset of samples within each tissue), centrifuged for 20min at 4°C (9,500 g), and then supernatants were centrifuged again under the same conditions to remove lipid constituents. Heart, rectal gland, and brain homogenates were only centrifuged once.

mRNA Transcript Abundance

Transcript abundance for five genes of interest were investigated in all sampled tissues using the same protocols as outlined described in Chapter 4. Genes of interest included: *glut1, glut4* (glucose transporters), *mct1, mct2* (potential ketone transporters), and *gr* (glucocorticoid receptor). Transcript abundance in the short-term protocol was normalized to the 0min group and for in the long-term protocol was normalized to the control group using NORMA-gene (Heckmann et al., 2011) and analyzed using the comparative C_t method (Schmittgen and Livak, 2008). Of note, serial dilutions of *mct1* in brain were too lowly expressed and did not meet the primer efficiency requirements (90-110%), thus *actin* transcript abundance was used in this tissue to satisfy the minimum number of genes for NORMA-gene.

Statistical Analysis

All models were subject to Shapiro-Wilks and Levine's tests to assess normality and equal variance, respectively. If assumptions were not met, data sets were transformed using rank (short-term protocol: plasma 3-HB concentration and osmolality, SCOT activity in liver, GP activity in brain, *mct1* transcript abundance in white muscle, *gr* transcript abundance in brain; long-term protocol: 3-HBDH activity in brain, SCOT activity in rectal gland, *glut1* transcript abundance in heart, *glut4* transcript abundance in liver, *glut4* transcript abundance in brain, *mct2* transcript abundance in white muscle) square-root (short-term protocol: plasma 1α-OHB concentration, 3-HBDH activity in white muscle, SCOT activity in heart, PEPCK activity in liver, *glut1* transcript abundance in heart, *mct2* transcript abundance in liver, *mct2* transcript abundance in brain; long-term protocol: 3-HBDH activity in liver and heart, HEX activity in heart, SCOT activity in heart

and white muscle, *glut4* transcript abundance in heart) or double square-root transformations (short-term protocol: HEX activity in heart). Non-parametric Kruskal-Wallace with Dunn post-hoc tests using 'holm' corrections were conducted on data sets where transformations did not meet assumptions (long-term protocol: SCOT activity in liver). Data sets in Series A were analyzed using one-way ANOVAs. Tukey's post-hoc tests ('glht' function in 'multcomp' package) (Hothorn et al., 2008) were used to determine significance of time on metabolite concentration. Data sets in the long-term were analyzed using Welch Two Sample t-tests to compare control and treatment groups. Of note, enzyme samples for the 1hr brain treatment were thawed prematurely, and thus were omitted from enzyme analysis in this study. Therefore, Welch Two Sample t-tests were used to compare enzyme activity in the short-term in the brain over time. All statistical significance of post-hoc tests were accepted at $\alpha = 0.05$. All statistical analysis was conducted in R (version 2023.03.0+386).

5.4. Results

Short-term

Plasma glucose, 3-HB, and osmolality concentrations did not change over time (Figures 5.1A, 5.1B, 5.1D), while plasma lactate concentrations significantly increased at 30min ($t = 7.165$, $p < 0.001$) and 1hr ($t = 7.542$, $p < 0.001$) post-air exposure (Figure 5.1C). Further plasma corticosteroid concentrations did not change over time (Figure 5.1E, 5.1F, 5.1G). Enzyme activities for HEX, GP, 3-HBDH, and PEPCK in all tissues did not significantly change over time (Figure 5.2A, 5.2B, 5.2C, 5.2E). SCOT activity significantly decreased at 30min ($t = -2.644$, $p = 0.047$) and 1hr ($t = -3.098$, $p = 0.020$) post-air exposure only in heart (Figure 5.2D).

glut1 ($t = 2.817$, $p = 0.031$) and *glut4* ($t = 3.276$, $p = 0.012$) transcript abundance significantly increased in white muscle at 30min post-air exposure (Figure 5.3A, 5.3B). *glut4* transcript abundance also decreased at 1hr in liver as compared to 0min ($t = -3.516$, $p = 0.008$) and at 30min ($t = -3.764$, $p = 0.004$) and 1hr ($t = -5.825$, $p < 0.001$) in heart post-air exposure (Figure 3B). *mct1* (compared to 0min, $t = -2.963$, $p = 0.024$; compared to 30min, $t = -4.913$, $p < 0.001$), *mct2* (compared to 0min, $t = -2.792$, $p = 0.033$; compared to 30min, $t = -4.400$, $p = 0.001$), and *gr* (compared to 0min, $t = -2.992$, $p = 0.022$; compared to 30min, $t = -3.994$, $p = 0.003$) transcript abundance decreased at 1hr post-air exposure in liver as compared to 0 and 30min (Figure 5.3C,

5.3D); *mct2* transcript abundance decreased at 1hr in heart (compared to 0min, t = -4.781, p < 0.001; compared to 30min, t = -5.390, p < 0.001) as compared to 0 and 30min (Figure 5.3D).

Long-term

Plasma glucose concentration was significantly less in the treatment group as compared to the control group (t = 2.838, df = 9.097, p = 0.019; Figure 5.4A). Plasma 3-HB, lactate, osmolality and corticosteroid concentrations did not differ between treatment and control groups (Figure 5.4B, 5.4C, 5.4D, 5.4E, 5.4F, 5.4G). HEX activity was significantly elevated in heart (t = -11.212, df = 6.969, p < 0.001) and rectal gland (t = -3.894, df = 9.024, p = 0.004) in the treatment group, as compared to the control group (Figure 5.5A). GP and SCOT activities were significantly elevated in heart (GP, t = -5.773, df = 7.072, p < 0.001; SCOT, t = -4.093, df = 5.749, p = 0.007), rectal gland (GP, t = -6.823, df = 7.878, p < 0.001; SCOT, t = -3.905, df = 6.013, p = 0.008); only SCOT activity was elevated in the treatment group in the brain (SCOT, t = -2.789, df = 7.908, p = 0.024) as compared to the control group (Figure 5.5B, 5.5D). 3-HBDH activity was elevated in the treatment group, as compared to the control group, in liver (t = -3.766, df = 7.244, p = 0.007), heart (t = -8.998, df = 7.655, p < 0.001), and rectal gland (t = -3.436, df = 8.970, p = 0.007) (Figure 5.5C). PEPCK activity significantly differ between treatment and control groups (Figure 5.5E; Table 5.2).

glut1 (t = -2.866, df = 7.093, p = 0.024) and *glut4* (t = -8.530, df = 7.810, p < 0.001) transcript abundance was significantly elevated in the treatment group, as compared to the control group, in heart (Figure 5.6A, 5.6B); *glut4* transcript abundance was also elevated in the treatment group in liver (t = -4.697, df = 5.205, p = 0.005) and rectal gland (t = 3.392, df = 7.152, p = 0.011) (Figure 6B). *mct1* transcript abundance significantly decreased in the treatment group in rectal gland (t = 3.356, df = 5.409, p = 0.018) as compared to the control group (Figure 5.6C), while *mct2* transcript abundance was significantly elevated in the treatment group in liver (t = -4.747, df = 9.977, p < 0.001) (Figure 5.6D). Finally, *gr* transcript abundance was significantly elevated in the treatment group, as compared to the control group, in liver (t = -3.479, df = 7.268, p = 0.001) and heart (t = -3.574, df = 5.954, p = 0.012) (Figure 5.6E).

5.5. Discussion

In the present study, we demonstrate tissue specific and time dependent changes in the pathways associated with glucose and 3-HB mobilization and usage in *S. suckleyi* post air-exposure. Data indicated no effect in the short- or long-term on classic plasma parameters used to infer activation of the endocrine stress response and subsequent mobilization of energy reserves in other vertebrates. However, patterns of tissue specific enzyme activity and mRNA abundance suggested an effect at the tissue level that varied between treatment groups. Interestingly, a more consistent significant change in measured cellular parameters was observed in the long-term treatment group. Reasons for this are unclear as air exposure, handling, and holding tanks were the same regardless of treatment with one exception. The long-term treatment group were held in groups of six fish per tank compared to the short-term treatment and control in groups of two fish per tank. It is possible that air-exposed fish in our long-term study were also subjected to a more chronic stressor of crowding. Although, there was no evidence of aggressive interactions recorded between fish in any of the treatment or control groups, previous studies indicate *S. suckleyi* exhibited heightened levels of corticosteroids and metabolites post-surgical insertion of an in-dwelling cannula and placement in a confined space (Chapter 2).

Plasma

There was an increase in plasma lactate following the stress events in the short-term, indicative of an anaerobic stress, which has been seen previously in air-exposed elasmobranchs (i.e. Hoffmayer and Parsons, 2001; Manire et al. 2001; Fick et al., 2010; Lambert et al., 2018; Chapter 2). Interestingly, plasma concentrations of glucose did not change in the short-term. Classic activation of the endocrine stress response in vertebrates is in part defined by the downstream increase of plasma glucose via glycogenolysis and gluconeogenesis. While this is consistent in a variety of elasmobranch species (Bouyoucos et al., 2017; Bouyoucos et al., 2018b; Chapman and Renshaw, 2009; Cliff and Thurman, 1984; Hoffmayer et al., 2012; Hoffmayer et al., 2015; Hoffmayer and Parsons, 2001; Ruiz-Jarabo et al., 2019; Schoen et al., 2021), there are some situations where plasma glucose does not change (Bouyoucos et al., 2018a; Bouyoucos et al., 2018b; Brinn et al., 2012; Chapman and Renshaw, 2009; Frick et al., 2009; Frick et al., 2010; Shea et al., 2022) or even decreases after a stress event (Frick et al., 2010; Lambert et al., 2018; Manire et al., 2001). Variability in plasma glucose after a stress event may be influenced by a preference

for ketone body oxidation; indeed, perfused white muscle of *S. suckleyi* demonstrated a greater influx of 3-HB compared to glucose post-exercise (Richards et al., 2003) and plasma 3-HB increased post-surgery and confinement stress in the same species (Chapter 2). However, plasma 3-HB concentrations also did not change in the short-term, suggesting either a differential fuel under these circumstances, the stressor employed was insufficient to induce a change in plasma metabolites, or that fish were stressed prior to experimentation.

Chapter 2 provides support that fish were stressed prior to experimentation in that air exposure did not cause a change in either plasma glucose or 3-HB in *S. suckleyi* (although there was a predictable increase in plasma lactate), presumably because fish were previously stressed via surgical cannulation and confinement, which caused an increase in both metabolites 24hrs prior to air exposure. A similar pattern occurred in the dominant circulating corticosteroids, 1α-OHB and B (Chapter 2), which also did not change over time in the present study. When comparing metabolite and corticosteroid values from Chapter 2 and this study to those taken from *S. suckleyi* immediately following hook-and-line angling (unpublished data, n = 6; glucose, 2.0-2.8mM; 3-HB, 0.3-1.1mM; 1α-OHB, 0.00-1.96ng.mL^{-1}; B, 0.07-0.27ng.mL^{-1}), it is clear that at least 3-HB and corticosteroid concentrations are elevated in fish housed in holding tanks. A glucocorticoid role for the dominant corticosteroids has not yet been fully determined in any elasmobranch species and the correlations between these corticosteroids and measured metabolites are weak or non-existent (Ruiz-Jarabo et al., 2019; Schoen et al., 2021; Chapter 2); but both plasma 1α-OHB (Iki et al., 2020; Ruiz-Jarabo et al., 2019; Chapter 2) and B (Brinn et al., 2012; Iki et al., 2020; Chapter 2) have been reported to increase following exposure to a stressor in several elasmobranch species. Therefore, it may be plausible that the raised corticosteroid concentrations in captive fish are a result of capture and holding in the aquarium and a greater amount of time is needed for circulating concentrations to return to pre-capture levels; subsequently, fish may not have been able to appropriately mount an endocrine stress response to the additional stressors during experimentation (Romero et al., 2009).

There was a negligible change in plasma lactate concentration in long-term, which confirms that the initial air exposure stress 7 days prior to sampling was resolved in terms of anaerobic metabolism. In contrast to the short-term, there was a decrease in plasma glucose concentration in the long-term and no significant changes in any other plasma measurements between control and treatment groups. In may be possible that the decrease in plasma glucose

indicates either a reduction in glucose mobilization or an increase in extrahepatic consumption, which is further elucidated by tissue enzyme and molecular results.

Liver

There were no changes in hepatic enzyme activity in the short-term. The liver is an essential source of catecholamine and corticosteroid-mediated metabolite mobilization following a stress event in most vertebrates investigated to date (Romero and Butler, 2007). Following exposure to stressor, catecholamines rapidly activate GP to break down hepatic glycogen. In the present study, although there was no increase in hepatic GP activity following the air-exposure in the short-term, this result is consistent with 15min of E perfusion in the livers of *S. suckleyi* in Chapter 4, which did not alter hepatic GP activity or perfusate glucose concentrations, possibly indicating mechanistic differences between elasmobranchs and other vertebrate GP activation. GP activity also did not differ between treatments in the long-term, further supporting an alternate mechanism of GP activation. However, it is important to note that while total hepatic GP enzyme activity, as measured in the present study, may not have changed in either treatment the percent change of the active form of the enzyme (%GP*a*) may have given a more accurate representation of changes in GP activity (Moon et al., 1999) under the present experimental conditions.

In contrast, there was elevated 3-HBDH activity in fish 7 days post air exposure, indicative of an increase in the capacity for 3-HB flux through ketogenic pathways. It has been shown that hepatic ketones are a preferential fuel source to long-chain fatty acids in a number of extrahepatic tissues (Driedzic and Hart, 1984; Speers-Roesch and Treberg, 2010; Zammit and Newsholme, 1979) and possibly in some cases exogenous glucose (deRoos, 1994; Richards et al., 2003) particularly during fasting conditions (Wood et al., 2010; Zammit and Newsholme, 1979). Both treatments in the long-term experiment were fasted for the same amount of time, so the increase in 3-HBDH suggests an additive effect of more fish being present in the air-exposure treatment on hepatic 3-HBDH activity; the mechanism of action of this is unknown. Of note, as the elasmobranch liver is not considered a ketolytic tissue (Speers-Roesch and Treberg, 2010), SCOT activity did not change in either the short- or long-term experiments.

Transcript abundance of *glut* and *mct* transporters either do not change (*glut1*) or decrease (*glut4*, *mct1*, and *mct2*) in the short-term. These results support the lack of hepatic glucose or 3-HB mobilization, potentially as a mechanism of saving energy by reducing translation and

translocation of transporters to the hepatocyte membrane; potentially these transporters are not important under the present stress conditions. On the other hand, it is important to consider that mRNA transcript abundance is the sum of multiple regulatory mechanisms at the transcription, translation, and post-translation modification levels; thus, an increase in mRNA has numerous interpretations. Here, we could speculate that a decrease in transporter transcript abundance in the short-term might also infer an increase in protein translation (an example of this type of proposed mechanism was suggested in Deck et al. (2016) in respect to *glut* transcript abundance in *S. suckleyi* following feeding), at least of MCTs. MCTs are predominate lactate transporters in mammals (Halestrap, 2013) and presumptively teleosts (Ngan and Wang, 2009; Omlin and Weber, 2013; Tseng et al., 2014; van der Meer et al., 2005), and have also been found to increase protein expression (MCT1 and MCT4) in the brain of *S. chilensis* exposed to hypoxic conditions – which was attributed to an increase in lactate transport (Balmaceda-Aguilera et al., 2012). Given the air exposure stress event chosen in this study and the resulting increase in plasma lactate in the short-term, it is possible that the decrease in *mct1* and *2* transcript abundance corresponded to an increase in transporter translation to support efflux of hepatic lactate.

In contrast, changes in transcript abundance in the long-term are more likely to infer an increase or decrease in metabolite transport given the length of time fish were exposed to the stress event. In the long-term there was an increase in hepatic *glut4* transcript abundance. *Glut4* transcript abundance previously increased in the liver of *S. suckleyi* steadily over 48hrs after a bolus glucose injection and was related to a concurrent increase in hepatic glycogen synthesis (Deck et al., 2017b). Glycogen content was not measured in this study, but it may be conceivable that *glut4* transcripts increased to allow an influx of glucose into the liver for glycogen storage, particularly given the significant decrease in circulating plasma glucose in the long-term. Additionally, there was an increase in hepatic *mct2* transcript abundance that corresponded with the increase in hepatic 3-HBDH activity, inferring that this transporter might be responsible for 3-HB transport in the liver under these conditions.

Finally, there was a decrease in *gr* transcript abundance in the short-term and an increase in the long-term. Thus it does not appear that changes in *gr* transcript abundance corresponded to changes in hepatic glucose balance, which is contrary to the classic vertebrate role of the GR in regulating glucose (Romero and Butler, 2007). Alternatively, the changes in *gr* transcript

abundance could be associated with the changes in *mct* transcript abundance in both the short- and long-term, either in relation to ketone or lactate transport.

Heart

In the short-term following air-exposure, the negligible change in HEX or GP activity combined with the decrease in *glut4* transcript abundance suggests a lack of mechanisms associated with a change in glucose transport and consumption in this tissue under these conditions. Elasmobranchs are relatively glucose intolerant (Deck et al., 2017b; Patent, 1970) as compared to mammals, which supports a lack of a change in HEX and GP activity if the heart is not reliant on exogenous glucose and glycolysis flux to increase in the short-term. However, in long-term, HEX and GP activities, as well as *glut1* and *4* transcript abundance, were elevated, suggesting both exogenous and endogenous glucose consumption that is consistent with previous studies (Driedzic, 1978; Driedzic and Hart, 1984). This demonstrates a clear difference between metabolite handling of air-exposed fish over the short- and long-term where glucose may be of greater importance fueling cardiac function.

Regarding 3-HB balance in short-term, SCOT was the only enzyme to show changes in activity, which decreased at 30min and 1hr. SCOT is the rate limiting step of ketolysis (Laffel, 1999) and thus a decrease in activity infers a reduced capacity for the flux of 3-HB through this ketolytic pathway. *mct2* transcript abundance also decreased at 1hr, supporting a reduction in 3-HB influx. In contrast, both 3-HBDH and SCOT activity increased in the long-term, indicating an increase in the capacity for 3-HB flux through a ketolytic pathway; although there was no change in *mct* transcript abundance, which may indicate that MCT1 and 2 are not the dominant 3-HB transporters in this tissue. Nevertheless, both glucose (Driedzic, 1978) and ketones (acetoacetate) (Driedzic and Hart, 1984) have previously been shown to be efficient fuel sources for the heart of *L. erinacea*. It is of interest that enzymes associated with both metabolites increase in the long-term and are unchanged or decrease in the short-term, again demonstrating context dependency of fuel preference in different tissues.

Finally, there was an increase in *gr* transcript abundance in the long-term. Since there is evidence that both glucose and 3-HB consumption increase in the heart under these conditions, it is unclear if an increase in *gr* transcript abundance corresponds to the classic GR glucose regulatory role or a novel ketone regulatory role. Further, since there were no changes in the

measured plasma corticosteroids, the identity of a factor or mechanism that could be stimulating an increase in *gr* transcript abundance remains unknown.

White Muscle

Similar to the liver, an expected outcome in vertebrates following initiation of the stress response is an increase in glycogenolysis in the white muscle by the activation of GP via catecholamine stimulation (Fischer et al., 1978); however, GP activity did not change in either the short- or long-term. As previously discussed in regards to the liver, this may be due to an alternative mechanism regulating GP activation or the assay methods used in this study.

Another expected outcome following activation of the stress axis in vertebrates is the glucocorticoid-mediated internalization of insulin-sensitive GLUT receptors (principally GLUT4), primarily in white muscle and adipose tissue in tetrapods and teleosts (Dimitriadis et al., 1997; Romero and Beattie, 2022). Transcript abundance of *glut1* (Díaz et al., 2009; Polakof et al., 2010) and *glut4* (Capilla et al., 2002; Díaz et al., 2007; Polakof et al., 2010) in skeletal muscle has been shown to increase following insulin administration in several teleost species and *S. suckleyi* (Deck et al., 2017b). Here, we show a significant increase in both *glut1* and *glut4* transcript abundance in white muscle at 30min in the short-term, We propose that an increase in *glut* transporter transcript abundance might infer down-regulation of *glut* translation into functional proteins and subsequent accumulation of transcripts within the cell (for storage or prior to degradation), which can occur during stress (Coller and Parker, 2004). It was hypothesized that this occurred in the rectal gland of *S. suckleyi* where both *glut1* and *glut4* transcript abundance decreased post-feeding, suggesting that transporters were synthesized from stored *glut* transcripts rather than *de novo* transcription (Deck et al., 2016b). Interestingly, in the present study, transcript abundance of both *glut1* and *4* returned to baseline values after 1hr, either showing a restoration of protein translation or the degradation of internalized transcripts. In contrast, *glut* transcript abundance does not change in the long-term, suggesting no change in glucose transport in white muscle between treatments.

There were no changes in enzyme activity or mRNA transcript abundance associated with 3-HB balance in either the short- or long-term. Previously in *S. suckleyi* post-exhaustive exercise, 3-HB significantly increased in the perfused tail-trunk white muscle and was estimated to account for up to 21% of post-exercise ATP production (Richards et al., 2003). Here there is no evidence

of an increase in 3-HB white muscle consumption post-stressor, which may further indicate a difference in 3-HB handling among stress events (e.g. exhaustive exercise versus air exposure).

Rectal Gland

There were no changes in enzyme activity or transcript abundance associated with either glucose or 3-HB flux in the short-term. The rectal gland of elasmobranchs has an osmoregulatory function of excreting excess NaCl. Therefore, the rectal gland may not be an organ of substantial importance in the short-term as osmotic balance was not affected in either the short- or long-term. Indeed, there was no change in HEX activity in the rectal gland following air exposure in *S. canicula* (Ruiz-Jarabo et al., 2022),

In the long-term, there was an increase in HEX, GP, 3-HBDH, and SCOT activity illustrating that the energy demand of the rectal gland under these conditions may have increased. The rectal gland is a glucose dependent tissue, but the rate of secretion is significantly enhanced by 3-HB (Walsh et al., 2006). Therefore, it is likely that both metabolites were used by the rectal gland under periods of increased energy demand. It is unclear why the long-term conditions would cause an increase in rectal gland energy use as there was no apparent osmotic challenge; however, we did not measure plasma sodium, chloride or urea, which would provide a clearer picture of any changes in rectal gland function.

Interestingly, *glut4* and *mct1* transcript abundance decreased in the long-term, suggesting a reduction in metabolite flux, despite enzymatic evidence of the contrary. As previously mentioned, the rectal gland is glucose-dependent and uses 3-HB to augment function (Walsh et al., 2006). Both GLUTs (Gould and Holman, 1993) and MCTs (Halestrap and Price, 1999) transport respective metabolites across a concentration gradient and are critical for the rectal gland when energy demand increases and cellular metabolites are low. However, a decrease in *glut4* and *mct1* transcript abundance over 7 days may infer that there is a higher concentration of metabolites within the rectal gland than the plasma, thus reducing the need for transporters to prevent a loss of intracellular metabolites. Alternatively, the rectal gland may employ additional transporters not measured in this study that may be more reflective of a change in metabolite use, such as SGLT for glucose (Deck et al. 2017a) or MCT7 for 3-HB (Hugo et al. 2012).

Brain

There were limited measurable responses in the brain, perhaps suggesting the importance for maintaining fuel use and balance in this tissue. The only significant change was an increase in SCOT activity in the long-term. Glucose is the predominate fuel for the brain in vertebrates; however, there is conflicting evidence in elasmobranchs that suggest glucose (Moon and Mommsen, 1987) or 3-HB (deRoos, 1994) may serve as primary fuel sources. In response to stress the data is limited, but Balmaceda-Aguilera et al. (2012) did show an increase in *mct* transcirpt abundance in hypoxia treated *S. chilensis*. In the present study the increase in SCOT activity supports that 3-HB may serve a role in fueling the brain during chronic stress.

5.6. Conclusions

In the present study we suggest there is a difference in the capacity for the flux of glucose and 3-HB following a short-term and long-term stress event in *S. suckleyi*. While fish may have already been stressed prior to air exposure, there was an added anaerobic stress in the short-term, as indicated by an increase in plasma lactate. Under these conditions there were surprisingly few changes in the short-term in enzyme activity, with a decrease in SCOT activity in the heart being the exception, suggesting a reduction in 3-HB flux through this ketolytic pathway. There was evidence of predicted mechanisms following activation of the stress response, such as the presumed internalization of GLUT receptors in the white muscle. Furthermore, *mct* transcript abundance may have decreased due to translation of MCTs to transport lactate in the liver and heart; although, additional work is needed to confirm protein expression and if this response is correlated with changes in *gr* transcript abundance. Ultimately, there was no evidence to support that either glucose or 3-HB play a major role in fueling the increased demand for energy during stress response under these conditions.

The capacity for metabolite flux through catabolic pathways differed in the long-term response in that it appeared both glucose and 3-HB played a more substantial role. A decrease in circulating plasma glucose may be explained by an increase in hepatic *glut4* transcript abundance and an increase in HEX activity in the heart and rectal gland. While there were no changes in circulating 3-HB between treatment groups, there is evidence to support an increase in hepatic 3-HB efflux and extrahepatic influx in the heart, rectal gland, and brain. Transport of both metabolites under these conditions in the tissues investigated remains elusive and may involve transporters that were not investigated in this study. Finally, activation of the *gr* in liver and heart

suggests that there was hormonal influence on metabolite balance in these tissues, but further work is needed to determine the identity of those hormones.

5.7. Acknowledgements

The authors thank Bamfield Marine Science Centre for the use of facilities and financial assistance to A.N.S. through the Dick and Leona Peter Student Bursary, and to Ryan Wahl and Jess MacPherson and for assistance with sample collection. Further, we thank the additional funding sources of the Natural Science and Engineering Research Council of Canada (NSERC) Discovery grant awarded to W.G.A. the University of Manitoba Graduate Fellowship awarded to A.N.S., a NSERC PDF awarded to A.R.W., and the University of Manitoba Faculty of Science Field work support program. We also would like to acknowledge that the Bamfield Marine Sciences Centre sits within the traditional territory of the Huu-ay-aht First Nations and the University of Manitoba campuses are located on the original lands of the Anishinaabeg, Cree, Oji-Cree, Dakota, and Dene peoples, and on the homeland of the Métis Nation.

5.8. Tables

Table 5.1. qPCR primer sequences, concentrations, cycling conditions, efficiency, and sources.

Target Gene	Forward Primer	Reverse Primer	Tissue	Primer Concentration	Cycling Conditions	Primer Efficiency	Source
glut1	AGTCGGATTGTTCGTCAACC	GCCGGAGTAGATGCCAATAA	Liver	400nM	95°C for 10min, and 40 cycles of 95°C for 10sec and 60°C for 15sec	96.20%	(Deck et al., 2016b)
			Heart	200nM	95°C for 3min, and 40 cycles of 95°C for 15sec, 58.8°C for 30sec, and 72°C for 30sec	90.54%	
			White Muscle	200nM	95°C for 3min, and 40 cycles of 95°C for 15sec, 62°C for 30sec, and 72°C for 30sec	90.14%	
			Rectal	200nM	95°C for 5min, and 40 cycles of 95°C for 5sec, 61.6°C for 10sec, and 72°C for 15sec	101.97%	
			Brain	400nM	95°C for 3min, and 40 cycles of 95°C for 15sec, 68.5°C for 30sec, and 72°C for 30sec	100.93%	

glut4	GTGGATGTGCG ATTCTGATG	GATGAAATTTGC GGTCCAGT	Liver	200nM	95°C for 3min, and 40 cycles of 95°C for 15sec, 58.5°C for 30sec, and 72°C for 30sec	107.91%	(Deck et al., 2016b)
			Heart	160nM	95°C for 3min, and 40 cycles of 95°C for 15sec, 58.8°C for 30sec, and 72°C for 30sec	90.54%	
			White Muscle	400nM	95°C for 3min, and 40 cycles of 95°C for 15sec, 64.9°C for 30sec, and 72°C for 30sec	106.80%	
			Rectal	200nM	95°C for 5min, and 40 cycles of 95°C for 5sec, 58.5°C for 10sec, and 72°C for 15sec	107.62%	
			Brain	400nM	95°C for 3min, and 40 cycles of 95°C for 15sec, 56.9°C for 30sec, and 72°C for 30sec	98.05%	
mct1	CAGCAGTCTCCT GGTGAACA	AGTTGAAGGCGA GTCCAAGA	Liver	400nM	95°C for 10min, and 40 cycles of 95°C for 10sec and 60°C for 15sec	108.59%	(Deck et al., 2016a)
			Heart	200nM	95°C for 3min, and 40 cycles of 95°C for 15sec, 61.5°C for 30sec, and 72°C for 30sec	91.95%	

			White Muscle	200nM	95°C for 3min, and 40 cycles of 95°C for 15sec, 67.6°C for 30sec, and 72°C for 30sec	100.65%	
			Rectal	200nM	95°C for 5min, and 40 cycles of 95°C for 5sec, 55°C for 10sec, and 72°C for 15sec	93.88%	
mct2	GTGAGGCC AAG GATCCAGTA	TCCCAGAA GTAC AGGGCAAC	Liver	200nM	95°C for 3min, and 40 cycles of 95°C for 15sec, 61.5°C for 30sec, and 72°C for 30sec	97.28%	(Deck et al., 2016a)
			Heart	200nM	95°C for 3min, and 40 cycles of 95°C for 15sec, 58.8°C for 30sec, and 72°C for 30sec	91.74%	
			White Muscle	400nM	95°C for 3min, and 40 cycles of 95°C for 15sec, 62°C for 30sec, and 72°C for 30sec	106.38%	
			Rectal Gland	200nM	95°C for 5min, and 40 cycles of 95°C for 5sec, 56.9°C for 10sec, and 72°C for 15sec	100.40%	
			Brain	200nM	95°C for 3min, and 40 cycles of 95°C for 15sec, 61.5°C for 30sec, and 72°C for 30sec	93.95%	

gr	CGGTCTTGGCTG GAGATCTTA	TGCATCCGTTCC TCATTGAG	Liver	400nM	95°C for 10min, and 40 cycles of 95°C for 10sec and 60°C for 15sec	104.56%	(Chapter 4)
			Heart	400nM	95°C for 10min, and 40 cycles of 95°C for 10sec and 60°C for 15sec	105.39%	
			White Muscle	200nM	95°C for 3min, and 40 cycles of 95°C for 15sec, 58.8°C for 30sec, and 72°C for 30sec	106.02%	
			Rectal Gland	200nM	95°C for 5min, and 40 cycles of 95°C for 5sec and 60°C for 10sec	95.47%	
			Brain	400nM	95°C for 10min, and 40 cycles of 95°C for 10sec and 60°C for 15sec	103.42%	
actin	TGCACTGGACTTTGAACAGG	TTCCACAGGATTCCATACCC	Brain	400nM	95°C for 2min, and 40 cycles of 95°C for 15sec and 60°C for 30sec	102.01%	(Weinrauch et al., 2022)

5.9. Figures

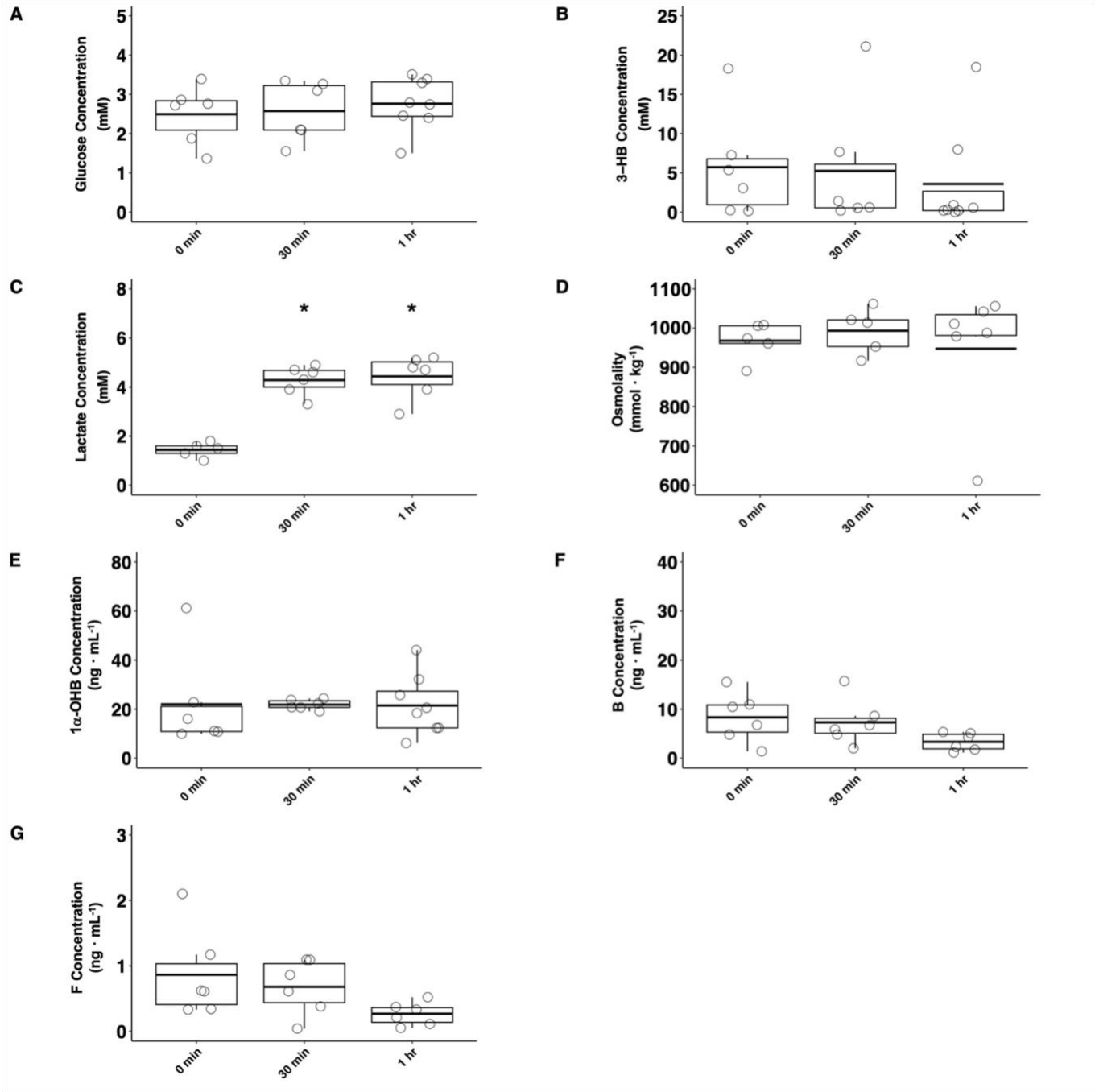

A
Glucose Concentration (mM)
0
1
2
3
4
5
0 min
30 min
1 hr
B
3–HB Concentration (mM)
0
5
10
15
20
25
0 min
30 min
1 hr
C
Lactate Concentration (mM)
0
2
4
6
8
*
*
0 min
30 min
1 hr
D
Osmolality (mmol · kg⁻¹)
600
700
800
900
1000
1100
0 min
30 min
1 hr
E
1α-OHB Concentration (ng · mL⁻¹)
0
20
40
60
80
0 min
30 min
1 hr
F
B Concentration (ng · mL⁻¹)
0
10
20
30
40
0 min
30 min
1 hr
G
F Concentration (ng · mL⁻¹)
0
1
2
3
0 min
30 min
1 hr

Figure 5.1. Plasma A) glucose concentrations (mM; n = 6-7), B) 3-HB concentrations (mM; n = 6-8), C) lactate concentrations (mM; n = 5-6), D) osmolality ($mmol \cdot kg^{-1}$; n = 5-6), E) 1α-OHB concentrations ($ng \cdot mL^{-1}$; n = 6-8), F) B concentrations ($ng \cdot mL^{-1}$; n = 5-6), and G) F concentrations ($ng \cdot mL^{-1}$; n = 6) over time in *Squalus suckleyi*. Boxplots represent the mean (solid black line inside box), interquartile range (box edges), and maximum and minimum (box whiskers) of respective data. Statistical significance ($\alpha = 0.05$) of the mean from 0min is indicated by an asterisk (*).

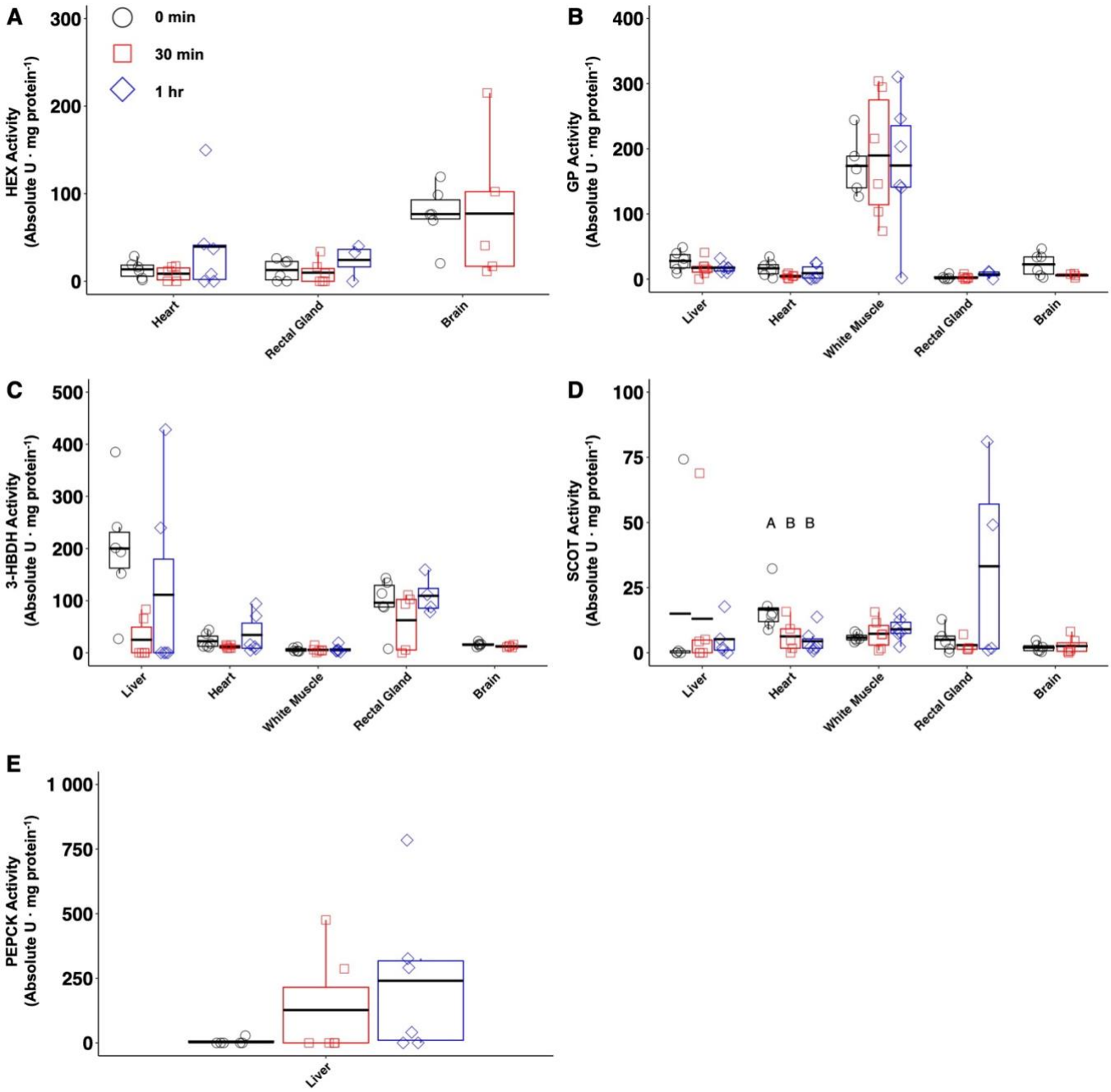


Figure 5.2. Enzyme activity (U·mg protein^{-1}) of A) HEX (n = 3-6), B) GP (n = 3-6), C) 3-HBDH (n = 4-6), D) SCOT (n = 4-6), and E) PEPCK (n = 6) in various tissues over time in *Squalus suckleyi*. Boxplots (0min = black circles, 30min = red squares, and 1hr = blue diamonds) represent the mean (solid black line inside box), interquartile range (box edges), and maximum and minimum (box whiskers) of enzyme activity data. Statistical significance (α = 0.05) of the mean over time within tissue is indicated by different letters (A or B).

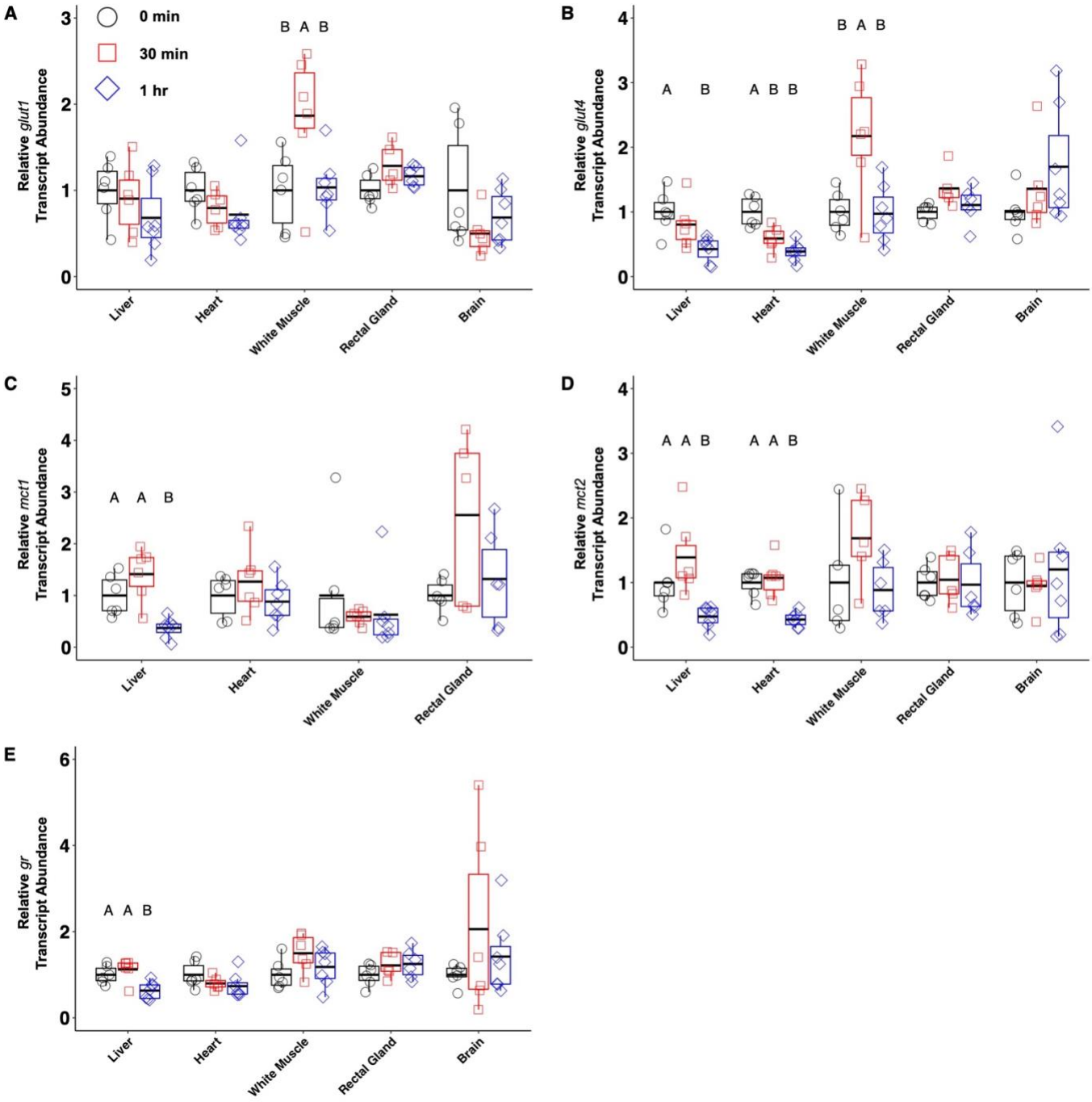


Figure 5.3. Transcript abundance of A) *glut1* (n = 5-7), B) *glut4* (n = 5-7), C) *mct1* (n = 5-7), D) *mct2* (n = 5-7), and E) *gr* (n = 5-7) in various tissues over time (relative to 0min within tissue) in *Squalus suckleyi*. Boxplots (0min = black circles, 30min = red squares, and 1hr = blue diamonds) represent the mean (solid black line inside box), interquartile range (box edges), and maximum and minimum (box whiskers) of transcript abundance data. Statistical significance ($\alpha = 0.05$) of the mean over time within tissue is indicated by different letters (A or B).

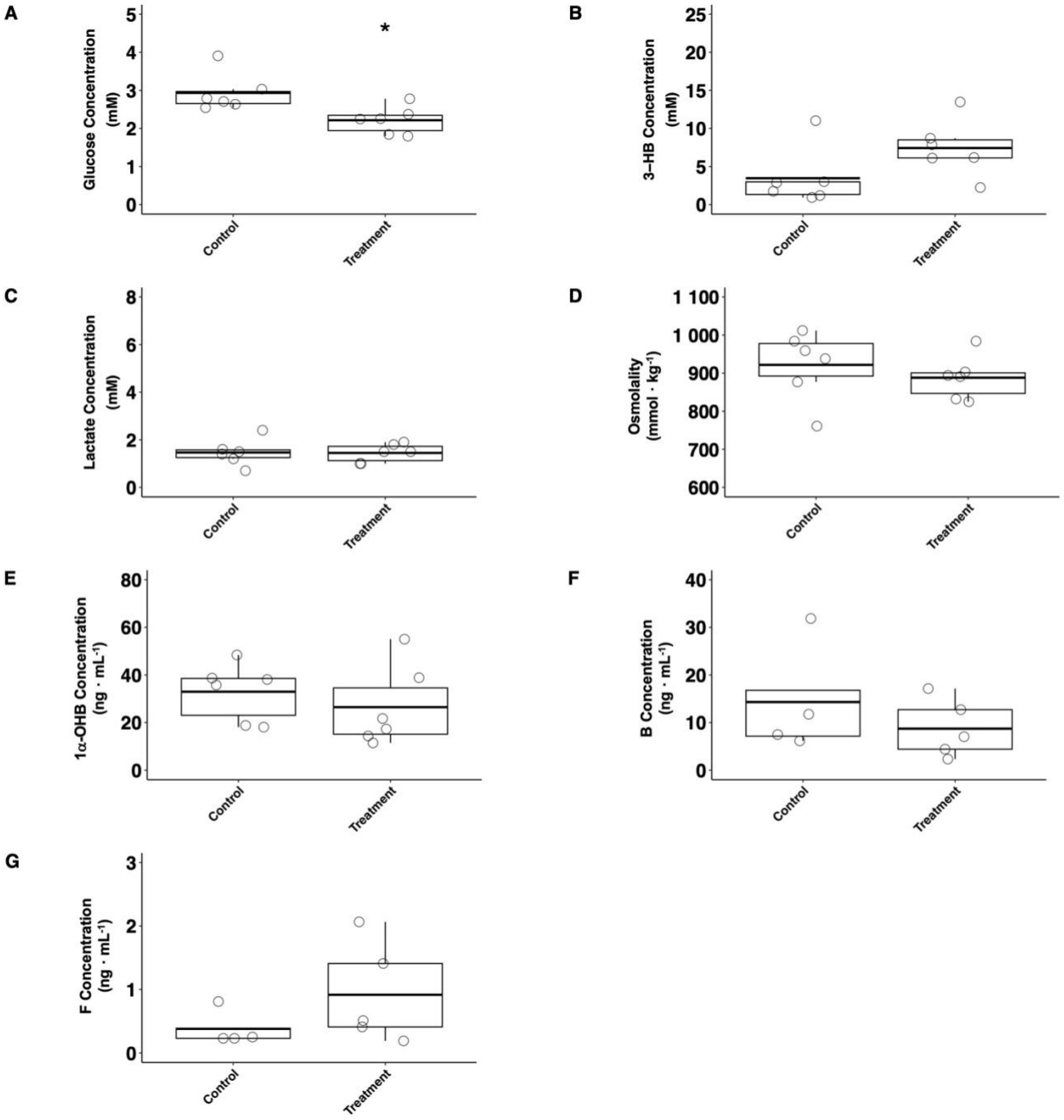


Figure 5.4. Plasma A) glucose concentrations (mM; n = 6), B) 3-HB concentrations (mM; n = 6), C) lactate concentrations (mM; n = 6), D) osmolality (mmol·kg^{-1}; n = 6), E) 1α-OHB concentrations (ng·mL^{-1}; n = 6), F) B concentrations (ng·mL^{-1}; n = 4-5), and G) F concentrations (ng·mL^{-1}; n = 4-5) over time in *Squalus suckleyi*. Boxplots represent the mean (solid black line inside box), interquartile range (box edges), and maximum and minimum (box whiskers) of

respective data. Statistical significance ($\alpha = 0.05$) of the mean from 0min is indicated by an asterisk (*).

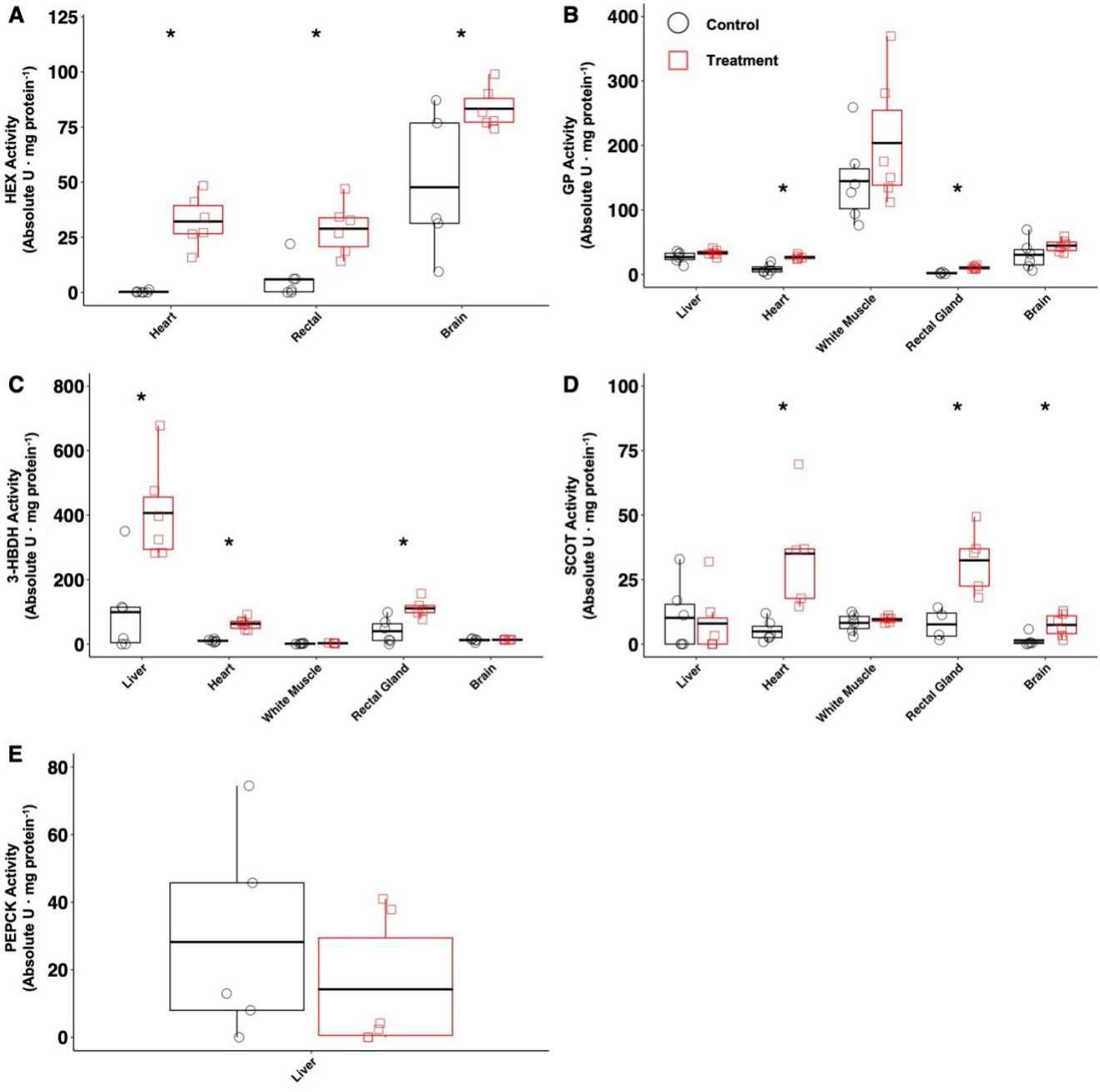

A
HEX Activity
(Absolute U · mg protein-1)
125
100
75
50
25
0
Heart
Rectal
Brain
B
Control
Treatment
GP Activity
(Absolute U · mg protein-1)
400
300
200
100
0
Liver
Heart
White Muscle
Rectal Gland
Brain
C
3-HBDH Activity
(Absolute U · mg protein-1)
800
600
400
200
0
Liver
Heart
White Muscle
Rectal Gland
Brain
D
SCOT Activity
(Absolute U · mg protein-1)
100
75
50
25
0
Liver
Heart
White Muscle
Rectal Gland
Brain
E
PEPCK Activity
(Absolute U · mg protein-1)
80
60
40
20
0
Liver

Figure 5.5. Enzyme activity (U·mg protein^{-1}) of A) HEX (n = 5-6), B) GP (n = 4-6), C) 3-HBDH (n = 5-6), D) SCOT (n = 4-6), and E) PEPCK (n = 6) in various tissues over time in *Squalus suckleyi*. Boxplots (controls = black circles, air exposure treatment = red squares) represent the mean (solid black line inside box), interquartile range (box edges), and maximum and minimum (box whiskers) of enzyme activity data. Statistical significance ($\alpha = 0.05$) of the mean over time within tissue is indicated by an asterisk (*).

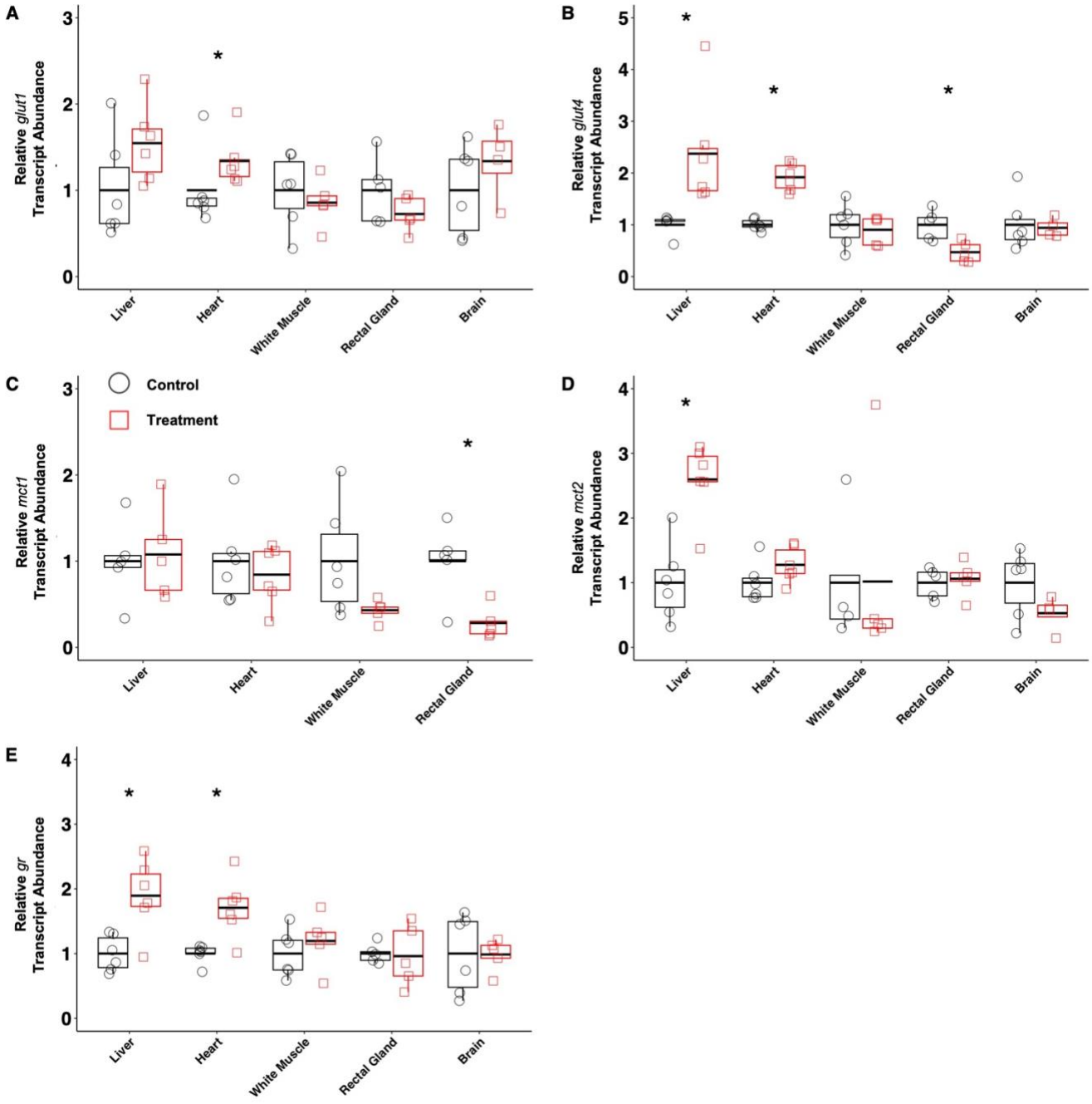


Figure 5.6. Transcript abundance of A) *glut1* (n = 4-6), B) *glut4* (n = 4-6), C) *mct1* (n = 5-6), D) *mct2* (n = 4-6), and E) *gr* (n = 5-6) in various tissues over time (relative to 0min within tissue) in *Squalus suckleyi*. Boxplots (controls = black circles, air exposure treatment = red squares) represent the mean (solid black line inside box), interquartile range (box edges), and maximum and minimum (box whiskers) of transcript abundance data. Statistical significance ($\alpha = 0.05$) of the mean over time within tissue is indicated by an asterisk (*).

5.10. Works Cited

Ballantyne, J. S. (1997). Jaws: The Inside Story. The Metabolism of Elasmobranch Fishes. *Comparative Biochemistry and Physiology, Part B* **118B**, 703-742.

Balmaceda-Aguilera, C., Cortés-Campos, C., Cifuentes, M., Peruzzo, B., Mack, L., Tapia, J. C., Oyarce, K., García, M. A. and Nualart, F. (2012). Glucose Transporter 1 and Monocarboxylate Transporters 1, 2, and 4 Localization within the Glial Cells of Shark Blood-Brain-Barriers. *PloS One* **7**, e32409.

Bouyoucos, I. A., Schoen, A. N., Wahl, R. C. and Anderson, W. G. (2021). Ancient fishes and the functional evolution of the corticosteroid stress response in vertebrates. *Comparative Biochemistry and Physiology, Part A* **260**, 111024.

Bouyoucos, I. A., Suski, C. D., Mandelman, J. and Brooks, E. J. (2017). The energetic, physiological, and behavioral response of lemon sharks (*Negaprion brevirostris*) to simulated longline capture. *Comparative Biochemistry and Physiology, Part A* **207**, 65-72.

Bouyoucos, I. A., Talwar, B. S., Brooks, E. J., Brownscombe, J. W., Cooke, S. J., Suski, C. D. and Mandelman, J. (2018a). Exercise intensity while hooked is associated with physiological status of longline-captured sharks. *Conservation Physiology* **6**, coy074.

Bouyoucos, I. A., Weideli, O. C., Planes, S., Simpfendorfer, C. A. and Rummer, J. L. (2018b). Dead tired: evaluating the physiological status and survival of neonatal reef sharks under stress. *Conservation Physiology* **6**, coy053.

Brinn, R. P., Marcon, J. L., McComb, D. M., Gomes, L. C., Abreu, J. S. and Baldisseroto, B. (2012). Stress responses of the endemic freshwater cururu stingray (*Potamotrygon* cf. *histrix*) during transportation in the Amazon region of the Rio Negro. *Comparative Biochemistry and Physiology, Part A* **162A**, 139-145.

Capilla, E., Díaz, M., Gutiérrez, J. and Planas, J. V. (2002). Physiological regulation of the expression of a GLUT4 homolog in fish skeletal muscle. *American Journal of Physiology Endocrinology and Metabolism* **283**, E44-E49.

Chapman, C. A. and Renshaw, G. M. C. (2009). Hematological Responses of the Grey Carpet Shark (*Chiloscyllium punctatum*) and the Epaulette Shark (*Hemiscyllium ocellatum*) to Anoxia and Re-Oxygenation. *Journal of Experimental Zoology* **311A**, 422-438.

Cliff, G. and Thurman, G. D. (1984). Pathological and physiological effects of stress during capture and transport in the juvenile dusky shark, *Carcharhinus obscurus*. *Comparative Biochemistry and Physiology, Part A* **78A**, 167-173.

Coller, J. and Parker, R. (2004). Eukaryotic mRNA Decapping. *Annual Review of Biochemistry* **73**, 861-890.

Deck, C. A., Anderson, W. G., Conlon, J. M. and Walsh, P. J. (2017a). The activity of the rectal gland of the North pacific spiny dogfish *Squalus suckleyi* is glucose dependent and stimulated by glucagon-like peptide-1. *Journal of Comparative Physiology, Part B* **187**, 1155-1161.

Deck, C. A., Anderson, W. G. and Walsh, P. J. (2017b). Effects of glucose and insulin administration on glucose transporter expression in the North Pacific spiny dogfish (*Squalus suckleyi*). *General and Comparative Endocrinology* **247**, 46-52.

Deck, C. A., Bockus, A. B., Seibel, B. A. and Walsh, P. J. (2016a). Effects of short-term hyper- and hypo-osmotic exposure on the osmoregulatory strategy of unfed North Pacific spiny dogfish (*Squalus suckleyi*). *Comparative Biochemistry and Physiology, Part A* **193**, 29-35.

Deck, C. A., Lemoine, C. M. R. and Walsh, P. J. (2016b). Phylogenetic analysis and tissue distribution of elasmobranch glucose transporters and their response to feeding. *Biology Open* **5**, 256-261.

deRoos, R. (1994). Plasma ketone, glucose, lactate, and alanine levels in the vascular supply to and from the brain of the spiny dogfish shark (Squalus acanthias). *Journal of Experimental Zoology* **268**, 354-363.

deRoos, R. and deRoos, C. C. (1978). Elevation of Plasma Glucose Levels by catecholamines in Elasmobranch Fish. *General and Comparative Endocrinology* **34**, 447-452.

Dimitriadis, G., Leighton, B., Parry-Billings, M., Sasson, S., Young, M., Krause, U., Bevan, S., Piva, T., Wegener, G. and Newsholme, E. A. (1997). Effects of glucocorticoid excess on the sensitivity of glucose transport and metabolism to insulin in rat skeletal muscle. *Biochemical Journal* **321**.

Driedzic, W. R. (1978). Carbohydrate Metabolism in the Perfused Dogfish Heart. *Physiological Zoology* **51**, 42-50.

Driedzic, W. R. and Hart, T. (1984). Relationship bewteen exogenous fuel avaiability and performance by teleost and elasmobranch hearts. *Journal of Comparative Physiology, Part B* **154**, 593-599.

Díaz, M., Antonescu, C., Capilla, E., Klip, A. and Planas, J. (2007). Fish Glucose Transporter (GLUT)-4 Differs from Rat GLUT4 in Its Traffic Characteristics but Can Translocate to the Cell Surface in Response to Insulin in Skeletal Muscle Cells. *Endocrinology* **148**, 5248-5257.

Díaz, M., Vraskou, Y., Gutiérrez, J. and Planas, J. V. (2009). Expression of rainbow trout glucose transporters GLUT1 and GLUT4 during in vitro muscle cell differentiation and regulation by insulin and IGF-1. *American Journal of Physiology: Regulatory, Integrative and Comparative Physiology* **296**, R469-R843.

Fabbri, E., Capuzzo, A. and Moon, T. W. (1998). The role of circulating catecholamines in the regulation of fish metabolism: An overview. *Comparative Biochemistry and Physiology, Part C* **120**, 177-192.

Fischer, E. H., Alaba, J. O., Brautigan, D. L., Kerrick, W. G. L., Malencik, D. A., Moeschler, H. J., Picton, C. and Pocinwong, S. (1978). Evolutionary aspects of the structure and regulation of phosphorylase kinase. In *Versatility of Proteins*, (ed. C. H. Li), pp. 133-149. New York, New York: Academic Press.

French, R. P., Lyle, J., Tracey, S., Currie, S. and Semmens, J. M. (2015). High survivorship after catch-and-release fishing suggests physioloical resilience in the endothermic shortfun mako shark (*Isurus oxyrinchus*). *Conservation Physiology* **3**, cov044.

Frick, L. H., Reina, R. D. and Walker, T. I. (2009). The Physiological Response of Port Jack Sharks and Austrailian Swellsharks to Sedation, Gill-Net Capture, and Repeated Sampling in Captivity. *North American Journal of Fisheries Management* **29**, 127-139.

Frick, L. H., Walker, T. I. and Reina, R. D. (2010). Trawl capture of Port Jackson sharks, *Heterodontus portusjacksoni*, and gummy sharks, *Mustelus antarcticus*, in a controlled setting: Effects of tow duration, air exposure and crowding. *Fisheries Research* **106**, 344-350.

Gould, G. W. and Holman, G. D. (1993). The glucose transporter family: structure, function and tissue-specific expression. *Biochemical Journal* **295**, 329-341.

Halestrap, A. P. (2013). Monocarboxylic Acid Transport. *Comprehensive Physiology* **3**, 1611-1643.

Halestrap, A. P. and Price, N. T. (1999). The proton-linked monocarboxylate transporter (MCT) family: structure, fuction and regulation. *Biochemical Journal* **343**, 281-299.

Heard, M., Van Rijn, J. A., Reina, R. D. and Huveneers, C. (2014). Impacts of crowding, trawl duration and air exposure on the physiology of stingarees (family: Urolophidae). *Conservation Physiology* **2**, cou040.

Heckmann, L.-H., Sørensen, P. B., Krogh, P. H. and Sørensen, J. G. (2011). NORMA-Gene: A simple and robust method for qPCR normalization based on target gene data. *BMC Bioinformatics* **12**, 250.

Hoffmayer, E. R., Hendon, J. M. and Parsons, G. R. (2012). Seasonal modulation in the secondary stress response of a carcharhinid shark, *Rhizoprionodon terraenovae*. *Comparative Biochemistry and Physiology, Part A* **162**, 81-87.

Hoffmayer, E. R., Hendon, J. M., Parsons, G. R., Driggers III, W. B. and Campbell, M. D. (2015). A comparison of single and multiple stressor protocols to assess acute stress in a coastal shark species, *Rhizoprionodon terraenovae*. *Fish Physiology and Biochemistry* **41**, 1253-1260.

Hoffmayer, E. R. and Parsons, G. R. (2001). The physiological response to capture and handling stress in the Atlantic sharpnose shark, *Rhizoprionodon terraenovae*. *Fish Physiology and Biochemistry* **25**, 277-285.

Hothorn, T., Bretz, F. and Westfall, P. (2008). Simultaneous Inference in General Parametric Models. *Biometrical Journal* **50**, 346-363.

Huang, R., Han, S., Qiu, Y., Zhou, T., Wu, Y., Du, H., Xu, J. and Wei, X. (2022). Glucocorticoid regulation of lactate release from spinal astrocytes contributes to the induction of spinal LTP of C-fiber-evoked field potentials and the development of mechanical allodynia. *Neuropharmacology* **219**, 109253.

Hugo, S. E., Cruz-Garcia, L., Karanth, S., Anderson, R. M., Stainier, D. Y. R. and Schlegel, A. (2012). A monocarboxylate transporter required for hepatocyte secredtion of ketone bodies during fasting. *Genes and Development* **26**, 282-293.

Iki, A., Anderson, G., Deck, C. A., Ogihara, M. H., Ikeba, K., Kataoka, H. and Hyodo, S. (2020). Measurement of 1α-hydroxycorticosterone in the Japanese banded houndshark, *Triakis scyllium*, following expsure to a series of stressors. *General and Comparative Endocrinology* **292**, 113440.

Jackson, V. N. and Halestrap, A. P. (1996). The Kinetics, Substrate, and Inhibitor Specificity of the Monocarboxylate (Lactate) Transporter of Rat Liver Cells Determined Using the Fluorescent Intracellular pH Indicator, 2',7'-Bis(carboxyethyl)-5(6)-carboxyfluorescein*. *The Journal of Biological Chemistry* **271**, 861-868.

Krebs, H. A., Bennett, A. H., de Gasquet, P., Gascoyne, T. and Yoshida, T. (1963). Renal Gluconeogenesis: The Effect of Diet on the Gluconeogenic Capacity of Rat-Kidney-Cortex Slices. *Biochemical Journal* **86**, 22-27.

Laffel, L. (1999). Ketone Bodies: a Review of Physiology, Pathophysiology and Application of Monitoring to Diabetes. *Diabetes/Metabolism Research and Review* **15**, 412-426.

Lambert, F. N., Treberg, J. R., Anderson, W. G., Brandt, C. and Evans, A. N. (2018). The physiological stress response of the Atlantic stingray (*Hypanus sabinus*) to aerial exposure. *Comparative Biochemistry and Physiology, Part A* **219-220**, 38-43.

Lipshaw, L. A., Patent, G. J. and P, F. P. (1972). Effects of Epinephrine and Norepinephrine on the Hepatic Lipids of the Nurse Shark, *Ginglymostoma cirratum*. *Hormone and Metabolic Research* **4**, 34-38.

Mandelman, J. and Farrington, M. A. (2007). The estimated short-term discard mortality of a trawled elasmobranch, the spiny dogfish (*Squalus acanthias*). *Fisheries Research* **83**, 238-245.

Manire, C. A., Hueter, R., Hull, E. and Spieler, R. (2001). Serological Changes Associated with Gill-Net Capture and Restraint in Three Species of Sharks. *Transactions of the American Fisheries Society* **130**, 1038-1048.

Moon, T. W., Busby, E. R., Cooper, G. A. and Mommsen, T. P. (1999). Fish hepatocyte glycogen phosphorylase - a sensitive indicator for hormonal modulation. *Fish Physiology and Biochemistry* **21**, 15-24.

Moon, T. W. and Mommsen, T. P. (1987). Enzymes of Intermediary Metabolism in Tissues of the Little Skate, *Raja erinacea*. *Journal of Experimental Zoology* **244**, 9-15.

Nathanson, M. H. and Mariwalla, K. (1996). Characterization and function of ATP receptors on hepatocytes from the little skate *Raja erinacea*. *American Physiological Society* **270**, R561-R570.

Newsholme, E. A. and Start, C. (1973). Regulation in metabolism. London and New York: Wiley Interscience.

Ngan, A. K. and Wang, Y. S. (2009). Tissue-specific transcriptional regulation of monocarboxylate transporters (MCTs) during short-term hypoxia in zebrafish (*Danio rerio*). *Comparative Biochemistry and Physiology, Part B* **154**, 396-405.

Omlin, T. and Weber, J.-M. (2013). Exhausting exercise and tissue-specific expression of monocarboxylate transporters in rainbow trout. *American Journal of Physiology Regulatory, Integrative, and Comparative Physiology* **304**, R1036-R1043.

Pardridge, W. M. (1983). Brain Metabolism: A Perspective From the Blood-Brain Barrier. *American Physiological Society* **63**, 1481-1535.

Patent, G. J. (1970). Comparision of Some Hormonal Effects on Carbohydrate Metabolism in an Elasmobranch (*Squalus acanthias*) and a Holocephalan (*Hydrolagus colliei*). *General and Comparative Endocrinology* **14**, 215-242.

Polakof, S., Skiba-Cassy, S., Choubert, G. and Panserat, S. (2010). Insulin-induced hypoglycemia is co-ordinately regulated by liver and muscle during acute and chronic insulin stimulation in rainbow trout (*Oncorhynchus mykiss*). *Journal of Experimental Biology* **213**, 1443-1452.

Richards, J. G., Heigenhauster, J. F. and Wood, C. M. (2003). Exercise and recovery metabolism in the pacific spiny dogfish (*Squalus acanthias*). *Journal of Comparative Physiology, Part B* **173**, 463-474.

Romero, L. M. and Beattie, U. K. (2022). Common myths of glucocorticoid function in ecology and conservation. *Journal of Experimental Zoology, Part A* **337**, 7-14.

Romero, M. L. and Butler, L. K. (2007). Endocrinology of Stress. *International Journal of Comparative Psychology* **20**, 89-95.

Romero, M. L., Dickens, M. J. and Cyr, N. E. (2009). The reactive scope model - A new model integrating homeostasis, allostasis, and stress. *Hormones and Behavior* **55**, 375-389.

Ruiz-Jarabo, I., Berragán-Méndez, C., Jerez-Cepa, I., Fernández-Castro, M., Sobrino, I., Mancera, J. M. and Aerts, J. (2019). Plasma 1α-Hydroxycorticosterone as Biomarker for Acute Stress in Catsharks (*Scyliorhinus canucula*). *Frontiers in Physiology* **10**.

Ruiz-Jarabo, I., Paullada-Salmerón, J. A., Jerez-Cepa, I., Neto, J. B. G., Bystriansky, J. S. and Mancera, J. M. (2022). Acute Stress in Lesser-Spotted Catshark (*Scyliorhinus canicula* Linnaeus, 1758) Promotes Amino Acid Catabolism and Osmoregulatory Imbalances. *Animals* **12**, 1192.

Schmittgen, T. D. and Livak, K. J. (2008). Analyzing real-time PCR data by the comparative CT method. *Nature Protocols* **3**, 1101-1108.

Schoen, A. N., Bouyoucos, I. A., Anderson, W. G., Wheaton, C. J., Planes, S., Mylniczenko, N. D. and Rummer, J. L. (2021). Simulated heatwave and fishing stressors alter corticosteroid and energy balance in neonate blacktip reef sharks, *Carcharhinus melanopterus*. . *Conservation Physiology* **9**, coab067.

Shea, B. D., Coulter, S. K., Dooling, K. E., Isihara, H. L., Roth, J. C., Sudal, E., Donovan, D. J., Hoopes, L. A., Dove, A. D. M., Cooke, S. J. et al. (2022). Recreational fishing fight times are not correlated with physiological status of blue sharks (*Prionace glauca*) in the Northwestern Atlantic. *Fisheries Research* **248**, 106220.

Speers-Roesch, B., Ip, Y. K. and Ballantyne, J. S. (2006). Metabolic organization of freswater, euryhaline, and marine elasmobranchs: implications for the evolution of energy metabolism in sharks and rays. *Journal of Experimental Biology* **209**, 2495-2508.

Speers-Roesch, B. and Treberg, J. R. (2010). The unusual energy metabolism of elasmobranch fishes. *Comparative Biochemistry and Physiology, Part A* **155**, 417-434.

Tseng, Y.-C., Liu, S.-T., Hu, M. Y., Chen, R.-D., Lee, J.-R. and Hwang, P.-P. (2014). Brain functioning under acute hypothermic stress supported by dynamic monocarboxylate utilization and transport in ectothermic fish. *Frontiers in Zoology* **11**, 53.

van der Meer, D. L. M., van der Thillart, G. E. E. J. M., Witte, F., de Bakker, M. A. G., Besser, J., Richardson, M. K., Spaink, H. P., Leito, J. T. D. and Bagowski, C. P. (2005). Gene expression profiling of the long-term adaptive response to hypoxia in the gills of adult zebrafish. *American Journal of Physiology: Regulatory, Integrative, and Comparative Physiology* **289**, R1512-1519.

Walsh, P. J., Kajimura, M., Mommsen, T. P. and Wood, C. M. (2006). Metabolic organization and effects of feeding on ezyme activities of the dogifsh shark (Squalus acanthias) rectal gland. *Journal of Experimental Biology* **209**, 2929-2938.

Watson, R. R. and Dickson, K. A. (2001). Enzyme Activities Support the Use of Liver Lipid-Derived Ketone Bodies as Aerobic Fuels in Muscle Tissues of Active Sharks. *Physiological and Biochemical Zoology* **74**, 273-282.

Weinrauch, A. M., Fehrmann, F. and Anderson, W. G. (2022). Sustained endocrine and exocrine function in the pancreas of the Pacific spiny digfish post-feeding. *Fish Physiology and Biochemistry* **48**, 645-657.

Widnell, C. C. (1995). Control of Glucose Transport by GLUT1: Regulated Secretion in an Unexpected Environment. *Bioscience Reports* **15**, 427-443.

Wood, C. M., Walsh, P. J., Kajimura, M., McClelland, G. B. and Chew, S. F. (2010). The influence of feeding and fasting on plasma metabolites in the dogfish shark (*Squalus acanthias*). *Comparative Biochemistry and Physiology, Part A* **155**, 435-444.

Zammit, V. A. and Newsholme, E. A. (1979). Activities of Enzymes of Fat and Ketone-Body Metabolism and Effects of Starvation on Blood Concentrations of Glucose and Fat Fuels in Teleost and Elasmobranch Fish. *Biochemical Journal* **184**, 313-322.

6. General Discussion

6.1. Thesis Summary

Elasmobranchii is one of the most ancient taxon of jawed-vertebrates, diverging from other vertebrates between 370-380 million year ago, with extant lineages dating back 66-200 million years (Janvier and Pradel, 2016). This phylogenetic position gives unique insight into the evolution of energy balance and the stress response in vertebrates. As such, my thesis investigates metabolite (glucose and 3-HB) balance and use in this primitive group, specifically the North Pacific spiny dogfish, *Squalus suckleyi*, by using the stress axis as a paradigm to alter metabolite mobilization and consumption. The overarching questions of my thesis were 1) What are the dynamics of key energy metabolites (glucose and 3-HB) and corticosteroids following a stress response, 2) What influence do hormones of interest have on metabolite mobilization, and 3) What is fueling the stress response in elasmobranchs? I attempted to answer these questions by using a "big to small" approach; first by analyzing metabolite mobilization following a stress event *in vivo* using a whole organism, next focusing on the tissue level of metabolite mobilization using a whole-liver perfusion, and finally, examining metabolite balance from a cellular level using enzymatic and molecular techniques.

Initially, I showed an increase in key circulating plasma metabolites (glucose and 3-hydroxybutyrate [3-HB]) and corticosteroids (1α-hydroxycorticosterone [1α-OHB] and corticosterone [B]) following an anesthetic bath, surgical cannulation, and 24hrs of confinement (Chapter 2). Subsequent air exposure did not increase these plasma parameters, likely because the initial set of stressors chronically activated the stress response, which seemed to only be alleviated 48hrs after air exposure when plasma glucose returned to baseline values. Further, an intravascular injection of B did not increase plasma glucose. B was previously shown to cause hyperglycemia in the spiny dogfish, *S. acanthias*, although this was measured after 10 days of repeated intramuscular B injections (Patent, 1970); thus, the duration of B exposure and/or repeated handling may have a significant effect that was not observed in Chapter 2. Alternatively, the lack of a response again suggests chronic stress prior to experimentation or that B is not directly involved in glucose regulation under these conditions. Furthermore, using data from the control and air-exposed treatments in Chapter 2, plasma 3-HB positively correlated to plasma 1α-OHB, plasma glucose positively correlated to plasma B, and plasma 3-HB negatively correlated to plasma B. These relationships gave initial insight into the potential roles the predominate

corticosteroids may have in regulating glucose and 3-HB; however, the relationships were largely weak and inferred alternative regulatory mechanisms. Interestingly, plasma 3-HB and glucose were also negatively correlated, which has been shown following handling and air exposure in blacktip reef sharks, *Carcharhinus melanopterus* (Schoen et al., 2021), and inferred from seasonal analysis of plasma samples in *S. canicula* (Gutiérrez et al., 1987) and angled *I. oxyrinchus* at increasing sea surface temperatures (French et al., 2015). The relationship between glucose and ketones in mammals is in part regulated by insulin, glucagon, and catecholamines; thus, these results added additional hormones of interest to investigate further.

To delve into the underlying mechanisms of hormonal control of metabolite balance, I developed an *in situ* liver perfusion in a shark species. The perfusion was determined viable for at least 3hrs based on consistent oxygen consumption and predictable vasoconstriction in response to angiotensin II (Chapter 3). By removing and reintroducing key metabolites to the perfusion (glucose and 3-HB), I showed that the liver in *S. suckleyi* produced 3-HB and that glucose balance was only affected by the exogenous manipulation of this metabolite. This perfusion was used to test the function of insulin and glucagon, as well as relevant corticosteroids, B and DOC, and a catecholamine, epinephrine (E) (Chapter 4). There were no detectable changes in the measured metabolites following any hormonal stimulation; however, a second set of livers were then perfused to elucidate if cellular mechanisms (enzyme activity and mRNA transcript abundance) were stimulated by hormones.

Enzymes and gene transcripts of interest were chosen based on involvement in hepatic glucose (glycogenolysis, glycogen phosphorylase [GP] activity; and gluconeogenesis, phosphoenolpyruvate carboxykinase [PEPCK] activity; glucose transport, *glut1* and *glut4* transcript abundance) and 3-HB (ketogenesis, 3-hydroxybutyrate [3-HBDH] activity; ketolysis, succinyl-CoA transferase [SCOT] activity; *mct1* and *mct2* transcript abundance) balance. There were no changes in transcript abundance of metabolite transporters following hormone perfusion, supporting the lack of hepatic glucose or 3-HB efflux. There was also no change in SCOT activity following hormone perfusion, which is consistent with the limited use of ketones by the elasmobranch liver (Zammit and Newsholme, 1979; Moon and Mommsen, 1987). Similarly, there was no change in GP activity, which is surprising particularly following E perfusion and may indicate alternative activation of this enzyme as compared to mammals (Fischer et al., 1978). E perfusion did increase 3-HBDH activity, inferring an increase in ketogenesis, and all hormones

increased PEPCK activity, suggesting an increase in gluconeogenesis. There was also an increase in *gr* transcript abundance following DOC perfusion, suggesting upregulation of the glucocorticoid receptor (GR) and subsequent increase in gluconeogenesis as one might predict following a stress event that activates the endocrine stress axis (Romero and Butler, 2007).

Finally, I focused on the same enzymatic and molecular responses associated with plasma metabolites and corticosteroids (outlined in Chapter 4) following two stress experiments that were similar to the stress methodology in Chapter 2: 1) handling and air exposure followed by tissue sampling in the short-term and 2) air exposure followed by tissue sampling in the long-term (Chapter 5). There were no changes in key metabolites or corticosteroids in the short-term but there was an increase in plasma lactate, indicative of anaerobic metabolism. As outlined in Chapter 2, the lack of a response in plasma parameters (except lactate) potentially indicates that fish may have been stressed prior to experimentation. Still, there was a detectable decrease in SCOT activity in the heart that suggested a reduction in 3-HB flux through a ketolytic pathway. Interestingly, there were increases in *glut1* and *glut4* transcript abundance in white muscle, which may be indicative of a reduction in transcript translation to functional proteins; this is the predicted response in mammals (Dimitriadis et al., 1997) and some teleosts (Díaz et al., 2007, 2009). Interestingly, *mct1*, *mct2*, and ,*gr* transcript abundance decreased in the liver and *mct2* transcript abundance decreased in the heart, which may infer changes in the transport of lactate following air exposure.

In the long-term, there was a decrease a plasma glucose, which may correspond to an increase in glycolysis in the heart and rectal gland (increased HEX activity). These tissues also showed an increase in GP activity, showing that glucose may be of more importance under these conditions, as compared to the short-term. Furthermore, there was an increase in hepatic 3-HBDH activity that correlated with an increase in both 3-HBDH and SCOT activity in the heart and rectal gland (as well as an increase in SCOT activity in the brain); these results suggest an increase in hepatic ketogenesis and extrahepatic ketolysis in these tissues. Transcript abundance of *glut1* and *glut 4* increased in the heart, as well as an increase in *glut4* transcript abundance in the liver, suggesting an increase in glucose flux in these tissues that may be responsible for the decrease in plasma glucose. In the liver, *mct2* transcript abundance also increased, again matching enzyme results that infer an increase in hepatic ketogenesis. Interestingly, *mct1* and *glut4* transcript abundance in the rectal gland decreased, contrary to the increase in enzyme activity associated

with glycolysis and ketolysis, which may be a function of reducing transporters in the plasma membrane to prevent intracellular metabolite loss. Finally, there was an increase in *gr* transcript abundance in the liver and heart, which shows glucocorticoid stimulation, although the identity of the stimulant remains unknown.

6.2. What are the dynamics of key metabolites following a stress response?

A number of different stressors were employed across the chapters of my thesis including air exposure (Chapters 2 and 5), surgical cannulation (Chapter 2), handling, (Chapters 2 and 5), presumptive confinement/crowding (Chapters 2 and 5), and stimulation using hormonal candidates that may be mobilized following a stress event (Chapters 3 and 4). This is important to note because the use of these stressors sequentially or alone may influence energy dynamics, and different stressors will inevitably result in nuanced differences in how an organism may respond. Despite this, there are patterns that repeatedly appear in the data presented in this thesis, speaking to conserved metabolic mechanisms regardless of the imposed stress event.

The most prominent pattern is the inverse relationship between circulating plasma glucose and 3-HB. In Chapter 2, there was a significant negative correlation between these metabolites using all the datapoints across each treatment (control, air exposure, and B-injection; n=203, R^2=-0.296, p< 0.001). This correlation is repeated in both the short- and long-term stress events in Chapter 5 (short-term: n = 20, R^2 = -0.788, p < 0.001; long-term: n = 12, R^2 = -0.579, p = 0.048). Previous work in other shark species have also found this relationship under a variety of conditions (French et al., 2015; Gutiérrez et al., 1987; Schoen et al., 2021), showing that mechanisms regulating this pattern are potentially related to stress. In mammals, there is a similar inverse relationship between plasma glucose and ketones, where glucose predominates during satiation and ketones increase during starvation to provide a fuel source for the brain. This is in part a result of oxaloacetate in the citric acid cycle being diverted towards gluconeogenesis, which increases the pool of acetyl-CoA to undergo ketogenesis (Laffel, 1999); although it is unknown if this is the same mechanism in elasmobranchs. Elasmobranchs have elevated ketones in both satiated and starved states, so the inverse relationship may reflect this groups slow rate of glucose utilization (Deck et al., 2017; Patent, 1970). A possible mechanism of this slow rate is illustrated in Chapter 5, where HEX activity in the heart and rectal gland does not change in the short-term but increases in the heart and rectal gland were observed at seven days post-exposure to the stressor.

This also raises the question as to if the pattern between glucose and 3-HB is largely regulated by the liver or use by extrahepatic tissues, or both. In Chapters 3 and 4, there is no discernable relationship between glucose and 3-HB in the outflowing perfusate of liver perfusions, suggesting that the inverse relationship between these metabolites deduced in Chapters 2 and 5 is not at the hepatic level. However, there was a trending decrease in hepatic 3-HBDH activity (one-way ANOVA, $t = -2.386$, $p = 0.074$) in the short-term at 30min post-air exposure in Chapter 5, while HEX activity remained the same in the extrahepatic tissues analyzed. These changes in enzyme activities may allude to a possible mechanism of describing the inverse relationship between plasma glucose and 3-HB and provides an intriguing route for further investigation.

To further complicate matters, plasma 3-HB concentrations are highly variable compared to glucose values in Chapters 2 and 5, which is consistent with previous literature (Gutiérrez et al., 1987; Lambert et al., 2018; Wood et al., 2010) and speaks to individual variation. If 3-HB is an important energy source, it is curious why there is not tighter regulation, which clearly is strongly influenced by feeding status (Wood et al., 2010; Zammit and Newsholme, 1979). Feeding status may explain why [A-V 3-HB] in Chapters 3 and 4 were so variable, where there was an inferred net production of 3-HB in some treatments, while in others there was a net consumption. Ultimately, these discrepancies across all chapters highlight the intricacies of metabolic regulation, particularly of ketones in elasmobranchs when their recent history is unknown.

6.3. What are the dynamics of major corticosteroids following a stress response?

Patterns of corticosteroid mobilization and suspected responses following a stress event in elasmobranchs remain elusive, although there are some interesting clues in this thesis. There were parallel increases in measured plasma metabolites (glucose and 3-HB) and corticosteroids (1α-OHB and B) following surgical cannulation and confinement in Chapter 2, but no changes following air exposure in all plasma metrics in both Chapter 2 and 5. A presumed longer confinement stress in Chapter 5 (7 days versus 24hrs in Chapter 2) only decreased plasma glucose, again conflicting with the results in Chapter 2. As previously mentioned, the type, duration, and synergy of stress events will inevitably result in different corticosteroid responses. Further, there may be individual variation in corticosteroid response level, which may be influenced by social hierarchy in Chapter 5 (Gilmour et al., 2005); although, there are currently no studies of hierarchical influence on hormones in elasmobranchs.

Another property of corticosteroid mobilization in elasmobranchs (at least the dominant corticosteroids measured in this thesis) may be feeding status. Iki et al. (2020) found that both 1α-OHB and B are influenced by feeding status, where fasted individuals had greater plasma concentrations of both corticosteroids. Additional analysis of Chapter 5 showed that plasma B concentrations (Welch Two Sample t-tests, $t = 2.305$, $df = 23.272$, $p = 0.030$), as well as plasma 3-HB concentrations (Welch Two Sample t-tests, $t = 2.071$, $df = 29.973$, $p = 0.047$), were significantly lower in the short-term (at least two days fasted) than in the long-term (at least seven days fasted); plasma 1α-OHB and glucose were unaffected by feeding status. These results are consistent with previous work and further supports that at least corticosterone is strongly impacted by feeding status. Overall, there is evidence in this thesis that both 1α-OHB and B are mobilized under certain stress conditions (Chapter 2), although type and duration of the stressor, and prior feeding status certainly serve a role in this hormonal response.

6.4. What influence do hormones of interest have on metabolite mobilization?

A key aspect of my thesis was to determine the hormonal influence on glucose and 3-HB balance, specifically following a stress event. Again, given the diversity of stressors employed and the likelihood that fish in Chapters 2 and 5 were stressed to some degree prior to experimentation, it is difficult to definitively say if the hormones investigated have a role in the stress response. There are conflicting results between Chapters 2 and 5, in that several correlations between metabolites and corticosteroids in Chapter 2 (3-HB and 1α-OHB, $n= 203$, $R^2 = 0.230$, $p = 0.001$; glucose and B, $n = 220$, $R^2 = 0.349$, $p < 0.001$; 3-HB and B, $n = 212$, $R^2 = 0.180$, $p = 0.008$) were not repeatable in Chapter 5. Further, an intravascular B injection in Chapter 2 and hepatic perfusion in Chapter 4 did not result in concurrent changes in glucose, despite previous literature suggesting a hyperglycemic effect of this corticosteroid (Patent, 1970); although, as previously mentioned, the timeframe of B exposure in Patent (1970) was different than those employed in this thesis. The lack of a glucose response to B in Chapter 4 also further demonstrates that the hepatic role in glucose balance may be negligible within the 15min of B exposure used in this chapter. Ultimately, these results provide conflicting evidence as to the role of 1α-OHB and B in glucose and 3-HB balance during the stress response and raises the question of whether other hormones serve a more potent role in metabolite regulation under these conditions.

A major finding of this work is the change in *gr* transcript abundance following DOC perfusion in Chapter 4. DOC is the proposed biosynthetic precursor to B and 1α-OHB (Anderson, 2012) and can activate the GR of *L. erinacea* with about 3-fold greater sensitivity than 1α-OHB (Carroll et al., 2008), suggesting promiscuity of the GR and a potential role of this corticosteroid. However, hepatic perfusion with DOC did not yield changes in either glucose or 3-HB; although, there may have only been enough time for DOC to enact a molecular response, given the 15min perfusion time, and no metabolic response. Further, the lack of a corticosteroid response (1α-OHB, B, and cortisol) simultaneously with deviations in hepatic *gr* transcript abundance following both stress series in Chapter 5 (and in the heart in the long-term) suggests an alternative hormone or mechanism may have altered *gr* transcript abundance in these tissues. DOC was not measured in this study and lacks investigation in the literature, but is worth considering in the future as a potential regulator of metabolite balance.

Finally, non-corticosteroid hormones (insulin, glucagon, and E) were added to liver perfusions in Chapters 3 and 4 to demonstrate the known physiological responses of these hormones. Surprisingly, there was a lack of a response from all three hormones. While this confirms negligible 3-HB regulation by insulin (Anderson et al., 2002) and relative glucose insensitivity to glucagon (Grant, 1964; Patent, 1970), it is unclear why insulin did not cause hypoglycemia (Deck et al., 2017; deRoos and deRoos, 1979; deRoos et al., 1985; Patent, 1970) or why E did not result in hyperglycemia (deRoos and deRoos, 1978; Patent, 1970). Given the relative glucose intolerance of elasmobranchs as compared to mammals, perfusion time may have a critical role in glucose balance; thus, longer perfusions with these hormones are warranted. E perfusions are curious because catecholamines should cause changes in glucose mobilization seconds to minutes following a stress event; however, elasmobranchs may have a more primitive mechanism of GP activation that is not mediated by catecholamines (Fischer et al., 1978). In Chapter 4, E perfusion did not result in changes to hepatic GP activity, supporting this claim. Likewise, GP activity in all tissues except white muscle is low in Chapter 5, and hepatic GP activity did not change in the short- or long term, suggesting activation of hepatic GP via catecholamines may not be a primary mechanism of action in elasmobranchs. This hypothesis was previously postulated by Moon and Mommsen (1987), even though hyperglycemia does occur *in vivo* following catecholamine injections; it remains unclear from where this glucose originates if not the liver.

Overall, I show here that there may be glucose and 3-HB balance functions of 1α-OHB, B, and DOC, although further research is needed to conclusively determine if and what role. Additionally, while insulin and glucagon have defined roles in tetrapods and specifically mammals, these hormones may exert their function over longer timeframes and/or require larger concentrations in elasmobranchs to elicit a response. The same might be said of E, but it is critical to elucidate the mechanism of action of this hormone.

6.5. What is fueling the stress response in elasmobranchs?

Since glucose and 3-HB are key energy molecules in elasmobranchs and both were shown to increase following surgical cannulation and confinement in Chapter 2, it is reasonable to assume that these metabolites are involved in fueling the stress axis. Although, these changes were not consistent in both the short- and long-term in Chapter 5, despite the metabolite plasma concentrations remaining in the same relative range across both chapters. However, if both chapters are split into short- (handling and air exposure) and long-term (confinement in Chapter 2 and presumed crowding in Chapter 5) stress events, some patterns appear. Following the short-term stress events, there are no changes in metabolites. Chapter 5 further shows that there may be influx of glucose into tissues such as the heart following the short-term, but activity of the enzyme associated with glycolysis (HEX) does not change across the tissues investigated. Additionally, there is no change in hepatic PEPCK activity; thus glucose may not be a predominate fuel source in the short-term. Enzyme activity describing 3-HB ketolysis decreases only in the heart and remains unchanged in the other tissues investigated, suggesting that alternative fuel sources to glucose and 3-HB may be preferential under these conditions.

Metabolite balance after the long-term stress events are more variable across chapters, with both metabolites increasing in Chapter 2 and only glucose decreasing in Chapter 5. As these stressors were less comparable to each other across chapters, these differences in metabolite balance may be a result of variable stress treatments. However, glucose may play a larger role following long-term stress, as enzymatic and molecular endpoints infer an increase in glycolysis and glycogenolysis in tissues such as the heart and rectal gland. Endpoints associated with ketone balance are also elevated in the long-term in Chapter 5, confirming hepatic ketogenesis and extrahepatic ketolysis. In both the short- and long-term in Chapter 5, the heart (and possibly the

liver) appears to be affected energetically following stress events, which gives insight into the tissues that corticosteroids may be targeting for glucose and 3-HB mobilization and consumption.

6.6. Caveats and Future Directions

The foremost caveat that is discussed throughout my thesis is the activation of the stress axis prior to the intended experimentation. To date, the glucocorticoid in elasmobranchs remains elusive, which is predominately used to determine stress status in most vertebrates. Thus, I can only postulate based on changes in plasma glucose, 3-HB, and corticosteroids in Chapters 2 and 5 that fish were stressed in captivity. However, the previously mentioned changes in these plasma parameters as compared to immediately following capture from the ocean demonstrate that fish physiology changed between the ocean and captivity. This is an interesting finding as the majority of work conducted on this species has been in a recently captured, laboratory setting, suggesting that these findings may not be reflective of wild fish physiology. This highlights the drawbacks of studying wild animals and is all but impossible to remedy in a long-lived shark species that cannot be maintained for generations in captivity. Yet, future work should focus on finding an appropriate baseline in these fish, particularly when studying stress. This might be accomplished by first extending the time between capture and experimentation, and second taking blood samples immediately following capture and periodically during captivity to assess when plasma parameters (glucose, 3-HB, corticosteroids, etc.) return to baseline values.

Another important aspect of studying stress and metabolism in elasmobranchs is to determine feeding status. The fish used in this thesis were fed *ad libitum* every two days and were not monitored for feeding. Therefore, inevitably fish in each chapter were at different stages of feeding/fasting status, which has been shown to impact plasma 3-HB (Zammit and Newsholme, 1979) and corticosteroids (Iki et al., 2020). While force-feeding fish may also activate the stress response, it might be important in the future to definitively know feeding status. This also may be accomplished by fasting fish in the long-term, although metabolite mobilization following stress may differ between fed and fasted animals, which is also an interesting route for further investigation.

In respect to the types of metabolites that are mobilized and used following a stress event, a major source of energy that was not studied in this thesis was amino acids. Amino acids are a major fuel source in elasmobranchs (Ballantyne, 1997). Thus, future work in this area of study

should measure plasma amino acids, particularly glutamine and alanine, following a stress event to investigate the role that these metabolites serve to fuel the stress response; this should also be done in conjunction with the dominant corticosteroids to assess correlations between amino acid and corticosteroid mobilization. In Chapters 3 and 4, glutamine and alanine were added to the inflowing Ringer's of liver perfusions in order to serve as nitrogen donors to maintain urea homeostasis. However, it is possible that these amino acids served as energy metabolites for perfused livers, which may have been the reason why there was no change in glucose or 3-HB following hormonal stimulation. It is crucial to conduct these liver perfusions without amino acids in the inflowing Ringer's to determine if changes in glucose and 3-HB can be perceived. Furthermore, it would be prudent to measure amino acid concentrations in the outflow of perfused livers to see if these metabolites were consumed.

Finally, the gold-standard experiment that must be conducted to determine the role of 1α-OHB is to inject 1α-OHB into a shark and measure circulating plasma metabolites (glucose, 3-HB, amino acids, etc.). Unfortunately, this experiment is not possible until there is enough 1α-OHB synthetically synthesized, which is a difficult process. It would also be interesting to conduct this same experiment with DOC, since this corticosteroid increased hepatic *gr* transcript abundance in Chapter 4. Future corticosteroid analysis of elasmobranch plasma would benefit from including DOC as a corticosteroid of interest.

6.7. Conclusion

In summary, my thesis shows that the use of glucose and 3-HB as fuel following activation of the endocrine stress response in elasmobranchs is likely situational, and dependent on synergistic stress events, duration of stress, and feeding status. Regulation of energy balance following stress in this taxon remains equivocal, but this work highlights a number of hormonal candidates. I also show limitations of peptide/peptide-derived hormones to cause changes in hepatic metabolite efflux, suggesting 1) the importance of metabolite regulation at the extrahepatic level and 2) the presumptive primitive nature of these peptides and mechanisms of action.

6.8. Works Cited

Anderson, W. G. (2012). The endocrinology of 1α-hydroxycorticosterone in elasmobranch fish: A review. *Comparative Biochemistry and Physiology Part A: Molecular & Integrative Physiology* **162**, 73-80.

Anderson, W. G., Ali, M. F., Einarsdóttir, I. E., Schäffer, L., Hazon, N. and Conlon, J. M. (2002). Purification, Characterization, and Biological Activity of Insulins from the Spotted Dogfish, *Scyliorhinus canicula*, and the Hammerhead Shark, *Sphyrna lewini*. *General and Comparative Endocrinology* **126**, 113-122.

Ballantyne, J. S. (1997). Jaws: The Inside Story. The Metabolism of Elasmobranch Fishes. *Comparative Biochemistry and Physiology, Part B* **118B**, 703-742.

Carroll, S. M., Bridgham, J. T. and Thornton, J. W. (2008). Evolution of Hormone Signaling in Elasmobranchs by Exploitation of Promiscuous Receptors. *Molecular Biology and Evolution* **25**, 2643-2652.

Deck, C. A., Anderson, W. G. and Walsh, P. J. (2017). Effects of glucose and insulin administration on glucose transporter expression in the North Pacific spiny dogfish (*Squalus suckleyi*). *General and Comparative Endocrinology* **247**, 46-52.

deRoos, R. and deRoos, C. C. (1978). Elevation of Plasma Glucose Levels by catecholamines in Elasmobranch Fish. *General and Comparative Endocrinology* **34**, 447-452.

deRoos, R. and deRoos, C. C. (1979). Sever Insulin-Induced Hypoglycemia in the Spiny Dogfish Shark (*Squalus acanthias*). *General and Comparative Endocrinology* **37**, 186-191.

deRoos, R., deRoos, C. C., Werner, C. S. and Werner, H. (1985). Plasma Levels of Glucose, Alanine, Lactate, and ß-Hydroxybutyrate in the Unfed Spiny Dogfish Shark (*Squalus acanthias*) after Surgery and following Mammalian Insulin Infusion. *General and Comparative Endocrinology* **58**, 28-43.

Dimitriadis, G., Leighton, B., Parry-Billings, M., Sasson, S., Young, M., Krause, U., Bevan, S., Piva, T., Wegener, G. and Newsholme, E. A. (1997). Effects of glucocorticoid excess on the sensitivity of glucose transport and metabolism to insulin in rat skeletal muscle. *Biochemical Journal* **321**.

Díaz, M., Antonescu, C., Capilla, E., Klip, A. and Planas, J. (2007). Fish Glucose Transporter (GLUT)-4 Differs from Rat GLUT4 in Its Traffic Characteristics but Can Translocate

to the Cell Surface in Response to Insulin in Skeletal Muscle Cells. *Endocrinology* **148**, 5248-5257.

Díaz, M., Vraskou, Y., Gutiérrez, J. and Planas, J. V. (2009). Expression of rainbow trout glucose transporters GLUT1 and GLUT4 during in vitro muscle cell differentiation and regulation by insulin and IGF-1. *American Journal of Physiology: Regulatory, Integrative, and Comparative Physiology* **296**, R469-R843.

Driedzic, W. R. and Hart, T. (1984). Relationship bewteen exogenous fuel avaiability and performance by teleost and elasmobranch hearts. *Journal of Comparative Physiology, Part B* **154**, 593-599.

Fischer, E. H., Alaba, J. O., Brautigan, D. L., Kerrick, W. G. L., Malencik, D. A., Moeschler, H. J., Picton, C. and Pocinwong, S. (1978). Evolutionary aspects of the structure and regulation of phosphorylase kinase. In *Versatility of Proteins*, (ed. C. H. Li), pp. 133-149. New York, New York: Academic Press.

French, R. P., Lyle, J., Tracey, S., Currie, S. and Semmens, J. M. (2015). High survivorship after catch-and-release fishing suggests physioloical resilience in the endothermic shortfun mako shark (*Isurus oxyrinchus*). *Conservation Physiology* **3**, cov044.

Gilmour, K. M., DiBattista, J. D. and Thomas, J. B. (2005). Physiological Causes and Consequences of Social Status in Salmonid Fish. *Intergrative and Comparative Biology* **45**, 263-272.

Grant, W. C. (1964). Effect of insulin and glucagon on blood glucose levels in the skate, R. erinacea. *American Zoologist* **4**, 325-326.

Gutiérrez, J., Fernández, J. and Planas, J. (1987). Seasonal Variations of Insulin and Some Metabolites in Dogfish Plasma, *Scyliorhinus canicula*, L. *General and Comparative Endocrinology* **70**, 1-8.

Iki, A., Anderson, G., Deck, C. A., Ogihara, M. H., Ikeba, K., Kataoka, H. and Hyodo, S. (2020). Measurement of 1α-hydroxycorticosterone in the Japanese banded houndshark, *Triakis scyllium*, following expsure to a series of stressors. *General and Comparative Endocrinology* **292**, 113440.

Janvier, P. and Pradel, A. (2016). Elasmobranchs and Their Extinct Relatives: Diversity, Relationships, and Adaptations Through Time. In *Physiology of Elasmobranch Fishes: Structure*

and Interacton with Environment, vol. 34B eds. R. E. Shadwick A. P. Farrell and C. J. Brauner), pp. 1-17. London, San Diego, Waltham, Oxford: Academic Press.

Laffel, L. (1999). Ketone Bodies: a Review of Physiology, Pathophysiology and Application of Monitoring to Diabetes. *Diabetes/Metabolism Research and Review* **15**, 412-426.

Lambert, F. N., Treberg, J. R., Anderson, W. G., Brandt, C. and Evans, A. N. (2018). The physiological stress response of the Atlantic stingray (*Hypanus sabinus*) to aerial exposure. *Comparative Biochemistry and Physiology, Part A* **219-220**, 38-43.

Metcalf, V. J. and Gemmell, N. J. (2005). Fatty acid transport in cartilaginous fish: absence of albumin and possible utilization of lipoproteins. *Fish Physiology and Biochemistry* **31**, 55-64.

Mommsen, T. P. and Moon, T. W. (1987). The Metabolic Potential of Hepatocytes and Kidney Tissue in the Little Skate, *Raja erinacea*. *Journal of Experimental Zoology* **244**, 1-8.

Moon, T. W. and Mommsen, T. P. (1987). Enzymes of Intermediary Metabolism in Tissues of the Little Skate, *Raja erinacea*. *Journal of Experimental Zoology* **244**, 9-15.

Patent, G. J. (1970). Comparision of Some Hormonal Effects on Carbohydrate Metabolism in an Elasmobranch (*Squalus acanthias*) and a Holocephalan (*Hydrolagus colliei*). *General and Comparative Endocrinology* **14**, 215-242.

Romero, M. L. and Butler, L. K. (2007). Endocrinology of Stress. *International Journal of Comparative Psychology* **20**, 89-95.

Schoen, A. N., Bouyoucos, I. A., Anderson, W. G., Wheaton, C. J., Planes, S., Mylniczenko, N. D. and Rummer, J. L. (2021). Simulated heatwave and fishing stressors alter corticosteroid and energy balance in neonate blacktip reef sharks, *Carcharhinus melanopterus*. . *Conservation Physiology* **9**, coab067.

Speers-Roesch, B. and Treberg, J. R. (2010). The unusual energy metabolism of elasmobranch fishes. *Comparative Biochemistry and Physiology, Part A* **155**, 417-434.

Wood, C. M., Walsh, P. J., Kajimura, M., McClelland, G. B. and Chew, S. F. (2010). The influence of feeding and fasting on plasma metabolites in the dogfish shark (*Squalus acanthias*). *Comparative Biochemistry and Physiology, Part A* **155**, 435-444.

Zammit, V. A. and Newsholme, E. A. (1979). Activities of Enzymes of Fat and Ketone-Body Metabolism and Effects of Starvation on Blood Concentrations of Glucose and Fat Fuels in Teleost and Elasmobranch Fish. *Biochemical Journal* **184**, 313-322.